Development of Reliable Erosion Indices for Climate-Informed Soil Conservation in the Southeastern United States

by

Ryan Patrick McGehee

A thesis submitted to the Graduate Faculty of
Auburn University
in partial fulfillment of the
requirements for the Degree of
Master of Biosystems Engineering

Auburn, Alabama
December 10, 2016

Climate Change, Climate Variability, Erosion Index, Erosivity, Soil Loss

Approved by

Puneet Srivastava, Chair, Professor of Biosystems Engineering
Latif Kalin, Professor of Forestry and Wildlife Sciences
Joey Shaw, Professor of Agronomy and Soils
Jasmeet Lamba, Assistant Professor of Biosystems Engineering

Abstract

A new methodology and corresponding dataset are recommended for a more accurate calculation of erosion index (EI) and erosivity (R) that was more consistent with observations from superior data sources. NOAA NCDC DSI-3260 (quarter-hour) station data from 1970 to 2010 was screened and a water balance was performed to compare measured precipitation with the expected values at each station having matching climate normal data. The results of the water balance were used to select the screening method that most accurately accounts for precipitation at a high spatial resolution (about 3 times more dense than the previous publication of EI values). It was found that most stations have a slight deficit (averaging 5.9%) with a comparable missing data percentage of 5.77%, which might be the reason for the deficit. Updated annual, seasonal, and monthly EI distributions were calculated along with an analysis of single storm EI for 1, 2, 5, 10, and 20-year recurrence intervals. Annual EI values were found to be higher than AH703 by an average of 18.6% for unadjusted data, and values should be increased at least another 4% for the type of recording station being used. Station observations were gridded by geostatistical interpolation for better spatial representation of the data. The effects of limiting the maximum 30-minute intensity and adjusting for known uncertainties was quantified for the preferred screening method within each analysis. Station data was compared to a reliable literature source to validate the new methodology. Results were further analyzed for climate variability influences from ENSO by the statistical method known as joint-rank fit (JRfit). Data was analyzed under various clusters, and ENSO was found to have a significant effect on multiple precipitation parameters. Changes in the distribution of EI throughout the year, based on ENSO phase, was used to highlight general implications for BMPs aimed at soil conservation and reductions of sediment yield. With known variabilities accounted for, observed changes in erosivity from the influence of climate change can be accurately assessed in the future.

Acknowledgments

There were a number of people without whose sacrifice this thesis would not exist. First, and of the greatest sacrifice, was that of my wife and family. Thank you Mary Hope, Esmen, and Iah for allowing me to pursue a dream and to grow myself. Secondly, I thank my advisor and mentor, Dr. Puneet Srivastava. You have been faithful and unwavering in your commitment to my well-being and the best interest of my family. You were always good to all your students financially, ethically, and most of all personally. I always felt free to ask questions, make mistakes, and respectfully disagree. I do not think many students can speak as I have, nor can they boast of their experiences as I do. Thank you for that. Thank you to my committee, all of whom I greatly respect and revere. You were all very helpful and understanding throughout the process, and I am grateful for each of you. Lastly, to my colleagues and friends whom I considered a great encouragement and source of energy throughout my studies. You have all made a strong impression on me and my family culturally and philosophically. I consider it an honor to call you friends. Thank you Subhasis and Sarmistha for your guidance and friendship.

Table of Contents

List of Tables

List of Figures

List of Abbreviations

AMO	Atlantic Multidecadal Oscillation
ANN	Artificial Neural Network
AOGCM	Atmosphere-Ocean General Circulation Model
ARS	Agricultural Research Service
ENSO	El Niño Southern Oscillation
EPA	Environmental Protection Agency
GCM	General Circulation Model
IPCC	Intergovernmental Panel on Climate Change
NARCCAP	North American Regional Climate Change Assessment Program
NCA	National Climate Assessment
NCDC	National Climate Data Center
NMO	Northern Hemisphere Multidecadal Oscillation
NOAA	National Oceanic and Atmospheric Administration
NRCS	Natural Resources Conservation Service
PDO	Pacific Decadal Oscillation
PMO	Pacific Multidecadal Oscillation
RCM	Regional Circulation Model
RUSLE	Revised Universal Soil Loss Equation
RUSLE2	Revised Universal Soil Loss Equation Version 2
SST	Sea Surface Temperature
USDA	United States Department of Agriculture
USLE	Universal Soil Loss Equation
WEPP	Water Erosion Prediction Project

Chapter 1: Introduction to Study

1.1 Motivation

The conservation of natural resources is an issue of the utmost importance for our society. At this time in history, there is more talk of the food-water-energy nexus than ever before, and yet the human population continues to increase rapidly. These resources are intricately related to each other and to their varying climate, which in many cases determines the immediate utility of those resources. Furthermore, climate change has increased the complexity, uncertainty, and the strain on these relationships. Science and engineering are already discovering that the direct impacts of agriculture, urbanization, pollution, etc. can be matched or exceeded by the indirect impacts of these practices via climate and climate change. The indirect nature of this interaction makes observation, analysis, and communication much more difficult for the science than those resulting from more direct impacts (e.g. water quality). Despite these challenges, modern data, increased computing power, and governmental collaboration has enabled the implementation of relatively consistent, science-based conservation policies and practices. Yet, current conservation efforts still lag behind the state of the science. This is particularly evident in soil loss conservation practices and erosion prediction technology.

Climate—whether it is changing or not—plays a major role in soil interactions. It is one of the four factors of soil formation, and it is one of two soil loss 'driving' factors (erosivity and erodibility) in the USLE family of soil loss equations (not considering 'modifying' factors L, S, C, and P). In understanding how soils form and erode, it is important to understand climate, how it varies over different time scales, how it changes under external forcing, and most importantly that it is not in a steady state…ever. It has been well documented that our climate oscillates due to factors affecting intercepted solar radiation and more recently that anthropogenic contributions to greenhouse gas emissions are affecting measureable climate changes around the globe. It is not a single change; it is multiple changes, often not in the same direction for different locations. For example, some places will see higher amounts of precipitation and some will not. Precipitation is a good example to contrast with temperature because temperature is relatively well mixed, whereas precipitation is highly dependent on the moisture holding capacity of a column of air and how that column of moisture heats and cools as it moves. Despite these complex, dynamic relationships that drive soil loss, the climate aspect of erosion technologies is

usually approximated as a steady state factor. In USLE, RUSLE1, and RUSLE2 it is more obvious, since the R-factor only changes spatially. WEPP on the other hand, allows for new daily data to be incorporated in its CLIGEN weather generator for updated precipitation distributions. However, WEPP still relies on steady state determination of other parameters such as time-to-peak, which were derived from 15-minute NCDC stations. Therefore, **these technologies will need to at least occasionally evaluate whether or not changes in precipitation characteristics have occurred for the study area and time period of interest.** To be clear, the climate has changed—physics and thermodynamics proves this. What is left to determine was whether or not the change is significant and how our technologies can be updated to appropriately reflect these changes.

The goal of resource conservation is to sustain a net-zero or slightly net-positive flux of the resource being protected. In order to accomplish this, it is critical that our technologies are not outpaced by a dynamic climate. Otherwise, it is possible for conservation efforts to insufficiently predict, and therefore, insufficiently regulate and enforce conservation tolerances. Current regulations for soil conservation have not been too restrictive, and they have for the most part, conserved our soil resources. However, as some have begun to point out (Nearing et al., 2004), these current practices are at risk of becoming obsolete in the face of observed and projected climate change, and to a large degree have ignored climate variability.

To keep up with our changing climate, I propose that policy-makers and researchers adopt a three-point approach for a more intelligent conservation which focuses on observed change, observed variability, and subsequently, projected change. This approach is becoming more common among climatologists and climate scientists for communicating the science to the public, and an example is shown in Figure 1-1. Under this approach, one begins by identifying observed changes in the topic of interest. Once the total change has been identified, the impact of known climate cycles (e.g. ENSO, PMO, AMO, etc.) should be evaluated as they pertain to that topic. This will help to identify how much of the observed change is attributable to variability, and whether or not the relationship is significant. This may not ultimately yield better impact studies from climate projections since our understanding of climate variability is still maturing. However, it could prove to be useful in the near-term prediction of climate impacts due to

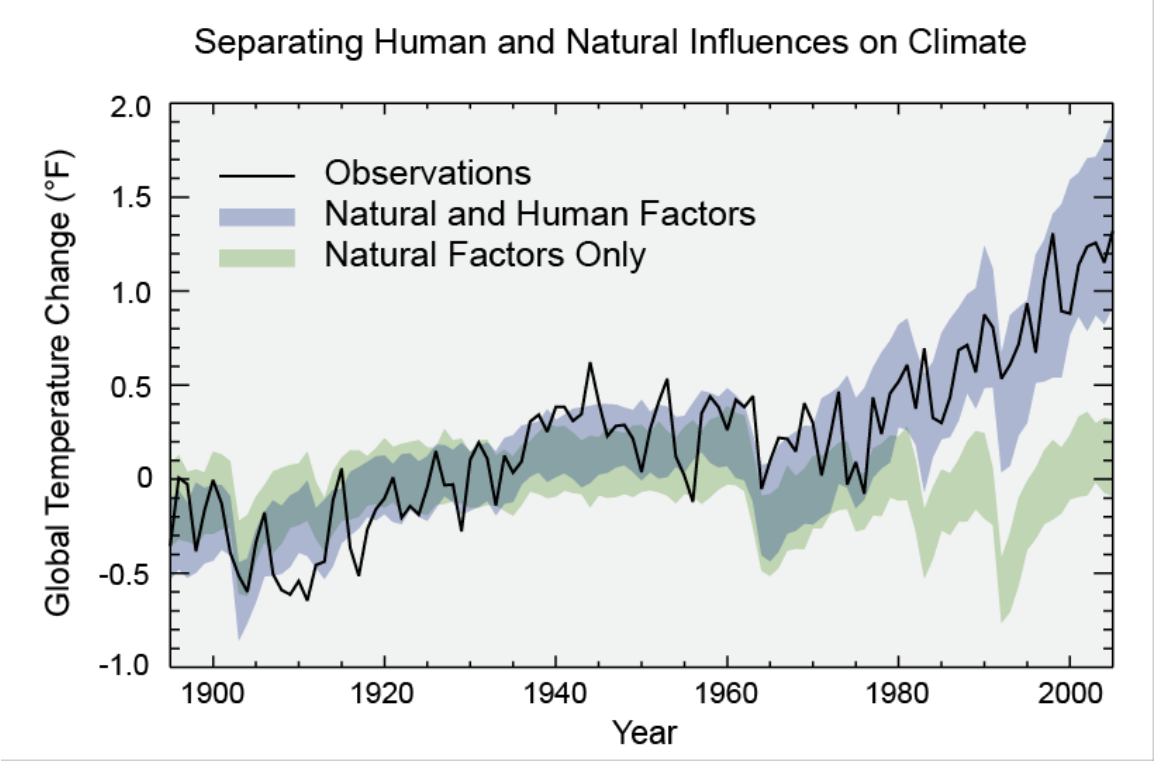

Figure 1-1 Separating Human and Natural Influences on Climate—an Approach for Assessing Climate and Climate Impacts. (Huber and Knutti 2012)

variability, and as models improve, climate projections can be informed through these studies. For instance, although the IPCC is highly confident that ENSO will continue to exist, it is not confident in the effect(s) climate change will have on ENSO and the future variability of ENSO (Cubasch et al., 2013). In short, ENSO and how it impacts a relatively steady state climate is understood, but climate change impacts on the drivers of ENSO are not understood. Most models predict that the climate will favor El Niño more in the future, but models do not agree on the variation of that warmer future. I suspect that until the scientific community can confidently identify the effects of climate change on climate variability, our projections for moderate to high resolution temporal and spatial scales will remain uncertain since they are highly dependent on these inter-annual variations. On global scales, the general implications of climate change can be predicted with relatively high confidence, but at regional scales, especially for variables such as precipitation, there may not be a clear pattern. Figure 1-2 shows precipitation patterns (driven by convection pathways in the atmosphere), which are the sources of this uncertainty. At our current level of understanding, these convection pathways are too difficult to predict with confidence.

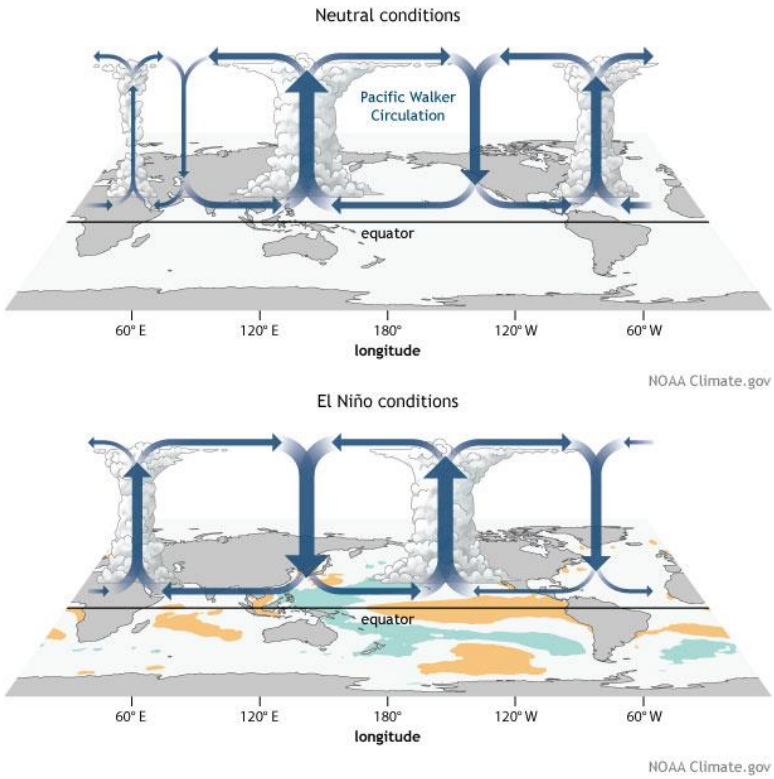

Figure 1-2 ENSO Driven Atmospheric Circulation Patterns Affecting Regional Convection and Precipitation (Credit: Fiona Martin, NOAA)

Therefore, the way to view this approach is from most confident to least confident: observed change, observed variability, and projected change. The projected change is the most uncertain because it relies on our understanding of a) climate change b) climate variability and c) how climate change will impact climate variability. Despite these uncertainties, there are some things which are certain, and it would be a mistake to simply ignore these due to ill-conceived notions of the science. The most obvious example of this was the well-documented fact that the temperature of the earth is increasing. This and other similar findings would be classified as observed change and as such are the most confident findings. Following this approach, the first objective of this study would be to determine what exactly these changes were as they pertain to erosivity in the Southeast United States. The second objective will attempt to quantify the effect of climate variability on the observed change, whether it was significant or not, and how to anticipate changes from variability in the future. Ultimately these two objectives set the stage for the ultimate goal of the research, which is the prediction of erosivity for the purpose of a more intelligent conservation of soil. For a more specific outline of objectives see Section 1.2.1.

1.2 Research Outline and Purpose

This thesis is a scientific document, but it is one that reads more like that of a narrative. The language becomes much more scientific as it progresses further into the body, but the goal is to arrive there in such a way that anyone could pick up this thesis, read it, and for the most part, understand what was done and how the results can be interpreted. Since this is a scientific document, the scientific method was the guiding principle for this study and the logic behind its implementation will be documented here. Relevant results are presented regularly throughout the body of the thesis as appropriate, but final conclusions are presented in Chapter 4 as they pertain to the hypothesis of each objective. Each chapter in the body of the thesis was organized similarly to that of a scientific journal article, which I plan to submit for publication after the completion of this thesis.

1.2.1 Objectives

The justification for the following objectives can be found in Section 1.1. In general, **these objectives were formulated in order to give the best possible insight into the relationship of climate—through climate variability and climate change—to the erosive nature of precipitation in the Southeast.** I want to eventually draw conclusions for the continental US at the same resolution as this study and potentially draw more general conclusions for erosivity globally in the context of changing climate. This first effort begins with a study area familiar to us and that will benefit significantly from the study, which is the southeastern region. I provide a detailed explanation for this decision in Chapter 2. The objectives for this study were as follows:

1. **Determine the change in erosion index and erosivity including:**
    a. Change Resulting from an Updated Methodology (and Data), and
    b. Other Change, Especially that Resulting from Climate Change, Regarding:
        i. Average Annual EI (R-Factor), and
        ii. Single Storm EI (Frequency Analysis)

2. **Determine the impact of climate variability on erosivity including:**
    a. Intra-Annual Variability and Changes (Monthly / Seasonal EI), and
    b. Inter-Annual Variability (ENSO), and
    c. Decadal Variability (PDO/PMO, AMO, NMO)*

3. **Determine the potential future impact of climate change on erosivity based on climate projections (potentially) including:***
    a. Effect of Climate Model (GCM-RCM) Temporal Resolution, and
    b. Effect of Bias Correction, and
    c. Trend-Analysis of Historical Data, and
    d. Prediction Method (ANN, PCA, etc.)

*Denotes that the objective was not evaluated in this thesis although some references may be made to the objective as these components remain the goal of the study. I plan to publish these results in journal articles following the approval of this thesis.

1.2.2 Experimental Design

In 1965, the first large-scale erosivity map was published in a document commonly referred to as Agriculture Handbook No. 282 (AH282). This document provided R values in the Southeast ranging from 125 to less than 700 hundreds of foot-tonf-inch per acre-hour-year. In 1978, AH537 was published using the same data and included a limit on intensity (3.0 in/hr for raindrop size) and maximum 30-minute intensity (2.5 in/hr for ponding in the Southeast). The values in AH537 decreased in the deep-south due to many storms being impacted by these limits. Values ranging from 100 to less than 600 were published at that time and considered to be better for that region. In 1992, AH703 was published with a new method for considering ponding in the Southeast based on slope and the 10-year storm EI, but it still used the same data from the previous two handbooks. The values in AH703 range from 100 to more than 700 and were contoured with more modern methods (McGregor et al. 1995). Each of these Agriculture Handbooks were considered slightly better than the previous publications. Although the values appear inconsistent at first look, each sequential improvement provided a better calculation of erosivity for locally specific observations. **This was good for the science and for steps towards a better and more accurate conservation, but it was challenging for climate science to see the role of climate change related to erosivity over this period. Therefore, the first challenge was to establish a 'benchmark' for future climate studies.**

Of the original Ag. Handbooks, AH703 was the best fit. Unfortunately, AH703 was not a suitable benchmark. It has been presented twice that AH537 (McGregor et al. 1980) and AH703 (McGregor et al. 1995) provide EI values that were consistently and significantly too low. All the Ag. Handbooks utilized 15-minute stations in their calculations of EI,

which was the same type of station used in this study. However, regression equations were developed that related EI to certain return period storm events for each location so that EI values could be drawn at a higher resolution for the eastern United States. In order to establish a benchmark for future experiments, I used the base methodology of AH537 with the exception that all storms were included in our analysis and the abandonment of regression equations for erosivity interpolations. EI values were reported with both a limited and an unlimited I_{30} component. Limited EI values reflect a general observation that the potential erosive power of storms cannot be realized due to negative feedbacks from high intensity storms. More specifically, highly erosive storms, which have high intensities will not infiltrate or runoff quickly enough to allow the incoming rainfall to impact the soil. Therefore, the energy of rainfall can be absorbed by ponded water after sufficient time is allowed for initial abstractions to take place. The limited EI values will provide better insight as to more realistic impacts on climate-driven soil loss, while the unlimited EI values allow a deeper understanding of changes in storms themselves and the potential erosive power of such storms. I made the decision to use the AH537 energy equation despite the fact that AH703 and McGregor recommend using the Brown-Foster (BF) or McGregor-Mutchler (MM) equation for superior energy determination in EI calculations. This allowed for better comparisons between AH537, AH703, McGregor's study, and my study. I plan to expand the methodology in the future, pending publication of the new methodology, to the entire continental US. At that time I will evaluate the BF equation for comparisons with the methodology used in this study.

1.2.3 Anticipated Outcomes

This study utilizes modern datasets and provides an appropriate methodology for an accurate erosion index calculation. The results from this new methodology were evaluated to determine whether or not true EI values can be obtained for the Southeast United States since previous publications, namely that of the Agriculture Handbooks, have been shown to be unreliable. AH537 was primarily included as a point of reference for limited EI values and single storm EI, and AH703 was included for unlimited EI values and EI distribution throughout the year. This will demonstrate the differences in the methodology (mainly the incorporation of small storms less than 0.5 inches of relatively light intensities, which has been omitted in all Ag. Handbooks) as well

as the effect of regression equations used in the Ag. Handbooks. If the methodological differences can be quantified, I will have a baseline for comparison at two different time periods (1930s-1950s and 1970-2010) for climate change analysis. If these differences cannot be determined, it is still possible to evaluate the new methodology for observed influences from climate variability in the form of ENSO (others may be considered for study later, especially as the observed record improves). **Even if I cannot currently make conclusive statements about climate change impacts on erosivity, this study will a) provide a benchmark and direction for that specific purpose and b) result in recommendations for better conservation practices, which change according to the ENSO phase, and c) prepare for a study of projected climate impacts on erosivity.**

1.2.4 Broader Impacts

Conservation regulations attempt to maintain equilibrium between the natural environment and designated uses of the land or water body. Climate change and variability invoke a state of non-equilibrium, which suggests the need of a prediction technology for conservation regulation. **Prediction of climate change and climate variability outcomes for soil loss will allow agricultural, mining, ranching, construction, landfill, and military training operations to better maintain compliance with government regulation of soil loss tolerances in the future.** The primary benefactors of this project include EPA, NRCS, USDA, and other government agencies that have an interest in conservation of soil resources or that use erosion index (EI) for estimating soil loss. Additionally, RUSLE2 was capable of predicting climate change and climate variability outcomes for sediment yield based on soil loss and deposition calculations. Updating this erosion prediction technology creates an opportunity for understanding climate-driven sediment yields in watershed and water quality management.

1.3 Soil Background

Soil is a critical component of the terrestrial ecosystem. This natural resource provides the medium for biological growth and is responsible for a number of life sustaining services within the ecosystem. From a human perspective, soil is at the physical intersection of the food-water-energy nexus. Its landform and porosity (along with other properties) determine both the immediate and long-term availability of water and nutrients. Vegetation and fauna find habitat in the soil, and provide vital ecosystem services such as decomposition and runoff reduction by interception and infiltration. More specific to humans, soils used in agriculture require significant inputs of water and energy to yield food. Protecting this resource is of the utmost priority for sustaining the human population and the health of the ecosystem at large. In the event that relatively fertile agricultural soils were lost, more water and energy resources must be provided to the system to make up for decreased yields. Therefore, conservation that protects the soil health and fertility is critical. In order to understand the basis of conservation and a healthy flux of soil in a system, it is imperative to understand the natural process of how soils are generated through pedogenesis and how they are lost through erosion.

1.3.1 Soil Forming Factors

The basic unit of soils is the pedon, and perhaps even more than climate, this soil unit is thought of as a steady state, even though on large timescales, it is not. The pedon is the result of soil forming factors combined with unique processes that yield a unique individual much like DNA, mitosis, and meiosis yield a unique individual human. If the factor changes, you can expect that the individual will also change. Therefore, conservation is focused on reducing human-induced factor changes such as anthropogenic climate change as well as the direct modification of soils due to human disturbances. I would thusly argue that it is our responsibility not only to protect the soil from direct disturbances but also from those more indirect disturbances, such as climate change. More on this will be discussed in the climate background. Figure 1-3 is a diagram of how factors and processes interact to produce different pedons. I will add to this figure that some of the processes (although it is not obvious in the diagram) are also results of the climate and have large degrees of influence on the pedon over time. Figure 1-4 better shows the impact of the past and present climate on the future of the pedon. It is easy to see that significant changes in

climate can have significant changes on the soil, not only from the perspective of loss, but also from the perspective of formation. On a global scale, these changes are probably significant, but on a local scale it is highly dependent on local and regional climate patterns such as ENSO. If climate change favors El Niño, then what was once an oscillation could become a normal occurrence for the local regions impacted by ENSO the most. The oscillation will still exist, but it could be centered on the climate pattern of El Niño rather than the neutral phase of ENSO.

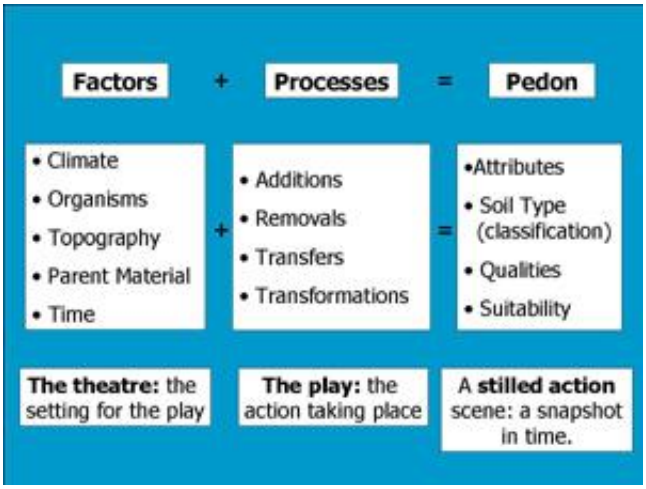

Figure 1-3 Soil Pedogenesis—Factors, Processes, and the Pedon (Hutchinson 1965)

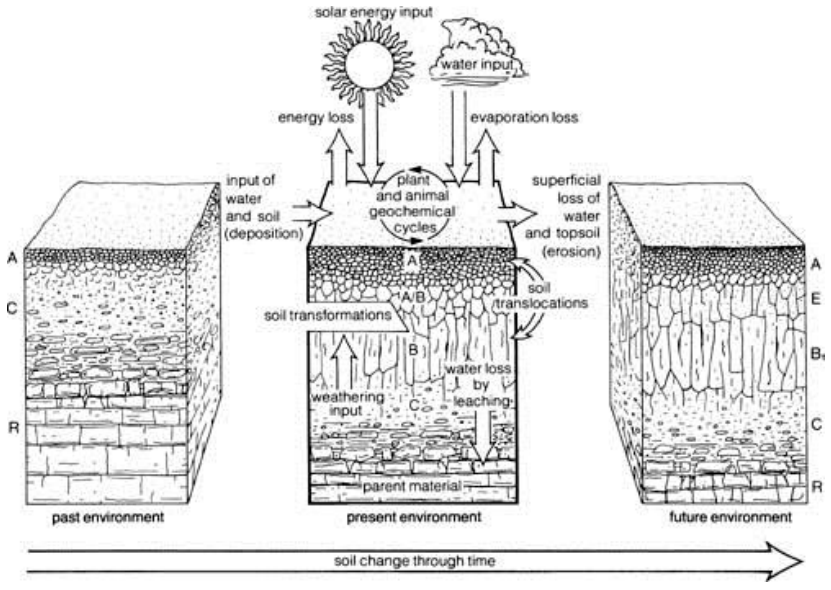

Figure 1-4 Illustration of the Evolution of Soil (Bridges 1978)

1.3.2 Soil Loss Mechanisms and Modeling

Soil loss models are driven by two primary functions including the climate and the soil. Since this thesis focuses primarily on the climate aspect of soil loss, only a brief background on the soil component is provided. In a nutshell, soil loss occurs when the energy of rainfall or runoff exceeds the critical shear force holding the soil together and it breaks off, or more correctly, it detaches. The climate component is essentially an energy calculation. Different models calculate this term in quite a dissimilar fashion, but it is ultimately about defining climate conditions that can overcome soil adhesiveness. In reality, this shear force is determined by the properties of the soil, hence the discussion of the pedon earlier, and fluctuating properties of the soil caused by climate. There is actually a debate in the soil community about whether these are properties of the soil or of the climate (e.g. soil moisture and temperature). Clearly these properties are driven by the recent precipitation and weather patterns, but different soils will react uniquely to the same climate pattern. It is easy to take a perspective on either side. For the purpose of this thesis, since the USLE incorporates these in the calculation of the K-factor, I will refer to them as temporary soil properties. Physically based models will actually calculate the shear force and the force of precipitation required to overcome it. Empirical models will use statistics to fit the best mathematical representation of the process to observations. What is important to gather from this was that both physically based and empirical models rely on these two 'driving' factors to estimate soil loss. Despite their vastly different approaches, the findings from using one model will still have significant value for the other.

In order to truly evaluate the total impact of climate change and climate variability on soil loss, both driving factors should be evaluated simultaneously as well as the indirect changes that will impact factors such as vegetation and human practices. These effects would be called either positive or negative feedback loops based upon whether they reinforce the direction of change or act against it. This would be an enormous undertaking, so I decided to focus my efforts on just the direct impacts of climate on soil loss. In addition to this, I had to select the way in which I would communicate changes in this soil loss mechanism. Since, I am familiar with modeling, I thought it would be best to present findings that would be relevant to at least one erosion prediction technology. **It is important at this point to note that I am not using any soil loss model**

to predict soil loss based on climate change and climate variability. Rather I am assessing the impact of climate change and climate variability upon one of the two soil loss 'driving' factors. I used the format of a soil loss model for communicating observations and analysis results so that practical applications may come from my work. Although there are many soil loss models from which to choose, there are only two popular choices, both of which have historically received the most support in US erosion prediction: RUSLE2 and WEPP.

1.3.3 Physical vs. Empirical Models

A more process-based model like WEPP could offer better insight on how climate change may interact with soil loss mechanisms, but most government agencies use the more empirically derived model due to better performance of empirical models over uncalibrated physical models. Physically based models have the potential to perform better, but they require more demanding inputs unique to the study area along with model calibration for the best results and they often fall short of their potential (Tiwari et al., 2000). The USLE family of equations have proven strength without any calibration or significant user input. Therefore, updating the R-factor from these soil loss models has a greater impact potential for erosion prediction technology. Additionally, even though WEPP is a more physically based model, it does not consider variations in the kinetic energy per unit quantity of rainfall. WEPP only varies the intensity of rainfall in its calculations, which if ignored in this study could result in only part of climate impacts being detected. I feel these important considerations outweigh any potential gains from using a more physically based model.

There are still several criticisms to using either USLE or RUSLE that should be addressed. WEPP offers a superior temporal and spatial resolution to either of these models in determining soil loss. Specifically, WEPP is able to predict soil loss on a non-annual basis unlike USLE and RUSLE. So not only were the calculations superior, but the soil loss reporting scheme is better as well. This is where RUSLE2 solidified my decision to stick with the empirical calculation of EI. RUSLE2 has the potential to outperform both USLE and RUSLE models owing to its integrative mathematical structure, which allows it to better model temporally small scale events that can comprise the majority of soil loss for the entire year. This is especially true in highly erosive summer precipitation events of

the southeastern region. RUSLE2 calculates the long-term average daily soil loss for each day along with 5 of 6 soil loss factors of the original USLE equation (slope steepness is assumed constant). Thus, **RUSLE2 benefits from high temporal and spatial resolutions as WEPP does, but RUSLE2 operates from the proven strength of the empirical nature of USLE.** This is particularly exciting for a study of erosivity, which varies daily and even between storms. Over long time periods, the distribution of erosivity throughout the year can be known and conservation practices effectively implemented and evaluated to meet soil loss tolerances.

1.3.4 The State of Erosion Prediction Technology

This is a brief section included to summarize a) the developments in and b) the most current state of erosion prediction technology as well as c) where I see the technology could and should be developed further. In AH282 (1965), the first isoerodent maps of the eastern US were developed based on the statistical relationship of energy and intensity to soil loss when all other factors were held constant for 22 years of precipitation data (1936-1957). These maps showed average annual erosion index (formally called erosivity) based on a mixture of data from 2000 locations evenly distributed across the 37 states analyzed. Actual EI values were calculated at 181 locations across 37 eastern states from stations similar to the DSI-3260 'quarter-hour' stations used in our study. An equation relating the 2-year precipitation depths of varying durations to average annual erosivity values was developed for the 181 stations used for EI calculations. This equation was used to estimate EI at about 2,000 locations, and these results were presented in all the Agricultural Handbooks (USDA, 2008). Thirteen years later, AH537 updated these values in the eastern US to include energy and intensity limits that better reflect the actual EI values across the region. At this point there was mention of 'cyclical rainfall patterns' that require longer station periods in order to calculate true EI values. Two years earlier an estimating procedure was used to extend the isoerodent map to the west coast, which was included in AH537. In 1980—two years later—McGregor publishes a troubling paper using far superior data claiming that the EI values recommended by AH537 should be much higher than reported. The same was observed in 1995 for erosivity values utilized by RUSLE. Some of this was from methodological changes made by McGregor, some from using a superior dataset (29 breakpoint gauging stations), and some undoubtedly from actual variations and changes in

the climate. Two years later, AH703 was published along with updates to the computer-based RUSLE program and databases. This update came with an updated isoerodent map, which used new methods for calculating maximum intensity limitations and modern contouring methods. Even with these updates, the area of McGregor's study (northern Mississippi) was largely unaffected by AH703 updates, and therefore, the values at that location were still too low. In 2008, RUSLE2 abandoned the 'standard approach' to erosivity calculation, and used an erosivity density function for its soil loss calculations. **Today, 21 years since the most recent update to 'standard approach' erosivity studies, I am recommending one of the largest overhauls of standard erosivity calculations in the history of erosion prediction technology (recommendations detailed below).**

Most of the methodology used in this study was previously recommended by McGregor and AH703 to provide the most accurate EI calculation possible. The best data available is breakpoint data. Unfortunately, it is not commonly available at significant spatial scales, but it would serve a great purpose as a validation dataset for EI calculations where it is available. The only viable alternative to breakpoint data is high-resolution temporal data. Therefore, the most obvious recommendation is to use the most widespread data of this kind—NOAA NCDC 15-minute data (DSI-3260). Second, the ideal methodology would include all storms in its calculation regardless of the size or intensity. These were historically omitted for ease of calculation, which is a non-issue with today's computing resources. Third, the BF energy equation should be used for better energy calculations (discussed earlier). Fourth, maximum intensity calculations should not be limited since the limitation is based on terrain not precipitation characteristics. Fifth, regression-based relationships of erosivity to rainfall should be abandoned since these relationships may change with climate variability and change. Sixth, EI calculations should be kept in context of climate anomalies including: natural variabilities of the observed period (phases of ENSO, AMO, PDO, etc.), exceptional storms of large recurrence intervals (intervals larger than the observation period), and exceptional droughts of recurrence intervals larger than the observation period. This last point is not evaluated in this study but is nonetheless an important consideration for EI studies. **These recommendations will require an update of the annual EI, storm probability of exceedance, and temporal distribution of EI throughout the year to benchmark the effects of the new methodology on EI values.**

1.4 Climate Background

Earth's climate could be expressed as the sum total of how solar radiation is intercepted, absorbed, transformed, transported, reflected, and emitted throughout the globe. In even simpler terms, it is how energy moves through the matter of Earth. Earth itself has an energy source at its core, but the relative impact this has on the surface and atmosphere is negligible compared to that of solar radiation from the sun. **Basic heat and mass transfer through the atmosphere and oceans is responsible for climate and the oscillations or patterns that exist in the climate system.** Figure 1-5 is an updated quantification of these energy fluxes that drive our climate. Obviously, internal or external forcings that change these fluxes will change the climate as a whole. **It is critical to understand that a change in the energy flux not only has the potential to change the magnitude of energy in the system, but it also has the potential to change energy distribution mechanisms.** In the context of Earth, these mechanisms may include the wind patterns and ocean currents that facilitate principles such as diffusion, convection, etc. Hopefully it is obvious that even relatively small changes in these energy patterns can have far-reaching effects on the climate system as a whole—and the impacts of those changes on such a complex system are not obvious. This is the reason that climate models have been developed as tools for understanding the climate system. These tools are central to the science and are constantly improving with greater understanding of the physical sciences as well as observation

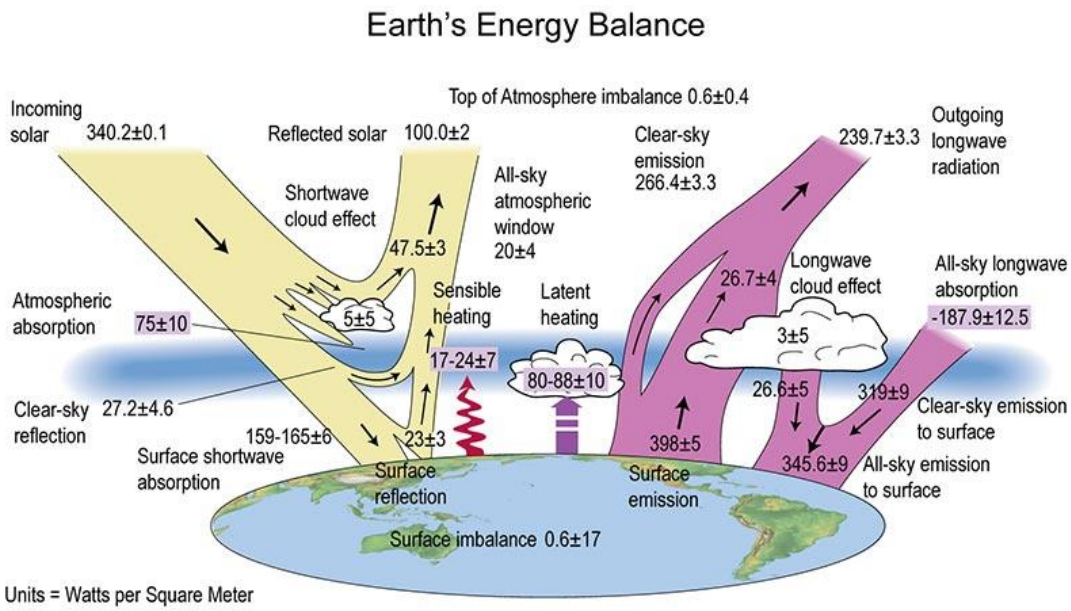

Figure 1-5 Updated Energy Balance of the Earth (Stephens et al. 2012)

strategies and technologies (e.g. weather stations, weather balloons, buoys, satellite-based remote sensing, etc.). The remainder of this section will attempt to present with a broad-stroke, a basic understanding of and some of the most recent advances in climatology, climate variability, and climate change.

1.4.1 Climate Modeling

As mentioned before, climate modeling is the backbone of modern climate science. It is not my role (the role of an agricultural engineer) to directly change these models. However, it is important to understand these models, how they were developed, how they work, their applications, their strengths and weaknesses, and how to evaluate them. Climate scientists produce and refine these models and engineers interpret the outputs for society in important areas such as hydrology, agriculture, infrastructure, etc. When these models are producing results comparable to observed data, they are performing relatively well. When they perform poorly, our work informs future modeling efforts, and the models get better after many iterations. Models are still making significant gains with each IPCC assessment, but the field is relatively young given a) the number of reporting cycles from which it has received feedback (entering the 6th cycle) and b) the level of model complexity. In general, the field has been limited not by understanding of different earth system components but rather their interactions with each other as a single continuous system. This understanding was once more restricted due to the computing limitations from the previous model generations. **As computing resources have evolved and become more widespread, the understanding of models (and the climate system) has grown proportionally.**

Despite the relative immaturity of the science to what it will be in the next decade, I believe that now is an appropriate time to begin integrating climate variability and climate projections into erosivity prediction. As the climate science (and related models) mature further, predictions will become more accurate. It is my opinion that the science is sufficiently matured and the observed data required to support these predictions is now available (partially resulting from an improved methodology to utilize these observations). As for accuracy, the first few cycles may have larger residuals than hoped for, but the prediction of erosivity for the year will be better with an accounting of climate variability than without it. The primary limitation is the limited observed data for analysis, but the length of observations is continuously growing (yielding more accurate EI calculations).

1.4.2 Climate Change

This is a sensitive topic at the time of this writing. Most of the scientific body is in agreement regarding the topic of climate change, but a minority of scientists and a large portion of the general population largely reject the claims of climate change. I would like to address some confusion that I think is partially responsible for the rejection of climate change findings. First, **climate change is a terminology that has been poorly understood.** Climate changes regularly, but these changes are not what has been called 'climate change' today. Rather climatology calls this 'climate variability' because over a long period of time there has been little to no net change in the climate. When there is significant change over a long period of time it is called 'climate change'. Within that term 'climate change' there is still room for confusion because not all change is the same. There are some documented 'natural changes' that do not have regular predictable fluctuations. The other change is called 'anthropogenic climate change', which is change resulting directly from human influence. Generally, people actually reject this small part of climate science's findings, but they will often grow skeptical of other findings too.

Second, **climate change reporting is not standardized.** Most of the science is actually in agreement with findings from the community, but the problem is that similar results are communicated differently. A common example may involve a GCM (operating at coarse spatial scales) may predict a slight increase in precipitation for a local region while an RCM (operating at finer scales) running on the same or another GCM may find a significant decrease in the same region. If you averaged the changes of that region with those neighboring regions, you would obtain the same results of the GCM or slightly different, but all that is considered in these studies are the outcomes and not the methodology. To complicate matters, there are multiple scenarios, time periods, models, techniques, etc. that make consistent reporting difficult. More recently, government bodies have begun producing consistent reports aimed at improving public understanding of climate change. The National Climate Assessment was a good example of this.

Third, **there is a general misunderstanding of how GHG emissions are responsible for so many changes in the general climate**, especially given what seems to be a steady increase in CO_2. The answer lies in the energy balance of the earth—something the general population is probably not willing to try and understand. Figure 1-5 shows the large

amounts of solar energy intercepted by Earth. Even a fractional change in the atmospheric composition will change the amount of energy stored in the atmosphere. Now combine this with the fact that Earth's orbit, spin, angle, wobble, etc. causes uneven heating of the atmosphere. There is essentially more energy retained in a revolving, spinning, wobbling system trying to reach equilibrium. I would expect the well-mixed aspects of climate (e.g. temperature) to experience marginal increases related to the increase in energy. Other variables that are not well-mixed will experience more varied and uncertain impacts. This uneven energy distribution is a major driver of climate variability. Scientists make these connections better than the general public, so their receptiveness was expected to be higher than that of the public.

Lastly, **climate change is not simple to observe, and it is even less simple to predict.** Figure 1-6 is an example of some observed changes in the climate. What is difficult to ascertain from this figure (and the data it represents) is how much can be attributed to variability. In this figure it appears that the Atlantic side of the country is experiencing far more change than the Pacific side, and it was true from the perspective that it was changing.

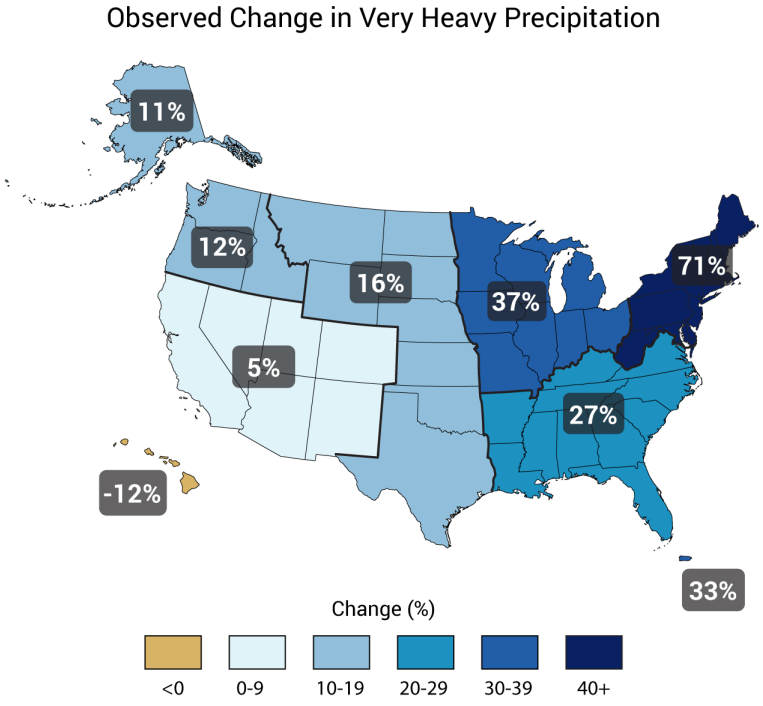

Figure 1-6 Observed Changes in Very Heavy Precipitation (Top 1% of Precipitation Events) by Region (Karl et al. 2009)

What must be evaluated now is how much of this change was resulting from climate variability—perhaps from the Atlantic Multi-decadal Oscillation (AMO). If a positive AMO causes an increase in observed heavy precipitation, then at least the negative phase should also be reported for a better picture of the trend. It is even better if the previous positive phase could be included to see if there has been any change under the same phase. As more phases are included, the trend becomes clearer, and the total change is more easily identified. Preferably, the discussion of climate variability should be placed after climate change but before this figure to better understand the coinciding effects in this figure. For an AMO background, please read Section 1.4.4 for more information.

It is understandable why there was confusion regarding this topic, even without considering political agendas, energy industry power brokering, lifestyle preferences, and other human factors. **The objectives for this study were formed in consideration of these issues.** For this reason, I proceed first by presenting only the highest quality analysis of observed EI in the Southeast. Only after having established reliable data and methods of erosivity calculation can I move on to analyzing climate change and variability. Once these are sufficiently understood, reliable projections can be presented for the future of erosivity. It is our goal to begin analyzing these projections using our current understanding, and to responsibly update these projections as our understanding matures. As mentioned earlier, this maturation comes as our observed data record increases so that there is a sufficient understanding of climate variability and its role in the observed change. This should ideally precede attempts to quantify climate change for a better understanding and confidence.

1.4.3 Climate Variability

Climate variability refers to the cyclical patterns of our climate that influence elements such as precipitation, temperature, humidity, etc. Generally, this refers to climate oscillations on larger time scales (greater than one year), but the terminology can be applied to any oscillation cycle. Examples of climate variability include ENSO, PMO, PDO, AMO, NMO, and more. These cycles have been effectively linked particularly to precipitation patterns although other patterns do exist. Figure 1-7 demonstrates how strongly variability can influence regional climate. The influence can range from a strongly positive force or a strongly negative (inhibiting) force. Generally, a few oscillations should be observed in order to determine the relationship.

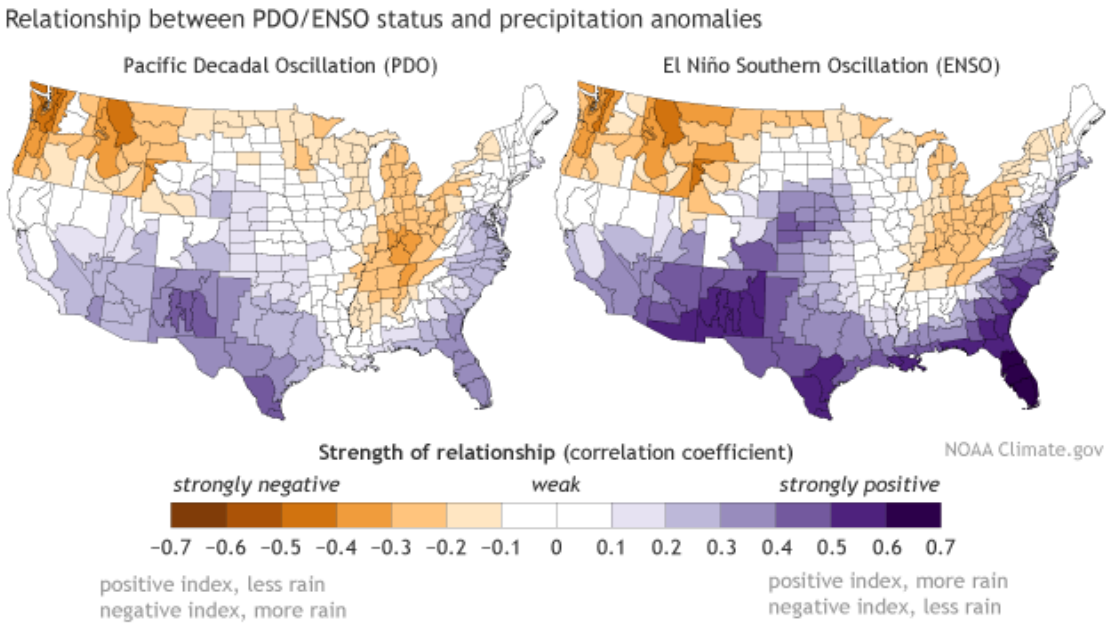

Figure 1-7 Correlation of Precipitation Anomalies, PDO, and ENSO During November-March from 1901-2014 (Credit: Matt Newman, NCEI)

From the figure above, it is clear that ENSO has a strong effect on the Southeast, whereas PDO is definitely less important than ENSO and arguably a weak influence on this region. A question then arises as to which variability cycles should be analyzed for their effect on the Southeast. The short answer is that all of these cycles affect the region, and therefore, eventually all of the cycles should be considered. However, this would take considerable amounts of time, which is ultimately why not all of these cycles are analyzed in smaller studies. Even in larger studies like the IPCC reports, some cycles tend to get far more attention than others. Since I cannot analyze all of these cycles I must ultimately 'guess' which will have the most impact (the highest impact will not truly be known until after the study). Fortunately, others have published analyses that help in these decisions. A perfect example of this was the Atlantic Multi-decadal Oscillation (AMO).

1.4.4 AMO Variability

This is a longer term climate cycle than PDO or ENSO, occurring only about every 25 years. Figure 1-8 summarizes the known effect of AMO on climate patterns in the Atlantic Ocean. Although AMO has been observed for over 120 years, there are probably no more than 2 complete observations of the AMO cycle at a spatial resolution significant enough to draw conclusions for large regions. A positive phase AMO causes more than double the

number of hurricanes to develop along with strong fluctuations in coastal rain for the Southeast (NOAA, AMOL). It is highly likely that AMO impacts erosivity in the Southeast, but there is currently not sufficient data (of the type used in this study) to perform a reliable analysis. Most of the 15-minute data used in this study occurs in the negative phase of AMO (about 25 years) with a smaller sample of the positive phase (about 15 years). More recent data of these stations are available (about 6 years of positive phase data), but it still may not be enough for a robust analysis, which would require more like 30 to 50 years of each phase. Supplemental data of another source may be required to determine the effects of AMO on the Southeast.

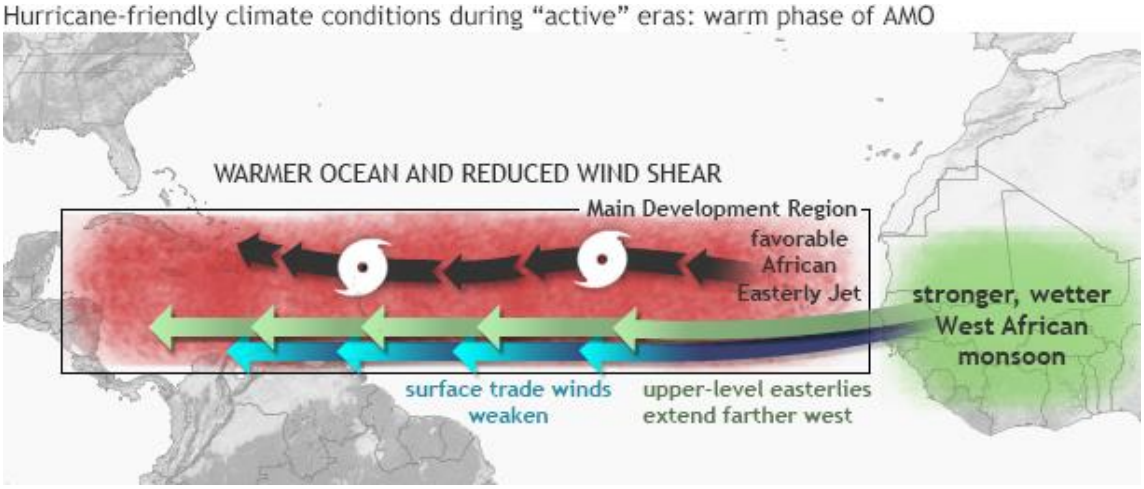

Figure 1-8 Climate Patterns Associated with the Warm Phase of the Atlantic Multi-decadal Oscillation (Credit: Gerry Bell, NOAA)

The most interesting aspect of AMO for this study is how it favors the development of large, high-intensity storms. **Large storms encompass the majority of erosivity, and if enough hurricanes are developed in a positive AMO phase, the EI calculations could be primarily driven by this one climate cycle.** It has also been observed that AMO tends to determine the pathway of hurricanes. Positive AMO favors the gulf, and negative AMO favors the Atlantic Coast. Therefore, both the magnitude and spatial distribution of EI can be significantly influenced by this particular oscillation. **The fact that AMO can affect the development of storms and their landfall locations means that it could be at least partially responsible for fluctuations in calculated erosivity values for the Southeast.** Depending on the strength of the AMO phase, the compounding effect of other climate cycles, and the data observation period, the calculated EI could be significantly different.

It is very likely that AMO (and other climate cycles) have played some role in differences in isoerodent maps published in the Ag. Handbooks and modern observations. There are methodological differences driving some variation in these maps but certainly not all of those differences. This is exactly the reason for this study, and although AMO would be a likely candidate for variation in the Southeast, I will focus my efforts on ENSO instead.

1.4.5 ENSO Variability

The El Niño Southern Oscillation is pictured in Figure 1-9. Along with the other climate oscillations, it is based on warming and cooling trends in specific parts of the various oceans. These variations in temperature cause changes in atmospheric winds, which can influence where precipitation tends to fall, how much, and how quickly.

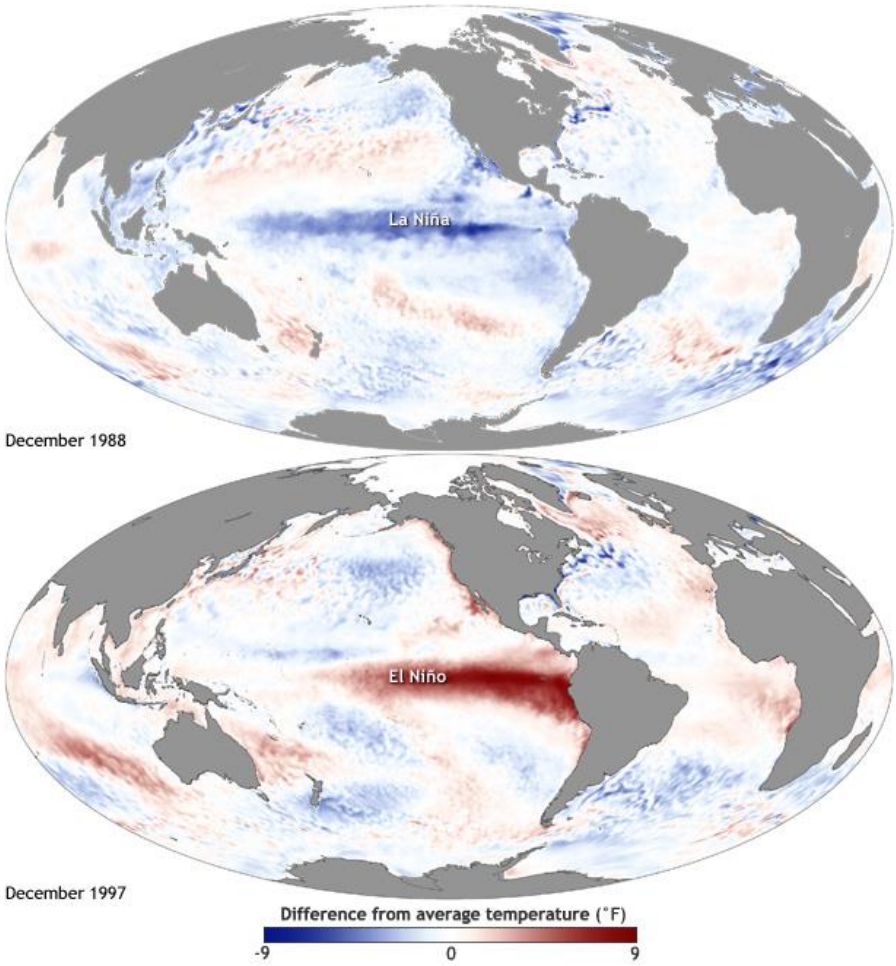

Figure 1-9 Maps of Sea Surface Temperature (SST) Anomaly in the Pacific Ocean During a Strong La Niña and El Niño (Credit: NOAA)

ENSO has been shown to have significant influence in parts of the Southeast regarding precipitation. Figure 1-10 portrays the differences in the two phases of ENSO as it pertains to precipitation (dominated by wind currents). Unlike most of the other climate cycles, ENSO occurs in shorter cycles (usually one or two years). Although it tends to oscillate from positive to negative and vice versa, ENSO can return to either a positive or negative phase regardless of the preceding phase. **The prediction technology for ENSO is more developed (partially due to more frequent cycling), which makes it possible to predict ENSO impacts for the near-term future erosivity.** Prediction capability along with short cycle duration (for multiple cycles to be analyzed) make ENSO an ideal choice for our variability analysis.

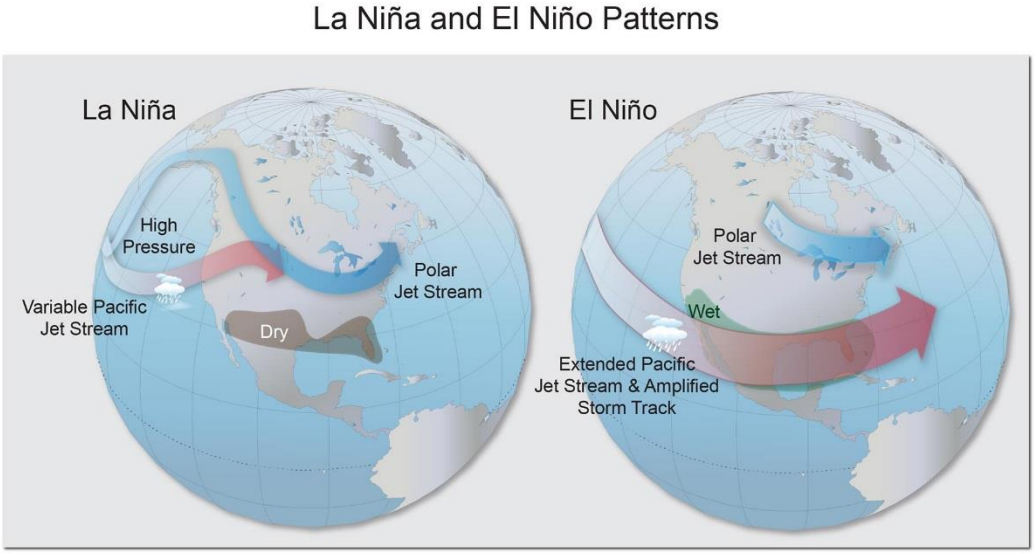

Figure 1-10 January-March Conditions for La Niña and El Niño (Credit: NOAA)

Chapter 2: Benchmarking Reliable Erosion Indices for Climate Studies in the Southeastern United States from Quarter-Hour Station Data

2.1 Abstract

Precipitation is one of many aspects of our changing climate that is under intense investigation by the scientific community. Although climate scientists generally predict that the amount of precipitation has and will continue to increase for the United States, the characteristics of that changing precipitation are not well understood. Some have reported significant observed and projected changes in precipitation characteristics, but existing studies have not adequately addressed this issue. One precipitation characteristic particularly vulnerable to climate change is the erosivity of rainfall. Unfortunately, there are published discrepancies in observed erosivity. Hence, the goal of this study is to update the erosion index (EI), specifically those in the southeastern US for two reasons. First, it is a region highly likely to be influenced by climate change and climate variability, and second, it is the setting of published discrepancies mentioned earlier. Observed quarter-hour precipitation data from 616 NOAA NCDC land-based stations (DSI-3260) for eleven states in the Southeast were used to calculate erosion index (EI) values for each station. The data was screened before calculation, resulting in 172 gauge locations to represent the 11 states in this study. A water balance was performed to validate the observed dataset and to select the best of 7 station screening methods. Annual and single storm EI statistics were calculated for stations passing the preferred screening method. EI values for the Southeast were found to be significantly larger than AH537 (1978) and AH703 (1997) confirming the findings of McGregor et al. (1995) while significantly increasing the spatial resolution of EI observations in the Southeast. The regional increase on average was 18.6% over the previous EI values (AH703) with a range of -19.5% to +57.5%. The unadjusted EI was based on 15-minute station data, which usually underestimates I_{30}. An adjusted EI was provided which accounts for this phenomenon and missing and deleted data for each station. The adjusted data, which represents the highest possible EI estimation from this methodology, reported an average increase of 39.0% with a range of -1.5% to +86.1%. These values were reasonable given the sensitivity of low erosivity regions in Kentucky and Virginia to relatively small changes in EI. There was no significant change in the 10-year storm EI with a regional average decrease of 2.3% for unadjusted data. **This study prepares the way for impact studies of climate variability and climate change related to erosivity for conservation efforts in the Southeast.**

2.2 Introduction

Precipitation is one of many aspects of our changing climate that is under investigation by the scientific community. Studies published in climate related reports like the National Climate Assessment (NCA) show trends of increasing precipitation amounts, increasing frequency of heavy precipitation events, and an increasing appearance of consecutive dry days (Melillo et al., 2014). It is apparent from these reports that the quantity of rainfall is indeed changing as well as the seasonal distribution of that rainfall. What is not well-understood, or is at least not well-published, are the characteristics of the precipitation, whether they are changing, and by how much. Yet, **it is the characteristics of rainfall that determine the utility of that rainfall and its interaction with the land surface.**

The Intergovernmental Panel on Climate Change (IPCC) published a rough magnitude change for total precipitation of about 1% to 2% K^{-1}, but the moisture-holding capacity of the atmosphere changes at a rate closer to 7% K^{-1} (Trenberth et al., 2003). These rates of change have become more certain as supercomputers have enabled higher resolution modeling. The increased absolute amount of precipitation coupled with the increased moisture-holding capacity make it possible for higher intensity precipitation events. Trenberth mentions other factors that must be considered in order for larger intensities to become a reality, but it is possible nonetheless. Beyond this, the article also argues that changes in localized intensities can even exceed changes in moisture-holding capacity due to latent heat feedbacks further stimulating storm energy. **The potential for significant change in rainfall characteristics combined with observed and projected changes in related precipitation variables suggests the need for studies in this area.**

The motivation for this study was that precipitation characteristics can eclipse the importance of mere quantities of rainfall for a host of applications. Soil conservation efforts and infrastructure development practices in particular stand to gain the most insight from studies of precipitation characteristics. Some work has already been done to quantify potential changes. Mirhosseini and Srivastava (2012) reported double-digit intensity decreases in projected intensity-duration-frequency (IDF) curves for shorter duration storms (less than 2 hours) and mixed results for longer durations. Nearing et al., (2004) reported projected magnitude changes in erosivity ranging from 17% to 58% across the continental United States over different time periods and model combinations. Despite total

precipitation only increasing 1% to 2% K^{-1} (Trenberth et al., 2003), the storm characteristics of precipitation are changing at a much higher rate. These changes are significant, especially since some regions will experience even larger magnitude changes than the specific publications mentioned, which only report spatial averages. These studies contribute to our understanding of projected changing precipitation characteristics, but **there is an increasing need for an observed high-resolution, large-scale study of erosive rainfall in sensitive regions.** Meeting this need has become the intended purpose for this erosivity study of the southeastern United States.

There have been three major publications to date using the 'standard approach' for EI calculation—not including the RUSLE2 study, which does not provide EI values but rather moved to a new approach using erosivity density. These three studies were Agriculture Handbooks published by USDA-ARS known as AH282 (Wischmeier and Smith, 1965), AH537 (Wischmeier and Smith, 1978), and AH703 (Renard et al., 1997). In AH282 (1965), the first isoerodent maps of the eastern US were developed based on the statistical relationship of energy and intensity to soil loss for 22 years of observed precipitation data (1936-1957). These maps showed the average annual erosion index (erosivity) based on a mixture of data from 2000 locations distributed across the 37 states analyzed. Actual EI values were calculated at 181 locations across 37 eastern states from stations similar to the DSI-3260 'quarter-hour' stations used in our study. An equation relating the 2-year precipitation depths of varying durations to average annual erosivity values was developed for the 181 stations used for EI calculations. These equations were used to estimate EI at about 2,000 locations, and these results form the basis of erosivity values presented in each of the Agricultural Handbooks (USDA, 2008). Thirteen years later, AH537 updated these values in the eastern US to include energy and intensity limits that better reflect the actual EI values across the region. In 1980—two years later—McGregor et al. (1995) used superior data which claimed EI values from AH537 (Figure 2-1) should be 30% higher than the published values. The same was observed in 1995 for erosivity values utilized by RUSLE. In 1997, AH703 was published with updates to previous isoerodent maps (Figure 2-2), which used new methods for calculating maximum intensity limitations and modern contouring methods. Even with these changes, EI values in northern Mississippi were largely unaffected by AH703 updates, and therefore, the values at that location were still

too low. Some of the differences in the Ag. Handbooks and McGregor's observations result from methodological differences (primarily the omission of small, low-intensity storms), some from McGregor's superior data (29 breakpoint stations), and some undoubtedly from climate variability and change. **Erosivity values with this much error—and uncertainty in the sources of error—call into question the reliability of those values and prevent their use in climate studies, which suggests the need for a benchmark erosivity calculation.** In 2008, these persistent issues led to an abandonment of the 'standard approach' to erosivity calculation in RUSLE2, and it used an erosivity density function and precipitation data to derive erosivity values. RUSLE2 moved to the erosivity density approach as a result of the perceived inconsistency of EI values from Ag. Handbooks and the strength of that approach with short observation periods (USDA, 2008).

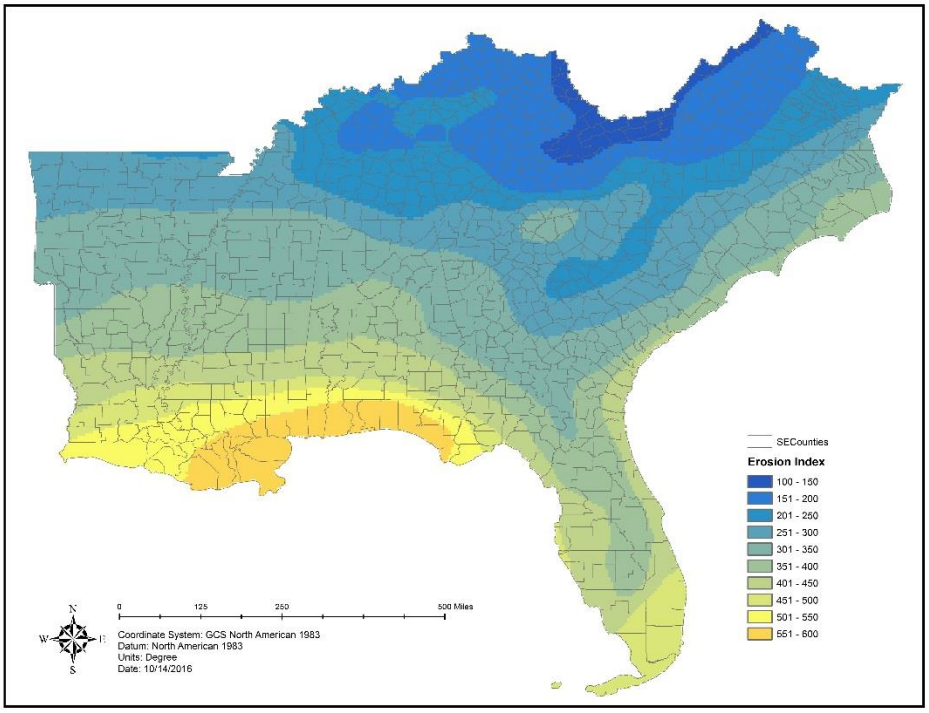

Figure 2-1 Erosivity for the Southeast US as from AH537

In order to establish a benchmark for future climate studies, I use an updated methodology of AH537 that only uses direct station calculations of EI and includes all storms in the analysis regardless of size or intensity. All other methodologies, including the energy equation, were identical. EI values will also be reported with I_{30} limited and unlimited (described later). Limited EI values reflect a general observation that the

potential erosive power of storms cannot be realized due to negative feedbacks from high intensity storms. More specifically, highly erosive storms, which have high intensities will not infiltrate or runoff quickly enough to allow the incoming rainfall to impact the soil. Therefore, the energy of rainfall can be absorbed by ponded water after sufficient time is allowed for initial abstractions to take place. The limited EI values will provide better insight as to more realistic impacts on climate-driven soil loss, while the unlimited EI values allow a deeper understanding of changes in storms themselves and the potential erosive power of such storms. I made the decision to use the AH537 energy equation despite the fact that AH703 and McGregor recommend using the Brown Foster (BF) or McGregor-Mutchler (MM) energy equation so comparisons may be made with AH537 and AH703. Pending the results from this study, I would expand this analysis to include the these energy equations and all parts of the continental United States.

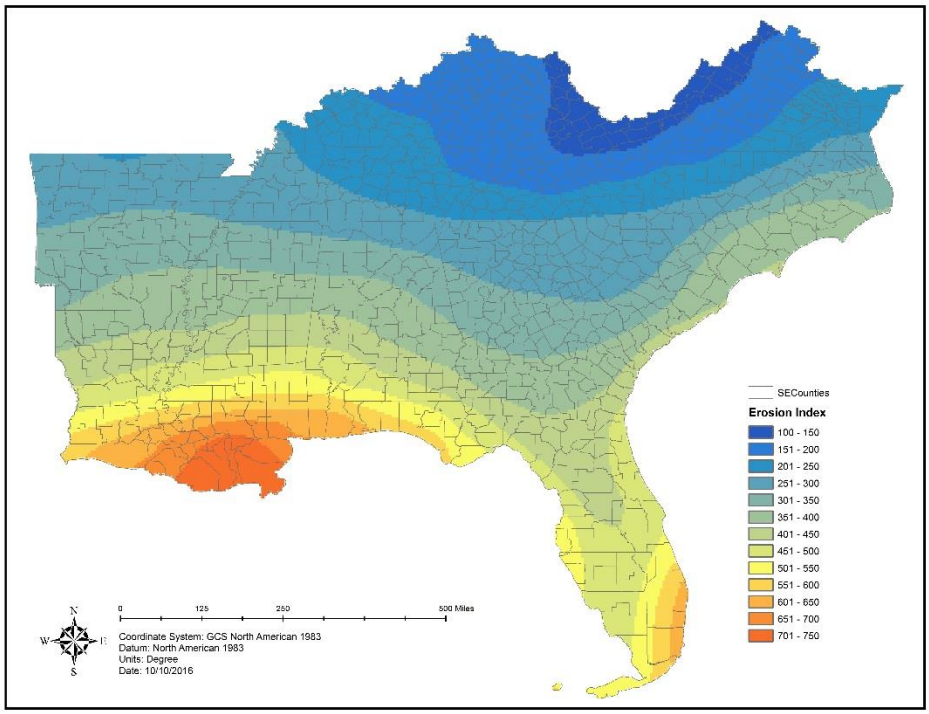

Figure 2-2 Erosivity for the Southeast US as from AH703

2.2.1 Erosion Index and Erosivity

The erosion index is a function of two precipitation components: storm kinetic energy (E) and maximum 30-minute intensity of the storm (I_{30}). The product of these values is the erosion index of a storm, which can be summed to obtain the erosion index for a given

location and time period. The most commonly reported value is the annual EI value, but it is also of interest to report the distribution of EI values for probable storm occurrences at a given location. EI values are summed annually and averaged over a long period of time—20 years or more—to find the average annual erosivity factor (R), which is in turn used with other soil parameters to find soil loss. The USLE family of empirical soil loss equations rely almost entirely on the R-factor to represent climate impacts on soil loss.

The EI value should not be considered merely a soil loss measure, as it is primarily a calculation of direct measurements of climate. Moreover, it is a measure of all storms at a specific location, their depths, kinetic energies, maximum intensities, and durations are all present when calculating this measure. This is both the advantage and disadvantage of using EI. On a positive note, there is more than one way to observe and communicate precipitation change due to its 'data intensive' nature. The disadvantage is that it is difficult to obtain a significant quantity of long-term, spatially distributed data while still preserving its quality. This disadvantage is the specific reason that the standard approach was abandoned for ongoing erosion prediction efforts through RUSLE2. I think that the new erosivity density approach offers an unexpected and exciting gain for erosion prediction technology, especially in western states where 15-minute station record length is perhaps insufficient for accurate EI calculation. **However, the standard approach may serve as a less obscure measure for climate variability and climate change analysis.**

2.2.2 Study Area Selection

When selecting an appropriate study area, it is most important to consider the area of greatest potential impact. That area for rainfall characteristics is found in the southeastern United States. Figure 2-3 shows the areas of highest erosivity across the continental United States, with annual R values ranging from 2,000 to greater than 10,000 MJ-mm ha^{-1} h^{-1} y^{-1} or the English equivalent of 125 to more than 600 hundreds of foot-tonf-inch ac^{-1} h^{-1} y^{-1}. Note that **the Southeast experiences far more erosivity than other areas of the country.** These are averaged annual values and single year values and even some single storm values (if no intensity limits are imposed) can exceed this range. In addition, one of the factors leading to potentially higher intensities in lower latitudes results from disproportionate rates of moisture convergence near the tropics, which means that **the Southeast could be more susceptible to impacts of climate change than other regions**. **These two facts**

alone make for an exceptionally high risk for impact along the coastal Gulf of Mexico and its surrounding areas. Texas also experiences high erosivity, but it was not included in the study primarily in order to be consistent with the regional groupings according to the NCA. Other reasons include changes in the calculation of EI values as the study approaches the western United States (changes in intensity limits), increasing complexity communicating the differences and their respective uncertainties, and the computational demand of a larger study area.

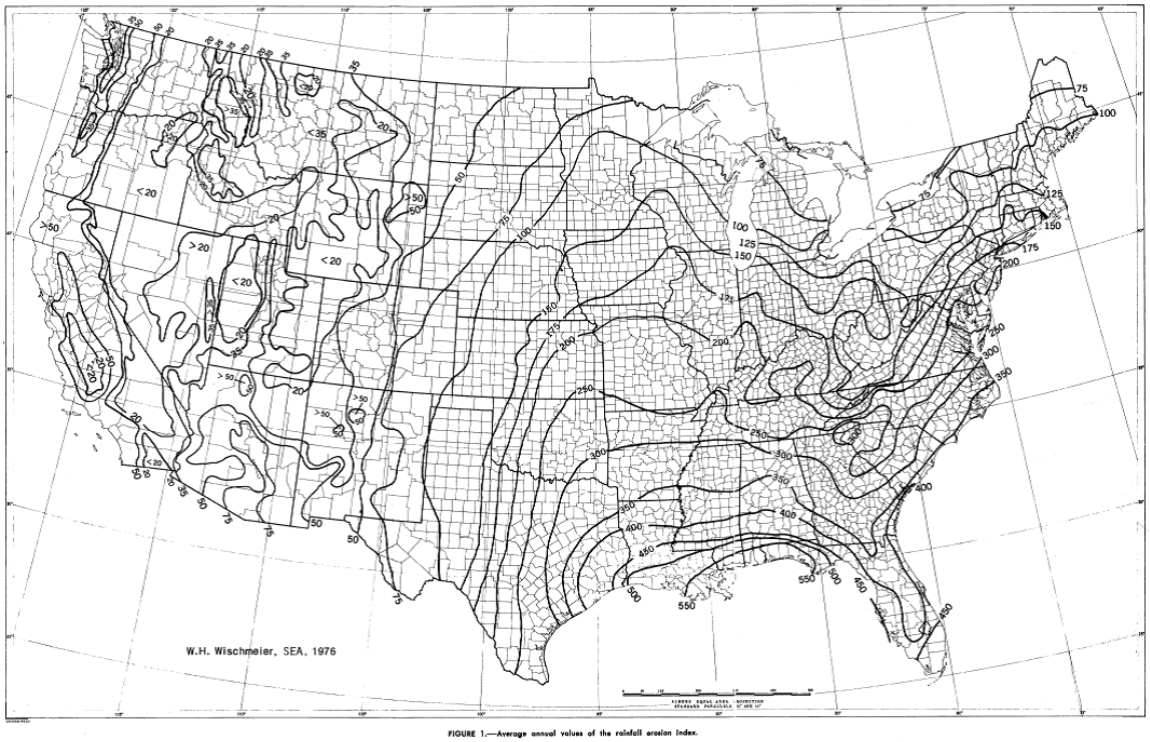

Figure 2-3 Erosivity for the Continental US (AH537). Note the Much Higher Erosivity in the Southeast (125-600) than the Northeast (50-125) and the West (10-100).

2.3 Methodology

Observed quarter-hour precipitation data from more than 600 NOAA NCDC land-based stations (DSI-3260) were obtained for eleven states in the southeastern region including Alabama, Arkansas, Georgia, Florida, Kentucky, Louisiana, Mississippi, North Carolina, South Carolina, Tennessee, and Virginia. These data included 15-minute rainfall observations for every day that there was measureable precipitation at a given station. Measureable precipitation was defined as 0.1 inches of rain for HT stations and 0.01 inches of rain for HI stations (HT and HI indicate the smallest unit of rainfall recorded by the station). Data prior to 1996 was exclusively QPCP stations and more recent data was a mixture of QPCP and QGAG stations (QPCP and QGAG indicate measurement method for each type of station). QPCP is a direct volume measurement of precipitation while QGAG is a volume calculation based on weight. QGAG reports the gauge value and the daily total. QPCP reports the incremental value and daily total. Only QPCP data was used in this study due to the greater complexity and computational demand of processing the QGAG data in tandem with QPCP data although it would be beneficial to do this as it would provide validation for the accuracy of the QPCP data. There were two notable transitions for the data that occurred in the years 1984 and 1996. These years mark the beginning of automated recording stations and a new automated data handling procedure, respectively (resulting in less manual handling of the data).

In addition to quantitative data, there were quality flags recorded with each data. NOAA maintains the necessary documentation for these flags. The data used in this study contained few to no cases of evaporation, frozen-precipitation, and extreme value failures. The flags that commonly appeared for the data signified single value errors and an occasional flag indicating that the record time was ‘suspect’. The somewhat frequent accumulation periods (described below) were noted by flags. Finally, there was also a significant portion of the data that was flagged either ‘missing’ or ‘deleted’ for most stations. The procedure for handling the data and its flags is discussed below.

2.3.1 Accumulations

Should there be only a small amount of precipitation (less than the smallest unit of measurement for the type of station—HT or HI), the depth was either a) retained in the gauge and reported when the next appreciable precipitation occurred or b) began an

accumulation. The difference between these two was that the accumulation noted when the first event began accumulating. The sole factor in determining whether the event was recorded as ‘a’ or ‘b’ was in knowing the beginning of the event. Our observation was that ‘a’ does not occur frequently and/or has minimal impact on the data (in regard to both depth and intensity). It should also be noted that this was not the only case in which an accumulation will be recorded. An accumulation by definition occurs anytime the exact beginning, ending, and depth were known, and there was no distribution data available. Therefore, accumulations can represent somewhat significant portions of precipitation amounts, which if ignored, can proportionately affect the resulting precipitation study. However, these tend to be low intensity events, and they may not account for a significant portion of EI. In an effort to quantify the effect of accumulations on the study, the analysis was completed with and without accumulations.

2.3.2 Storm Events

The definition of a storm was similar to AH537, which defined a break between storms as a period of 6 hours or longer with less than 0.05 inches of precipitation (Wischmeier and Smith, 1978). However, this study does not omit storm events less than 0.05 inches as AH537 does with storms that have a maximum intensity less than 0.95 inches per hour. This practice was from an age before the widespread adoption of computers, and as such was not a necessary practice. McGregor (et al., 1995) showed that omitting storms less than 0.05 inches (~13 mm) affected erosivity values up to 3.5%, and even when considering the intensity threshold of 0.95 inches per hour that number shrank by less than one percentage point. This study follows McGregor’s recommendations to include all storm events since that is more representative of the actual erosivity, and uses the same threshold for storm separation as AH537 for comparison.

Although the NOAA NCDC data is of a relatively high temporal resolution compared to other datasets, a majority of the data has a maximum depth resolution of 0.1 inches. This can have a small but noticeable impact on the kinetic energy of a storm for small storms, but not enough to significantly impact erosivity. Most storms were small storms, but erosivity was primarily a result of few large storms and a number of moderate storms—with small storms contributing the least. It was also noteworthy that the threshold of 0.05 inches used for storm separation was less than the smallest unit of measure for most of the

NCDC data (0.1 inches). However, McGregor et al. (1995) offers that small changes in this threshold value do not significantly change the resulting EI calculations. This too was negligible as it will only impact storms that have had between 0.05 and 0.1 inches of rain in 6 hours. These storms would still be included in calculations but will be accounted as a separate storm system. Newer data—mostly occurring after 1994—was of a much higher resolution of 0.01 inches. Many of the stations in this study have the higher resolution data, and I have found no significant difference in our calculations. The resulting storms and associated energy, I_{30}, and EI values were screened for improved representation of actual precipitation and erosivity at each station.

All accumulations were separated from other events without prejudice. They were separated because there was no definitive way of knowing whether an accumulation was a single event or a collection of events. Single storm events (accumulations 24 hours or less in duration) that were characterized by larger depths and shorter durations were fit to a storm distribution according to location and duration. Given that the study area was mostly represented by the SCS Type-II curve and that Type-II and Type-III SCS distributions were almost identical, all accumulations 24 hours or less were fit to the SCS Type-II curve and used to calculate EI values for those events. The use of SCS distributions could be argued since they are static distributions used to represent a changing precipitation regime. However, the knowledge gained from approximating EI of these otherwise unaccounted storm events outweighs the uncertainty inherited from a fitted distribution, especially since results were reported with and without accumulations. When the accumulation was longer than 24 hours, the depth was multiplied by a monthly EI rate (EI $inch^{-1}$) for each station.

2.3.3 Station Screening

On the whole, the DSI-3260 data suffers significantly from ‘gaps’ in the record. Gaps can be categorized as either a missing period or a deleted period. A number of possibilities could lead to the creation of one of these periods including regular maintenance, an unplanned interruption of service, correction of known errors, etc. These ‘gaps’ can be relatively extensive, occurring in multiple years, many times in a year, and sometimes for months at a time. This begs the question regarding the quality of the dataset as a whole. Although it was true that the issue was widespread among the dataset, there were still many stations that record sufficient quantities of good quality data. In order to obtain stations

meeting minimum quality and quantities a station screening method was implemented, which consisted of both a quantitative and a qualitative component.

The qualitative screening served primarily as a check for improbable or impossible precipitation values in the record whereas the quantitative screening limits 'gaps' in the data. NCDC does not provide edited or corrected data prior to 1996, and data prior to 1984 was processed using only a 'gross value check'. After the qualitative screening was complete, the handful of erroneous values were removed. The impact that this had on the data was insignificant by all measures, and the qualitative screening has been removed for concise documentation of our methods. The quantitative screening consisted of two screening parameters that limit temporal gaps in the data and the brevity of the station record. The first parameter required a minimum number of months to be 'present' in order for a station-year to pass screening. A month must have at least one measured event to count as present. The second parameter requires a minimum number of years to be present for the station to pass screening. Different combinations of the screening parameters were run concurrently with a water balance analysis in order to determine the best screening method. Screened values still have holes in the data, but there were much fewer compared to unscreened data.

2.3.4 Water Balance

In order to validate the screening method and the NCDC data, a water balance was conducted for every station. The water balance was used to test different screening methods that would result in a more accurate calculation of EI values. Stations in the original dataset and 7 screening methods were compared with climate normals for the same time period and locations. Monthly precipitation normals (CLIM81) published through NOAA NCDC for the period 1971 – 2000 were compared to observed monthly precipitation (DSI-3260) data means for the period 1970 – 2010. Months that were missing from the observed data (either from screening or a gap in the data) were filled with the climate normal value for that month. Monthly averages were summed for observed precipitation and climate normals to obtain annual amounts. Both annual and monthly performance was evaluated for the screening methods, but only the annual was reported here.

The water balance was computed for stations with and without accumulation depths. The depth for each time period and station (without accumulations) was expected to be up

to 15% lower than the corresponding climate normal. This difference resulted from the cumulative effect of accumulation events, missing periods, and deleted periods in the record. Missing and deleted percentages were calculated for each station by summing the total duration of missing and deleted periods and dividing by the total time of operation of the station respectively. Some of these differences were reduced by including accumulation events, which was reported for comparison.

2.3.5 EI Calculation

A modified procedure based on AH537 was used for EI calculation. Maximum intensity values in energy computation were limited to 3.0 inches per hour and the maximum 30-minute intensity was limited to 2.5 inches per hour. These limits reflect that the raindrop size, and therefore energy, does not continue to increase above intensities of 2.5 to 3.0 inches per hour and that ponding in the Southeast absorbs some energy for the occasionally high I_{30} intensity, respectively. The method further diverges from AH537 in the aspect that small storms (defined earlier) were not removed from annual EI values. The EI values were calculated with and without maximum intensity limitations for the region as a whole. In the past, this was practiced only in the gulf region of the Southeast, but both are included since more of the Southeast was impacted significantly by this limit. Years that passed screening with missing months were filled with the average EI value for that month if there were also no accumulations in that month. These filled gaps account for a percentage of the data according to the number of missing months allowed. The preferred method was the 11-month screening, so theoretically around 8.3% of the data could be filled. At the completion of our analysis, I found this to be 2.25% and 2.26% of the erosivity data for I_{30} unlimited and limited, respectively. Filled data was insignificant relative to calculated data, but should be included in the analysis. Accumulations and their associated EI values were merged with the data before filling such that after being filled the EI calculation was complete. The calculation of EI values for accumulations was processed separately from measured data. Accumulations less than or equal to 24 hours in duration were fitted to an SCS-Type II curve to determine intensity for each 15-minute period and used to calculate EI for that storm. Longer accumulations used the product of a monthly EI Rate (EI divided by monthly depth) averaged over the observation period and the depth of the accumulation to determine EI. EI values for accumulation events were not included in the single event

analysis; thus, only measured events were used in the storm EI frequency analysis. The return period of the storm EI was determined by performing a log-transformed cumulative frequency analysis of ranked annual maximum storm EI given by the general form: $P_c = M/(N+1)$. The 1, 2, 5, 10, and 20-year return period storm EI values were determined by linear interpolation of resulting probabilities of exceedance. The calculation method for individual storms (n = 1) or a period of n storms (same method) was included below:

$$for \begin{cases} i & \leq & 3.0\ inches\ h^{-1} \\ I_{30} & \leq & 2.5\ inches\ h^{-1} \end{cases}$$

$$e_{t,t+1} = 916 + 331\ log_{10}\ i_{t,t+1}$$

$$E_s = \frac{\sum_{t=1}^{m} e_{0,t} d_{0,t} + e_{t,t+1} d_{t,t+1} + \cdots + e_{m-1,m} d_{m-1,m}}{100}$$

$$EI = \sum_{s_1}^{n} \left(E_{s_1} \cdot I_{30 s_1}\right) + \left(E_{s_2} \cdot I_{30 s_2}\right) + \cdots + \left(E_{s_n} \cdot I_{30 s_n}\right)$$

Where:
e was kinetic energy of a period of rain in foot-tonf ac^{-1} inch^{-1}
i was average rainfall intensity of a period of rain in inches h^{-1}
t was a single time interval (15-minute intervals for this study)
d was the depth of precipitation for a period in inches
s was a single storm, previously defined
m was the number time periods within a storm
n was the number of storms within a given time period
E was the storm kinetic energy in hundreds of foot-tonf ac^{-1}
I_{30} was the maximum 30-minute storm intensity in inches h^{-1}
EI was the erosion index of a period of time or of n events in hundreds of foot-tonf-inch ac^{-1} hour^{-1}

Although the methods for EI calculation were almost totally identical in every aspect, the data used in the calculation was not. In its purest form, EI should be calculated using storm intervals of equal intensities (breakpoint data). This was the reason for using 15-minute data, which was the highest resolution observed precipitation data available at a significant spatial and temporal scale. This means that the true EI could actually be higher than the values reported in this study, and it would be at least 3-4% higher on average as reported by Hollinger et al. (2002) since I_{30} values calculated from 15-minute data are slightly lower than those from breakpoint data. EI values were reported showing the effect of I30 limitation, I30 adjustment (to mimic breakpoint observations), and filled data (explained in detail later).

2.3.6 Data Justification

Others that have calculated EI and related EI products from non-breakpoint data have used hourly, daily, and monthly precipitation data (Istok et al., 1986; Richardson et al., 1983; Nuno de Santos Loureiro, 2001; Angulo-Martínez, 2009). These studies were valuable where long term densified measurement of precipitation data were unavailable, but there was a common limitation to each method. None of these methods can capture the effect of intensity on the storm kinetic energy or the 30-minute maximum intensity, which were both needed to accurately determine EI. Furthermore, it was the intensity characteristic of precipitation which was expected to have changed and to continue to change with changing climate. This makes a strong case for the need of fixed-intensity data as opposed to fixed-interval data. However, if fixed-intensity data are unavailable, high-resolution, fixed-interval data can sufficiently capture intensity variation within storm events. It was for this reason I selected the DSI-3260 data for the study.

2.4 Results

EI values were calculated for every storm in the processed NOAA NCDC data (about 1.1 million storms in total). Unadjusted data was screened, filled, and limited (or unlimited)—see Section 2.3.5 for more information. These EI values were summed over different time periods to derive annual EI (also called erosivity or R-factor). In an effort to quantify some uncertainty in the data, adjusted EI calculations were provided. First, EI calculations were increased by 4.0% to account for quarter-hour stations not being able to capture the true I_{30}. Additionally, the EI calculations may or may not need to be increased by missing and deleted percentages. EI calculations and annual estimations were compared for a station in northern Mississippi to McGregor's 29 breakpoint stations. A comparison of two means is provided for both the years in common for these two studies and each data as a whole. The results of this comparison validate our methodology and dataset for EI calculation in the Southeast and hopefully for an imminent update of EI values in the continental US. Finally, a frequency analysis of single storm EI was performed for 1, 2, 5, 10, and 20-year return periods. This analysis was completed for unlimited and limited I_{30} values. Station data was processed into gridded data by using the geostatistical interpolation method—empirical Bayesian kriging. This method accounts for error in the kriging semivariogram by resampling the data. These grid values were used for gridded comparisons to digitized data from AH537 and AH703. Only the comparison to McGregor's data uses direct station data.

2.4.1 Water Balance and Screening

The mean, median, and standard deviation of percent differences at each station are shown both with and without accumulations (+/-) in Table 2-1. The 'Screening Method ID' is in the format YY.MM indicating the required number of years and months per year for each screening method. In general, the trade-off is primarily between spatial resolution (the number of stations passing screening) and temporal coverage of each station (the extent of 'gaps' in its record) which impacts percent difference statistics. The 'number of stations' is a count of stations passing the various screening method. Matching stations used to compute the difference could be less than this number (usually about two-thirds of the stations passing screening had matching climate data for the analysis).

Table 2-1 Percent Differences in Total Precipitation for All Screened Stations in the Southeast by Screening Method, with and without Accumulations (+/-), by Statistical Measure

Relative Difference in Avg. Annual Precip. and Normal Annual Precip.							
SCREENING METHOD ID	MEAN %		MEDIAN %		STANDARD DEV. %		NUMBER OF STATIONS
	-	+	-	+	-	+	
20.10	-8.03	-6.15	-8.19	-6.09	3.96	4.15	280
20.11	-7.21	-5.43	-7.59	-5.86	4.11	4.15	172
25.10	-7.55	-5.56	-7.96	-5.44	3.46	3.54	167
25.11	-6.78	-5.11	-6.25	-4.84	3.48	3.49	78
30.10	-6.62	-4.81	-6.57	-4.67	3.06	3.07	68
20.12	-5.64	-4.60	-5.63	-3.81	3.65	3.80	31
30.11	-6.50	-4.93	-6.74	-4.70	2.91	3.00	22

Note: Negative or positive results for mean and median measures indicate a deficit or surplus respectively.

Requiring longer periods of observations—25 to 30 years as opposed to the 20 year minimum—resulted in better performance. However, most screenings with 25 or 30 year requirements resulted in spatial distributions and resolutions that were not conducive for accurate EI analysis. This was mostly due to station distribution along the eastern coast where there were not enough years on record that meet other screening requirements. More months per year (11 or 12) always yielded better results and reduced uncertainty compared to 10-month results—since stations with more months of data in a year inherently have less missing and deleted data. For these reasons, the 20.11 screening was chosen over the 25.10 and 20.10 screenings. The 20.10 and 20.11 screenings were evaluated visually in order to spot any potential differences in the data resolution (280 stations vs. 172 stations). No significant trends could be noticed, although the 20.11 screening outperforms the 20.10 screening as expected. A potential benefit of the longer period screening, 25.10, was that it could present a better opportunity to analyze EI variability, which varies quite significantly from year to year. This will primarily benefit any climate variability study that uses this dataset and methodology, but it may provide a better annual and monthly EI.

Although the mean and median percent difference for every screening method was negative, there were a number of stations reporting higher than expected rainfall, but these were in the minority. This could be a result of stations having 2% - 16% missing data and 4% - 10% deleted periods. The states of Kentucky, North Carolina, South Carolina and Virginia tend to have slightly more ‘missing periods’ and noticeably more ‘deleted

periods'. NOAA does not provide a reason for this occurrence. There were two stations in southern Louisiana that report significantly higher 'missing periods' than surrounding areas. This could be from hurricane related damage, which would have caused the stations to be down for some time. During the study it was observed that some of these missing and deleted percentages may be too high since our method for calculating this used the beginning and ending dates of recording for each station and did not reduce the values for years that were screened out. For example, the stations in Louisiana were probably downed due to hurricane damage, but once they were repaired, observations continued. Our screening method removed the calendar years that were missing measured data, but the missing period still included the time that the station was downed. This was probably also true for deleted data. An updated methodology should remove these values for a better prediction of adjusted EI values that will yield reduced uncertainty for each screening method. Higher missing or deleted percentages do not necessarily correlate with missing rainfall (as shown by water accounting later for that area) because missing or deleted periods can occur in the dry season. Across all stations for the 20.11 screening, the arithmetic mean of missing and deleted percentages were 5.77% and 7.08%, respectively. Figures 2-4 and 2-5 show the spatial distribution of missing and deleted percentages for this screening method.

In summary, the water balance revealed that on an annual basis the observed rainfall falls slightly short of expected values—about 5.9% for the preferred screening method (20.11). Missing and deleted periods (as percent of each station's total operation history) are compared to the percent precipitation deficit in Table 2-2. Since missing and deleted percentages were greater than the total water deficit, it was possible that stations have observed more rainfall than what has actually occurred, which could theoretically register higher intensities than were real. Still, this is unlikely given the overestimation of missing and deleted percentages mentioned earlier and that some of these can occur in the dry season. It was still more likely true that intensities would be slightly underestimated from these type gauges as noted by Hollinger et al. (2002).

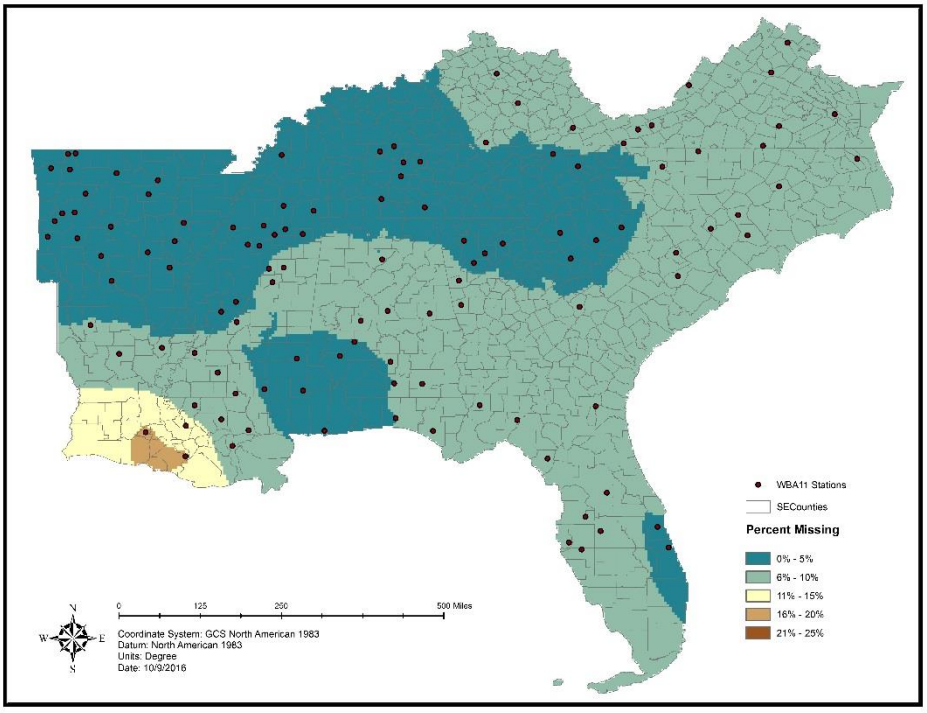

Figure 2-4 Spatial Distribution of Missing Percentages for 20.11 Screened Stations

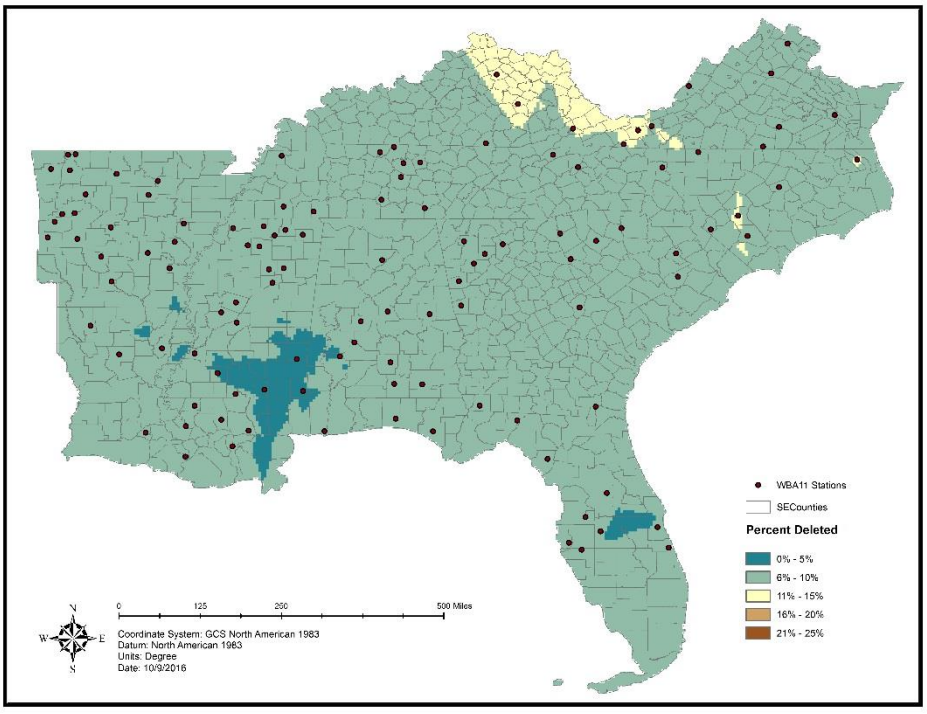

Figure 2-5 Spatial Distribution of Deleted Percentages for 20.11 Screened Stations

Table 2-2 Comparison of Water Deficit (as Percent Below Expected Precipitation) to Missing Data, Deleted Data, and Total Absent Data (Missing Plus Deleted Data)

Comparison of Water Deficits to Missing, Deleted, and Total Absent Data							
SCREENING METHOD ID	MEAN MISSING		MEAN DELETED		MEAN TOTAL		NUMBER OF STATIONS
	-	+	-	+	-	+	
20.10	-1.76	0.12	-0.02	1.86	6.25	8.13	280
20.11	-1.85	-0.07	-0.28	1.50	5.08	6.86	172
25.10	-2.15	-0.16	-0.74	1.26	4.66	6.66	167
25.11	-2.80	-1.13	-1.77	-0.10	2.21	3.88	78
30.10	-2.69	-0.87	-1.66	0.16	2.27	4.09	68
20.12	-2.60	-1.57	-1.50	-0.47	1.53	2.57	31
30.11	-3.51	-1.93	-2.24	-0.67	0.75	2.33	22

Note: Values determined by adding missing, deleted, or both to the mean water deficit for each screening with and without accumulations (+/-). Negative or positive results indicate a deficit or surplus respectively.

Using the 20.11 screening method, of the 172 screened stations 117 had matching climate normal data for the water balance. The absolute differences of the normal precipitation depth versus the observed depth were shown in Figures 2-6 and 2-7 with and without accumulations. The largest deficit occurs along the Atlantic coastline. In this area there were stations that reported about 5 inches below the expected precipitation depth for the same period. It was more apparent that these areas underestimated rainfall in relative terms. Figures 2-8 and 2-9 show the relative precipitation deficit as a percentage below expected depth with and without accumulations. Despite the lower-than-expected values reported for the Atlantic coast, no gridded value reported more than 11.9% below the expected precipitation depth, even if accumulations were not included. With accumulations the worst value was 10.2% below expected and the best was 2.0% below expected. These figures provide some spatial significance to uncertainty in the observed data. Thus, the Atlantic coast was the area which was most uncertain and reported the largest deficit in observed precipitation depths to expected climate normals. When reporting the EI for these areas, adjusted values may become more useful at least in communicating the uncertainty of the erosivity in these areas.

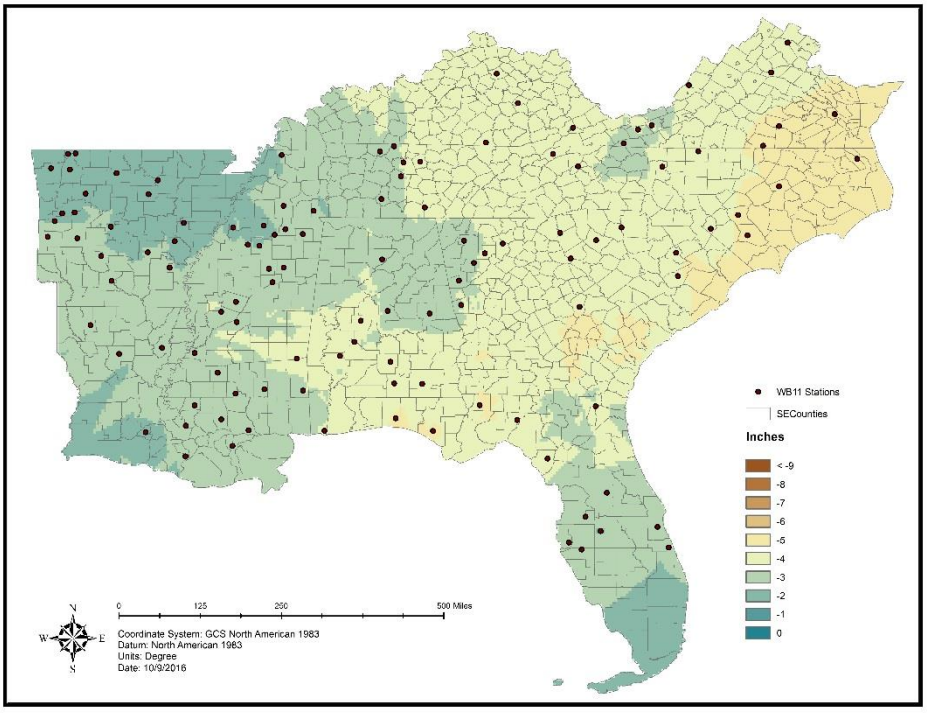

Figure 2-6 Absolute Difference from Normal Precipitation without Accumulations

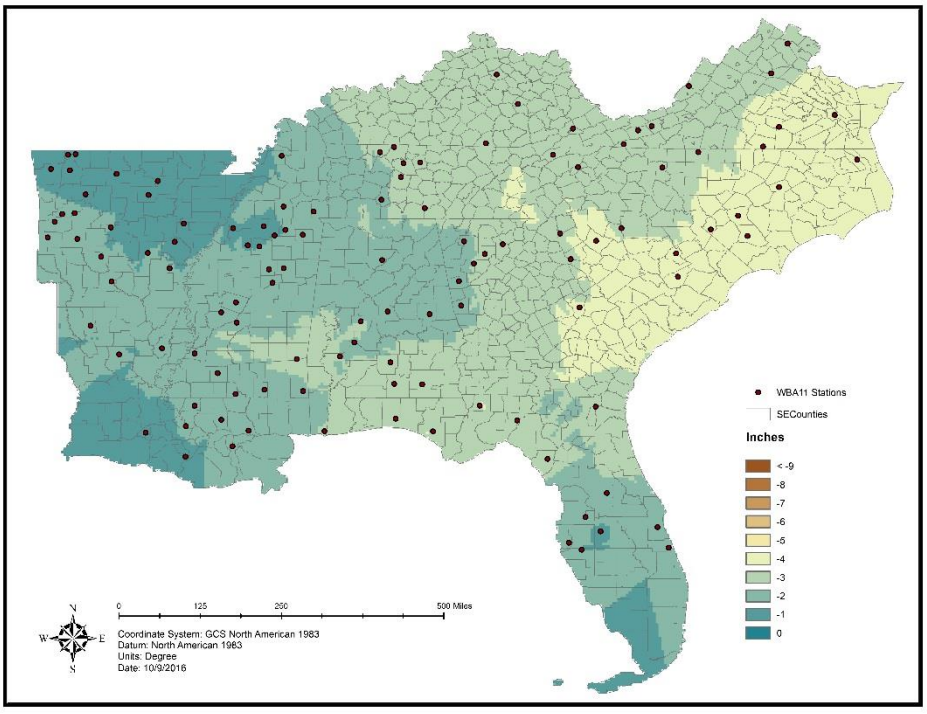

Figure 2-7 Absolute Difference from Normal Precipitation with Accumulations

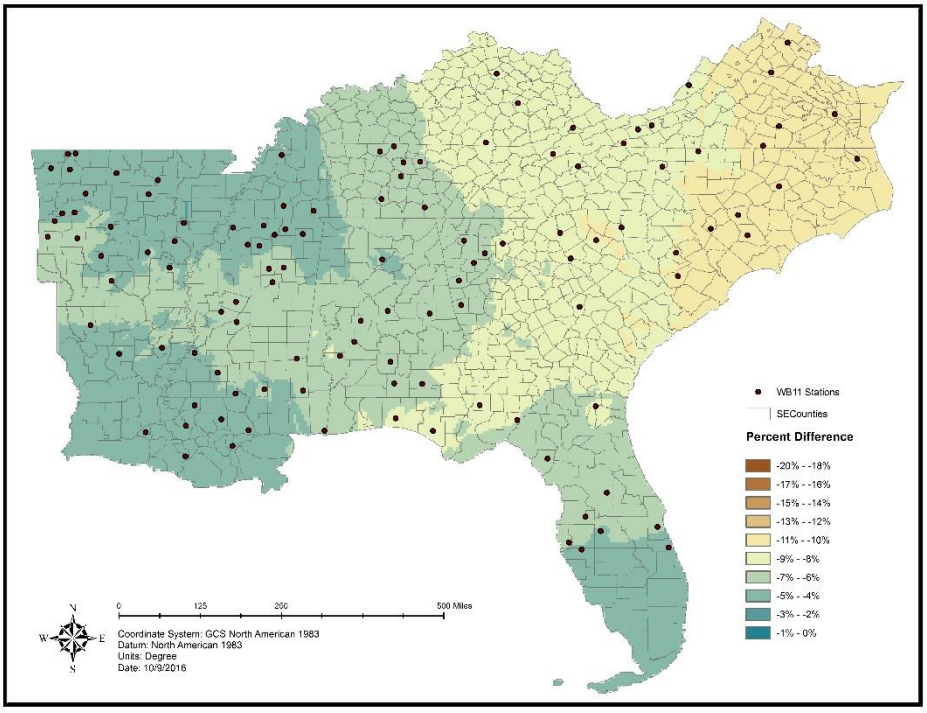

Figure 2-8 Relative Differences from Normal Precipitation without Accumulations

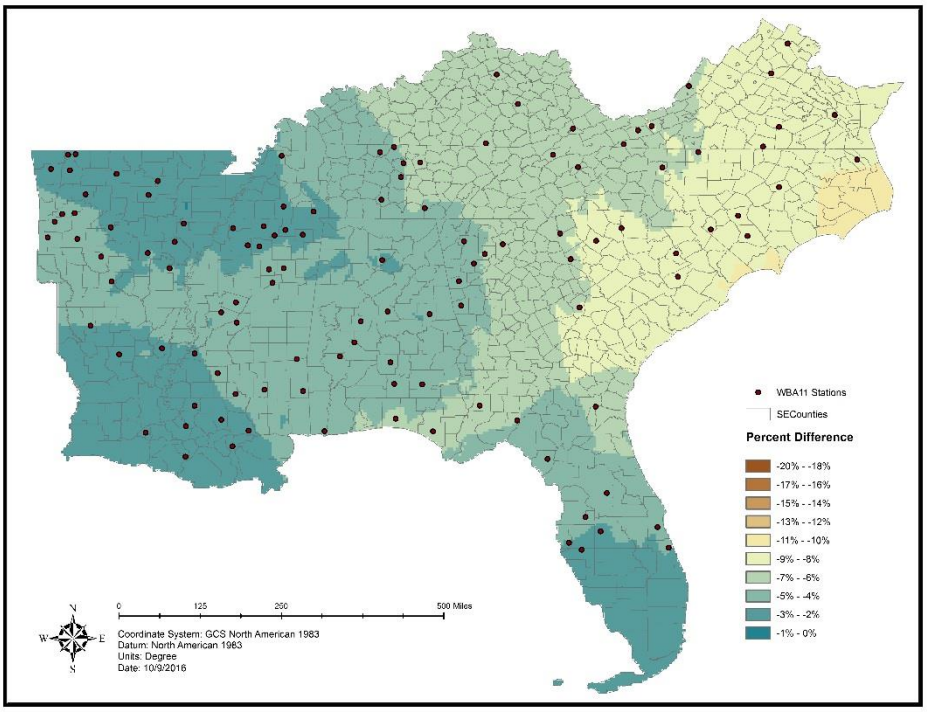

Figure 2-9 Relative Differences from Normal Precipitation with Accumulations

2.4.2 Annual EI

The annual EI (also called erosivity or R-factor) was calculated for unscreened data, 20.10 screened data, and 20.11 screened data for a) I_{30} limited and unlimited EI and b) filled and unfilled EI data. Only the filled 20.11 screened data calculations were systematically used to produce gridded isoerodent maps and analysis. A few gridded maps were produced as an exception to this rule in order to highlight potential differences of interest in the new methodology. Gridded data was provided for all calculations because of the large size of the data. The 20.11 screened gridded data is reported with and without adjustments to the data, and all gridded data for this method is provided in the appendix. A comparison of AH703 to AH537 is included in Figures 2-10 and 2-11 for reference. No significant difference was detected with or without accumulations or filled data. Accumulations have little effect because they were generally small storms with small depths. Filled data would be more important for less strict screening that has many more gaps to fill.

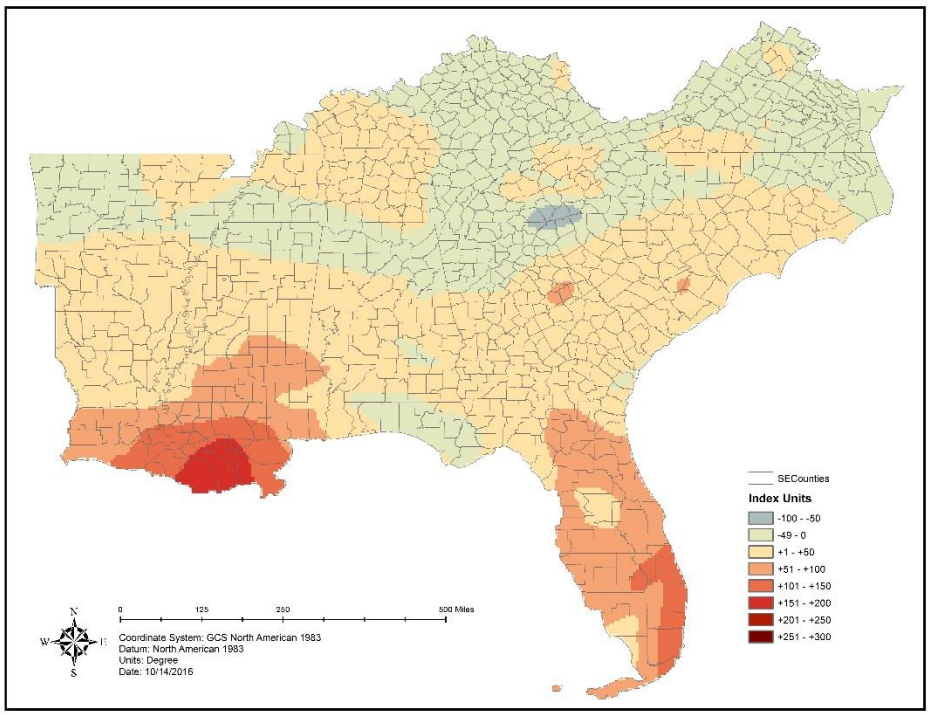

Figure 2-10 Absolute Difference in AH537 (Baseline) and AH703—Due to Unlimited I_{30} and Modern Contouring Methods in AH703

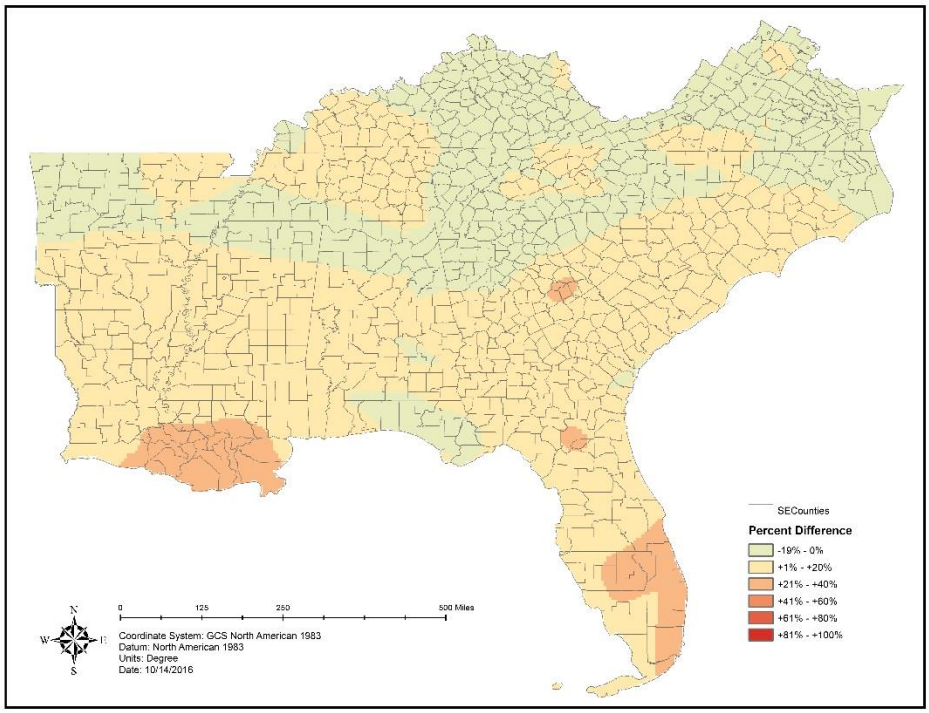

Figure 2-11 Relative Difference in AH537 (Baseline) and AH703—Due to Unlimited I_{30} and Modern Contouring Methods in AH703

Figures 2-12 and 2-13 show the annual EI with and without the effect of maximum 30-minute intensity limited to 2.5 inches per hour. Limiting the maximum intensity parameter has a strong effect on the EI calculation in Gulf States and was at least noticeable along the Atlantic Coast. The absolute effect in the Gulf was much higher, but due to the lower erosivity along the East Coast, the relative impact was apparent in both regions. Limiting this parameter may be even more important for the East Coast than these results indicate due to the lack of stations along the immediate coastline. The 20.10 screening cannot add much insight to this since it only adds one station to this critical region, but the unscreened data does have several stations in this area. Larger EI values exist on the Atlantic Coast from unscreened data, and these values were lower than expected due to larger missing percentages of data for unscreened stations. The unadjusted, unlimited, filled 20.10 screened and unscreened gridded EI values were depicted in Figures 2-14 and 2-15. Comparisons of Figure 2-12 to AH537 are shown in Figures 2-16 and 2-17. The average change over the entire region was +23.0% or a rounded increase of 73 EI units. Again, the Atlantic Coast did not see significant change in annual EI. Adjustments were highly

recommended for this area, since it saw the largest deficit of precipitation, which could mean lower-than-expected erosivity values in this area.

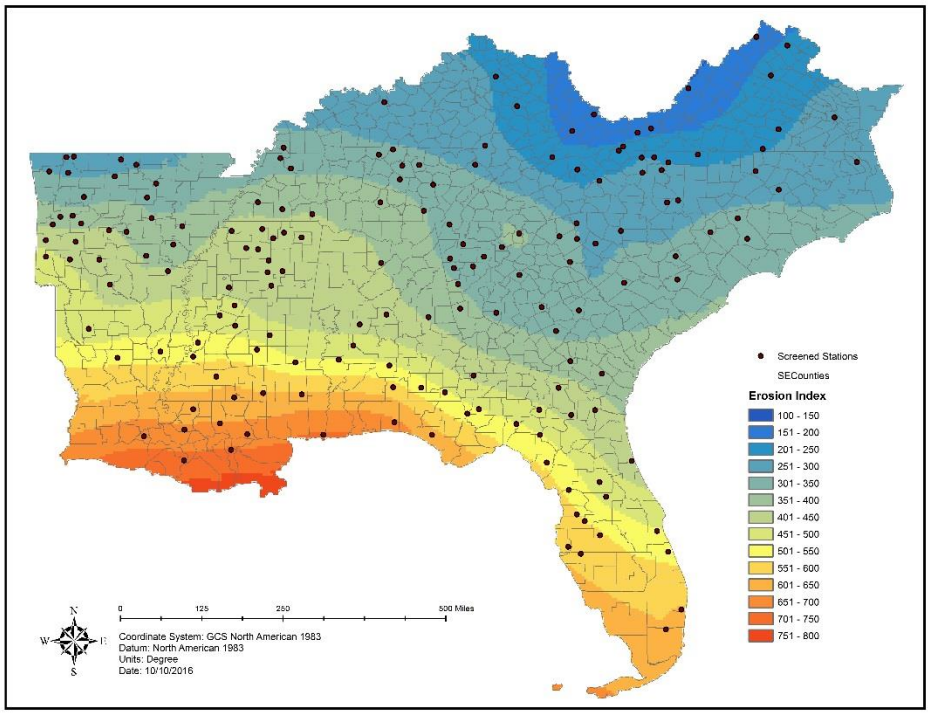

Figure 2-12 Gridded Annual EI (R-Factor) with Limited I_{30}

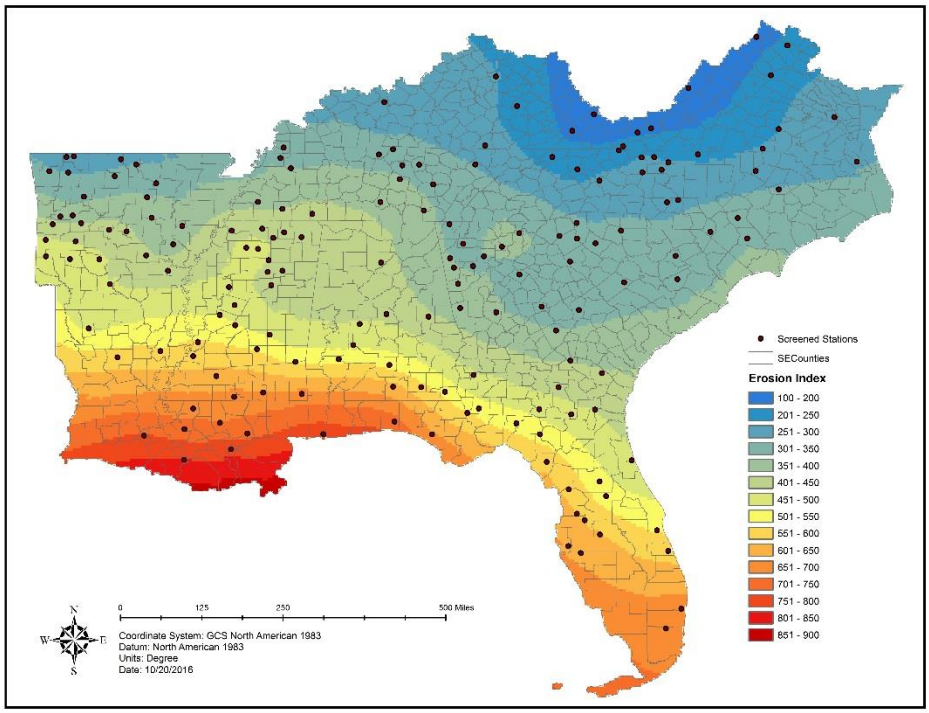

Figure 2-13 Gridded Annual EI (R-Factor) with Unlimited I_{30}

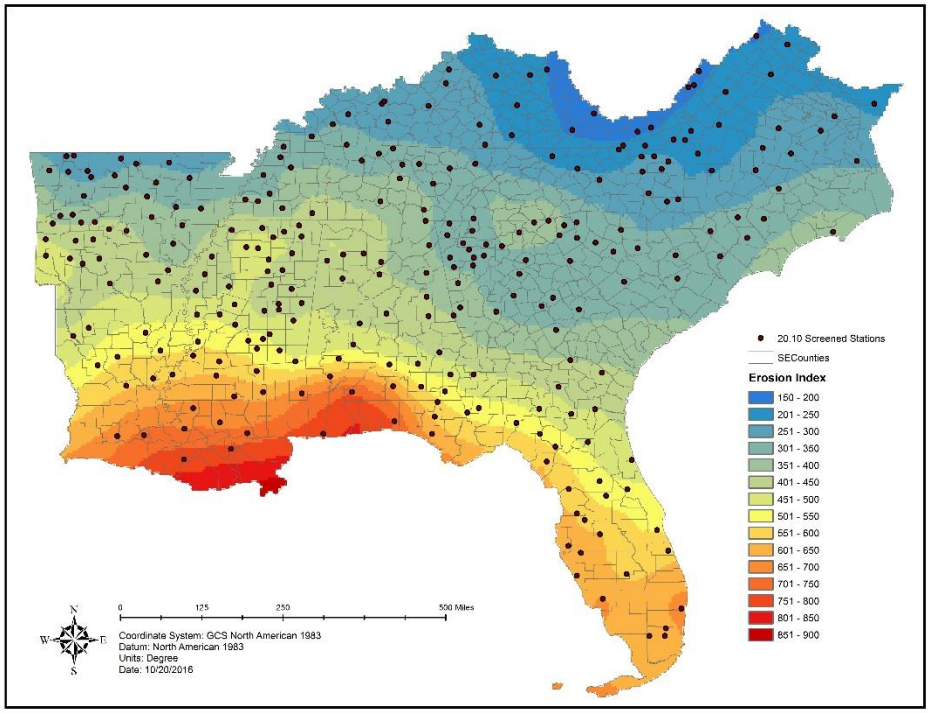

Figure 2-14 Gridded Annual EI for Unadjusted, Filled, Unlimited I_{30} Values for 20.10 Screened Stations (Right)—Shown for Visual Only (Actual EI Values Differ)

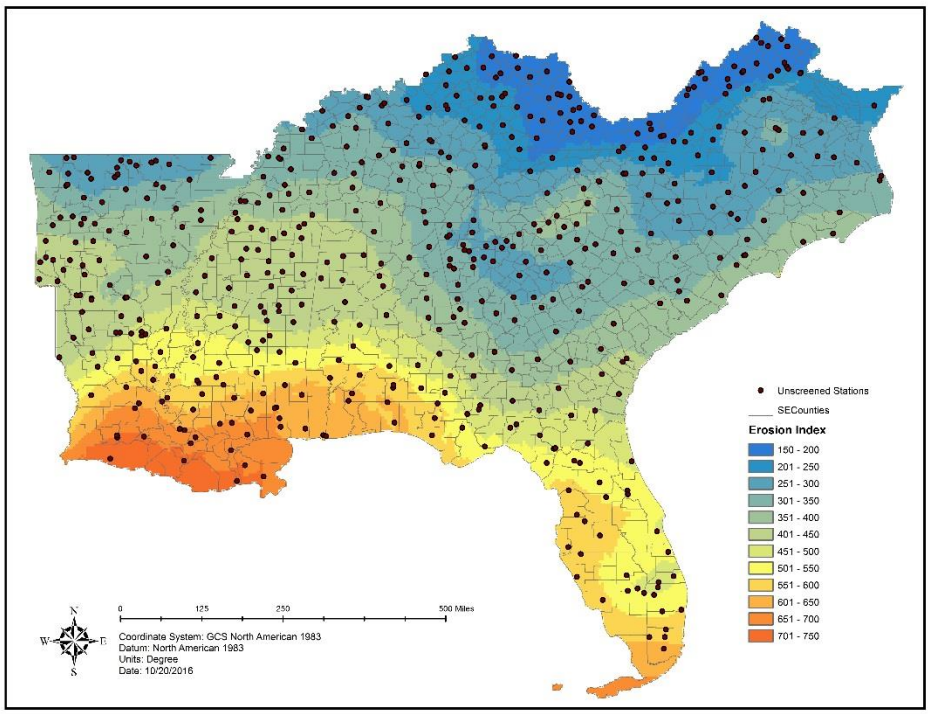

Figure 2-15 Gridded Annual EI for Unadjusted, Filled, Unlimited I_{30} Values for Unscreened Stations (Right)—Shown for Visual Only (Actual EI Values Differ)

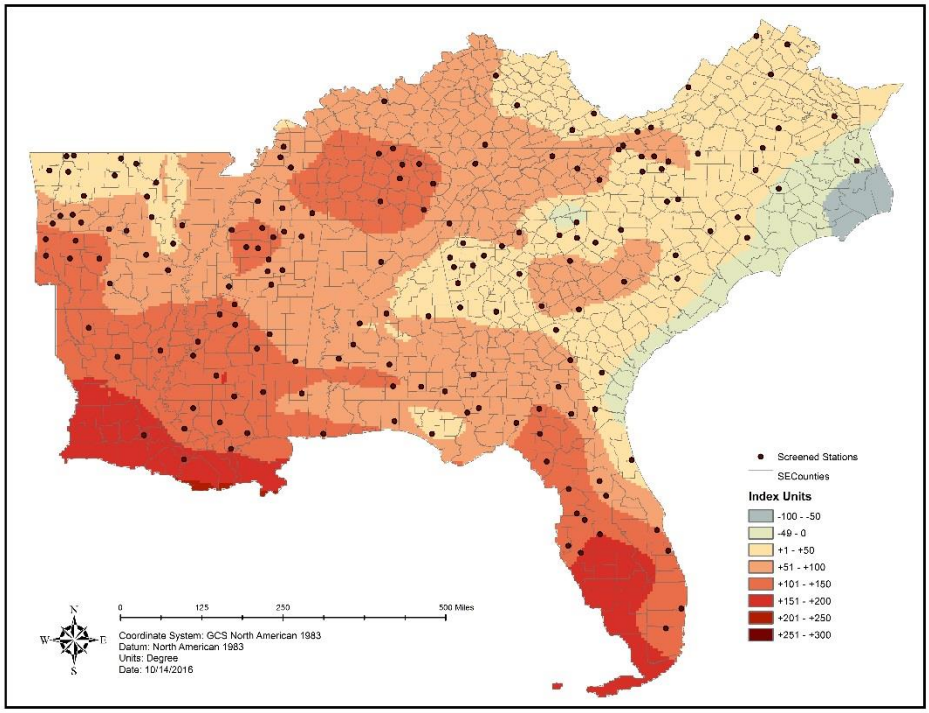

Figure 2-16 Absolute Differences in AH537 (Baseline) and Unadjusted, Filled, Limited, Gridded Annual EI for the 20.11 Screened Data

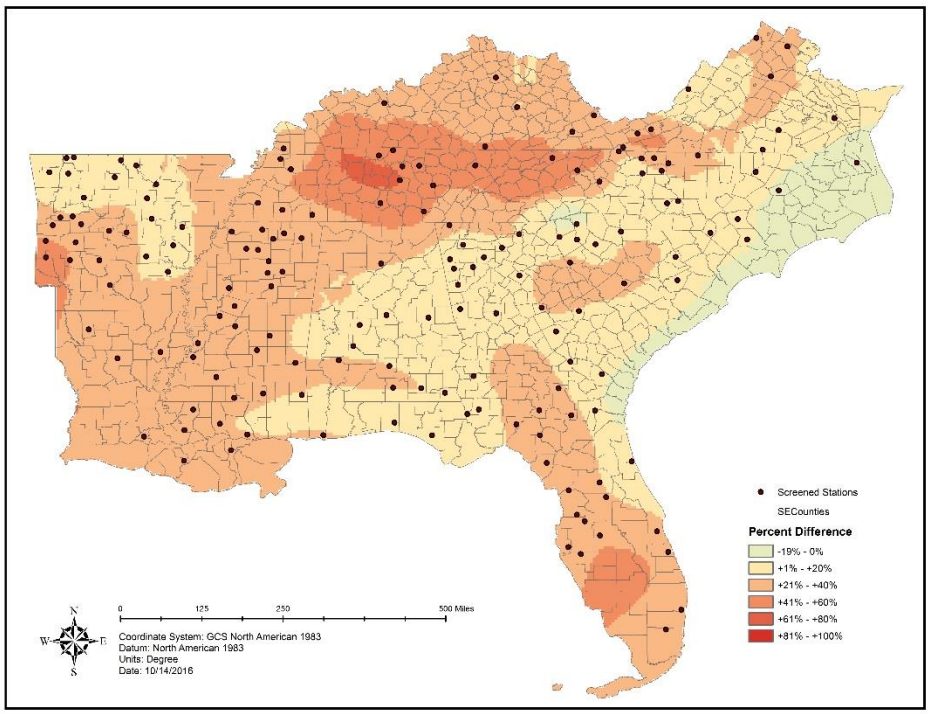

Figure 2-17 Relative Differences in AH537 (Baseline) and Unadjusted, Filled, Limited, Gridded Annual EI for the 20.11 Screened Data

In Figures 2-18, 2-19, and 2-20 gridded annual EI values were adjusted to better reflect a) adjusted I_{30} and b) 'a' plus gridded missing percentages from station metadata, and c) 'b' plus gridded deleted percentages from station metadata. In regards to the Atlantic Coast, adjusting for missing and deleted data did increase the absolute and relative difference from AH537, but it did little to remedy the unexpected decrease along the coast. This left only two options. The decrease in EI values on the coast was either a product of the station distribution (not having enough data entries close to the shoreline) or a result of climate variability influence (which I suspect is driven by AMO). This was a possibility that will be explored in the second objective along with other influences from climate variability, namely ENSO.

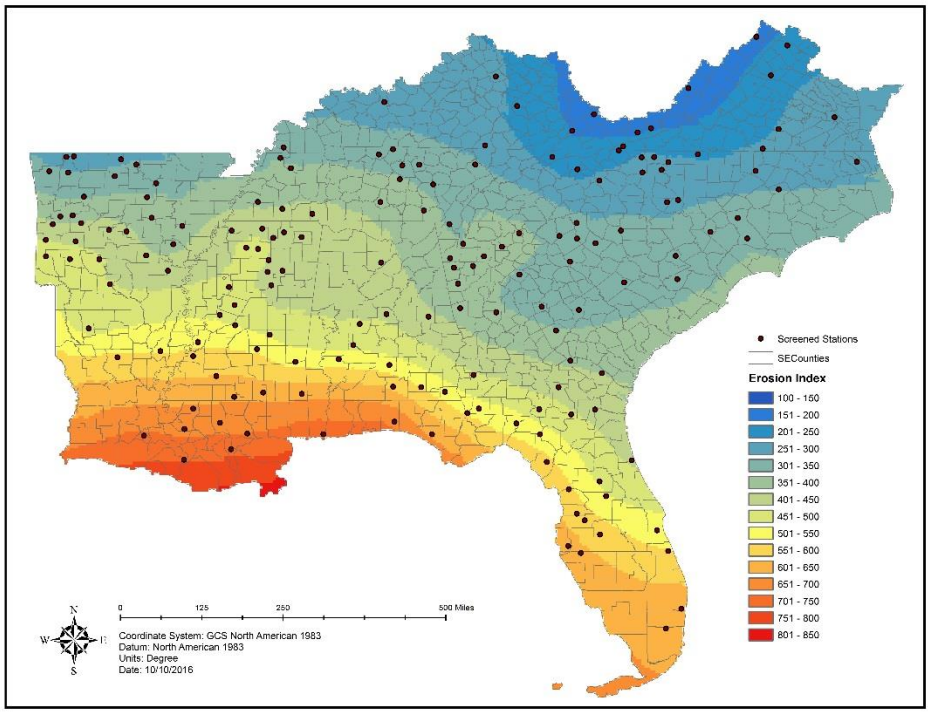

Figure 2-18 Gridded Annual EI with I30 Adjusted +4%

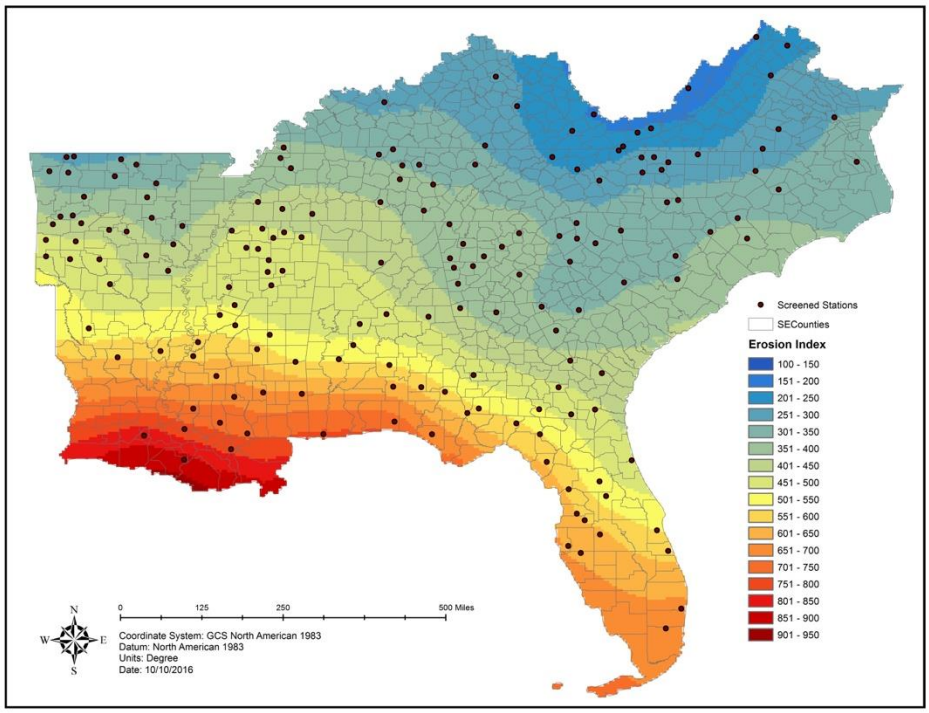

Figure 2-19 Gridded Annual EI with I30 and Missing Data Adjustments

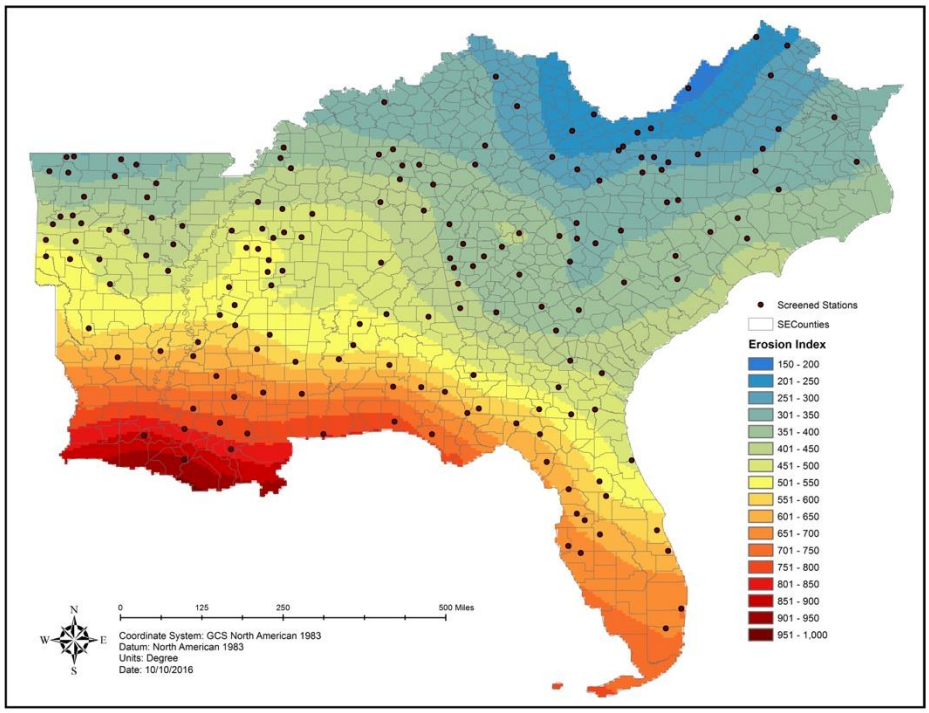

Figure 2-20 Gridded Annual EI with I30, Missing, and Deleted Data Adjustments

2.4.3 Single Storm EI

It is conceivable that the single storm EI could actually be a more important 'benchmark' for future climate studies than erosivity. This is because a storm is the 'building block' of erosivity much like an atom is to matter. Single storm EI is generally reported as a single value for a given return period storm. The 10-year storm erosivity is the most commonly reported value, and as such is the basis of comparison for this benchmarking analysis. Other return periods were included in the appendix. Figures 2-21 and 2-22 present the 10-year single storm EI value as reported by AH537 as well as the calculated value from 20.11 screened data, respectively. The AH537 single storm analysis was only computed at 181 stations for 37 states, while our analysis was of a higher quality, more recent, and a longer period for 172 stations in 11 states. These different return period storm events were highly varied across the Southeast for all return periods. Even smaller return periods show large amounts of spatial variability with areas in Kentucky and Virginia having a 1-year storm of only 9 EI units while the Gulf States consistently see storms of 60 EI units every year.

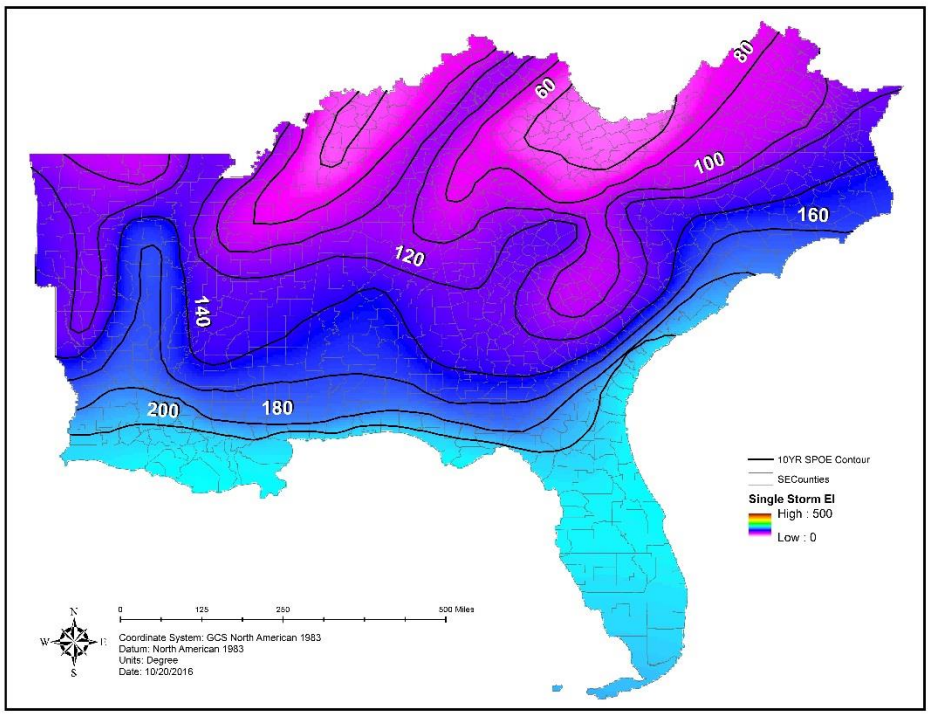

Figure 2-21 10-Year Single Storm EI from AH537

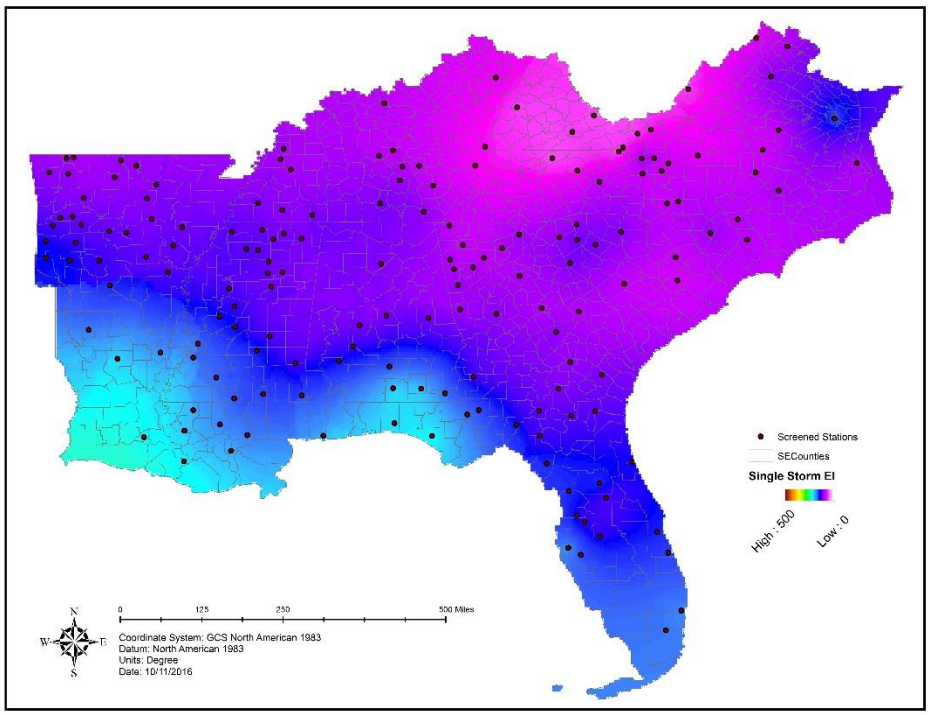

Figure 2-22 10-Year Single Storm EI for 20.11 Screened Stations with I_{30} Limited

Figures 2-23 and 2-24 compare AH537 to our analysis. There were significant decreases along the East Coast and some increases along the Gulf Coast as well as further inland. Much of the difference, especially in inland areas, was highly sensitive to small changes in EI. This creates an opportunity for storms of large return periods to have unrealistic impacts on the 10-year storm EI, especially for stations with short records. This may be a reason for such high relative changes seen in northern Mississippi, Tennessee, and Kentucky. A potential remedy for this may filter significantly larger return periods than the analysis return period or use a method more resilient to outliers (Hollinger et al. 2002). In general, our observations were consistent with Hollinger's, even perhaps some of the contouring issue Hollinger mentioned (dark red in Kentucky and Tennessee).

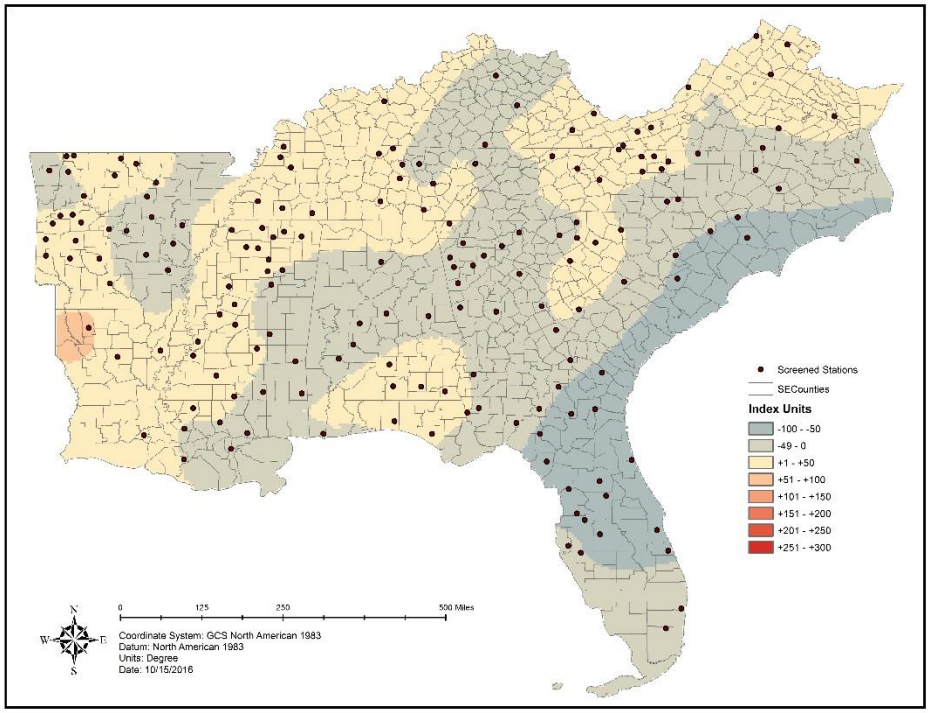

Figure 2-23 Absolute Differences in 10-Year Single Storm EI Values for AH537 and I_{30} Limited, Log-Transformed 20.11 Screened Data

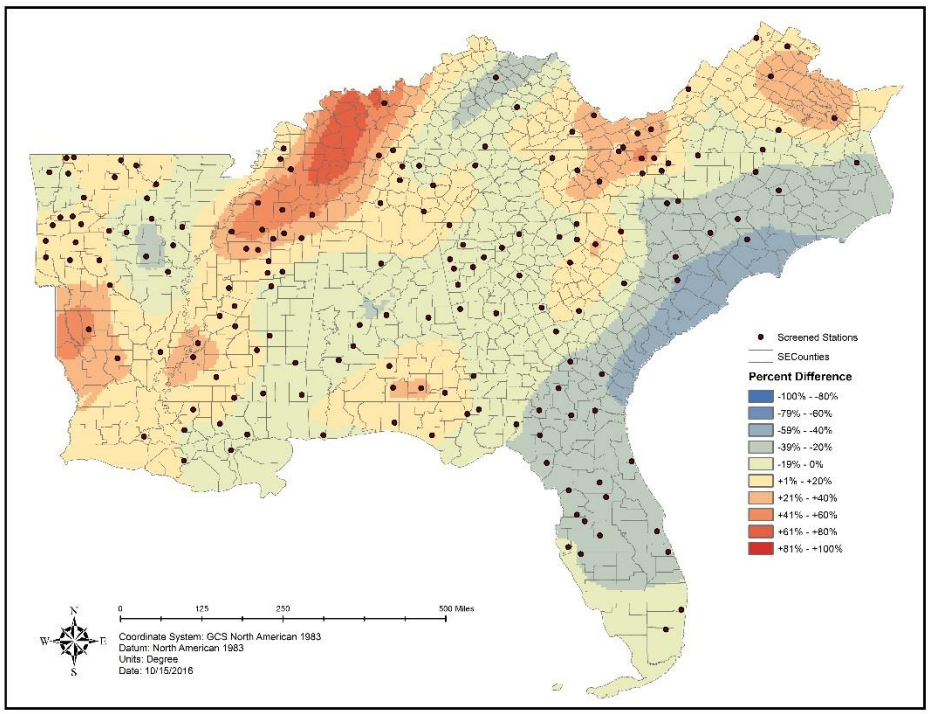

Figure 2-24 Relative Differences in 10-Year Single Storm EI Values for AH537 and I_{30} Limited, Log-Transformed 20.11 Screened Data

2.4.4 Comparison to Erosivity in Literature

It was important to address a concern raised by McGregor first in 1980 and again in 1995 regarding the underestimation of erosivity values in northern Mississippi—and probably elsewhere. This section is included to alleviate those concerns by providing a direct comparison of McGregor's 29 breakpoint stations to this study for EI calculations on an annual basis, annual EI estimation from station data, and gridded EI isoerodent mapping. Tables 2-3 and 2-4 display erosivity calculations for the same area in northern Mississippi for this study and McGregor's study, respectively. A new term called 'EI rate'—defined as the EI per unit depth (in this case EI Rate was in SI units)—was used to gain a deeper understanding of EI similar to erosivity density used in RUSLE2. The EI rate is found by dividing by precipitation measured at the quarter-hour station used to calculate EI. The EI rate was of the same unit as erosivity density, but a distinction was made since the EI rate was based on EI values and depths of each storm as opposed to averaging over any given period of time. The EI rate will show effects of precipitation depth differences on the calculated EI value similarly to erosivity density. Four calculations were compared directly for each year in Table 2-5 including: events, depth, EI, and EI rate. Standard statistics were provided appropriately. Keep in mind that this was a comparison of 29 breakpoint stations in a single watershed (of the same county) as our one quarter-hour station. Our station was located about 20 kilometers north of McGregor's study area, so the EI values would be expected to be slightly lower on average—a few percentage points at the most.

Table 2-3 EI Calculations for DSI-3260 Station No. 781500 in Northern Mississippi

Year	Events	Summation of All Events			SI Conversion		EI Rate	Median of All Events			
		Depth	Energy	EI	Depth	EI		Depth	Energy	I30	EI
		in	ft-tonf/ac	100-ft-tonf-in/ac-h	mm	MJ-mm/ha-h	MJ/ha-h	mm	ft-tonf/ac	in/hr	100-ft-tonf-in/ac-h
1984*	142	52.7	317	430	1338	7323	5.47	0.07	0.19	0.04	0.03
1986	83	52.0	455	505	1321	8599	6.51	0.20	1.57	0.20	0.63
1987	78	46.0	368	331	1168	5636	4.82	0.30	2.35	0.20	0.63
1988	85	48.5	415	376	1232	6398	5.19	0.40	2.83	0.40	0.94
1989	111	65.7	562	537	1669	9146	5.48	0.20	1.77	0.20	0.63
1990	97	61.2	513	444	1554	7554	4.86	0.30	2.55	0.20	0.63
1991	98	80.7	679	709	2050	12067	5.89	0.40	3.24	0.40	1.29
1992	90	45.8	388	312	1163	5307	4.56	0.30	2.55	0.20	0.78
1993	99	50.0	422	362	1270	6160	4.85	0.30	2.35	0.20	0.63
1994	89	59.7	483	449	1516	7642	5.04	0.40	3.14	0.40	1.10
1995	83	54.6	456	417	1387	7098	5.12	0.40	3.14	0.40	1.25
1996	89	53.3	457	490	1354	8344	6.16	0.30	2.83	0.40	1.25
1997	111	65.4	557	544	1661	9260	5.57	0.40	3.14	0.40	0.94
1998	99	51.4	432	338	1306	5761	4.41	0.30	2.35	0.20	0.71
1999	75	52.0	440	451	1321	7678	5.81	0.30	2.83	0.40	1.57
2001	76	70.9	600	604	1801	10283	5.71	0.50	4.02	0.40	0.98
2002	88	63.4	529	465	1610	7917	4.92	0.30	2.35	0.20	0.63
2003	85	57.6	497	598	1463	10181	6.96	0.40	3.14	0.20	1.02
2005	71	36.9	318	357	937	6071	6.48	0.30	2.35	0.20	0.63
2006	100	47.3	399	349	1201	5938	4.94	0.20	1.57	0.20	0.31
2007	97	41.3	359	407	1049	6929	6.60	0.20	1.57	0.20	0.47
2010	90	39.3	334	297	998	5048	5.06	0.10	0.78	0.20	0.16
2011	84	43.9	383	487	1115	8284	7.43	0.20	1.67	0.20	0.47
Avg.	**92**	**53.9**	**451**	**446**	**1369**	**7592**	**5.56**	**0.29**	**2.36**	**0.26**	**0.77**
S.D.	**15**	**10.6**	**93**	**104**	**269**	**1777**	**0.81**	**0.10**	**0.87**	**0.11**	**0.38**
C.O.V.	**0.16**	**0.20**	**0.21**	**0.23**	**0.20**	**0.23**	**0.15**	**0.36**	**0.37**	**0.41**	**0.49**

Table 2-4 EI Calculations from 29 Breakpoint Stations in Northern Mississippi*

Year	Events	Measured Precipitation Depth (mm)						EI	EI Rate
		Avg.	S.D.	Min	Median	Max	Range	MJ-mm/ha-h	MJ/ha-h
1982	89	1699	63	1568	1688	1811	243	10756	6.33
1983	74	1669	58	1523	1676	1775	252	10451	6.26
1984	77	1448	40	1361	1446	1512	151	9532	6.58
1985	76	1210	46	1160	1196	1319	159	7199	5.95
1986	63	1234	38	1133	1235	1314	181	7710	6.25
1987	70	1153	47	1059	1155	1237	178	5225	4.53
1988	70	1055	30	997	1056	1131	134	4816	4.56
1989	87	1792	47	1725	1789	1912	187	10177	5.68
1990	86	1497	52	1422	1494	1662	240	6909	4.62
1991	85	1999	60	1884	1998	2137	253	14161	7.08
1992	76	1123	34	1055	1120	1188	133	5786	5.15
Avg.	**78**	**1444**	**47**	**1353**	**1441**	**1545**	**192**	**8429**	**5.73**
S.D.	**8**	**314**	**11**	**298**	**314**	**335**	**47**	**2851**	**0.89**
C.O.V.	**0.11**	**0.22**	**0.23**	**0.22**	**0.22**	**0.22**	**0.25**	**0.34**	**0.16**

* Values were presented by McGregor et al. (1995)

Table 2-5 Direct Comparison of Common Years for McGregor's 29 Stations (Averaged) as the Baseline for Comparison and Station No. 781500 in Northern Mississippi

Year	Original Data			SI Unit Conversion			McGregor Data				Relative Difference			
	Events	Depth	EI	Depth	EI	EI Rate	Events	Depth	EI	EI Rate	Events	Depth	EI	EI Rate
	#	in	100-ft-tonf-in / ac-h	mm	MJ-mm / ha-h	MJ / ha-h	#	mm	MJ-mm / ha-h	MJ / ha-h	%	%	%	%
1986	83	52.0	505.2	1321	8599	6.51	63	1234	7710	6.25	31.7%	7.0%	11.5%	4.2%
1987	78	46.0	331.2	1168	5636	4.82	70	1153	5225	4.53	11.4%	1.3%	7.9%	6.4%
1988	85	48.5	375.9	1232	6398	5.19	70	1055	4816	4.56	21.4%	16.8%	32.8%	13.8%
1989	111	65.7	537.4	1669	9146	5.48	87	1792	10177	5.68	27.6%	-6.9%	-10.1%	-3.5%
1990	97	61.2	443.8	1554	7554	4.86	86	1497	6909	4.62	12.8%	3.8%	9.3%	5.3%
1991	98	80.7	709.0	2050	12067	5.89	85	1999	14161	7.08	15.3%	2.5%	-14.8%	-16.9%
1992	90	45.8	311.8	1163	5307	4.56	76	1123	5786	5.15	18.4%	3.6%	-8.3%	-11.5%
Avg.	**92**	**57.1**	**459.2**	**1451**	**7815**	**5.33**	**77**	**1408**	**7826**	**5.41**	**19.6%**	**3.1%**	**-0.1%**	**-1.5%**
S.D.	11	12.9	139.0	328	2366	0.68	9	366	3329	0.98				
Min	78	45.8	311.8	1163	5307	4.56	63	1055	4816	4.53				
Max	111	80.7	709.0	2050	12067	6.51	87	1999	14161	7.08				

The direct comparison of annual erosivity calculations (Table 2-5) was provided with relative differences for each year and the means of the two samples. Positive values correspond to overestimation while negative values convey the opposite. This was a small sample size, so conclusions are somewhat limited for this analysis. The quarter-hour stations observed more storm events, or more appropriately, observed them in a way that storm separation methods—identical for breakpoint data—resulted in more storms. This was expected since breakpoint data can detect very small intervals of precipitation, while quarter-hour stations have rigid intervals. This can have a significant impact on calculations since the portion of the storm that was separated by fixed-interval stations will usually have different maximum intensities multiplied by almost equal kinetic energies resulting in some calculation differences. This observation may partially explain EI differences for each year. Second, precipitation depth seems to be consistently well captured, although there will be some differences as these studies were located approximately 20 kilometers apart. Third, EI predictions vary quite widely within each year, which to a degree was acceptable due to location differences and how storms change as they move across the landscape. It would be expected, however, that the long-term average would be close to McGregor's findings. Lastly, the EI rate was much more consistent (coefficient of variation much lower than EI) with -16.9% being the largest difference in any given year. That particular year happened to be the maximum for this sample as well as all other data from both studies. In general, our calculations overestimate years with lower erosivity and underestimate years with

higher erosivity. Large values are underestimated because quarter-hour stations are not able to capture maximum intensities as well as breakpoint data and storms with low intensity tails are wrongly separated into smaller storms (resulting in lower maximum intensity multiplier for that portion of the storm). Small values are overestimated due to interval and measurement resolutions, which artificially increase intensities during small storms. Energy calculations are highly sensitive to small values, which is most likely responsible for the difference. Values averaged over a single 15-minute interval will always be underestimated, but values occurring over several intervals could register several zero-energy blocks before having one relatively large value (when the measurement threshold is finally reached). Table 2-6 summarizes the differences between all years on record for each study and provides basic statistical information regarding each. The total sample size for each study was 23 and 11, respectively. A two-tailed test of the two independent erosivity means found that differences in the means were not statistically significant with a p-value of 0.3008.

Table 2-6 Direct Comparison of All Years for McGregor's 29 Stations (Averaged) as the Baseline for Comparison and Station No. 781500 in Northern Mississippi

Stat.	Original Data			SI Unit Conversion			McGregor Data				Relative Difference			
	Events	Depth	EI	Depth	EI	EI Rate	Events	Depth	EI	EI Rate	Events	Depth	EI	EI Rate
	#	in	100-ft-tonf-in / ac-h	mm	MJ-mm / ha-h	MJ / ha-h	#	mm	MJ-mm / ha-h	MJ / ha-h	%	%	%	%
Avg.	**92**	**53.9**	**446.1**	**1369**	**7592**	**5.56**	**78**	**1444**	**8429**	**5.73**	**18.9%**	**-5.2%**	**-9.9%**	**-2.9%**
S.D.	15	10.6	104.4	269	1777	0.81	8	314	2851	0.89				
Min	71	36.9	296.6	937	5048	4.41	63	1055	4816	4.53				
Med	89	52.0	443.8	1321	7554	5.47	76	1448	7710	5.95				
Max	142	80.7	709.0	2050	12067	7.43	89	1999	14161	7.08				

After comparing the direct differences in EI calculation differences in gridded isoerodent maps and the expected erosivity provided by McGregor were evaluated. Table 2-7 shows this comparison across the different Ag. Handbooks and this analysis with adjusted and unadjusted data. Since these were gridded values being compared with station data, the minimum, geometric mean, and maximum values for Panola County, Mississippi were provided according to each isoerodent method. These values were compared with the expected value to determine relative differences. All of the Ag. Handbooks significantly underestimated the erosivity regardless of their varying methodologies as pointed out by McGregor et al., (1995). The Goodwin Creek Watershed was located in the southern

portion of Panola County (where the maximum values for the county were found). Station No. 781500 was located nearer to the minimum values for reference. The mean value for the two studies should result in a minimum gridded value slightly lower than 7,592 (from this study) and a maximum gridded value slightly higher than 8,429 (from McGregor's study). None of the gridded methods match this perfectly, and it was not significant that they do not. The interpolation method considers not only a single station but many stations within a certain distance of the cell being calculated to construct a semivariogram, which was used to determine spatial correlations among the dataset as a whole. Basically, even among the 29 stations there were strong variations in erosivity, and the gridded value takes that into consideration. It should be close to each target value, especially the Goodwin Creek study, but it can slightly differ from these. As expected, the most important adjustments were that of increasing I_{30} by 4% and accounting for missing data. If these two adjustments were made to gridded EI values—calculated from the DSI-3260 data—the resulting EI calculations were almost identical to McGregor's (discussed above).

Table 2-7 Comparison of Gridded Isoerodent Maps to Expected Values for Northern Mississippi

Isoerodent Method	Expected Value	Gridded Comparison Values			Relative Differences		
		Min.	*Mean	Max.	Min.	Mean	Max.
AH282	8374	5503	5584	5678	-34.3%	-33.3%	-32.2%
AH537	8196	5503	5584	5678	-32.9%	-31.9%	-30.7%
AH703	8196	5414	5589	5763	-33.9%	-31.8%	-29.7%
Unlimited I30	8677	7523	7737	7933	-13.3%	-10.8%	-8.6%
Limited I30	8429	7188	7405	7588	-14.7%	-12.1%	-10.0%
Adjusted I30	8429	7475	7702	7892	-11.3%	-8.6%	-6.4%
I30 & Missing	8429	7751	7989	8205	-8.0%	-5.2%	-2.7%
I30 & Deleted	8429	8059	8294	8486	-4.4%	-1.6%	0.7%
All Adjustments	8429	8335	8581	8801	-1.1%	1.8%	4.4%

*Mean was the geometric mean of the county of comparison. Units in MJ-mm ha^{-1} h^{-1} yr^{-1}.

2.5 Discussion

2.5.1 Data Quality and Screening

DSI-3260 (quarter-hour) station data was beset by significant amounts of gaps, errors, and flags that make data management and interpretation complex. The percent of missing and deleted data ranges widely from station to station, but it was manageable with screening. Strict screening methods were able to reduce the average missing percentage of unscreened data from 14.9% to 5.3% without taking into account missing percentages dropped within the record. Deleted percentages for screened and unscreened data hovered around 7.2% to 7.8% and would also be slightly better after accounting for removed gaps. Accumulations were processed differently than missing and deleted percentages, so the amount of accumulations was accurate. Accumulations as a percent of total measured depth also reduced from 6.2% to 3.6% with screening. Only 172 of 616 stations (27.9%) passed the stricter screening (20.11) while 280 passed the 20.10 screening. This was a much higher passing rate at 45.5%, but the trade-off was that a larger percentage of the data was filled data. This was probably more permissible for precipitation data, but erosivity was even more varied than precipitation. The coefficient of variation for erosivity in some locations can be more than double that of the precipitation depth. Therefore, I leaned towards a more strict station screening method, even though it results in fewer observations. The spatial density of actual erosivity station data for the 20.11 screening was still 3 to 4 times that of AH282, AH537, and AH703, which only used 181 locations across 37 states for direct EI calculations (the other roughly 2,000 locations were based on regression equations and not directly calculated values).

All flags must be considered in order to account for all precipitation. The issue noted by Hollinger et al., (2002) of stations inaccurately reporting as operational was true, but it can be mostly worked around with a more flexible screening method. The screening method used in this study permitted the ‘g’ flag to essentially be ignored, although I do still process it as a redundant measure. This screening method more effectively handles gaps in the data and results in a simpler implementation than that of Hollinger et al., (2002). There were still two considerations that must be made for this data, primarily in the form of potential bias towards stations experiencing drought and/or larger percentages of accumulations. Drought years sometimes do see no precipitation in a month, but it was rare

for more than one month to see no rainfall in the Southeast. It was especially rare for many stations in a larger area to experience drought and not see precipitation for multiple months. This will have an insignificant effect, if any, on individual stations and even less on regional outcomes regarding EI. Bias toward mid-latitude states such as Kentucky and Virginia is a larger concern. These areas have larger percentages of accumulations and precipitation characteristics likely to trigger event recording as an accumulation as opposed to a measured event. I compared the passing rate of stations by state and did not find any such bias. Station density, distribution, and quality seem to be state specific issues, and were not associated with the methodology of this study.

In short, **the methodology outlined in this study yielded the best documented quality of the NOAA NCDC 15-minute gauging stations.** Specifically, the missing percentage of data and the percent accumulation depth were significantly lower than values presented in Hollinger et al., (2002) and USDA (2008), and this is probably true of deleted percentages as well, although there was no mention of this parameter for comparison. Our values can be slightly improved with an updated processing of station metadata (post screening) and can be applied to other stations in the eastern US. Applications outside the Southeast may need to modify screening methods in stations with high accumulation percentages. Western states which can see several months with no precipitation will need to utilize 'g' flag processing for more accurate screening.

2.5.2 Water Balance and Uncertainty

Results of the water balance indicate that the 20.11 screening method was the best for the purposes of this study. In studies where longer record period was more critical, the 25.10 screened data can be used to increase the average station period from 25 years to nearly 30. Through screening, the issue of missing, deleted, and accumulated data can be mitigated to bring observed precipitation amounts to that of the expected climate normal of the period. Upon implementing recommended changes to the metadata handling, missing data can be compared to the total water deficit for further validation of these procedures. Currently the deficit was about 5.9% with 5.77% missing data (interestingly, station data in northern Mississippi was 5.2% below observations from breakpoint data).

The water balance also provided a statement on uncertainty within the data. Areas with larger water deficits from observed climate normals were missing precipitation data. **These**

results can be used specifically to inform erosivity calculations of areas where calculations could be different and by how much. This will not provide a reliable 'adjustment' to EI values, but could indicate where true EI values will be higher and where they were sufficiently captured by the data. Northern Mississippi, for example, has little missing or deleted data, so those adjustments do not have significant impacts on that area. This was particularly useful for the Atlantic Coast, which has evidence of a water deficit, large percentages of missing and deleted data (near 15% together), notable accumulation percentages, and potentially significant impacts of climate variability through AMO.

2.5.3 Annual EI and Climate Change

Our study confirms the analysis of several others regarding the underestimation of erosivity values by the procedure used in AH282, AH537, and AH703 (McGregor et al., 1995; Hollinger et al., 2002; USDA, 2008). Erosivity values should be increased on average by 23% for the unadjusted data, and I would argue that it was slightly larger than that. I suggest that at a minimum these values should be adjusted by +4% for the inability of quarter-hour stations to capture the true maximum values as breakpoint stations can. In addition to this, I believe that missing data should be incorporated at least to communicate uncertainties in the EI calculation and to demonstrate potential changes in the regional estimates of erosivity.

Climate change has undoubtedly impacted erosivity (most likely as an increase), but it was unclear exactly how much change has resulted from climate versus methodology or climate variability. This will almost certainly be an increase due to increasing temperatures of the Atlantic Ocean, which have been proven to invigorate high energy storms before they make landfall in the Southeast. In order to make a statement on climate change, supplementary, hourly or daily data may be required to capture at least a few oscillations of AMO. **It was likely that both AMO and ENSO were drivers behind erosivity in the Southeast and determining their impact will help identify climate change trends.**

2.5.4 Single Storm EI

The 10-year storm EI for the Atlantic Coast decreased significantly. This decrease was observed to be as high as -52.9% but was closer to -30% for most areas along the immediate coast. This resulted from two factors including sparse station distribution along the

coastline (which would explain differences in EI values along the coast) and the reflection of mostly negative phase AMO influences in our observation period. AH537 data was recorded during a strong positive AMO phase and the DSI-3260 data contained negative and positive phase AMO data, inversion occurred in 1995. This means that our data contains up to 25 years of negative phase data and 15 years of positive phase data, while AH537 contains up to 22 years of only positive phase AMO data. It is known that AMO affects the magnitude and track of high energy storms, and it was possible that many differences can be accounted for by AMO, especially on the Atlantic Coast. Whether this was the case or not, the single storm EI for the East Coast was significantly lower according to our analysis. This area also happened to be the area of the highest observed precipitation deficit (about -9% on average), but this was not likely to have a strong impact of the 10-year EI, especially given that the minimum station period was 20 years. **Analysis of single storm EI and annual EI values can be better understood in the context of climate variability, which this study does not directly investigate.**

2.6 Conclusion

Screened quarter-hour station data for 172 locations across 11 southeastern states were used to calculate erosivity (R) values and single storm EI return periods. A water balance was included to validate the precipitation observations against expected climate normals and to provide insight into uncertainties in the resulting EI calculations. Station and gridded data for northern Mississippi were compared to high-quality observations (McGregor et al., 1995) and were found to be satisfactory for this area. Previously published studies Hollinger et al. (2002) and USDA (2008) and the results of this study, indicate that EI data from NOAA NCDC should be screened, filled, and adjusted appropriately to derive accurate EI estimates. Methodology impacts on EI calculation from largest to smallest would be: screening, I_{30} limitation, I_{30} adjustment, missing data adjustment, and lastly, filling gaps. It is not recommended to adjust for deleted data; although it may be helpful to report the percent deleted data for each station. Using the recommended methodology for EI calculation, informed from McGregor's study, a benchmark was provided for future climate change and climate variability studies as well as updated erosivity values in the Southeast. **Conservation efforts using the standard approach (USLE and RUSLE) or the erosivity density approach (RUSLE2) can easily utilize or compare with more accurate erosion indices from densified observation of high-quality modern data under a simplified and robust data processing and EI calculation methodology.**

2.7 Chapter References

Angulo-Martínez, M., Begueria, S., 2009. Estimating rainfall erosivity from daily precipitation records: A comparison among methods using data from the Ebro Basin (NE Spain). Journal of Hydrology 379, 111–121. doi:10.1016/j.jhydrol.2009.09.051

Hollinger, S. E., Angel, J. R., and Palecki, M. A., 2002. Spatial distribution, variation, and trends in storm precipitation characteristics associated with soil erosion in the united states. Contract report CR 2002-08. Illinois State Water Survey. Champaign, IL. available at: www.isws.illinois.edu/pubdoc/CR/ISWSCR2002-08.pdf.

Istok, J. D., McCool, D. K., King, L. G., Boersma, L., 1986. Effect of rainfall measurement interval on EI calculation. Transactions of the ASAE 29, 0730–0734. doi:10.13031/2013.30221

McGregor, K.C., Bingner, R.L., Bowie, A.J., Foster, G.R., 1995. Erosivity index values for northern Mississippi. Research Gate 38, 1039–1047.

McGregor, K.C., Mutchler, C.K., Bowie, A.J., 1980. Annual R values in north Mississippi. Journal of Soil and Water Conservation 35(2), 81–84.

Melillo, J., Richmond, T., Yohe, G. (Eds.), 2014. Climate change impacts in the united states: the third national climate assessment. U.S. Global Change Research Program, 841 pp. doi:10.7930/J0Z31WJ2.

Mirhosseini, G., Srivastava, P., 2012. The impact of climate change on rainfall Intensity–Duration–Frequency (IDF) curves in Alabama. Regional Environmental Change. doi:10.1007/s10113-012-0375-5

Nearing, M.A., Pruski, F.F., O'Neal, M.R., 2004. Expected climate change impacts on soil erosion rates: a review. Journal of Soil and Water Conservation 59, 43–50.

Nuno de Santos Loureiro, M. de A.C., 2001. A new procedure to estimate the RUSLE EI30 index, based on monthly rainfall data and applied to the Algarve Region, Portugal. Journal of Hydrology 250, 12–18. doi:10.1016/S0022-1694(01)00387-0

Renard, K.G., Foster, G.R., Weesies, G.A., McCool, D.K., and Yoder, D.C., 1997. Predicting soil erosion by water: a guide to conservation planning with the Revised Universal Soil Loss Equation (RUSLE). Agriculture Handbook 703. U.S. Department of Agriculture. Washington, DC.

Richardson, C. W., Foster, G. R., Wright D. A., 1983. Estimation of erosion index from daily rainfall amount. Transactions of the ASAE 26, 0153–0156. doi:10.13031/2013.33893

Tiwari, A.K., Risse, L.M., Nearing, M., 2000. Evaluation of WEPP and its comparison with USLE and RUSLE. Transactions of the American Society of Agricultural Engineers 43, 1129–1135.

Trenberth, K.E., Dai, A., Rasmussen, R.M., Parsons, D.B., 2003. The changing character of precipitation. Bull. Amer. Meteor. Soc. 84, 1205–1217. doi:10.1175/BAMS-84-9-1205

USDA. 2008. User's reference guide: Revised Universal Soil Loss Equation, Version 2, (RUSLE2). Washington, D.C.: National Resources Conservation Service. Available at: http://www.ars.usda.gov/SP2UserFiles/Place/60600505/RUSLE/RUSLE2_User_Ref_Guide.pdf

Wischmeier, W. H., and Smith, D. D., 1965. Predicting rainfall erosion losses from Cropland east of the Rocky Mountains. USDA Agricultural Handbook No. 282. Washington, D.C.: GPO.

Wischmeier, W. H., and Smith, D. D., 1978. Predicting rainfall erosion losses. USDA Agricultural Handbook No. 537. Washington, D.C.: GPO.

Chapter 3: Intra-Annual Variability and ENSO Driven Impacts on Erosion Index (EI) in the Southeastern United States for Climate Resilient BMP Strategies

3.1 Abstract

Building on a previous benchmarking study of erosivity in the Southeast, this study analyzed climate variability influences of ENSO on erosion index for the southeastern United States. EI values consistent with observations from others (McGregor et al., 1995; Hollinger et al., 2002; USDA, 2008) were calculated using the methodology and dataset outlined in that study (Chapter 2). Five variability components of EI based on monthly and half-monthly EI values are studied. The first two studied 'intra-annual' variation and essentially benchmarked the magnitude and timing of 'normal' EI variations. The other three considered ENSO effects on variability and attempted to quantify 'inter-annual' variability. These included ENSO effects on EI magnitude (or the general strength of the change), EI distribution (the timing of EI throughout the year), and the characteristics of precipitation (mechanisms behind erosivity). Our analysis utilized a new and powerful statistical method known as joint-rank fit (JRFit) developed by Kloke et al. (2009). JRFit enables a more powerful statistical analysis of non-parametric data that is cluster correlated with heavy tails—data with outliers—such as erosivity data. ENSO was found to have a significant effect on both the magnitude and timing of erosivity throughout the year. Multiple precipitation parameters including number of events, precipitation depth, kinetic energy, EI, etc. were tested for significant influence of ENSO, which helped determine how erosivity was influenced by variability and which mechanisms were being impacted the most. The strongest influence of ENSO was that of the amount and timing of precipitation depth and kinetic energy, which was strongly correlated with depth. Monthly and biweekly EI distributions were benchmarked for future studies using the 25.10 screening method, which consisted of more recent, higher temporal and spatial resolution, more certain, and longer observation periods than either AH703 or RUSLE2 studies. Change in the magnitude and distribution of EI throughout the year—based on the ENSO phase—was used to highlight general implications for BMPs aimed at soil conservation and reductions of sediment yield. Having accounted for short-term variability, the time was ripe for a mid-term variability study of AMO and potentially PDO/PMO. This would likely result in a fuller picture of how mid-term oscillations influence erosivity. A mid-term variability study would also highlight clear patterns for a statement on observed climate change impacts regarding erosivity.

3.2 Introduction

Soil conservation efforts understand that climate is both a driving factor of erosion and that it is not a static parameter. Early attempts to define this relationship followed what has been called a 'standard approach' to calculating erosivity, but more recently has progressed to a newer method known as the 'erosivity density' approach. Both of these approaches quantify the changing characteristics of precipitation throughout the year using a time varying, long-term averaged distribution of either EI or erosivity density. However, in an attempt to simplify this relationship, neither of these approaches consider the impacts of climate change or climate variability on erosivity. These impacts are essential for the understanding and prediction of erosivity, especially those resulting from climate variability in the near to mid-term and those of climate change for the mid to long-term predictions. It would be a mistake to assume that erosivity changes proportionately with precipitation since **it is the characteristics of that precipitation which stand to change more than the quantity under a changing climate regime** (Trenberth et al., 2003).

The erosivity density approach does offer the ability to see variations in erosivity with respect to varying precipitation amounts, and this could potentially yield important results. However, the RUSLE2 erosivity density was derived for each station by calculating the EI (standard approach) of all storm events larger than 0.5 inches and less than 50 year return periods in a given month then subsequently dividing by the total precipitation depth for that month. There were two problems with this for evaluating climate impacts on erosivity including a) small storms were not included in calculation of EI but were included in the depth denominator and b) erosivity density values (calculated for each of the 12 months) were not allowed to vary each year. Although McGregor et al. (1995) found that small storms only account for up to 3.5% of EI in northern Mississippi for 29 breakpoint stations, quarter-hour station data do not support this finding. Using 20.11 screened data, events less than 0.5 inches accounted for 70.3% of events, 26.5% of total precipitation depth, and 8.7% of EI across all 172 stations. Therefore, the erosivity density approach would need to incorporate small events for a more accurate estimation. Furthermore, I defined a new term, EI rate, which allows us the opportunity to evaluate EI with respect to depth that includes EI from small storms and changes for every month and every year. EI rate was defined as the unaveraged, unique monthly EI divided by the depth for that unique month. Results for

the EI rate will reflect some variations in EI per unit depth that would be missed by conventional erosivity density. The inclusion of this term allows us to effectively analyze both the standard approach to EI as well as erosivity that changes with respect to precipitation depth while avoiding potential weaknesses of the erosivity density approach.

Unfortunately, observed discrepancies in erosion index values in northern Mississippi and those published in Agricultural Handbooks (Wischmeier and Smith, 1965; Wischmeier and Smith, 1978; Renard et al., 1997) raised concerns about the standard approach as it has been applied to different datasets (McGregor et al., 1980; McGregor et al., 1995). McGregor's results (from 29 breakpoint stations in Panola County, Mississippi) are superior to other datasets and are to be trusted over other studies including this one (Chapter 2), but McGregor's studies are confined to a small area. These results effectively nullify EI values from each of the Ag. Handbooks and diminish the ability to discern climate impacts on erosivity, especially long-term impacts. Therefore, it was necessary to create a benchmark that could be used for climate impact studies on erosion index including an appropriate methodology and dataset. Chapter 2 began to benchmark EI values on an annual and single storm basis, which can be used for climate change analysis in the future using the same methodology and dataset from that study. **This study used the annual EI benchmark and expanded the benchmarking to monthly magnitudes and half-monthly distributions using a more appropriate methodology for climate variability analysis.** These magnitude and distribution benchmarks can be used for variability analyses (estimating positive and negative phases against normal conditions) and change analysis (estimating differences of different time periods). As time progresses it will be possible to evaluate the impacts of observed climate change on erosivity in the region most sensitive to water erosion—the southeastern United States.

3.2.1 Study Objectives

In order to achieve an understanding of climate change impacts (observed and predicted), first, the effects of variability should be investigated. Climate variability occurs at multiple timescales (intra-annual, inter-annual, decadal, etc.) and involves different cycles (ENSO, PDO, AMO, etc.). Mid to long-term variability such as AMO is not well understood in comparison to shorter variability cycles. Unlike most of the other climate cycles, ENSO occurs in shorter cycles (usually one or two years). Although it tends to oscillate from

positive to negative and vice versa, ENSO can return to either a positive or negative phase regardless of the preceding phase. The prediction technology for ENSO is more developed (partially due to more frequent cycling), which makes it possible to predict ENSO impacts for the near-term future erosivity. Prediction capability along with short cycle duration (for multiple cycles to be analyzed) make ENSO an ideal choice for our variability analysis. ENSO has also been shown to have significant influence in parts of the Southeast regarding precipitation. **Therefore, the objective of this study is to evaluate the impact of ENSO on EI magnitude and distribution and to identify mechanisms of EI which are strongly impacted.** This study begins to identify variability impacts on erosivity. As other variability cycles are analyzed in future studies, it will be possible to determine observed effects of climate change on EI in the Southeast.

3.2.2 Broader Impacts

The findings of this study are key in predicting the magnitude of short to mid-term climate variability impacts, and eventually, mid to long-term climate change impacts. These predictions could be used to update or recommend new BMPs related to erosion and sedimentation, especially those that are dynamic in nature such as operational BMPs. There are at least two considerations that must be given to BMPs including maximum allowable conditions and the timing of practices. For example, maximum allowable conditions may include maintaining erosion and sedimentation TMDLs for water quality. TMDLs are maximum loads resulting from extreme events that could impair water bodies. In these cases, it is better to establish BMPs based on more vigorous climate cycles for each region (+AMO or El Niño for the Southeast), which have more frequent and intense events in a smaller amount of time compared to normal conditions. Most BMPs protecting against water erosion today are only concerned with long-term average sediment delivery, and predicting magnitude changes may prove to be—in most cases—unimportant. However, in regards to soil conservation, the biggest concern is agriculture practices, especially the timing of fallow soil, tilling, and crop rotation. In this case, timing should be the focus of these practices because EI varies over time. This is where ENSO is particularly interesting since it has been linked to seasonal changes in precipitation patterns as well as annual patterns. As all variability is incorporated in EI predictions, BMPs related to erosion and sedimentation will yield potentially much better conservation efficiency.

3.3 Methodology

After the data was formatted and processed, flags recorded and processed, and separated into storms (using the definition of a storm according to AH537 without omitting any storms), EI was calculated for each individual storm. EI values for 1.1 million storms during the period 1970 – 2010 across 616 stations were screened for a minimum of 10 months per year and 25 years for a station to pass screening. The 25.10 screening method (Chapter 2) was selected for this study due to superior results from a water balance analysis and longer station periods. Monthly and half-month EI values were calculated for each station. Monthly EI values calculated from station data were used to determine the effects of ENSO on erosivity using a novel approach to testing and estimating differences in cluster-correlated data (discussed in Section 3.3.3). The methodology for this study follows closely with that of Chapter 2. For more information regarding a detailed methodology, reference Section 2.3.

The 10-month screening was also selected since this analysis relies on monthly EI as opposed to annual EI calculations. Therefore, months that do not pass screening in years that do, will not need to be filled, and the analysis can tolerate more gaps in the data. This added the flexibility to increase the minimum number of years, since that was more important for variability studies. Similarly to Chapter 2, one measured event must be present for a month to pass screening. A concern then arises that this method could artificially increase the monthly EI since months with zero measured events would not be included in monthly EI probabilities. However, this was not prevalent since the study did not omit small storms (less than 0.5 inches) and there were many storms in this category (about 70% of all storm events). Months with no measured events would not be included in the monthly EI probability, but months with infinitesimally small EI values were included (down to 0.01 inches in a 15-minute period—the smallest possible with this dataset). For the Southeast, it was not common for a month to see no rainfall, and certainly not enough to significantly impact the median monthly EI (if at all). Also, not all months with no recorded precipitation were dry months. For many of these months it was possible that there was precipitation, but it was not recorded due to missing data periods. It was noted by Hollinger et al. (2002) that the ‘g’ flag—intended to note when stations were operational—was not a reliable indication of good station data. Our observation was that

our method was an effective filter of months that were assigned a 'g' flag but that do not have associated measured data. In short, **the incorporation of small storms combined with screening produce significant improvements in the calculation and probability analysis of monthly EI values**.

The coefficient of variation for erosivity is actually much higher than that of precipitation depth (Hastings et al., 2005), and in our own observations it can approach double or even triple that of depth. Since erosivity experiences much more variation than precipitation, it follows that the period of observation should be longer in order to obtain more reliable results. This is particularly true for variability studies which often will partition the dataset when analyzing positive and negative phases of climate oscillations. Utilizing the screening methods from Section 2.4.1, the 25.10 screening method was the preferred screening method since it increases the minimum number of years on record while maintaining a spatial resolution still about 3 times denser than observations reported in the Ag. Handbooks. Using this screening method results in water balance results superior to both 20.10 and 20.11 screenings while increasing the average station period from 24.8 years to 29.3 years and reducing standard deviations and coefficients of variation for the data. Filled data was not necessary for variability analysis which was based on monthly EI values alone, and since this was not needed, the 25.10 screening was by far the best choice.

Monthly and half-month EI were calculated identically to annual EI using the smaller observation periods of months and half-months. Although benchmarking of annual EI values was provided for both limited and unlimited I_{30} calculations, this study will only analyze the unlimited I_{30} in all calculations. This is primarily so that the true potential erosivity of storms can be studied as opposed to the correlated values for soil loss observations. Additionally, RUSLE1 and RUSLE2 have moved away from I_{30} limited calculations and include slope calculations instead to better represent true soil loss mechanisms. In reality, it is the slope in combination with intensity that determines ponding, rather than intensity alone.

Adjustments were not included in this study although the findings of Chapter 2 suggest that missing data and maximum intensity adjustments should be included. The missing adjustment was particularly small for this analysis, since the majority of missing data occurs outside months passing screening. Therefore, this adjustment is not included

because of its relatively small impact on the results. The maximum intensity was not adjusted in order to preserve actual EI signals from the station data, but the true values should be higher than quarter-hour data observations (Hollinger et al., 2002). Since only unlimited maximum intensity data is used, comparisons to AH703 were included where appropriate. Accumulations were processed identically to the annual EI analysis and merged with the measured data for a better estimation of the true monthly EI.

Since this study analyzed variability, which decreases the effective sample size of the dataset, it was therefore much more important to use a more powerful statistical method for the analysis. A more powerful statistical method is one that has a higher probability of correctly rejecting or failing to reject the null hypothesis when appropriate. Given certain data characteristics—heavy tails (data with outliers), smaller sample sizes, or strong correlation (Singh, 2016)—it is possible for statistical tests to not detect significant differences when there actually are differences. In effect, these differences are not easy to detect (due to the data or sample characteristics). More powerful methods can detect these differences despite the obscured sample and provide the correct test result. In addition to this, not all tests can provide estimations of the actual values for the different samples; some only provide the significance or p-value of the difference. One such test that is both powerful and provides the estimated median value for the two data partitions is called JRFit, which was developed by Kloke et al. (2009). JRFit is a Joint Rank Fit for non-parametric data such as erosivity. It has been evaluated for its performance among other common statistical methods, particularly among cluster-correlated data, and has outperformed them (Singh, 2016). An R implementation has been provided by Kloke et al. (2014), which was used in this study to perform the variability analysis for multiple precipitation parameters under several clustering ‘blocks’ and data partitions.

3.4 Results

EI values from station data were sometimes presented as gridded data—for better visualization—by means of empirical Bayesian kriging, which resamples locally derived semivariograms to map statistically significant spatial results. Although this analysis was based on monthly and half-month EI calculations, annual and seasonal EI was calculated to observe longer term impacts from inter-annual variability, namely that resulting from ENSO. Half-month EI values were graphed, since mapping becomes inefficient at finer temporal scales. Since half-month EI values were graphed and there were many stations, stations were classified according to climate divisions outlined in AH703 for comparison. The monthly EI and half-month EI values served as the benchmark for all present and future analyses. It was expected that significant increases in magnitude will be reported, which was consistent with findings from Chapter 2 in conjunction with McGregor et al. (1995). Any notable changes in the distribution of EI was reported and analyzed for variability impacts. **The variability analysis focused on two potential impacts including changes in the magnitude of EI values and in the distribution (timing) of those values.**

3.4.1 Monthly EI Benchmarks

Monthly EI for the 25.10 screening method (167) stations was computed for each month in each year during the period 1970 – 2010. The average station period was just under 30 years. Figures 3-1 and 3-2 compared annual EI values (calculated from summed monthly data as opposed to mean annual data in the previous study) from the two prevalent screening methods (20.11 and 25.10), which were discussed extensively in the prior section. The 25.10 screening was favored in the monthly analysis due to its longer record period and foregoing the need of a fuller record. Figure 3-3 showed unlimited, filled annual means (calculated from annual data) for comparison. **It was clear that the 25.10 screening better represents the annual EI better than the 20.11 method, and it will provide better monthly EI values (from longer station observation periods), which was critical for this variability study.**

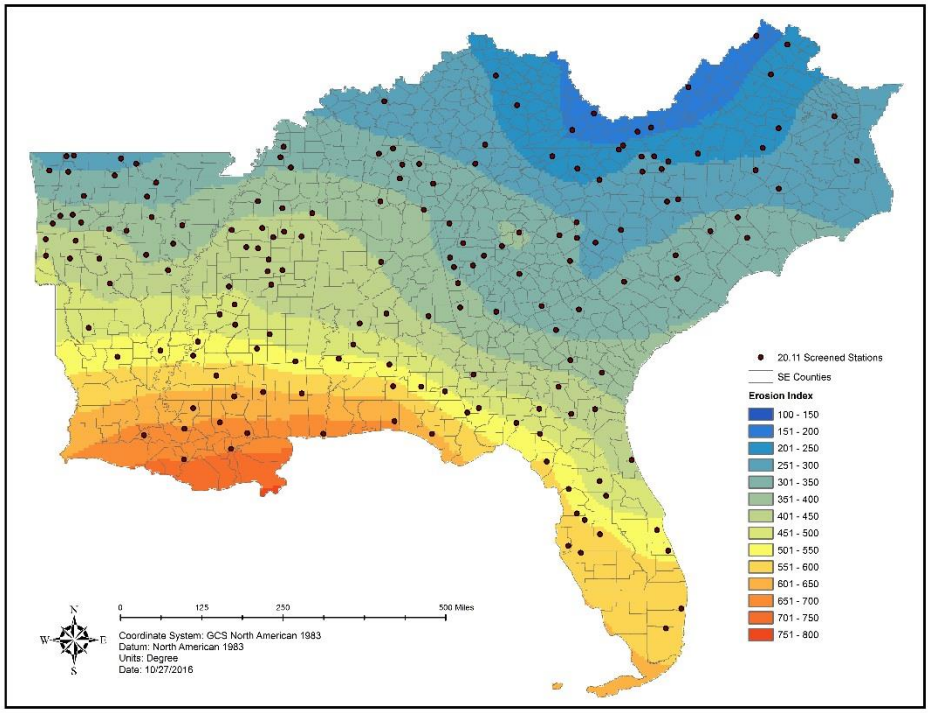

Figure 3-1 Unadjusted Annual EI from Monthly Mean EI for 20.11 Screened Data

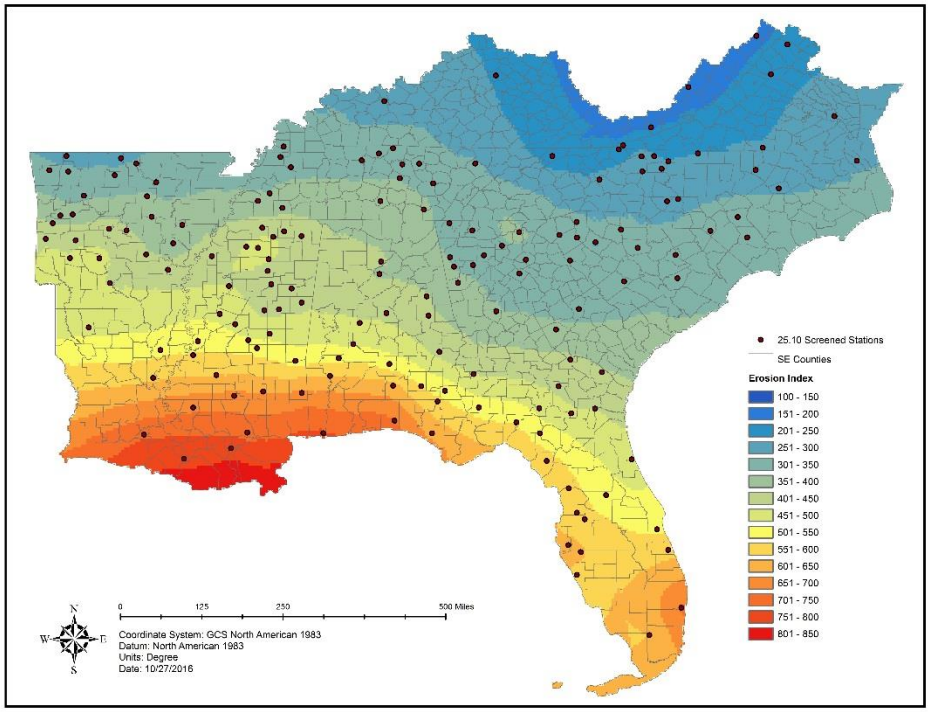

Figure 3-2 Unadjusted Annual EI from Monthly Mean EI for 25.10 Screened Data

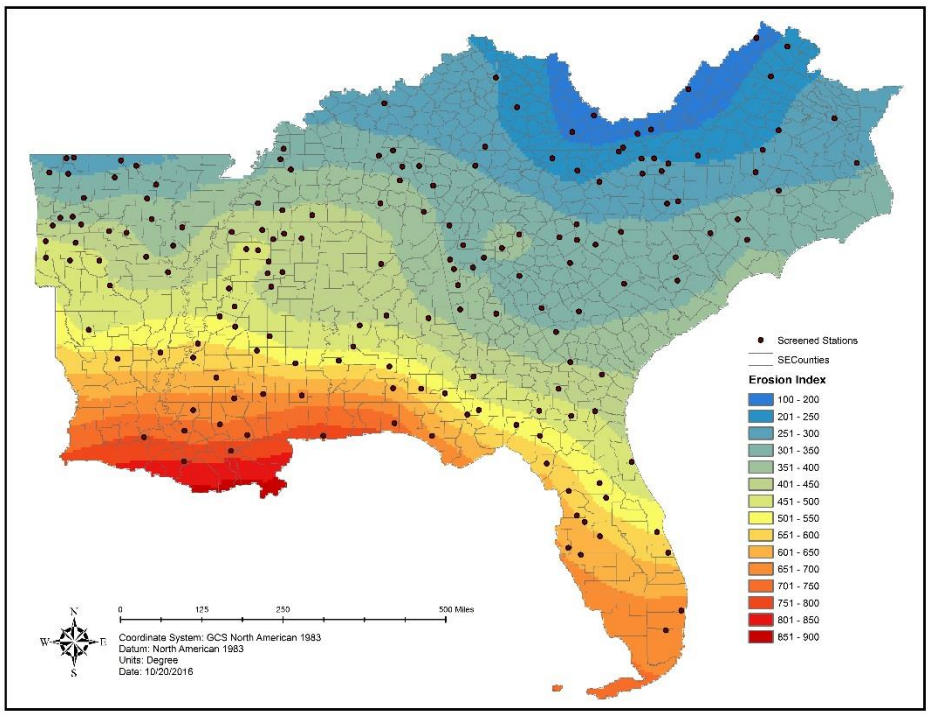

Figure 3-3 Annual EI from I_{30} Unlimited, Filled Annual Mean EI for 20.11 Screened Data—Preferred Method

Monthly EI values were also summed to determine the seasonal EI distribution. Figures 3-4, 3-5, 3-6, and 3-7 showed the seasonal distribution computed from mean monthly EI for 25.10 screened station data. This figure provided insight for spatial and temporal variations in EI, which were usually only presented as temporal variation for seasonal and monthly EI values. It was clear that both the Atlantic and Gulf Coasts received a majority of their erosivity in the summer season. A small exception was the Boca Raton, FL station, which observed many hurricanes in that particular location in the fall season. Significant understanding can be gained of the type of rain events driving EI from this figure. For example, convective rainfall along both the Gulf Coast and the Atlantic Coast was a significant factor in the annual EI values for those locations. These rains did not penetrate very far inland like other seasonal distributions, which was perhaps why unexpected decreases were observed in benchmarked EI values along the Atlantic Coast (due to stations not observing higher intensity rains along the immediate coastline). There were quarter-hour stations in these areas, but the current observation period of those stations was small. Therefore, they did not pass screening under any of the evaluated conditions. Over

time these stations will have stronger recording lengths, and they will capture coastal summer precipitation better. Monthly mean EI values were reported in the appendix.

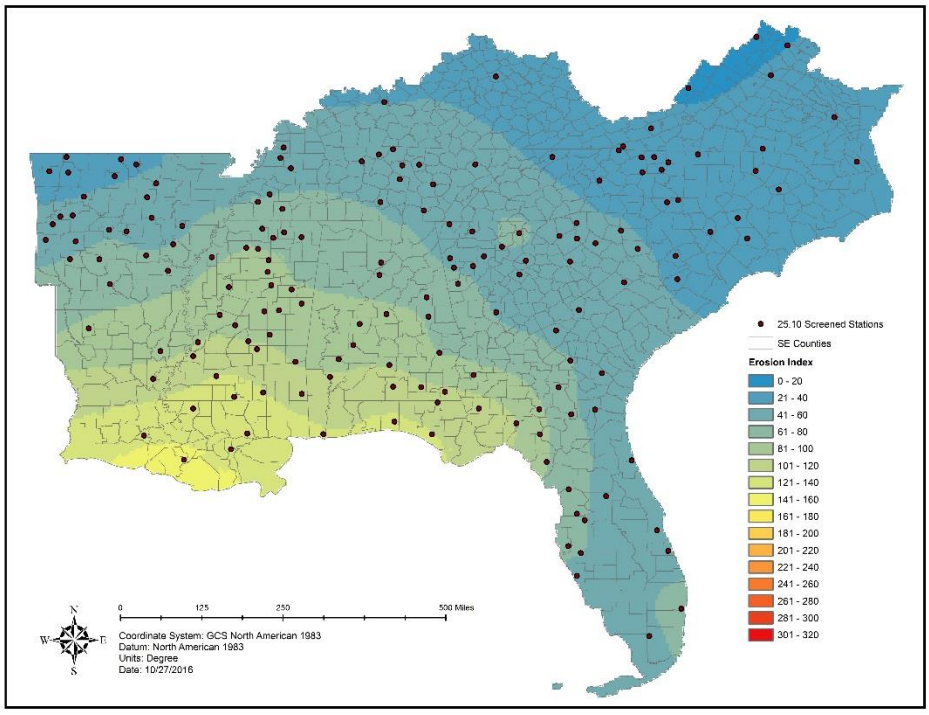

Figure 3-4 Average EI Values from Mean Monthly EI for Winter

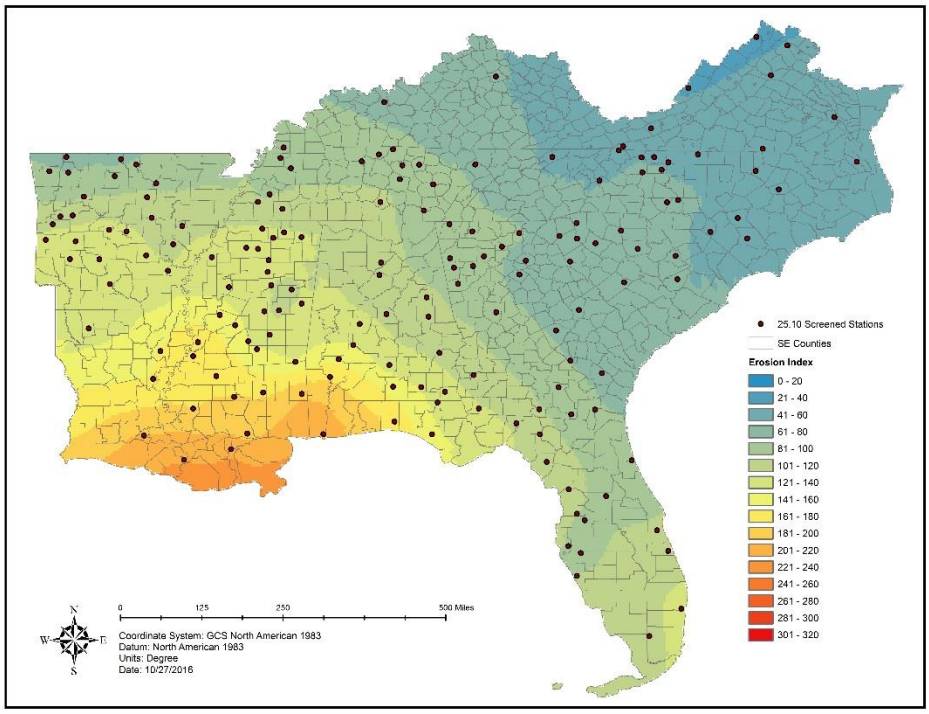

Figure 3-5 Average EI Values from Mean Monthly EI for Spring

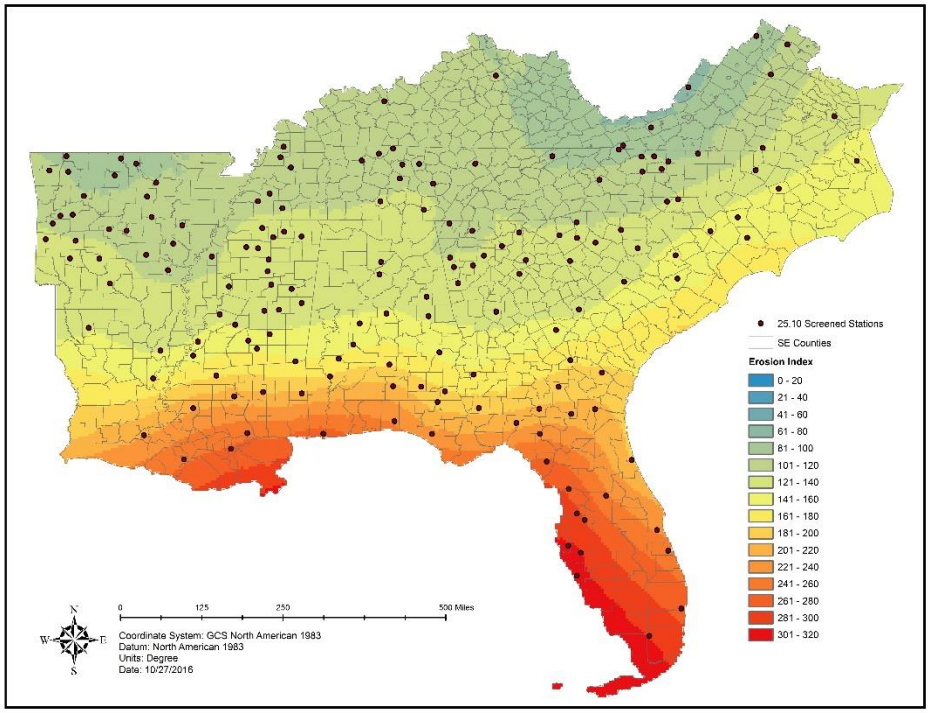

Figure 3-6 Average EI Values from Mean Monthly EI for Summer

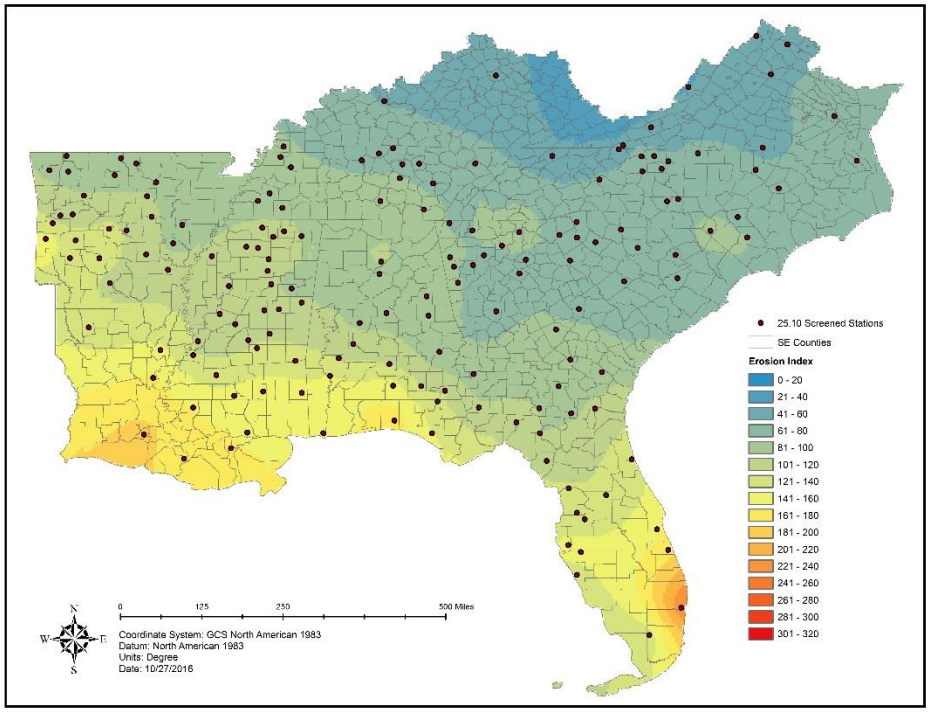

Figure 3-7 Average EI Values from Mean Monthly EI for Fall

3.4.2 Half-Month EI Distributions

Another necessary benchmark for the variability study evaluates even higher temporal resolutions using a convention outlined in AH703. Each 15 day period during a calendar year was lumped together and EI was summed for each period each year over the entire span of observations. The distribution statistics of these periods were calculated for each station and subsequently grouped by climate division. This convention was followed for comparison purposes, but there is no need to continue reporting EI according to climate division in the future. These data were important for communicating the actual range of EI values as opposed to averages. Figure 3-8 shows these climate divisions.

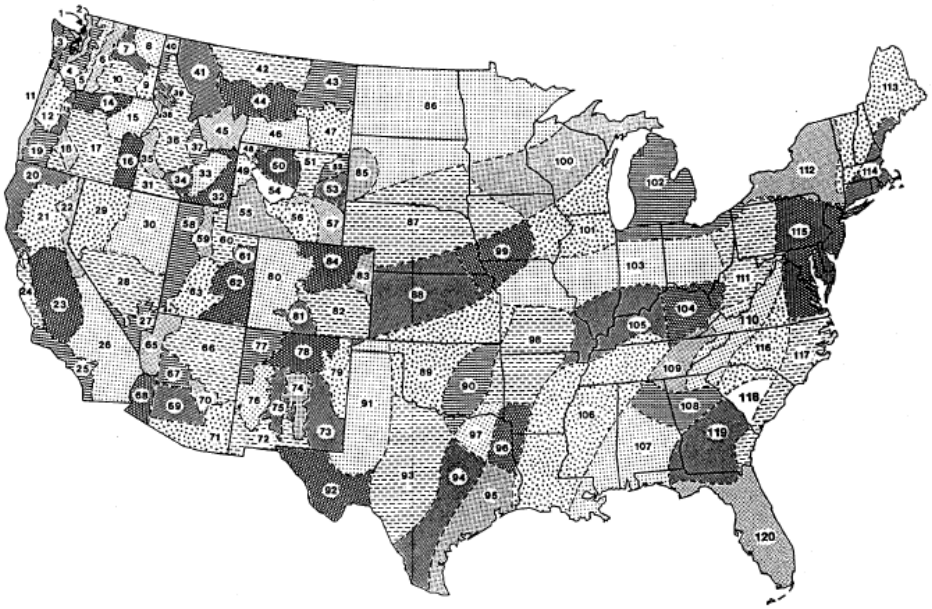

Figure 3-8 Climate Divisions Outlined by AH703

Figures 3-9, 3-10, 3-11, and 3-12 summarize the half-month distributions provided by AH703 for each climate division. Both the cumulative and fractional distribution of EI was presented. Figures 3-9 and 3-10 show these for the 120 climate divisions of the continental United States (CONUS) with an arithmetic mean of all climate divisions drawn in blue. Figures 3-11 and 3-12 do this for the Southeast and include the arithmetic national mean as well as the area-weighted mean for the Southeast alone (black). The impacts of the new methodology with small storms included, regression fitting of storm events and erosivity abandoned, etc. was pictured in Figures 3-13 and 3-14 with an area-weighted mean (red).

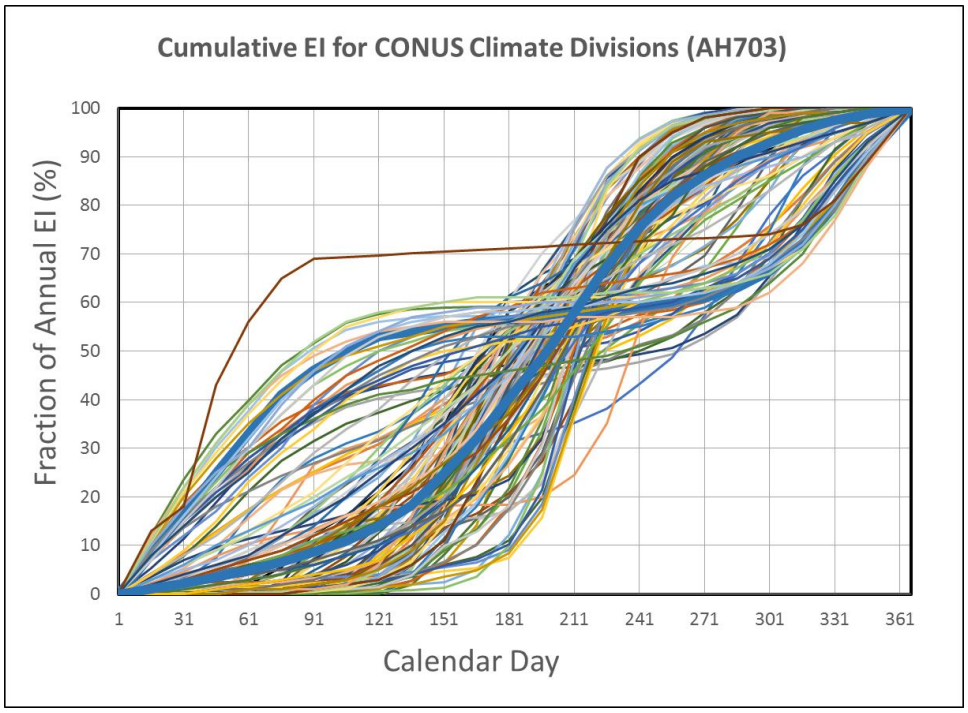

Figure 3-9 Half-Month Cumulative EI by Climate Division for CONUS (AH703) with National Avg. (Blue)

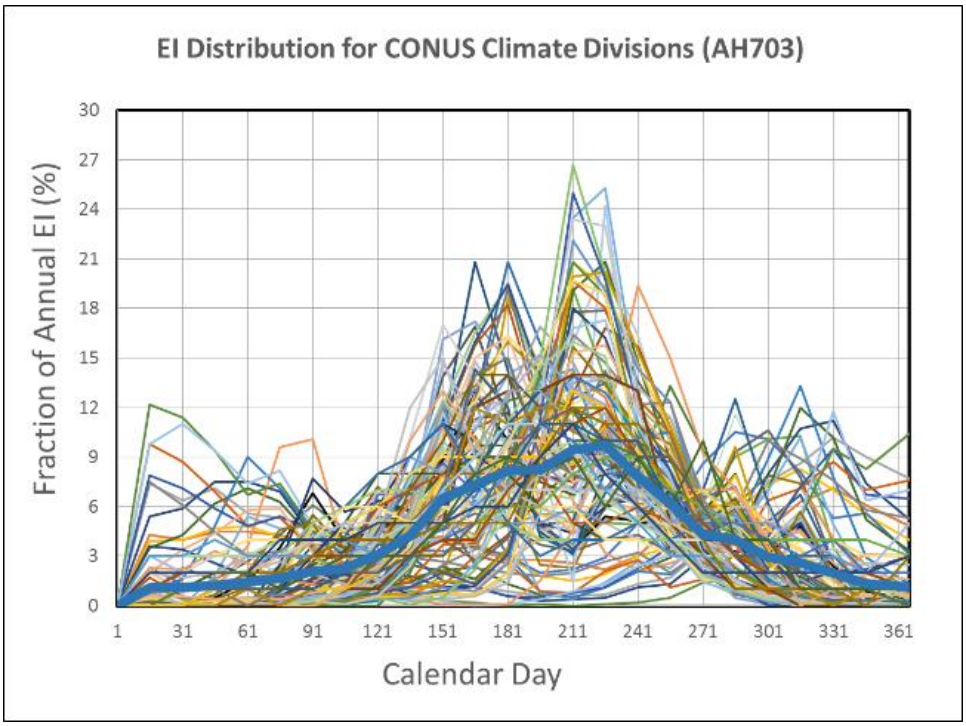

Figure 3-10 Half-Month EI Distribution by Climate Division for CONUS (AH703) with National Avg. (Blue)

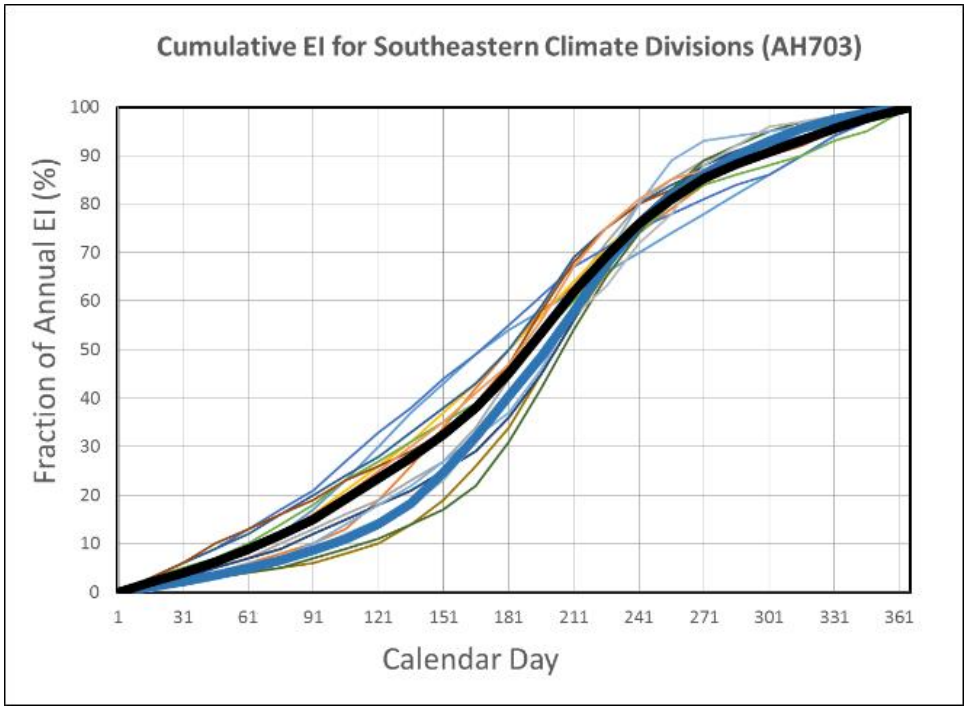

Figure 3-11 Half-Month Cumulative EI for the Southeast by Climate Division with Area-Weighted Avg. AH703 (Black) and National Avg. (Blue)

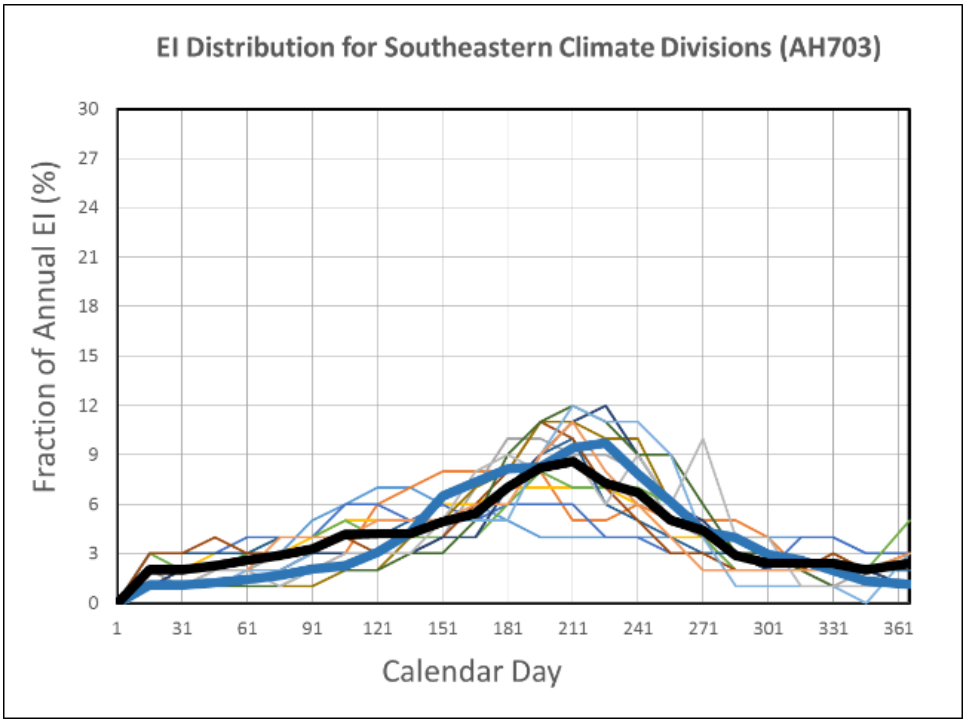

Figure 3-12 Half-Month EI Distribution for the Southeast by Climate Division with Area-Weighted Avg. AH703 (Black) and National Avg. (Blue)

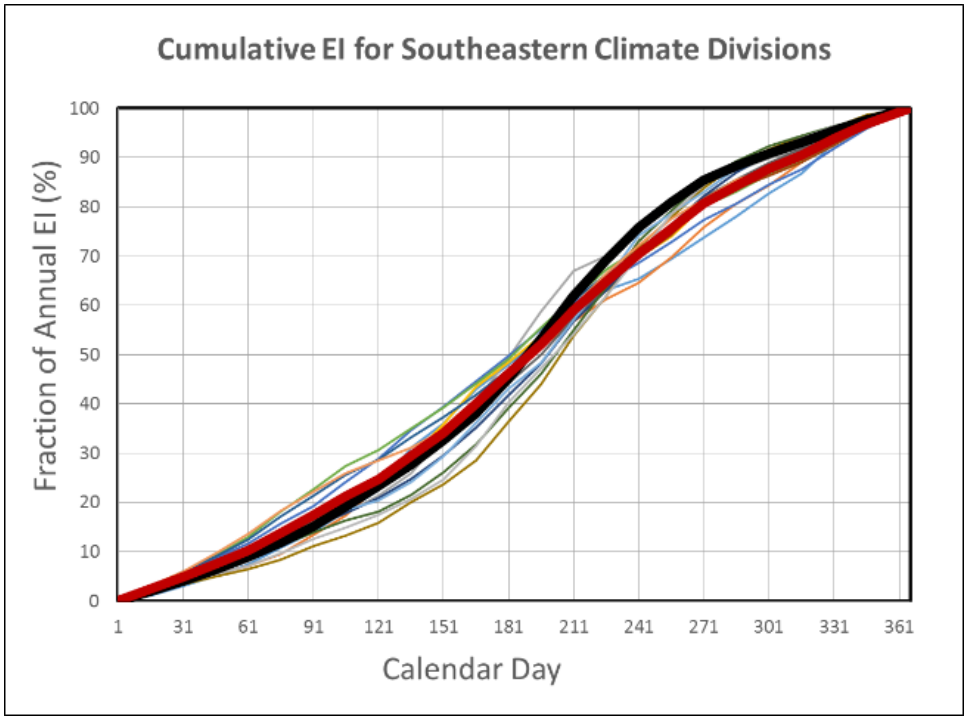

Figure 3-13 Half-Month Cumulative EI for the Southeast by Climate Division with an Area-Weighted Avg. for AH703 (Black) and for 25.10 Screened Stations (Red)

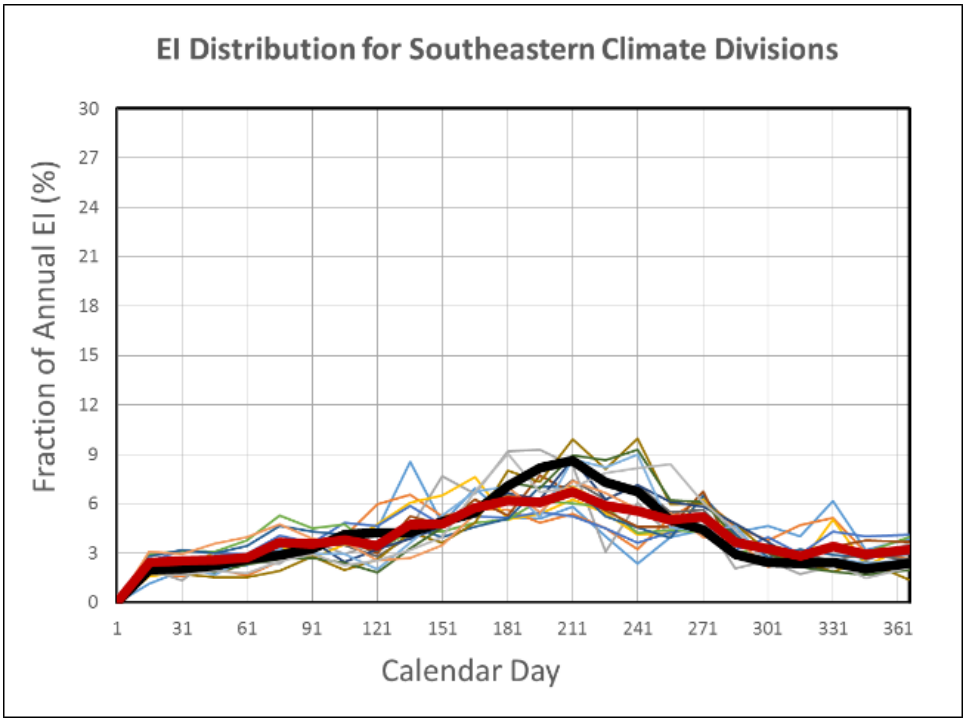

Figure 3-14 Half-Month EI Distribution for the Southeast by Climate Division with an Area-Weighted Avg. for AH703 (Black) and for 25.10 Screened Stations (Red)

It was expected that the variation of individual stations should decrease as pictured in Figures 3-11 and 3-12 due to more consistent EI patterns of the Southeast as compared to the rest of the nation. For the same area, probably a result of screening, the analysis was a much tighter fit along the weighted average than the analysis from AH703. A few things contributed to this including weaker data in AH703, densified spatial observations (more points of observation in a climate division for more consistent results), and lastly, the inclusion of small storms in the calculation of EI. The effect of small storms was most pronounced in Figure 3-14. The red line represented the general trend of new data as compared to AH703 in black. The most obvious change was the reduction of the peak in summer and the increase of EI values in the other three seasons. This was a graph of the fractional distribution of EI. If absolute values were presented (they were not since the focus of this section was on the actual distribution and timing of EI rather than the magnitude) one would notice that the inclusion of small storms—and the new methodology in general—increased EI estimations for all seasons. This was the primary reason for the monthly EI analysis, which does not need high temporal resolution, and was actually stronger for generalizing longer periods to better capture magnitude changes. However, this section seeks to understand the distribution of EI more than its magnitude.

From this analysis, it was still clear under the new methodology that summer and fall were the highest absolute periods of EI, but their relative difference was much reduced when a more accurate calculation of EI was utilized. It was likely that this dataset over-exaggerated the effect of small storms since quarter-hour station data wrongly separates precipitation into too many storm events. Those smaller events (with roughly the same energy content) were multiplied by different maximum intensities (Chapter 2) which produced different EI values than would actually be expected for each storm. Chapter 2 indicates this could shift 4-5% of EI values in those affected seasons by the measured difference in maximum intensity. This should be more than the observed difference in maximum intensity measurements reported by Hollinger et al. (2002), since these wrongly separated events (about 20% over a long period of time) were very small and maximum intensities could be quite different from the larger storm system from which they were separated.

3.4.3 ENSO and EI Magnitude

The most anticipated result from this study was the ability to forecast EI values based on the phase of ENSO variation. Therefore this analysis attempted to quantify the impact of ENSO on median monthly EI values and identify any particular spatial patterns. Median monthly EI values were computed for all months—irrespective of which month—in order to obtain the median for all climate variability observations from this dataset. The process was repeated for each phase of ENSO (El Niño and La Niña) while ignoring the neutral phase (weak SST variations). The results of this were shown in Figures 3-15, 3-16, and 3-17. All median values were determined using the longer station screening method (25.10). Relative differences for the respective ENSO phases were included in Figures 3-18 and 3-19. It was clear that ENSO impacted the median monthly EI, and a more thorough analysis was included in Section 3.4.5 to determine the mechanisms behind it.

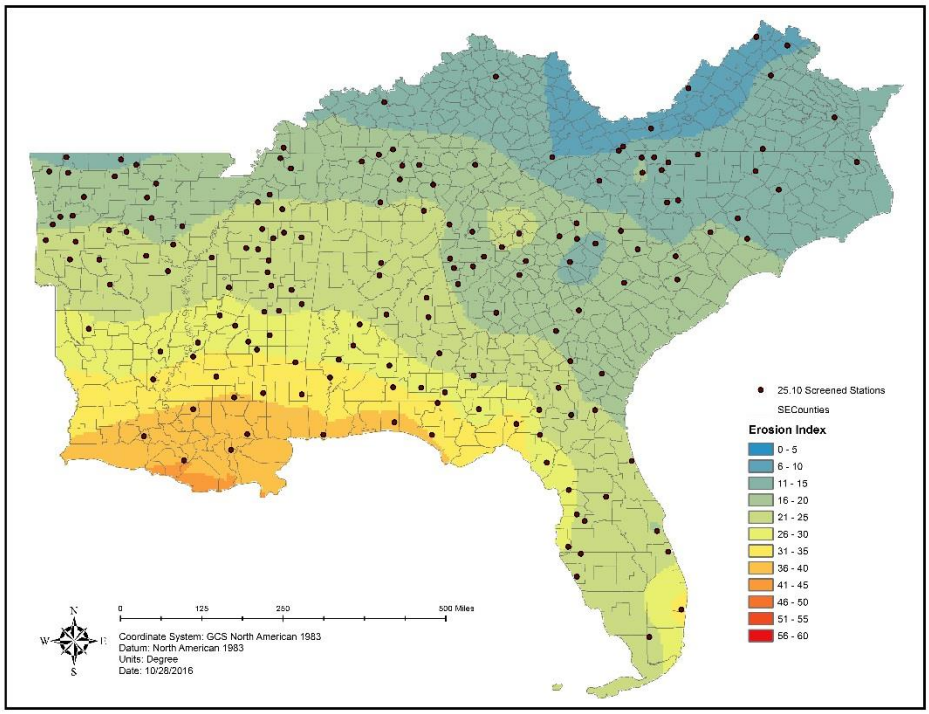

Figure 3-15 Median Monthly EI for 25.10 Screened Data

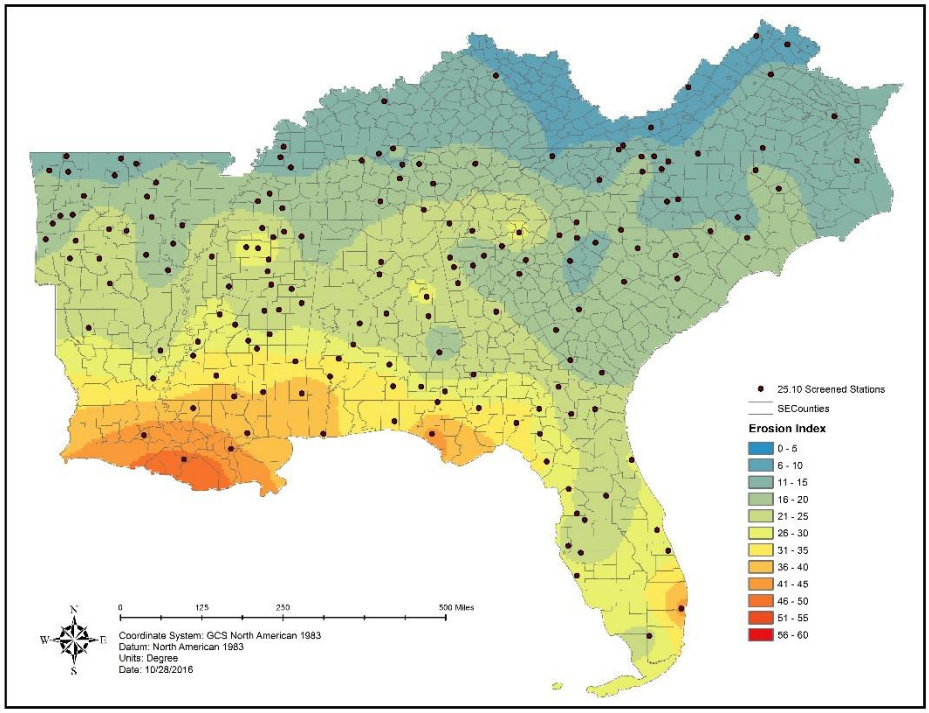

Figure 3-16 El Niño Median Monthly EI for 25.10 Screened Data

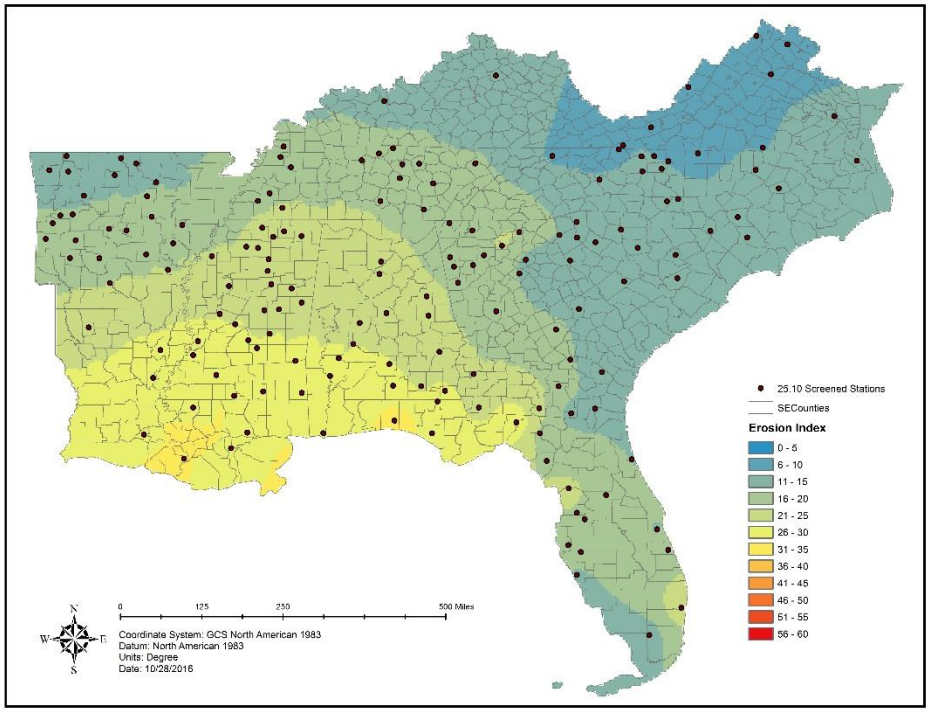

Figure 3-17 La Niña Median Monthly EI for 25.10 Screened Data

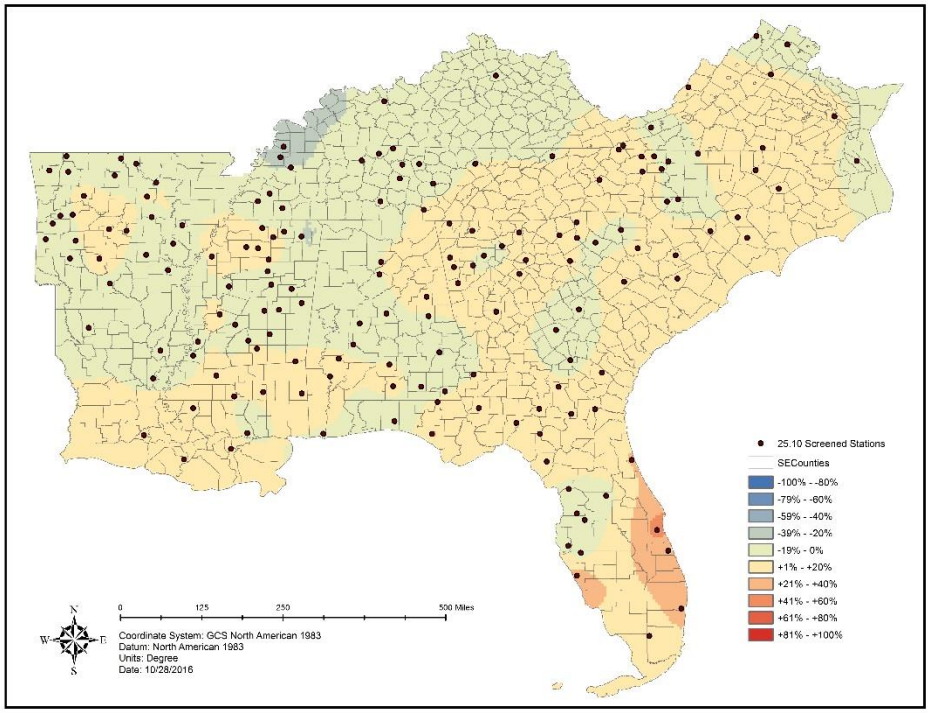

Figure 3-18 Relative Differences of El Niño from Normal Median Monthly EI

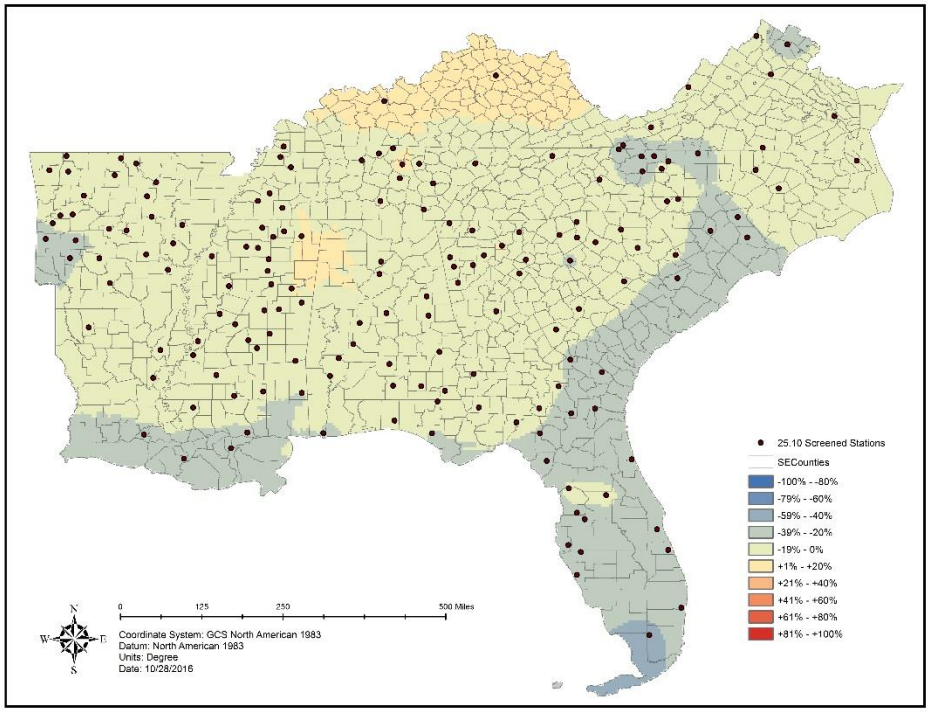

Figure 3-19 Relative Differences of La Niña from Normal Median Monthly EI

In general, ENSO had the strongest effect on the Gulf and Atlantic Coasts. El Niño tended to increase EI, and La Niña tended to decrease EI. Slight opposite trends were observed in both El Niño and La Niña as distance from the coast increased. This may be influenced by few observations in Kentucky (3) and Virginia (5). What was important to note about these observations was the number of stations in the areas of interest. It was likely that there were decreases related to El Niño because scores of stations were located in the light green areas. La Niña only has 3 stations in areas of observed increase, and two were located in a particularly sparse distribution of observations. In summary, **on the basis of median monthly EI, El Niño seems to polarize the EI values of the Southeast with higher EI associated with coastal rain and wind patterns of El Niño. La Niña, on the other hand cause a more even decrease of EI in all parts of the Southeast, still with areas along the coast affected the most.**

3.4.4 ENSO and EI Distribution

The second analysis looked at the effect of ENSO on distribution. With an understanding of general impacts of ENSO on EI magnitude, it may be possible to determine if those magnitudes were simple increases and decreases or if they were accompanied by shifts in the timing of erosivity. To do this, the analysis in Section 3.4.3 was performed, but the month of the year was considered. This was done for every month of the year, but mapping this would be cumbersome, so mapped data was not provided for monthly results and seasonal results were presented in gridded format for better visualization. Also, to reduce the number of figures, only relative differences were included, while the absolute median monthly EI values for each season was included in the appendix. Figures 3-20, 3-21, 3-22, and 3-23 showed the relative difference of median monthly EI for each season for El Niño. Figures 3-24, 3-25, 3-26, and 3-27 corresponded to La Niña.

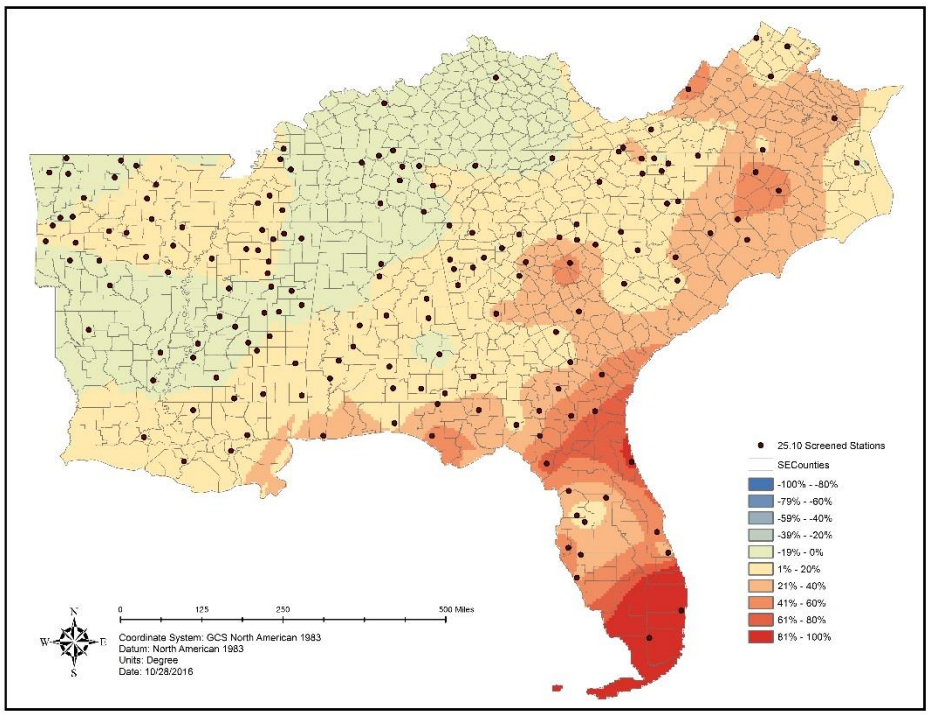

Figure 3-20 Relative Differences of Median Monthly EI from El Niño for Winter

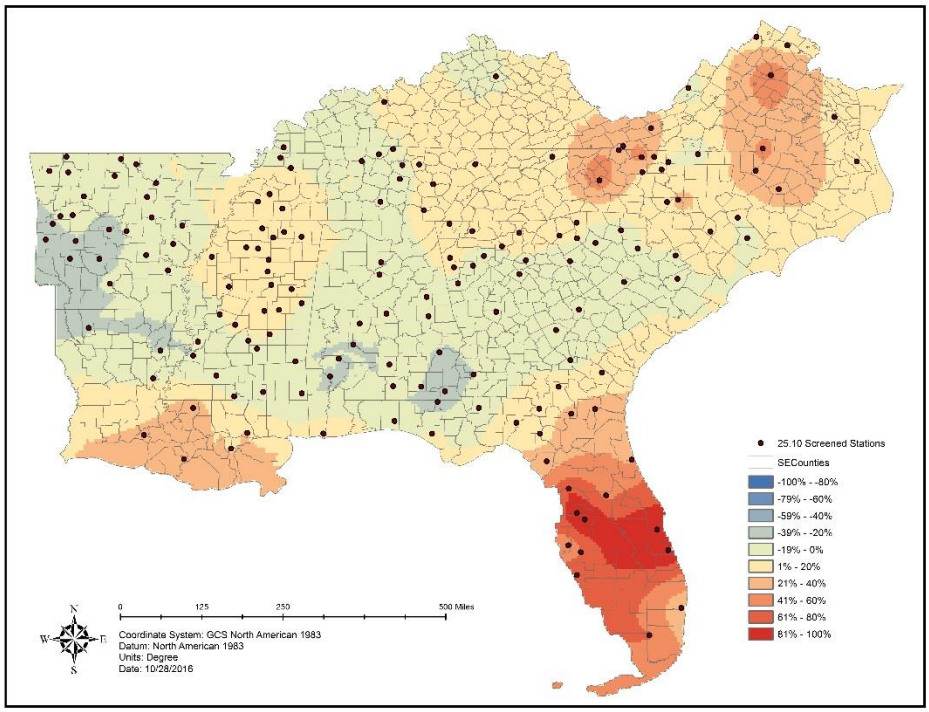

Figure 3-21 Relative Differences of Median Monthly EI from El Niño for Spring

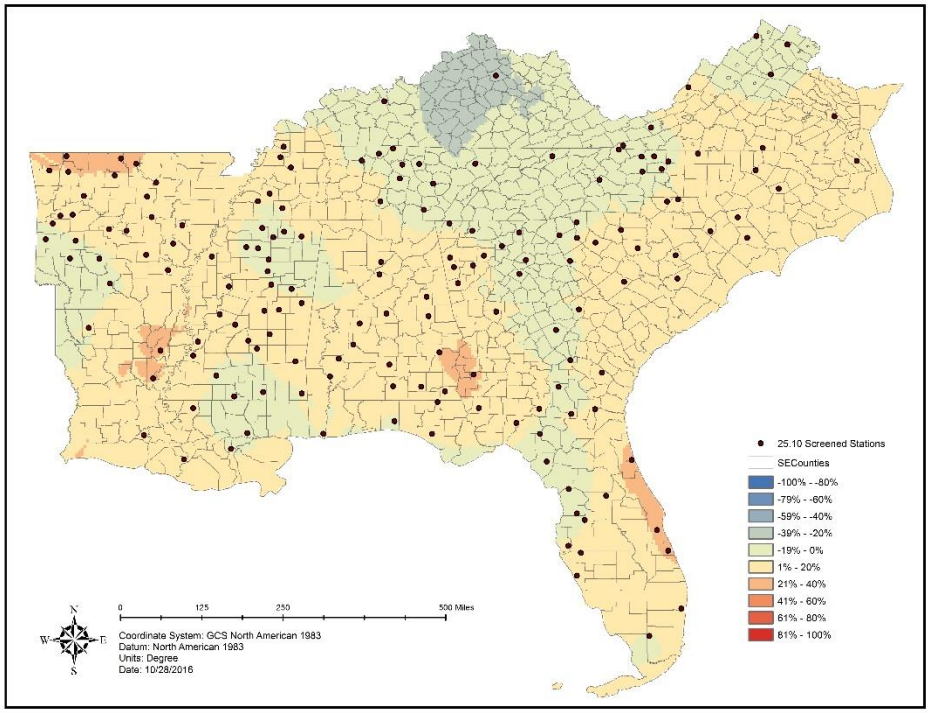

Figure 3-22 Relative Differences of Median Monthly EI from El Niño for Summer

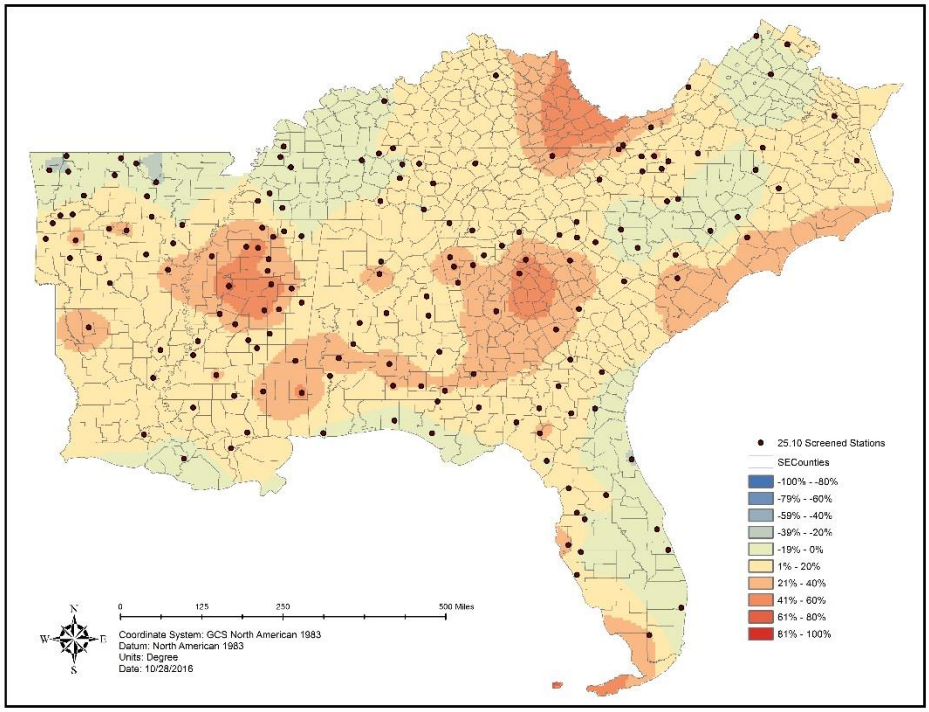

Figure 3-23 Relative Differences of Median Monthly EI from El Niño for Fall

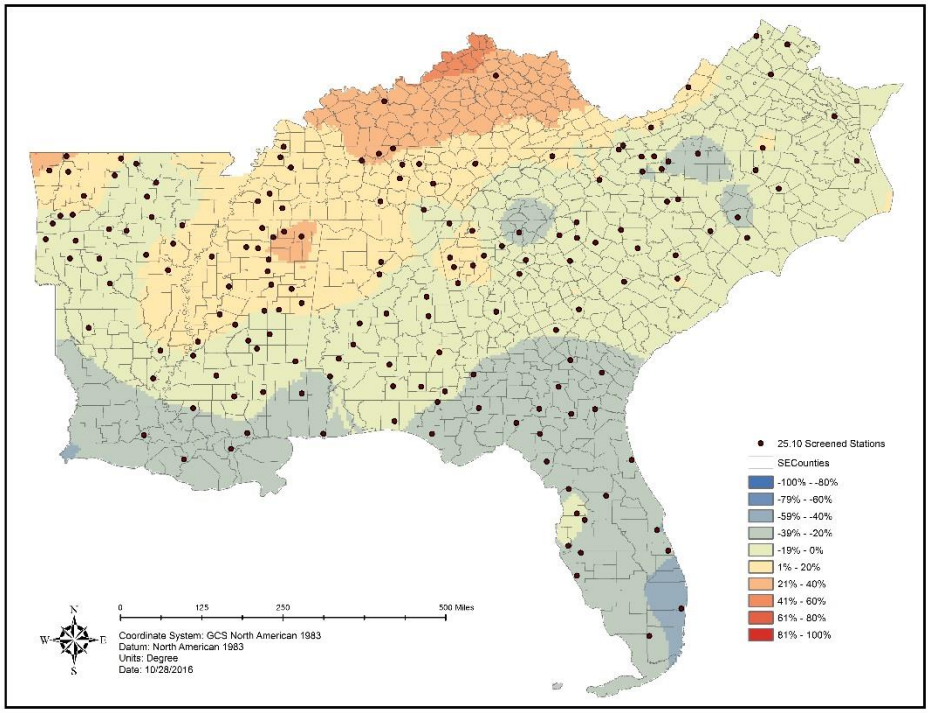

Figure 3-24 Relative Differences of Median Monthly EI from La Niña for Winter

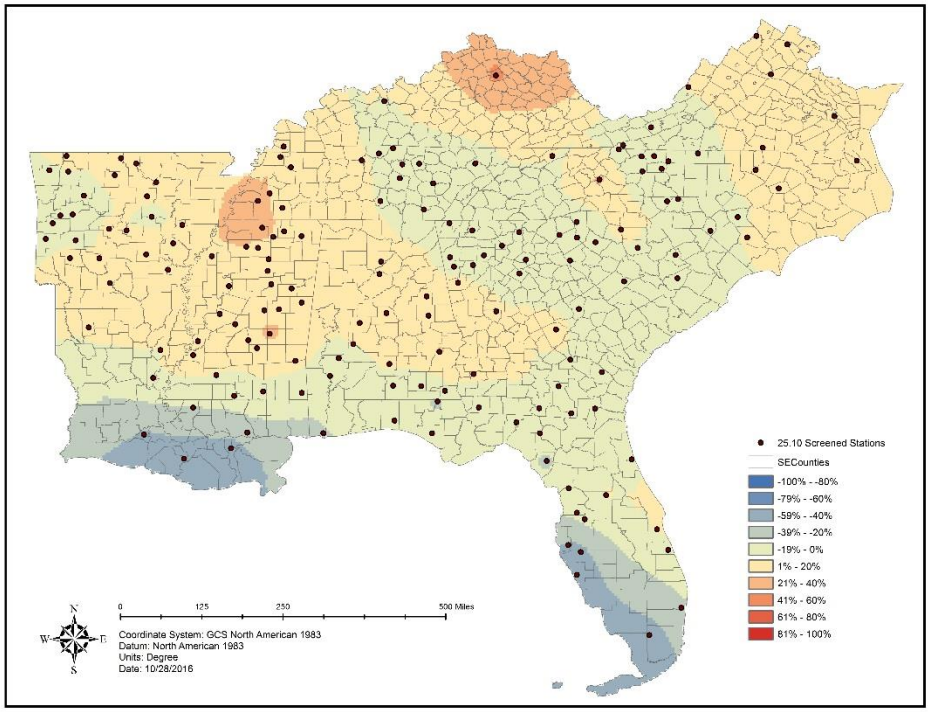

Figure 3-25 Relative Differences of Median Monthly EI from La Niña for Spring

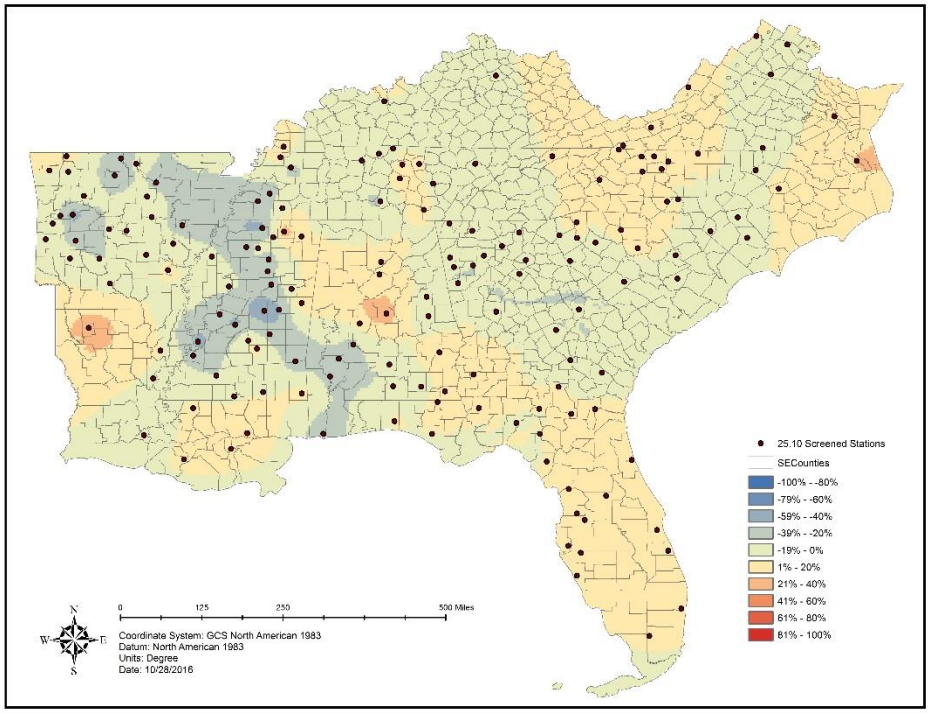

Figure 3-26 Relative Differences of Median Monthly EI from La Niña for Summer

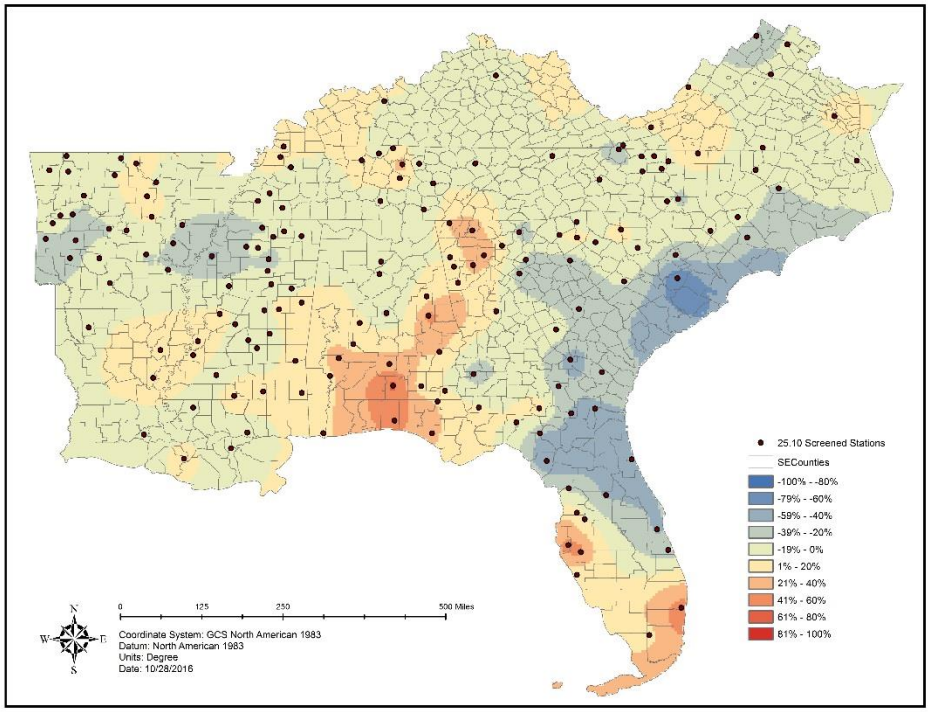

Figure 3-27 Relative Differences of Median Monthly EI from La Niña for Fall

From all of the above figures, it was clear that distribution changes were varied, and although the cumulative effects will support the general observations from Section 3.4.3, the timing of EI throughout the year was changing. El Niño was causing tremendous increases in both winter and spring for Florida. The Atlantic Coast appears to have strong influences in winter and fall, but there were few stations in these areas of increase to support gridded findings. A particularly interesting finding was that strong decreases in spring EI was detected in most central areas of the Southeast even approaching the coast. A significant portion of spring rain for the Southeast was frontal in nature, and it was possible that El Niño driven wind patterns were changing where these fronts meet or at least changing the temperament of that physical interaction. La Niña, consistently suppressed EI values for most of Georgia and South Carolina, as well as for most seasons in North Carolina and lower portions of Louisiana. A very strong decrease was detected for the Atlantic Coast in fall, which could be related to hurricane related EI values. All coastal areas experienced significant decreases in winter and spring while inland areas experienced stronger erosivity.

Differences within the seasonal EI distribution due to ENSO were evaluated for significance. This was presented as a lumped analysis in Section 3.4.3, but the variation within each season was considered for this analysis. The data was partitioned by season, then the JRFit analysis was performed using months as clusters. Clustered months meant that monthly EI values were used by this method to estimate median monthly EI under each phase of ENSO for each data partition and to determine the significance of the difference. To reduce the amount of data presented, only the p-values were reported for each individual station and the gridded p-values, which were used to determine spatially significant patterns as opposed to significance of ENSO for each station. Figures 3-28, 3-29, 3-30, and 3-31 showed the p-values for each station and gridded areas that were significantly impacted. These figures indicated that only winter was approximated well by the lumped approach. Areas of red indicated no significant differences. Therefore, the means by which ENSO impacts spring, summer, and fall seasons were not consistent (for most stations) among its component months and may require additional analysis of each month to determine influences of ENSO on EI distribution for these period. Ultimately, this does not contradict the earlier findings of ENSO impacts on seasonal EI, but it does

mean that within that time period these results were highly varied. All seasons had some stations that experienced consistent, significant differences.

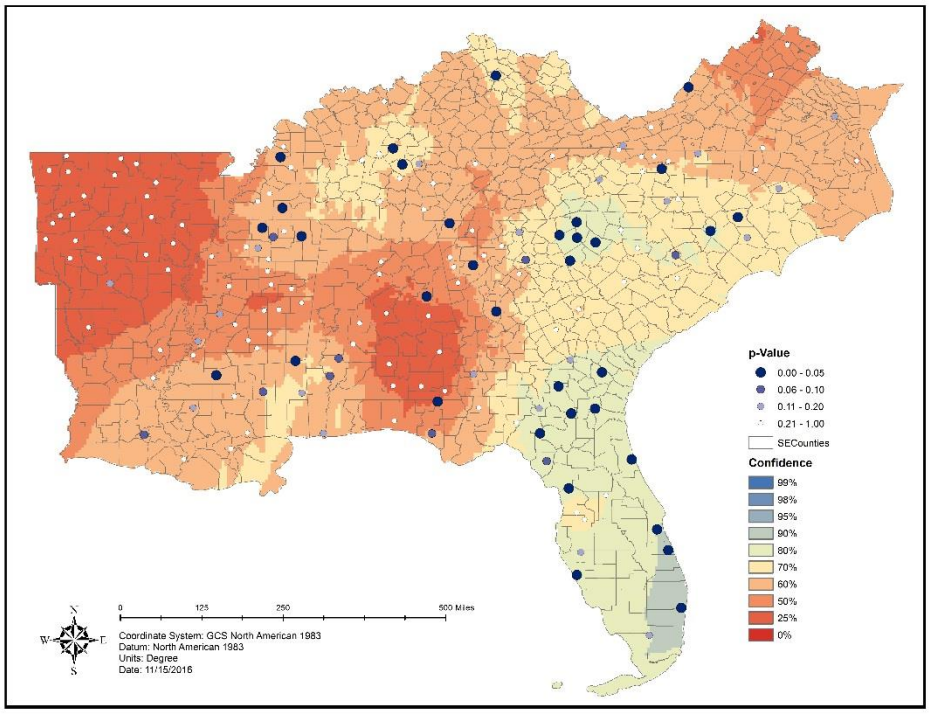

Figure 3-28 JRFit Test Results for Winter (Clustered Months)

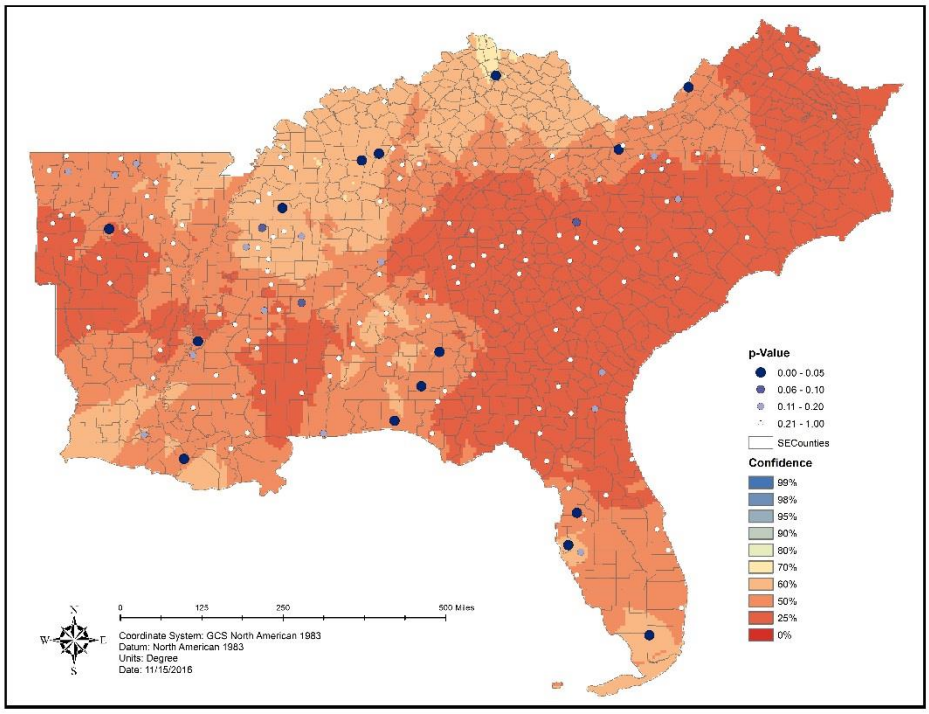

Figure 3-29 JRFit Test Results for Spring (Clustered Months)

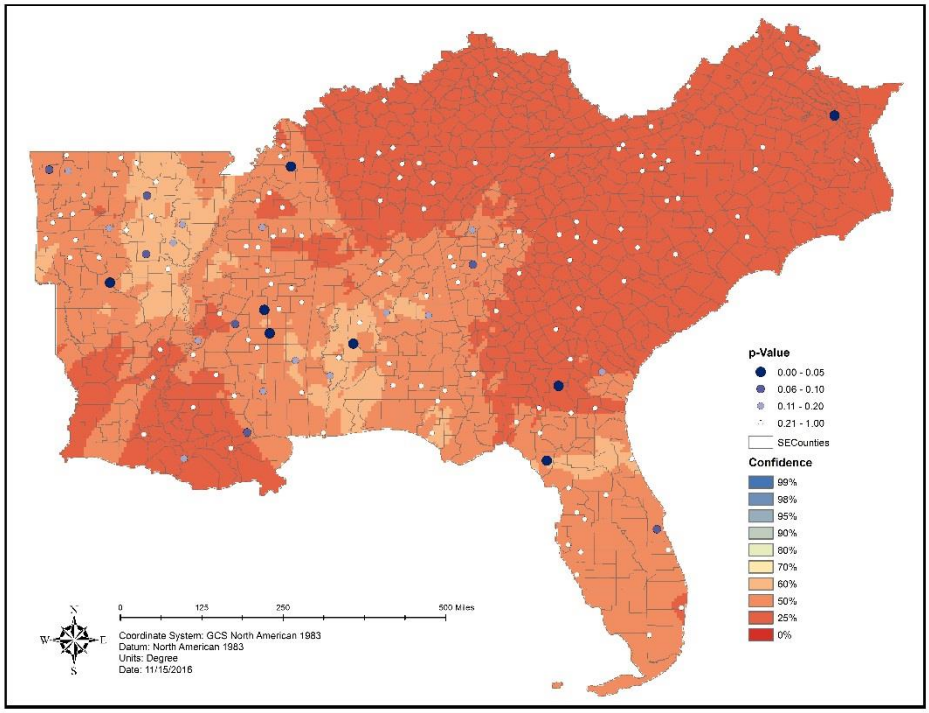

Figure 3-30 JRFit Test Results for Summer (Clustered Months)

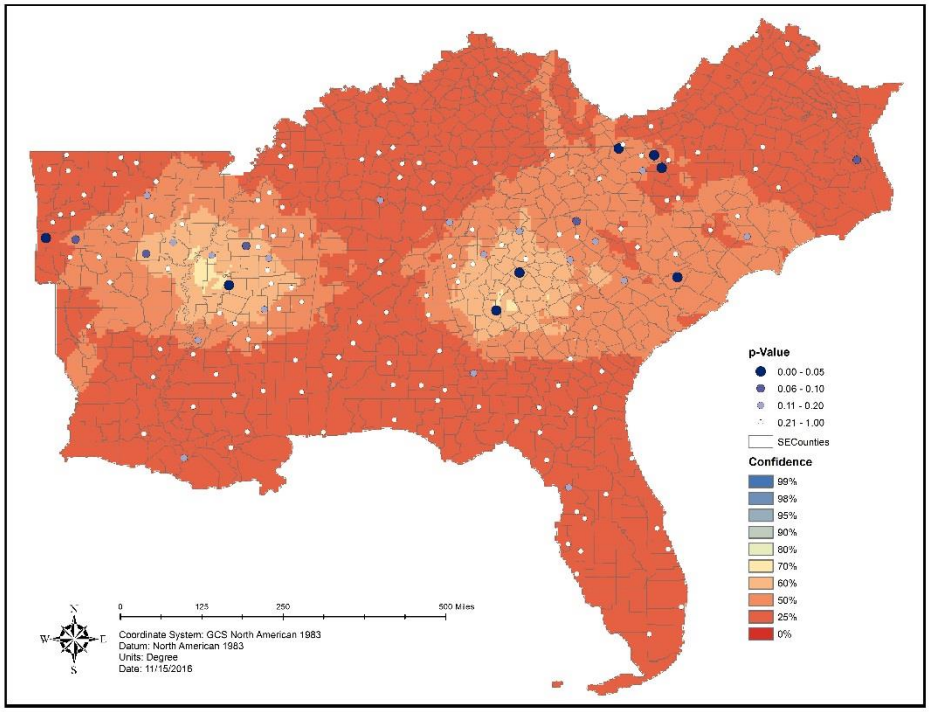

Figure 3-31 JRFit Test Results for Fall (Clustered Months)

3.4.5 ENSO and Precipitation Characteristics

The final analysis evaluated the effect of ENSO on precipitation characteristics—the mechanisms that drive EI calculation. **Identifying those mechanisms sensitive to ENSO which are driving EI fluctuations was the reason for this analysis.** The characteristics tested include: number of events, precipitation depth, kinetic energy, EI, EI rate, mean depth, mean kinetic energy, mean EI, and median I_{30}. Figures 3-32, 3-34, and 3-36 were provided for the most significant influences of ENSO for all precipitation characteristics. Figures 3-33, 3-35, and 3-37 demonstrate the impact of clustering seasons as opposed to months. Clustering seasons always produced higher p-values (less significant differences) since they sampled longer periods of time, which included a larger range of values for the tested parameter. This caused more overlapping values, and therefore, less confidence in the difference. This was the main reason for evaluating both the monthly and seasonal cluster effect on the analysis.

Figures 3-38, 3-39, 3-40, 3-41, 3-42, and 3-43 looked at a wider scope of potentially affected characteristics. One aspect of particular interest was not necessarily the sum total of depth, energy, or EI but rather the smaller increments in which these measures were observed—the storms themselves. It was evident that ENSO impacted the number of storms over which depth, energy, EI, etc. were observed. A few storm averaged parameters were analyzed—depth, energy, and EI—for changes with respect to the number of events observed. Perhaps more interesting than all the other results was the issue of energy and maximum intensity and their relationship to EI. ENSO had a strong influence on depth and energy, and this was confirmed mathematically since energy calculations, especially those based on the AH537 energy equation, were almost exclusively driven by the absolute depth of precipitation rather than intensity. This happened because the maximum impact of the intensity on energy was reached very quickly and raindrop size did not continue to increase beyond 3 inches hr^{-1}. About 80% of this impact was reached before 1.2 inches hr^{-1} using the AH537 equation, and similar results would be obtained using any energy equation (McGregor et al., 1995). Small storm energies vary due to the observed lognormal rate of increase in energy with linearly increasing intensities. Therefore, **depth—not intensity—was a controlling factor of energy for moderate and large storms and ENSO effects on energy closely followed those on depth.**

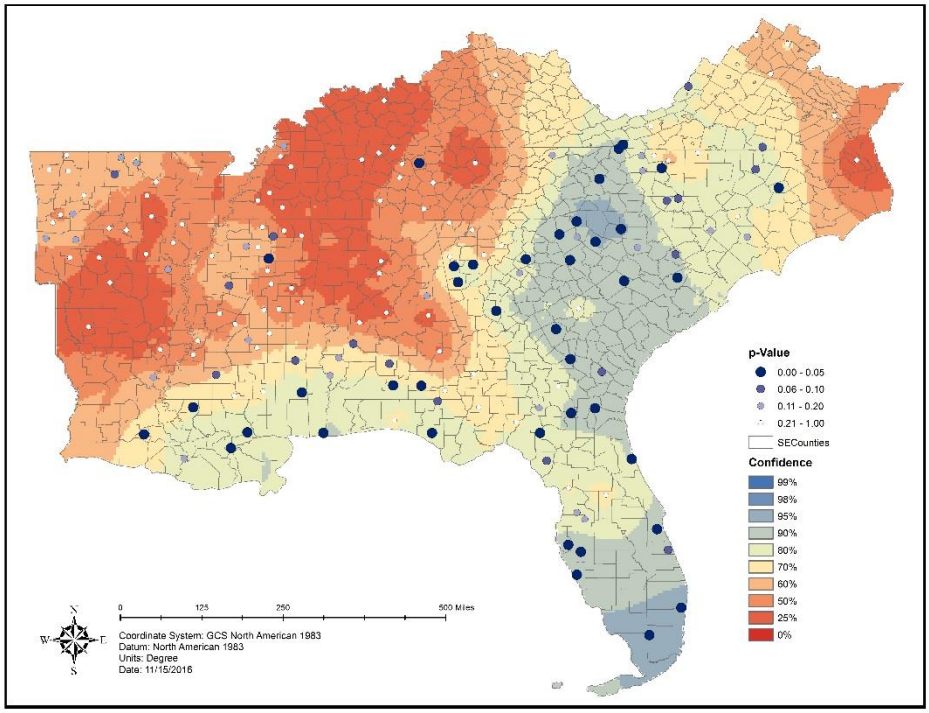

Figure 3-32 JRFit Test Results for ENSO Influence on Depth (Clustered Months)

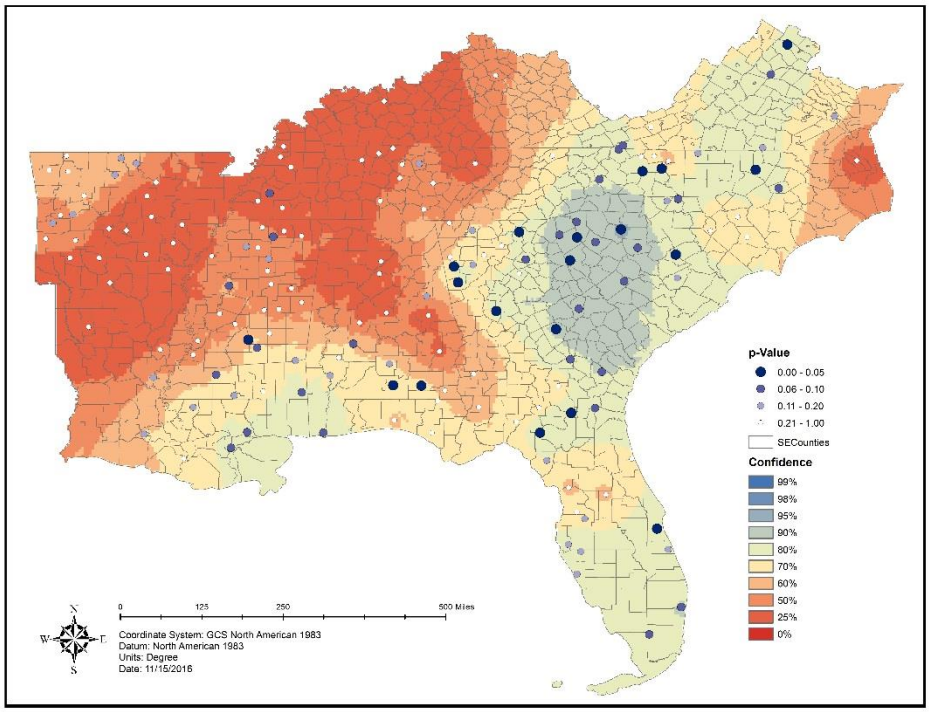

Figure 3-33 JRFit Test Results for ENSO Influence on Depth (Clustered Seasons)

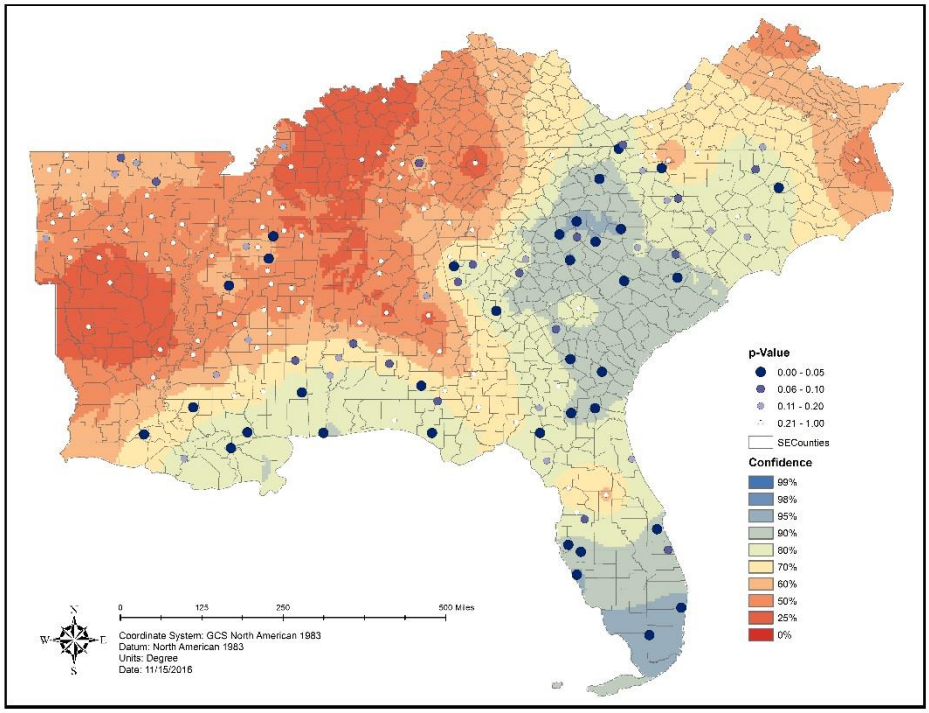

Figure 3-34 JRFit Test Results for ENSO Influence on Energy (Clustered Months)

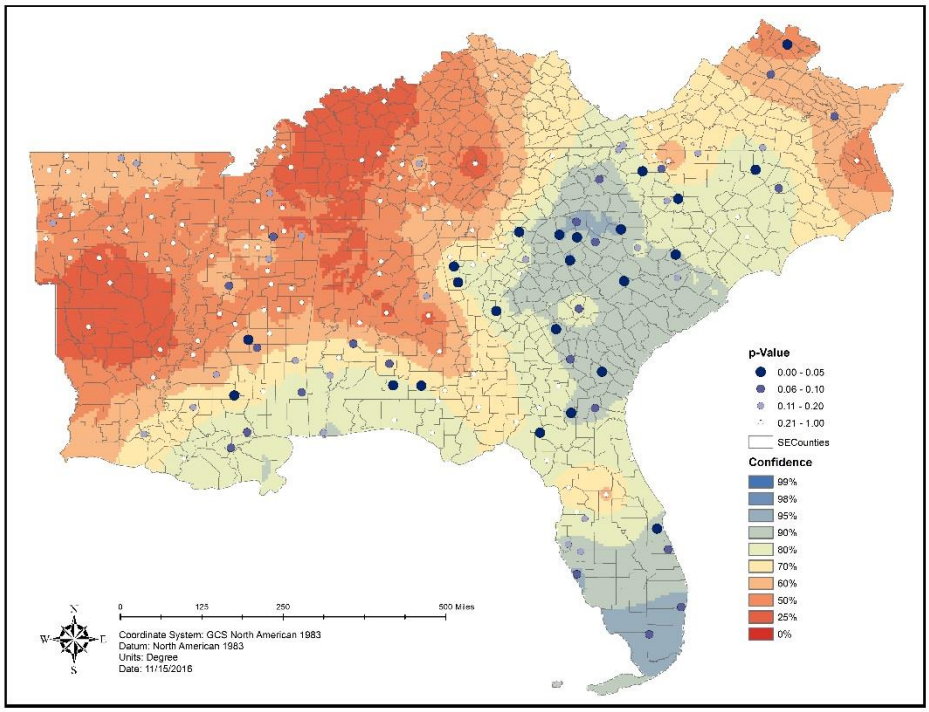

Figure 3-35 JRFit Test Results for ENSO Influence on Energy (Clustered Seasons)

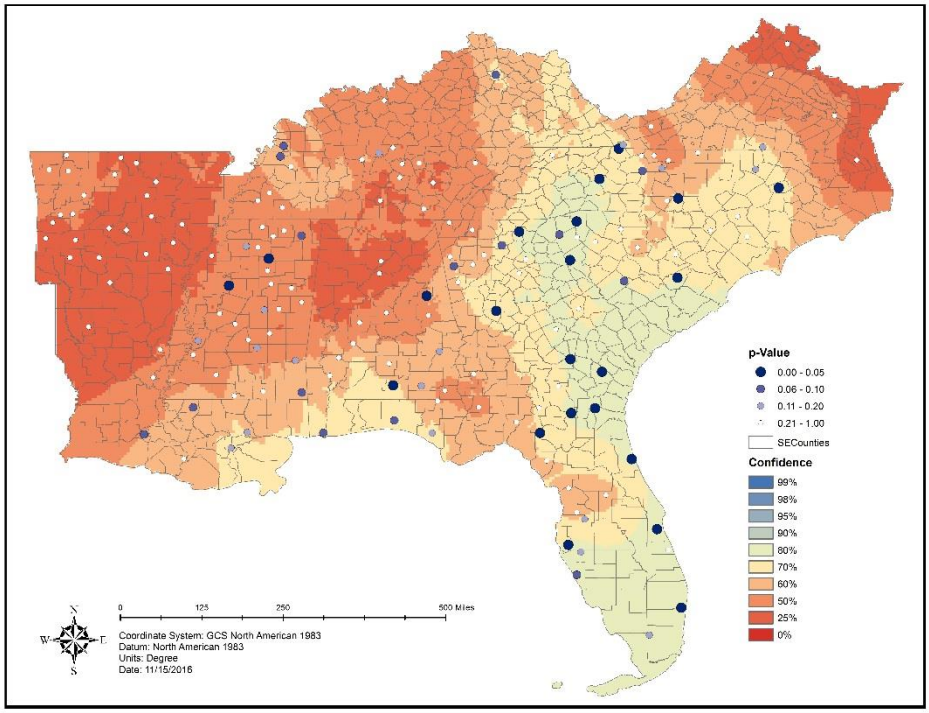

Figure 3-36 JRFit Test Results for ENSO Influence on EI (Clustered Months)

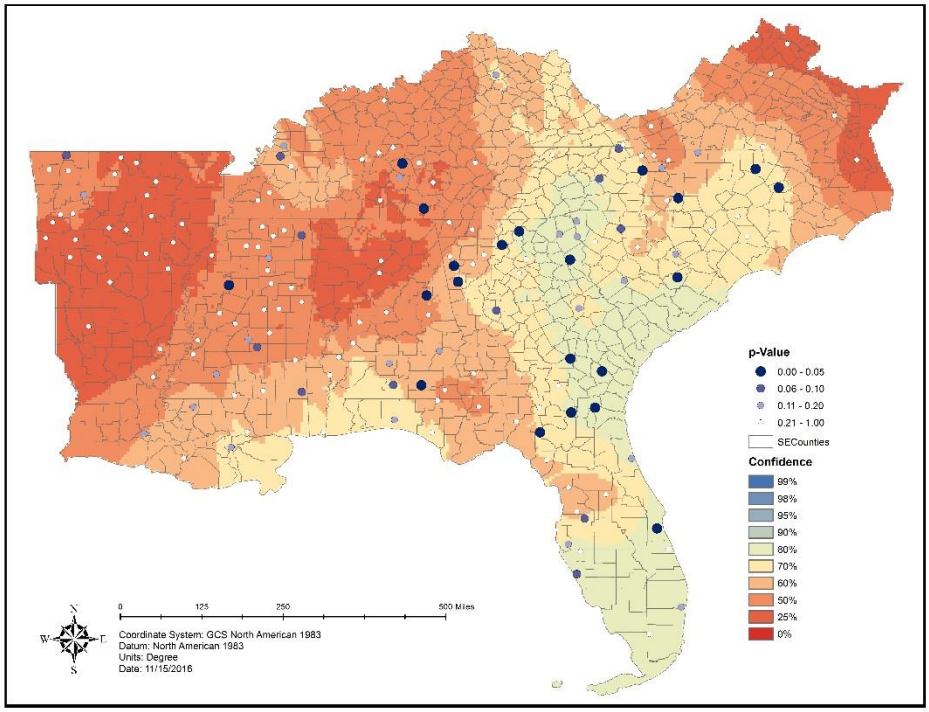

Figure 3-37 JRFit Test Results for ENSO Influence on EI (Clustered Seasons)

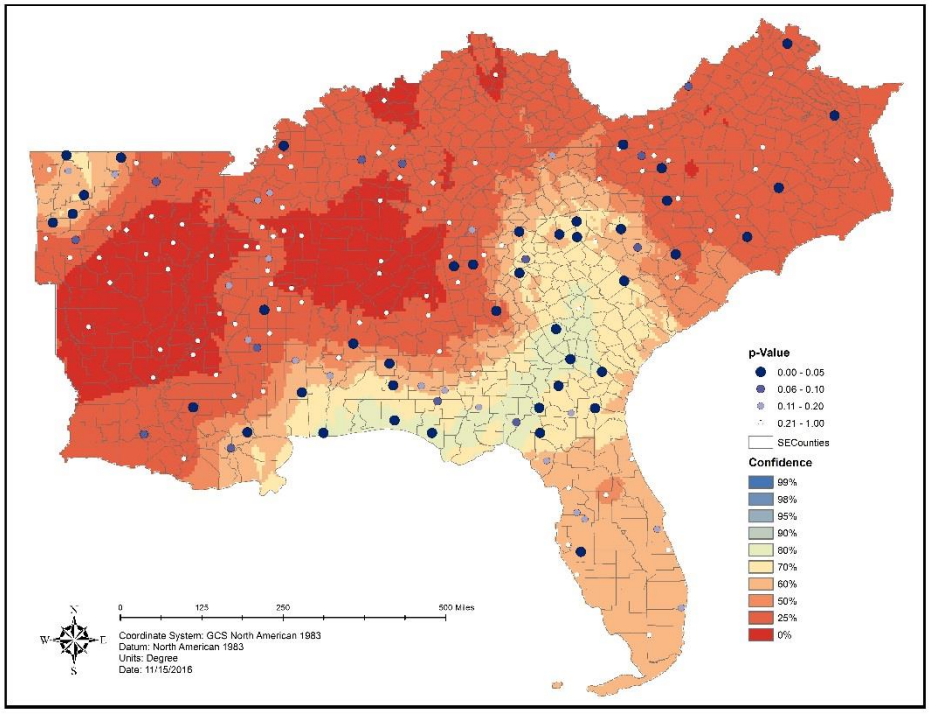

Figure 3-38 JRFit Test Results for ENSO Influence on Number of Events

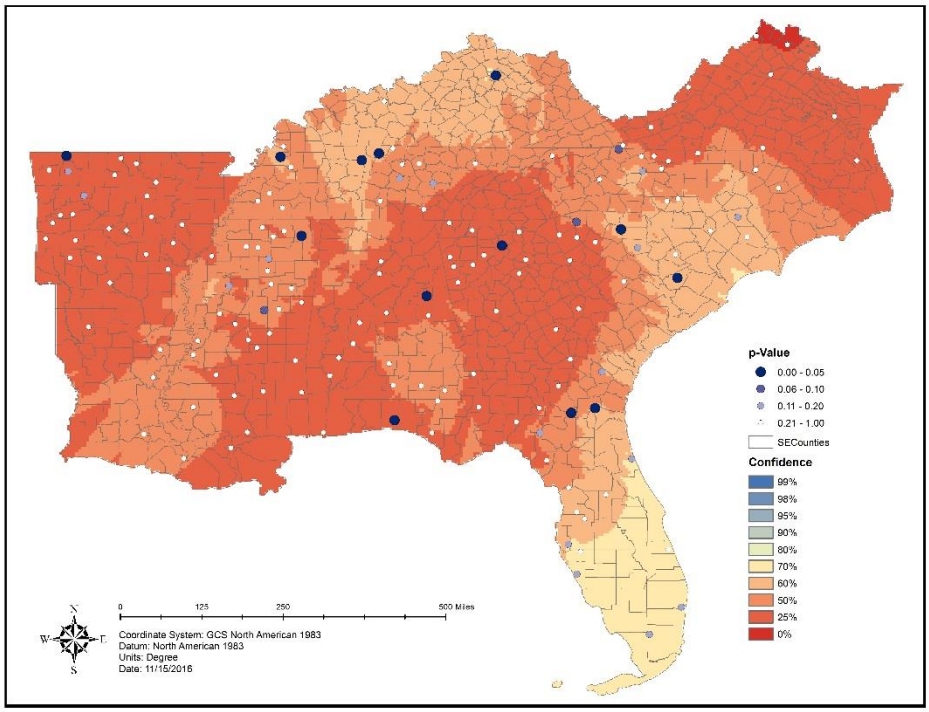

Figure 3-39 JRFit Test Results for ENSO Influence on EI Rate

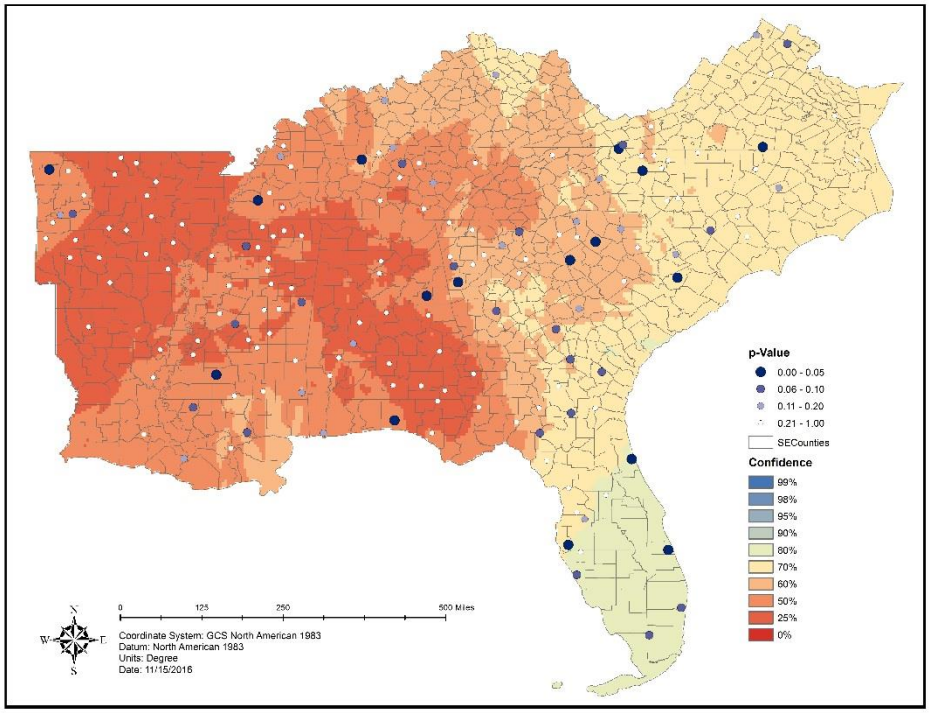

Figure 3-40 JRFit Test Results for ENSO Influence on Mean Depth

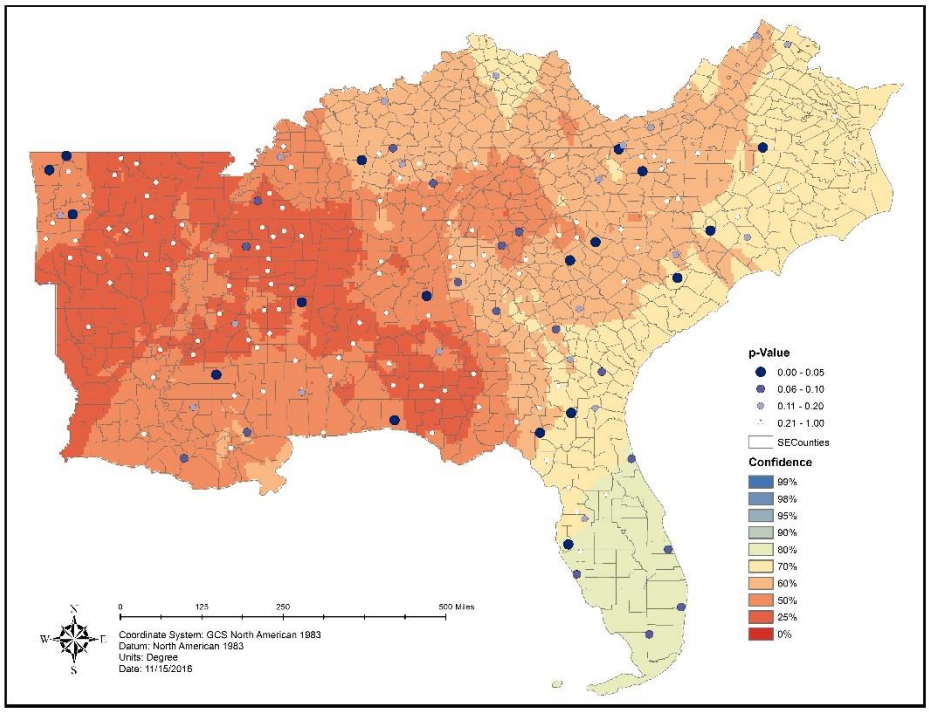

Figure 3-41 JRFit Test Results for ENSO Influence on Mean Energy

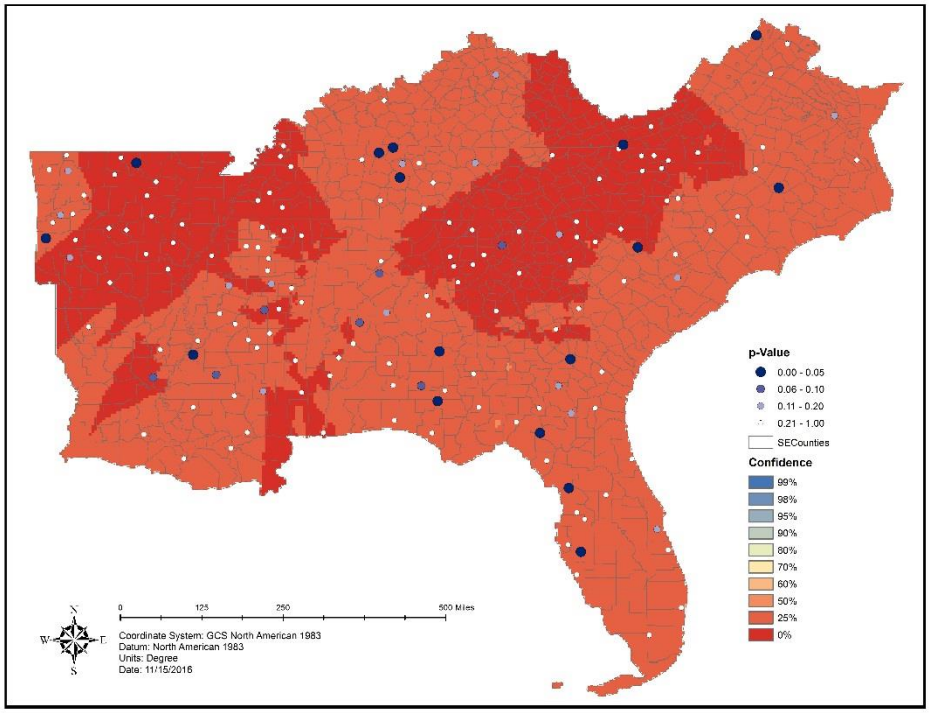

Figure 3-42 JRFit Test Results for ENSO Influence on Median I_{30} for Storms Greater than 1.0 Inch

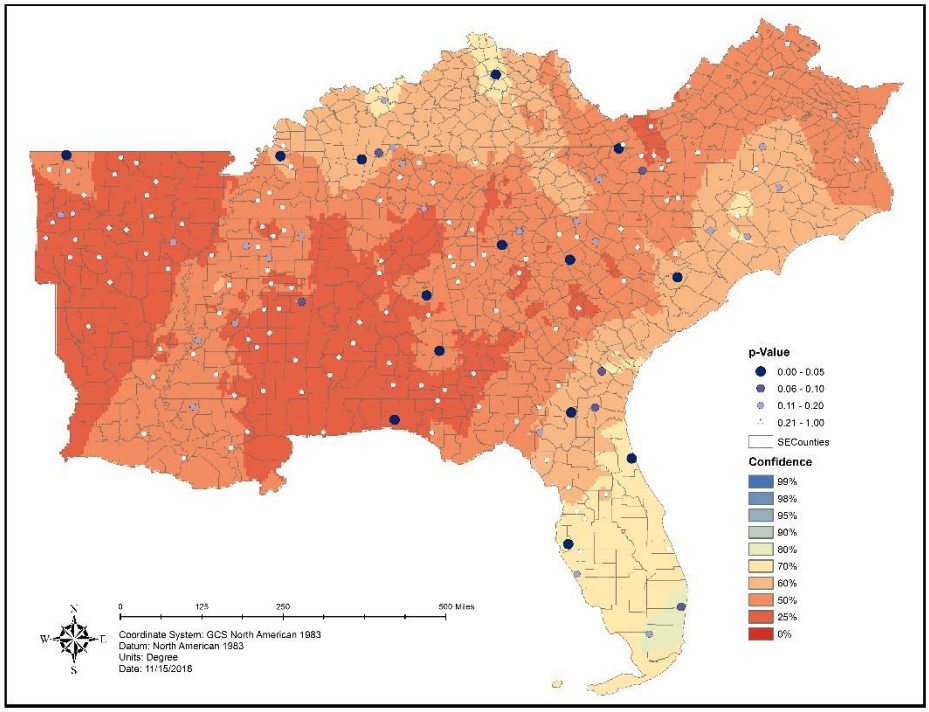

Figure 3-43 JRFit Test Results for ENSO Influence on Mean EI

3.5 Conclusions

Two key measures for climate variability studies were benchmarked including monthly EI magnitudes and their distribution. I reiterate the significance of unadjusted monthly EI values capable of producing erosivity values comparable if not superior to reliable observations (Chapter 2; McGregor et al., 1980 and 1995). Benchmarked EI distribution included omitted small storms that contributed significantly to EI for this methodology and dataset. Although these storms may not contribute more than a few percentage points to annual EI observed by breakpoint stations (McGregor et al., 1995), quarter-hour stations wrongly produced too many of these storms—accounting for about 8.7% of all erosivity, which was more than McGregor's observation of about 3.5%. Even if the percentage were lower than this, these storms would still need to be included, since they were not evenly distributed throughout the year, and most storms occurred in seasons of relatively low erosivity. Therefore, the relative impact of these small storms is significant for variability studies such as this one. **The completion of these benchmarking exercises provided trustworthy results for variability studies and analyses, especially since some have raised concerns regarding quarter-hour station data and its quality.**

Five variability components of EI were studied including two intra-annual components with results presented in Sections 3.4.1 and 3.4.2 and three inter-annual variability analyses related to ENSO. The latter included ENSO effects on EI magnitude (strength of change), EI distribution (timing of EI throughout the year), and the characteristics of precipitation (mechanisms behind erosivity). In general, intra-annual EI was very consistent, and even amidst a highly varying climate, these patterns were easily recognized. Summer, continued to be the period of the highest EI values across all southeastern states, and winter continued to be the lowest. This was true regardless of how strong ENSO has been and whether or not it was an El Niño or La Niña phase. However, especially after the inclusion of small events, the margins between these two can be highly affected by ENSO for specific regions, namely coastal areas. El Niño winters and springs can see anywhere from 20% to 80% increases in Florida, and La Niña seasons anywhere along the coast can expect significant decreases -20% to -60% for median monthly EI values in those periods. **These findings supported the conclusion that ENSO had a noticeable effect on both the magnitude and distribution of EI throughout the year.**

Observed differences from ENSO variability was then tested using the powerful statistical test, JRFit, to determine the most significant influences of ENSO on erosivity mechanisms. ENSO-driven precipitation qualities were felt most strongly along the Gulf and Atlantic Coast and as far inland as parts of Kentucky and Virginia. Characteristics which were most highly impacted included depth, energy, and EI. Only a few stations were found to have significant differences in I_{30} and EI rate (normalized for depth), which indicates that ENSO may not be totally responsible for variations in EI. **This creates the need for a study of a mid-term variability study such as AMO and PDO/PMO.**

The most practical outcome of this study is the implication of climate variability on BMPs related to soil conservation. The critical considerations to give regarding these implications include a) changes in average erosivity over a period of time b) changes in extreme erosivity over a short time or single event and c) changes in timing of erosivity. Both 'a' and 'b' should be considered particularly regarding sedimentation in water bodies. El Niño increased the median monthly EI for most locations across the Southeast and impacted different areas differently in each season of the year (La Niña generally had the reverse effect). Therefore BMPs aiming to meet specific targets within any given year should consider the ENSO phase in order to meet that target over a long period of time. ENSO was determined to have a strong effect on mean storm EI primarily in some stations across Florida, Georgia, South Carolina, and Kentucky. Therefore, BMPs related to maximum event tolerances should incorporate ENSO differences for those cases. This may be most important for easily eroded soils in these areas in which larger storms could cause mass wasting events. In order to determine this, more research should be directed at determining EI thresholds above which this occurs. Lastly, the type 'c' impact on BMPs is of the greatest concern and has the potential to impact soil conservation most. Since ENSO was shown to have a strong impact on the timing of EI throughout the year, agricultural operations (tilling, planting, harvest, residue cover, crop type, rotation, etc.) should incorporate ENSO prediction components for maximum effect. **The results of this variability study indicate that significant improvements in soil conservation may be achieved with the incorporation of ENSO-driven prediction of erosivity in the Southeast (and eventually prediction of other variability cycles and climate change) and the implementation of corresponding BMPs.**

3.6 Chapter References

Hastings, B. K., Breshears, D. D., Smith, F. M., 2005. Spatial variability in rainfall erosivity versus rainfall depth: implications for sediment yield. Vadose Zone Journal 4, 500-504. doi:10.2136.vzj2004.0036

Hollinger, S. E., Angel, J. R., and Palecki, M. A., 2002. Spatial distribution, variation, and trends in storm precipitation characteristics associated with soil erosion in the united states. Contract report CR 2002-08. Illinois State Water Survey. Champaign, IL. available at: www.isws.illinois.edu/pubdoc/CR/ISWSCR2002-08.pdf.

Kloke, J., and McKean, J. W., 2014. Nonparametric statistical methods using R. CRC Press, Taylor & Francis Group, FL.

Kloke, J.D., McKean, J.W., and Rashid, M., 2009. Rank-based estimation and associated inferences for linear models with cluster correlated errors. Journal of the American Statistical Association, 104 (485), 384-390.

McGregor, K.C., Bingner, R.L., Bowie, A.J., Foster, G.R., 1995. Erosivity index values for northern Mississippi. Research Gate 38, 1039–1047.

McGregor, K.C., Mutchler, C.K., Bowie, A.J., 1980. Annual R values in north Mississippi. Journal of Soil and Water Conservation 35(2), 81–84.

Renard, K.G., Foster, G.R., Weesies, G.A., McCool, D.K., and Yoder, D.C., 1997. Predicting soil erosion by water: a guide to conservation planning with the Revised Universal Soil Loss Equation (RUSLE). Agriculture Handbook 703. U.S. Department of Agriculture. Washington, DC.

Singh, S., Srivastava, P., 2015. Climate variability and irrigation impacts on stream-aquifer dynamics in the Apalachicola-Chattahoochee-Flint River Basin. Auburn, Alabama. Auburn University, Department of Biosystems Engineering. available at: https://etd.auburn.edu/handle/10415/4845.

Trenberth, K.E., Dai, A., Rasmussen, R.M., Parsons, D.B., 2003. The changing character of precipitation. Bull. Amer. Meteor. Soc. 84, 1205–1217. doi:10.1175/BAMS-84-9-1205

USDA. 2008. User's reference guide: Revised Universal Soil Loss Equation, Version 2, (RUSLE2). Washington, D.C.: National Resources Conservation Service. Available at:

http://www.ars.usda.gov/SP2UserFiles/Place/60600505/RUSLE/RUSLE2_User_Ref_Guide.pdf

Wischmeier, W. H., and Smith, D. D., 1965. Predicting rainfall erosion losses from Cropland east of the Rocky Mountains. USDA Agricultural Handbook No. 282. Washington, D.C.: GPO.

Wischmeier, W. H., and Smith, D. D., 1978. Predicting rainfall erosion losses. USDA Agricultural Handbook No. 537. Washington, D.C.: GPO.

Chapter 4: Study Conclusions

4.1 Objective Summary

A brief summary of each objective outlined in Section 1.2.1 is included below. For more information regarding each of the first two objectives, reference the conclusion sections of Chapters 2 and 3.

First Objective:

The first objective sought to determine the change in EI or erosivity with respect to a) methodology and b) climate change. I successfully determined the total change in EI from previously published values, but I was not able to separate (with confidence) how much of this can be attributed to either 'a' or 'b'. Significant progress was made toward this goal, which requires reliable erosion indices for future studies to determine these impacts. The EI values provided by the new methodology and dataset are consistent with McGregor et al. (1995), which provided reliable erosion indices for northern Mississippi.

Significant Findings:

- Screening drastically improved: water balance, metadata, and EI calculation (data quality assurance) for quarter-hour station data
- Annual EI was significantly higher than Ag. Handbook isoerodent maps
- Storm EI did not change significantly on a regional scale
- The Atlantic Coast experienced significant changes across both measures

Potential Leads:

- Storm EI may be driven by variability (location, timing, and magnitude)
- Storm EI may need to consider anomalies for accurate assessment
- Changes in the Atlantic Coast may be a direct reflection of AMO phase changes

Second Objective:

The second objective sought to determine changes in EI related to intra-annual and inter-annual variability, namely that resulting from ENSO. This objective also prepares for mid to long-term variability studies, but they are not evaluated in this thesis. I successfully determined that ENSO had a strong effect on nearly all aspects of EI (some more strong

than others) and quantified how much of an impact for various measures. I subsequently investigated the mechanisms by which this may have occurred, in order to gain a deeper understanding of ENSO impacts.

Significant Findings:

- Unadjusted mean monthly EI of longer observation periods (from 25.10 screened data) accurately approximated annual EI without filling gaps
- ENSO impacted the magnitude of monthly EI, the distribution of EI throughout the year, and the mechanisms behind EI (mainly depth and energy)
- ENSO most significantly impacted the Gulf and Atlantic Coasts
- Depth not intensity controlled energy of moderate and large storms

Potential Leads:

- Variability may need to consider combined effects (e.g. ENSO and AMO)
- AMO may impact maximum intensity more than ENSO
- Supplemental data may be required for mid to long-term variability analysis

Third Objective:

The last objective seeks to identify observed and predicted climate change impacts on erosivity and could not be completed for this thesis. This objective is included because it is the primary motivation for all other objectives and analyses. The groundwork has been laid for a successful result regarding this objective. Still there are a few pieces that must be studied first including the remaining variability oscillations, which could confuse climate change analysis. Once variability impacts have been assessed, the observed differences can be used to deconstruct oscillations for a better picture of climate change impacts on erosivity. Prediction methods can then be trained with the observed climate change signal and modeled historical data to predict erosivity from modeled future data.

4.1.1 Methodological Changes and Impacts

I managed to make significant improvements on quarter-hour station data quality assurance largely due to the implementation of station screening in conjunction with a water balance

analysis. This was the foundation for any advances in erosivity calculations. In bulleted form, these were the improvements that enabled better EI values or a deeper understanding of EI values resulting from quarter-hour station data:

- Reduced missing data from 21.6% to 5.3% (arithmetic mean of station metadata)
- Informed screening method selection with water balance (observed vs. normal)
- Quantified water deficit for roughly 2/3 of stations averaging -5.9% (gridded)
- Densified spatial resolution of stations used to calculate erosivity (3x AH703)
- Abandoned regression analysis of EI used by Ag. Handbooks
- Included all storms regardless of depth or intensity (more important for this data)
- Provided EI values from both limited and unlimited maximum intensities

These changes resulted in drastic improvements to EI values in the Southeast. These improvements will likely follow for the eastern United States and potentially even in western states given improvements in the observed data record. EI values were consistent with observations made by McGregor with superior data from 29 breakpoint stations. Calculations followed closely on a year-by-year and average annual basis for all statistics. Almost all calculations were within standard deviations for the 29 stations, despite the fact that our station was not located within the same local watershed.

These methodological changes were further applied to benchmarking for the purpose of climate variability studies. The most critical component of these studies was the 'monthly EI' construct, which was used to determine median values over long periods of time for shorter observation periods. Relatively small errors in these values could have widespread impact on all aspects of the overall goal of intelligent conservation (guided by climate studies that depend on testing those values throughout the study area), so much care must be given to the correct preparation and calculation of the median monthly EI. One must take into account the shorter observations of positive and negative variability states of the climate, so I use a longer minimum observation period as well as more powerful statistical tests to arrive at correct interpretations. I suggest that others follow this methodology to obtain better EI calculations for climate studies, which may enable erosion prediction technology to change from 'reactive' to 'proactive' soil conservation.

4.1.2 Concluding Statement

Since 1880, Earth has experienced a globally averaged increase in temperature of 0.8 K with two-thirds of this occurring since 1975 (NASA, Earth Observatory). Climate change projections range from a 1.1 to 5.4 K increase in globally averaged temperature by the year 2100, and these projections were highly influenced by the concentration of GHGs in the atmosphere resulting from human decisions (NOAA, Climate.gov). Using these values for the present day in conjunction with theoretical average values of 7% change in intensity and 2% change in precipitation depth K^{-1}. If these rates of change were reliable, then the globally averaged potential for climate change would look something like Table 4-1 for potential changes since 1880 and Table 4-2 for potential changes relative to today. Regional changes can fall below or exceed these theoretical global average changes.

Assumptions:

- Results are globally averaged (regional and local values will vary significantly)
- Depth controls kinetic energy (true for moderate to large storms)
- Latent heat feedbacks are not considered (does occur in reality)

Table 4-1 Theoretical Climate Change Impacts on Erosivity Since 1880

POTENTIAL CHANGE SINCE 1880				
Year	Temperature (K)	Precipitation (%)	Intensity (%)	Erosivity (%)
1880	0.00	0.0%	0.0%	0.0%
1975	0.27	0.5%	1.9%	2.4%
2016	0.80	1.6%	5.6%	7.3%
2100	1.90	3.8%	13.3%	17.6%
2100	6.20	12.4%	43.4%	61.2%

Table 4-2 Theoretical Climate Change Impacts on Erosivity Relative to Today

POTENTIAL CHANGE IN TODAY'S TERMS				
Year	Temperature (K)	Precipitation (%)	Intensity (%)	Erosivity (%)
1880	-0.80	-1.6%	-5.6%	-7.1%
1975	-0.53	-1.1%	-3.7%	-4.8%
2016	0.00	0.0%	0.0%	0.0%
2100	1.10	2.2%	7.7%	10.1%
2100	5.40	10.8%	37.8%	52.7%

These theoretical changes range widely based on forcing scenarios meaning that much of the change is still preventable, but these values also outline (based on current literature) what potential change may accompany varying temperature increases. For reference, the recent agreement in Paris has pledged to hold temperature changes below 2 °C, which corresponds to the lower bound of the year 2100 value. Many climate scientists predict that this is the path that the global society is currently following. If this is indeed the case, and if these theoretical values are correct, it seems that climate change will be responsible for about 17-18% of the change in globally averaged erosivity since 1880. Since regional values can exceed this average value, it follows that there should be some investigation into where precipitation bands could cause significant changes in erosivity. Ultimately, the research I am conducting aims to specify these areas for the United States, from which conclusions may can be applied to estimate these areas in other parts of the world. Although in the long-term climate change will outweigh climate variability impacts on erosivity, the short-term changes are highly dominated by variability. It is also important to note that there is uncertainty regarding whether the amplitude of these oscillations will continue to increase with climate change or not. **It is essential for the future of soil conservation that research efforts, such as those documented in this thesis, aim to transform erosion prediction technology into tools for intelligent (climate-informed) conservation in order to anticipate our dynamic climate.**

4.2 Future Work

As I progressed through the study, there were multiple changes I would have liked to incorporate into the final analysis. However, for practicality and the timeliness of completion, these changes were only mentioned here for future studies that intend to improve upon these analyses. Therefore, this section documents how I would have changed the study knowing what I know now and includes my short to mid-term research plans in regards to the study topic.

4.2.1 Immediate Updates

These are changes that will be incorporated immediately following the publication of this thesis and will render these chapters ready for publication in academic journals.

- **Calculate accumulation EI considering all SCS type storms**—accumulation EI values were calculated using only the SCS type II storm since most of the study area is of that type storm. This will be a necessary change going forward with EI estimation for the continental United States, where storm type would play a much more significant role in these calculations.
- **Reduce missing and deleted periods for intermediate years that did not pass screening**—missing and deleted periods were calculated as a percent of total station operation period, but they do not account for years between the start and end dates that would be removed by screening. A simple edit will slightly improve these values to reflect the actual percent missing and deleted.
- **Calculate EI using the superior Brown-Foster (BF) or McGregor-Mutchler (MM) energy equation**—both AH703 and McGregor recommend using the BF energy equation since it is a better fit for US rainfall data. The primary impact this will have on calculations is that the energy component of storms could vary for small and large storm intensities.
- **Calculate cumulative and fractional EI distributions for phases of ENSO**—ENSO was found to significantly impact the timing of EI throughout the year. Including this small improvement would communicate shifts in EI according to ENSO much more effectively than maps, which are strong for spatial variation and not necessarily temporal variation.

- **Perform PCA analysis for other clusters in variability analysis**—ENSO was not evaluated for effects on different types of storms (long vs. short duration, high vs. low intensity, large vs. small depths, etc.). These types of analyses would help to communicated changes in average and extreme precipitation. This could potentially decrease the sample size of observations for particular storm types, and may require some sort of climate division analysis, where data for an entire area is analyzed as opposed to a single station.
- **Update methodology for sufficient performance in western states**—the current methodology works well for the Southeast, but screening and accumulation methods may not perform as well in areas outside the Southeast, especially in low precipitation states in the western United States. Incorporating this would prepare for an eventual expansion of the analysis to western states.

4.2.2 Near-Term Work

The data used for this study included observations that were split almost evenly between a strong negative and a strong positive AMO (almost a full cycle with inversion occurring in 1995). This formulates a strong argument for studying the AMO variability cycle and potentially others too. Using this new found knowledge observed oscillations could be deconstructed to make a statement about climate change as it pertains to erosivity. Finally, with all observed changes identified, future climate projections could be used to predict the future climate change impacts on erosivity. These next steps outline the research plan necessary to successfully complete the third objective of predicting EI under a changing climate regime.

- **Perform other variability analyses**—currently the study only evaluated ENSO for impacts on erosivity. Expanding the analysis to other variability cycles (and looking at combined effects) will significantly improve our understanding of the role of climate variability in erosivity
- **Deconstruct variability oscillations**—variability oscillations make interpretation of climate change difficult. For example, quarter-hour station data was observed beginning with –AMO and ending with +AMO. If a trend analysis were performed on this data without processing, it is likely that the trend (for the Southeast) would

overestimate the change due to the coincidence of observations. Since the observation period is short relative to the number of cycles in the data, the oscillations will need to be accounted for in the data before trend analysis can accurately capture the observed change.

- **Evaluate observed climate change impacts on erosivity**—once oscillations have been deconstructed, the observed impact of climate change on erosivity should be communicated for further analysis.
- **Prepare climate change-erosivity signal**—in order to move from observed change to predicted change it is critical to establish a strong signal for the prediction method to detect. This will take a significant effort to ensure that training targets and input data are as true to the relationship as possible.
- **Predict erosivity using an artificial neural network**—using the training targets and change signal from observed climate change impacts on erosivity and modeled historical and projected data, an artificial neural network will be trained for predicting EI. These predictions will be computed for many models, potentially including downscaling, bias correction, and uncertainty analysis.

References

Angulo-Martínez, M., Begueria, S., 2009. Estimating rainfall erosivity from daily precipitation records: A comparison among methods using data from the Ebro Basin (NE Spain). Journal of Hydrology 379, 111–121. doi:10.1016/j.jhydrol.2009.09.051

Cubasch, U., Wuebbles, D., Chen, D., Facchini, M. C., Frame, D., Mahowald, N., and Winther, J. - G., 2013. Introduction. Climate Change 2013: The Physical Science Basis. Contribution of Working Group I to the Fifth Assessment Report of the Intergovernmental Panel on Climate Change, T.F. Stocker, D. Qin, G.-K. Plattner, M. Tignor, S.K. Allen, J. Boschung, A. Nauels, Y. Xia, V. Bex, and P.M. Midgley, Eds., Cambridge University Press, 119-158.

Hastings, B. K., Breshears, D. D., Smith, F. M., 2005. Spatial variability in rainfall erosivity versus rainfall depth: implications for sediment yield. Vadose Zone Journal 4, 500-504. doi:10.2136.vzj2004.0036

Hollinger, S. E., Angel, J. R., and Palecki, M. A., 2002. Spatial distribution, variation, and trends in storm precipitation characteristics associated with soil erosion in the united states. Contract report CR 2002-08. Illinois State Water Survey. Champaign, IL. available at: www.isws.illinois.edu/pubdoc/CR/ISWSCR2002-08.pdf.

Huber, M., and Knutti, R., 2012. Anthropogenic and natural warming inferred from changes in Earth's energy balance. Nature Geoscience, **5**, 31-36, doi:10.1038/ngeo1327.

Hutchinson, G.E., 1965. The ecological theatre and the evolutionary play. Yale University Press, New Haven, CT: USA.

Istok, J. D., McCool, D. K., King, L. G., Boersma, L., 1986. Effect of rainfall measurement interval on EI calculation. Transactions of the ASAE 29, 0730–0734. doi:10.13031/2013.30221

Karl, T. R., Melillo, J. T., and Peterson, T. C., 2009. Global climate change impacts in the united states. T.R. Karl, J.T. Melillo, and T.C. Peterson, Eds. Cambridge University Press, 189 pp.

Kloke, J., and McKean, J. W., 2014. Nonparametric statistical methods using R. CRC Press, Taylor & Francis Group, FL.

Kloke, J.D., McKean, J.W., and Rashid, M., 2009. Rank-based estimation and associated inferences for linear models with cluster correlated errors. Journal of the American Statistical Association, 104 (485), 384-390.

McGregor, K.C., Bingner, R.L., Bowie, A.J., Foster, G.R., 1995. Erosivity index values for northern Mississippi. Research Gate 38, 1039–1047.

McGregor, K.C., Mutchler, C.K., Bowie, A.J., 1980. Annual R values in north Mississippi. Journal of Soil and Water Conservation 35(2), 81–84.

Melillo, J., Richmond, T., Yohe, G. (Eds.), 2014. Climate change impacts in the united states: the third national climate assessment. U.S. Global Change Research Program, 841 pp. doi:10.7930/J0Z31WJ2.

Mirhosseini, G., Srivastava, P., 2012. The impact of climate change on rainfall Intensity–Duration–Frequency (IDF) curves in Alabama. Regional Environmental Change. doi:10.1007/s10113-012-0375-5

Nearing, M.A., Pruski, F.F., O'Neal, M.R., 2004. Expected climate change impacts on soil erosion rates: a review. Journal of Soil and Water Conservation 59, 43–50.

Nuno de Santos Loureiro, M. de A.C., 2001. A new procedure to estimate the RUSLE EI30 index, based on monthly rainfall data and applied to the Algarve Region, Portugal. Journal of Hydrology 250, 12–18. doi:10.1016/S0022-1694(01)00387-0

Renard, K.G., Foster, G.R., Weesies, G.A., McCool, D.K., and Yoder, D.C., 1997. Predicting soil erosion by water: a guide to conservation planning with the Revised Universal Soil Loss Equation (RUSLE). Agriculture Handbook 703. U.S. Department of Agriculture. Washington, DC.

Richardson, C. W., Foster, G. R., Wright D. A., 1983. Estimation of erosion index from daily rainfall amount. Transactions of the ASAE 26, 0153–0156. doi:10.13031/2013.33893

Singh, S., Srivastava, P., 2015. Climate variability and irrigation impacts on stream-aquifer dynamics in the Apalachicola-Chattahoochee-Flint River Basin. Auburn, Alabama. Auburn University, Department of Biosystems Engineering. available at: https://etd.auburn.edu/handle/10415/4845.

Stephens, G. L., Li, J., Wild, M., Anne Clayson, C., Loeb, N., Kato, S., L'Ecuyer, T., Stackhouse, P. W., Lebsock, M., and Andrews, T., 2012. An update on Earth's energy balance in light of the latest global observations. Nature Geoscience, **5**, 691-696, doi:10.1038/ngeo1580.

Tiwari, A.K., Risse, L.M., Nearing, M., 2000. Evaluation of WEPP and its comparison with USLE and RUSLE. Transactions of the American Society of Agricultural Engineers 43, 1129–1135.

Trenberth, K.E., Dai, A., Rasmussen, R.M., Parsons, D.B., 2003. The changing character of precipitation. Bull. Amer. Meteor. Soc. 84, 1205–1217. doi:10.1175/BAMS-84-9-1205

USDA. 2008. User's reference guide: Revised Universal Soil Loss Equation, Version 2, (RUSLE2). Washington, D.C.: National Resources Conservation Service. Available at: http://www.ars.usda.gov/SP2UserFiles/Place/60600505/RUSLE/RUSLE2_User_Ref_Guide.pdf

Wischmeier, W. H., and Smith, D. D., 1965. Predicting rainfall erosion losses from Cropland east of the Rocky Mountains. USDA Agricultural Handbook No. 282. Washington, D.C.: GPO.

Wischmeier, W. H., and Smith, D. D., 1978. Predicting rainfall erosion losses. USDA Agricultural Handbook No. 537. Washington, D.C.: GPO.

Appendices

Appendix A

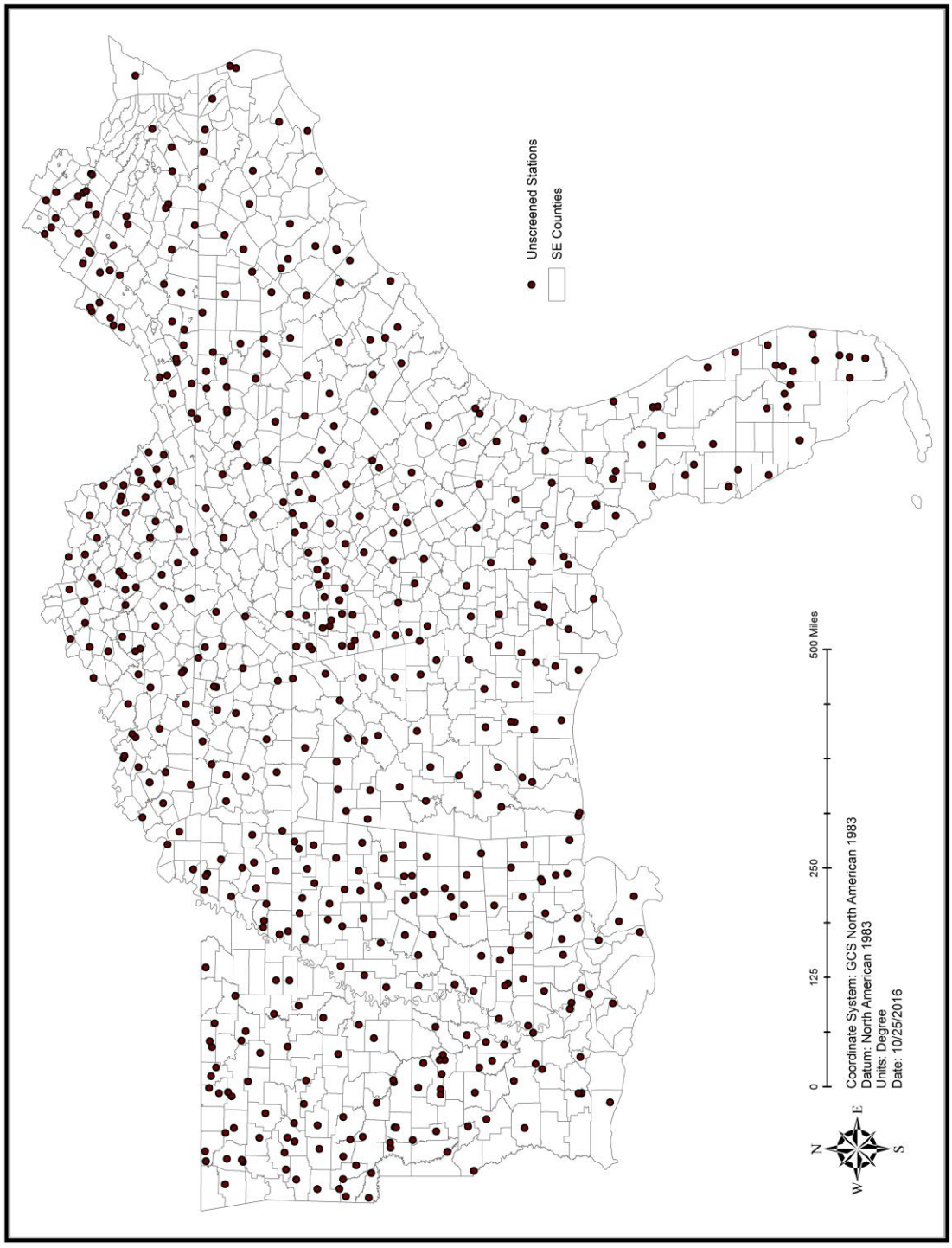
Unscreened Stations
SE Counties
0
125
250
500 Miles
N
E
S
W
Coordinate System: GCS North American 1983
Datum: North American 1983
Units: Degree
Date: 10/25/2016

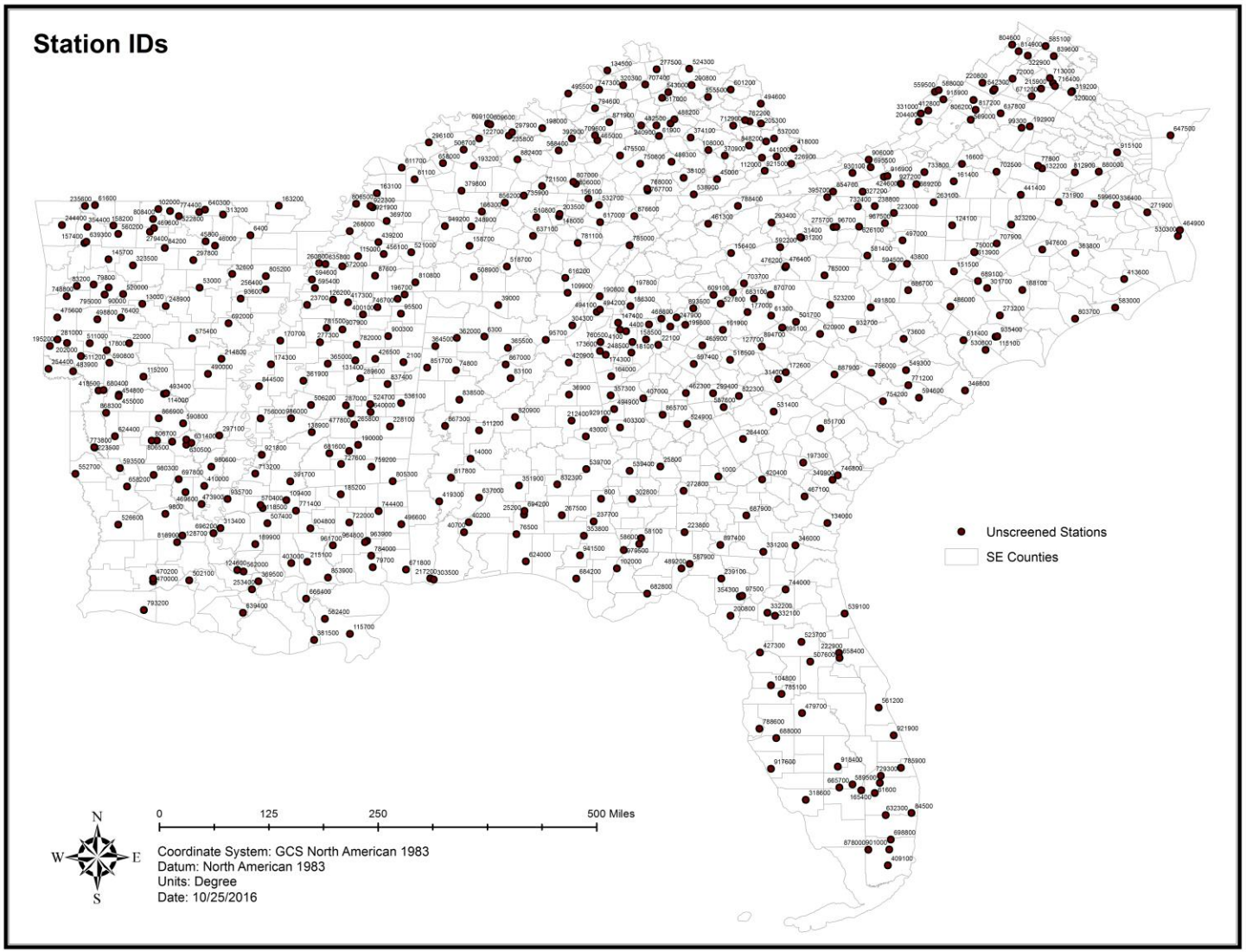
Station IDs
Unscreened Stations
SE Counties
N
W
E
S
0
125
250
500 Miles
Coordinate System: GCS North American 1983
Datum: North American 1983
Units: Degree
Date: 10/25/2016

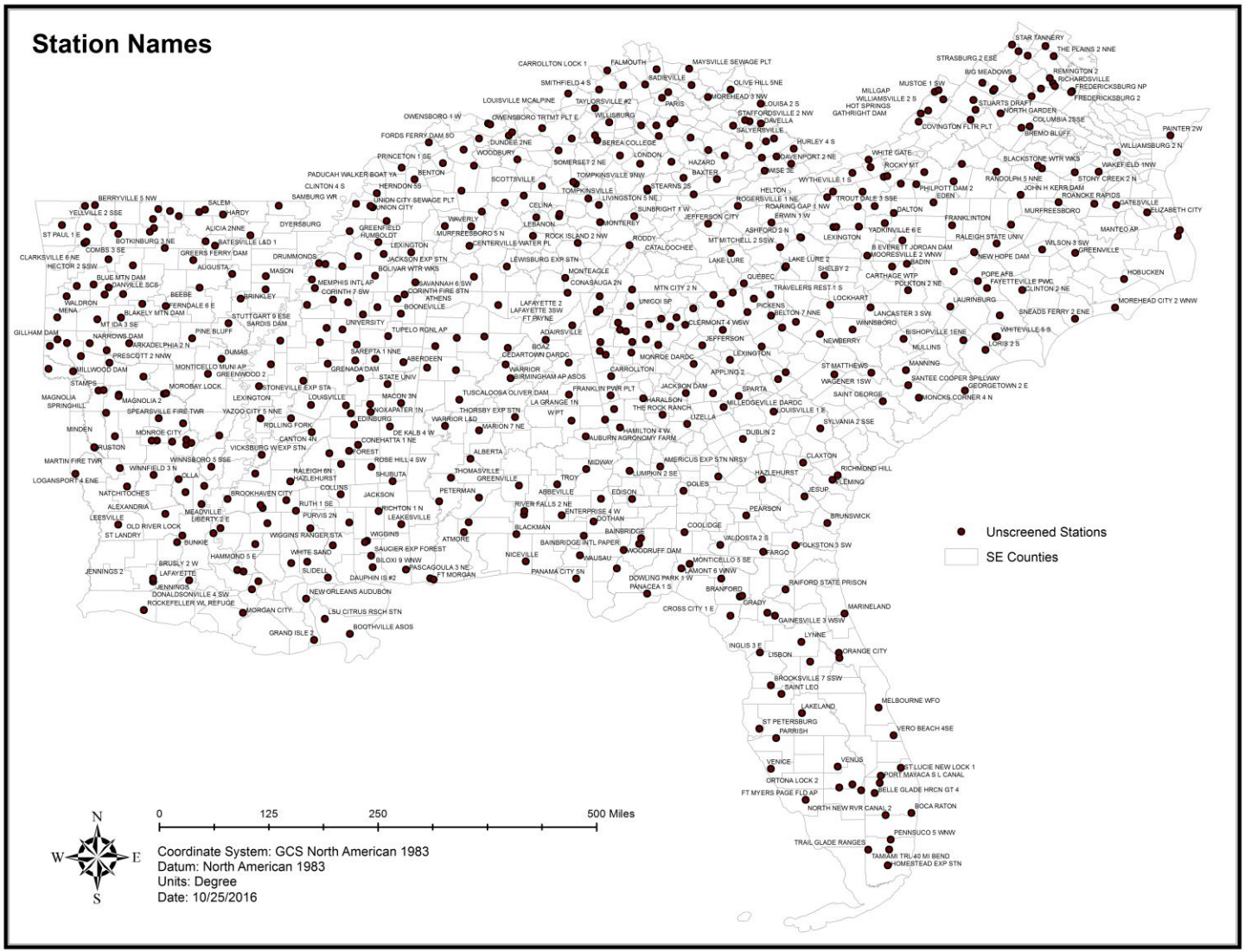
Station Names
Unscreened Stations
SE Counties
0
125
250
500 Miles
N
W
E
S
Coordinate System: GCS North American 1983
Datum: North American 1983
Units: Degree
Date: 10/25/2016

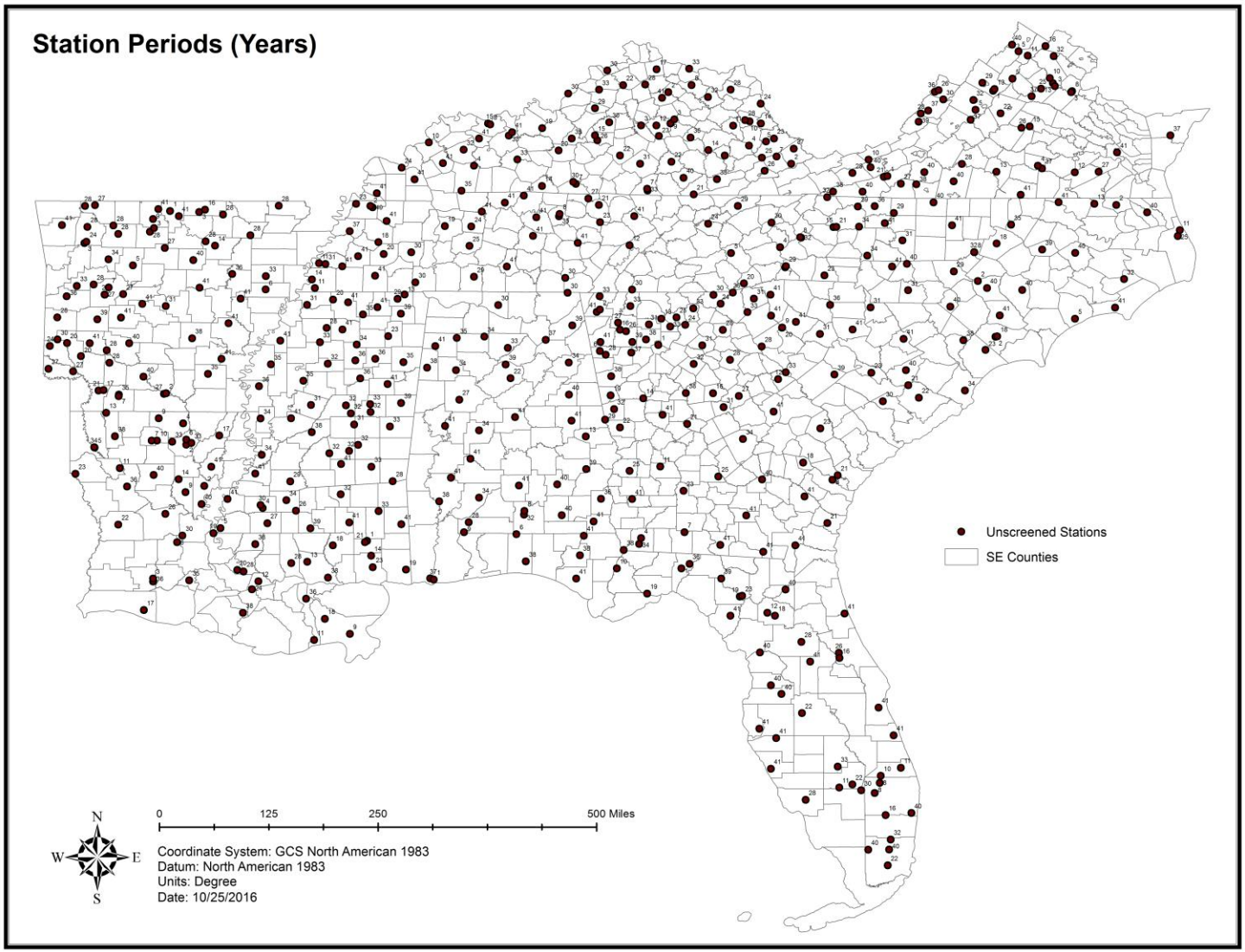
Station Periods (Years)
Unscreened Stations
SE Counties
N
W
E
S
0
125
250
500 Miles
Coordinate System: GCS North American 1983
Datum: North American 1983
Units: Degree
Date: 10/25/2016

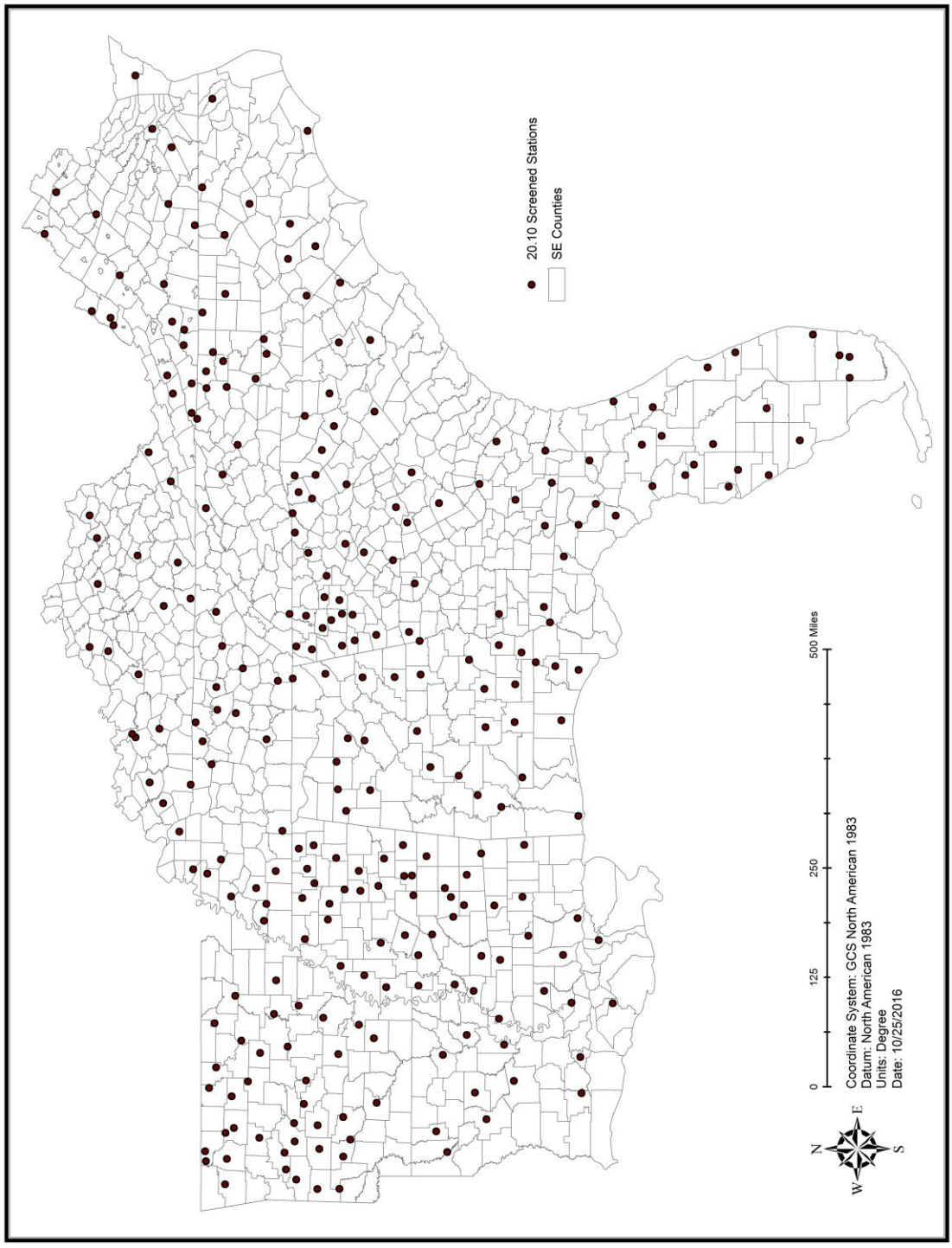
20.10 Screened Stations
SE Counties
0
125
250
500 Miles
Coordinate System: GCS North American 1983
Datum: North American 1983
Units: Degree
Date: 10/25/2016
N
E
S
W

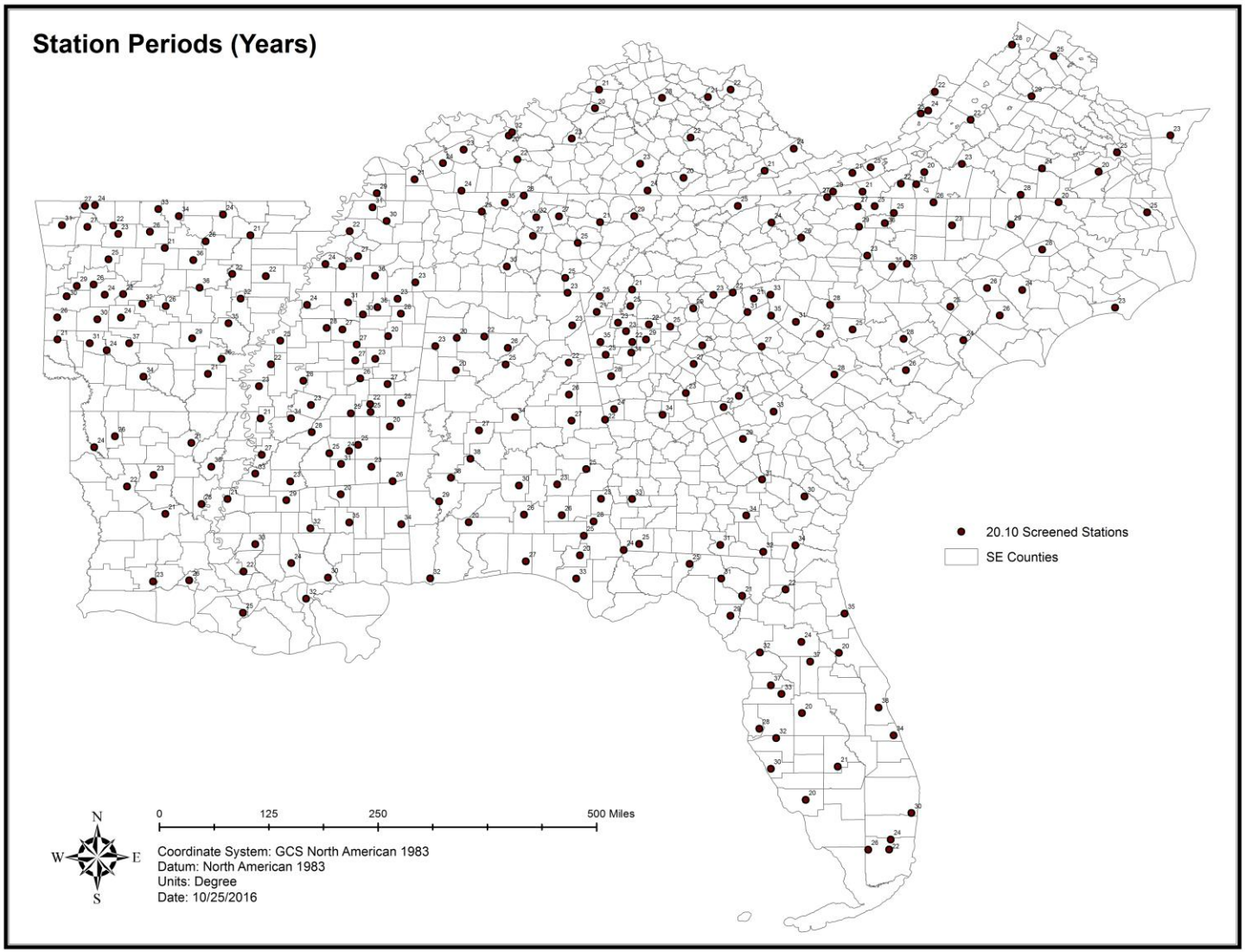
Station Periods (Years)
20.10 Screened Stations
SE Counties
0
125
250
500 Miles
N
W
E
S
Coordinate System: GCS North American 1983
Datum: North American 1983
Units: Degree
Date: 10/25/2016

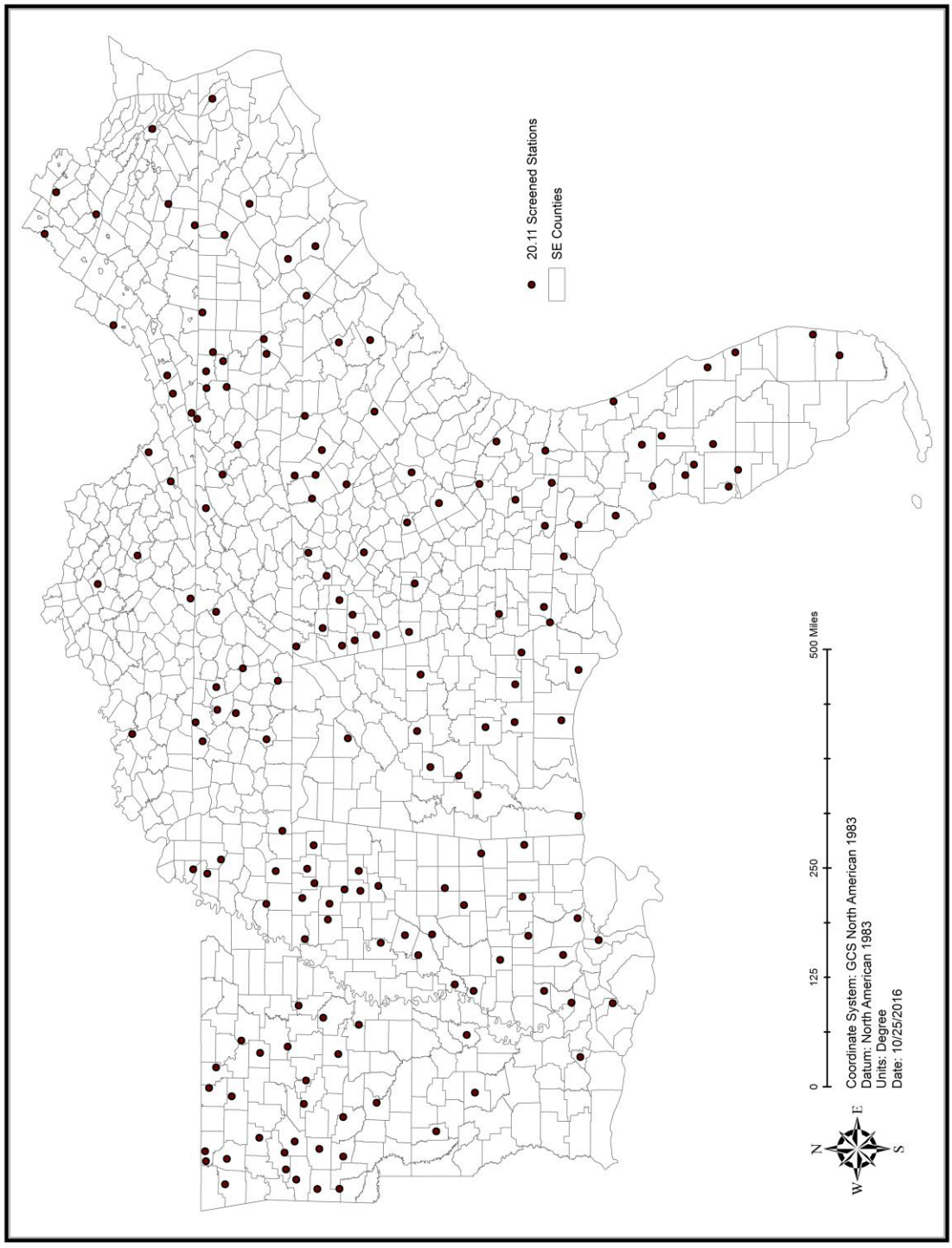
20.11 Screened Stations
SE Counties
0
125
250
500 Miles
N
E
S
W
Coordinate System: GCS North American 1983
Datum: North American 1983
Units: Degree
Date: 10/25/2016

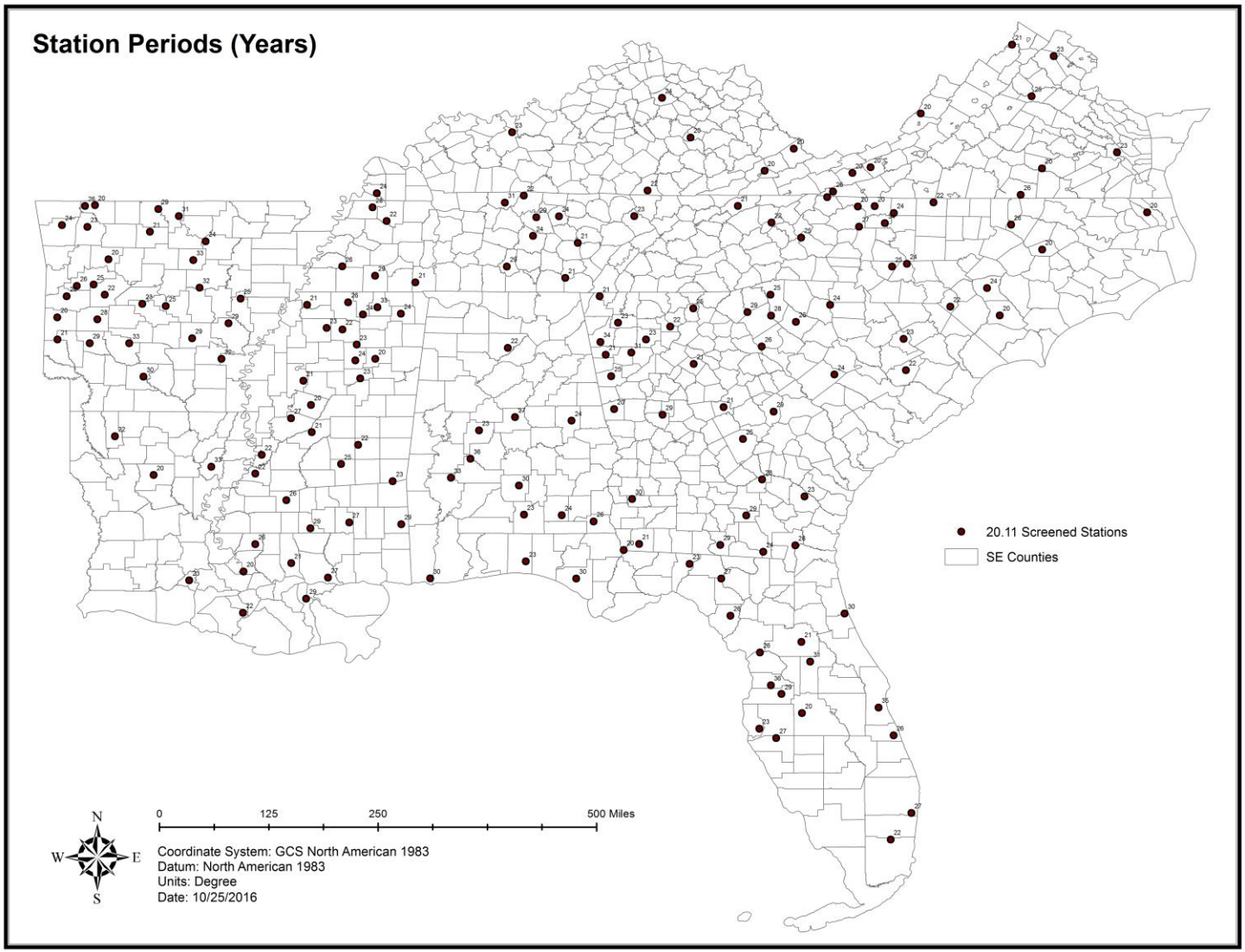
Station Periods (Years)
20.11 Screened Stations
SE Counties
N
W
E
S
0
125
250
500 Miles
Coordinate System: GCS North American 1983
Datum: North American 1983
Units: Degree
Date: 10/25/2016

Appendix B

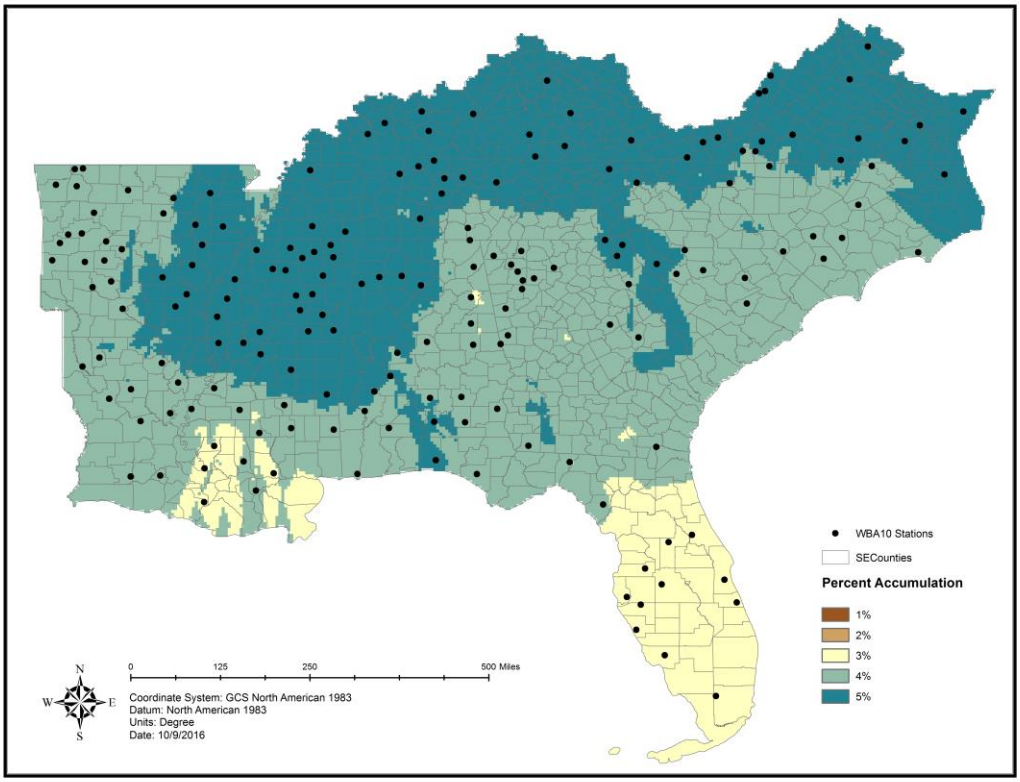

Figure 1 Distribution of Accumulation Percentages for the 20.10 Screening Method

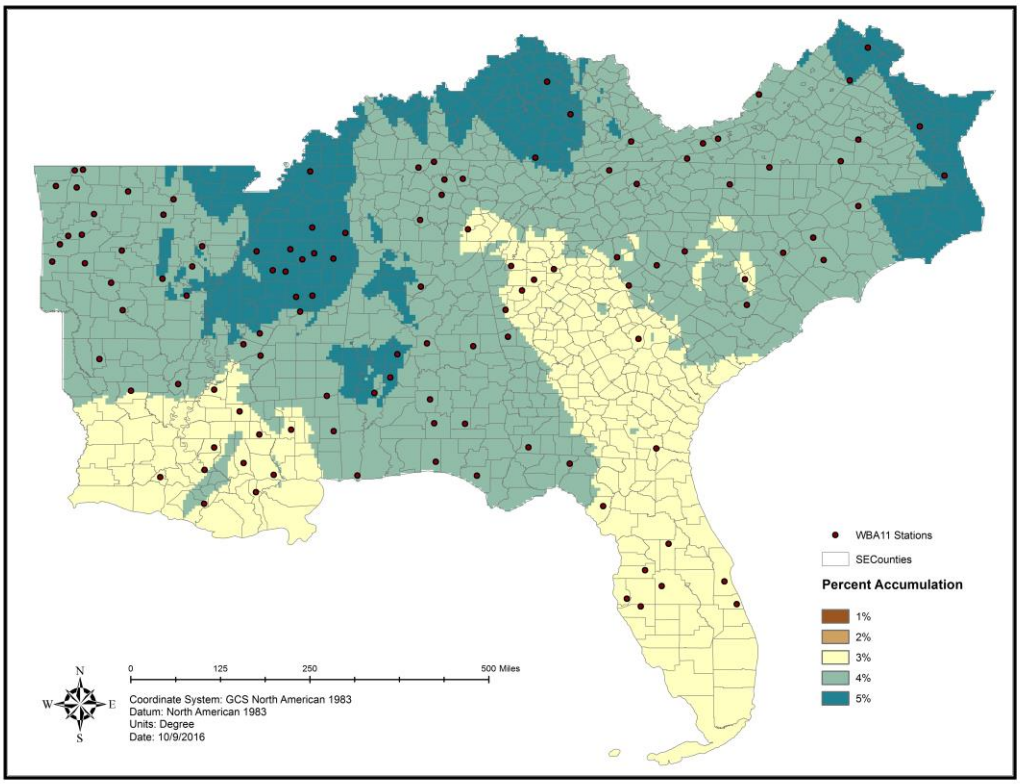

Figure 2 Distribution of Accumulation Percentages for the 20.11 Screening Method

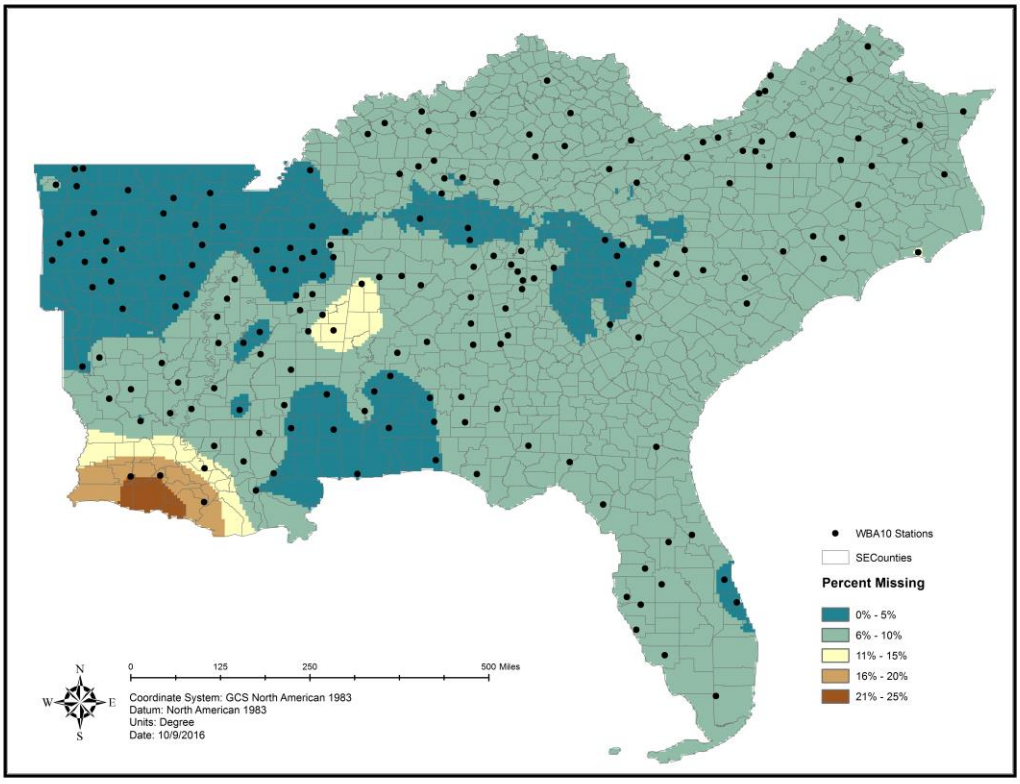

Figure 3 Distribution of Missing Percentages for the 20.10 Screening Method

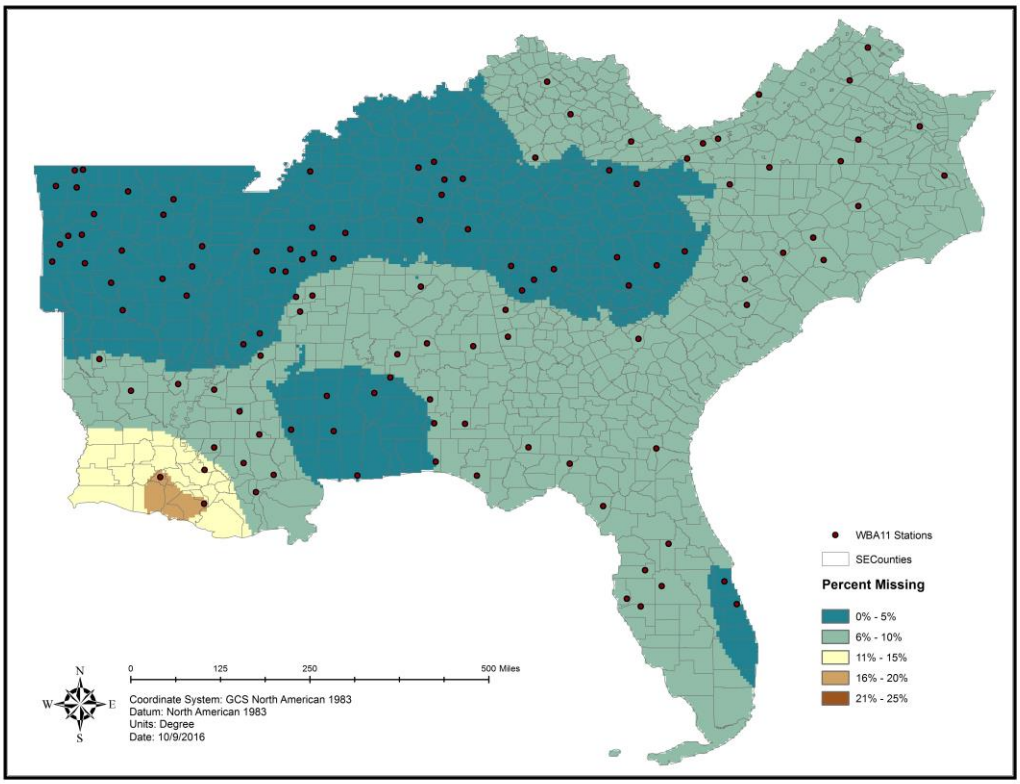

Figure 4 Distribution of Missing Percentages for the 20.11 Screening Method

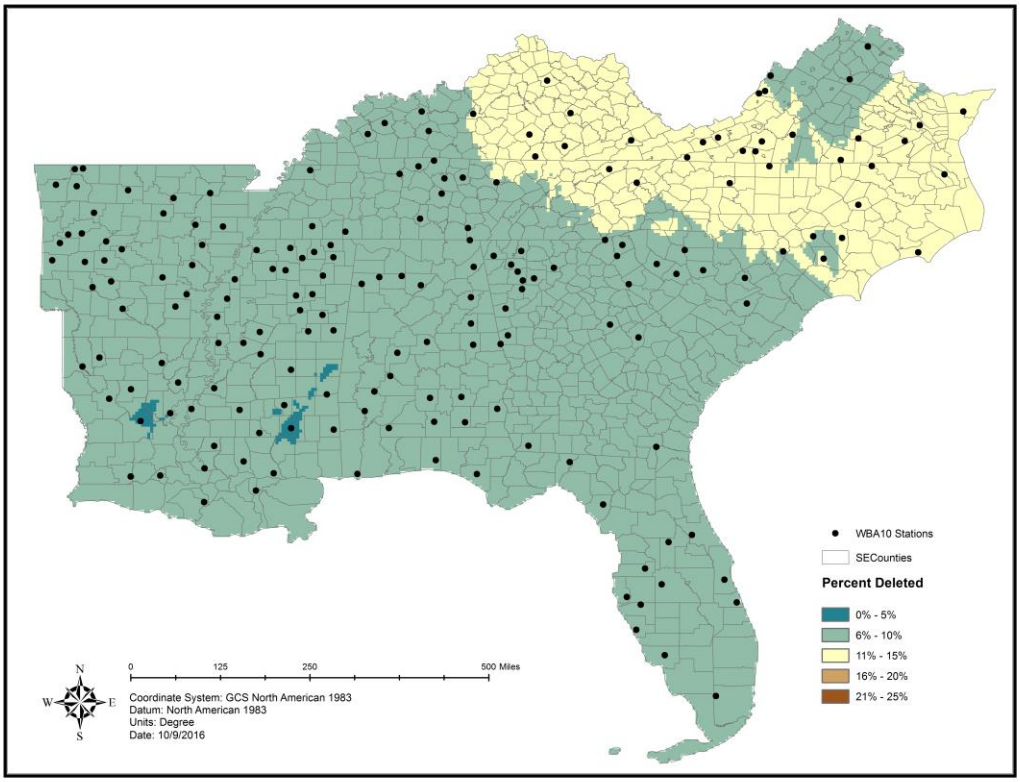

Figure 5 Distribution of Deleted Percentages for the 20.10 Screening Method

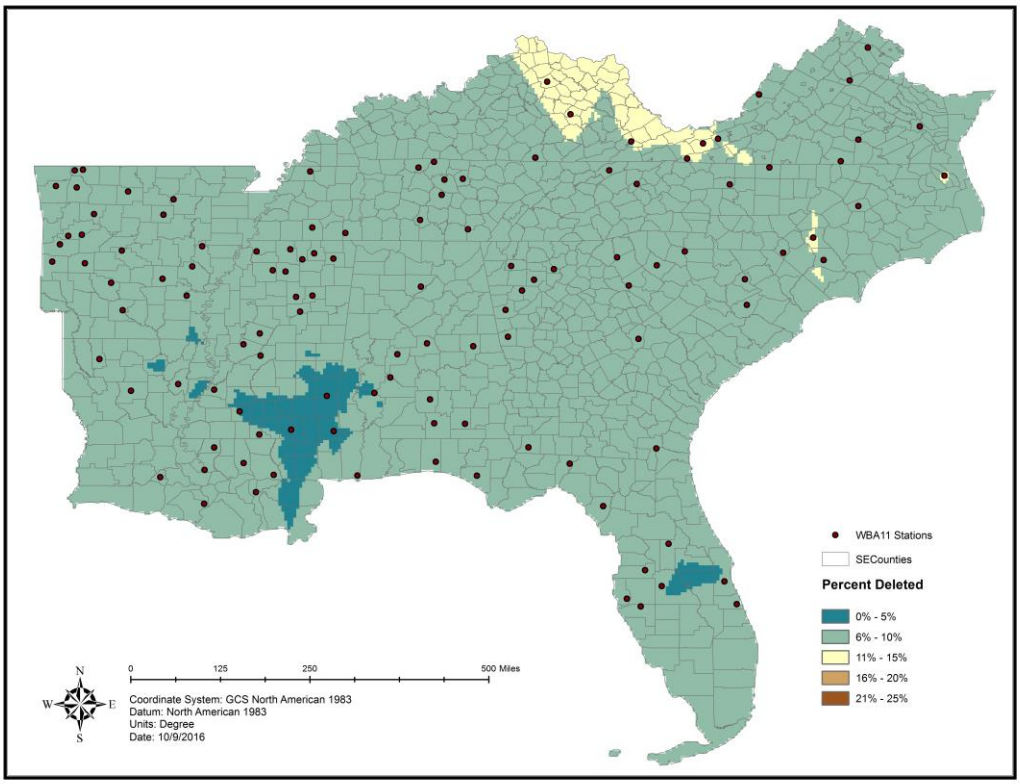

Figure 6 Distribution of Deleted Percentages for the 20.11 Screening Method

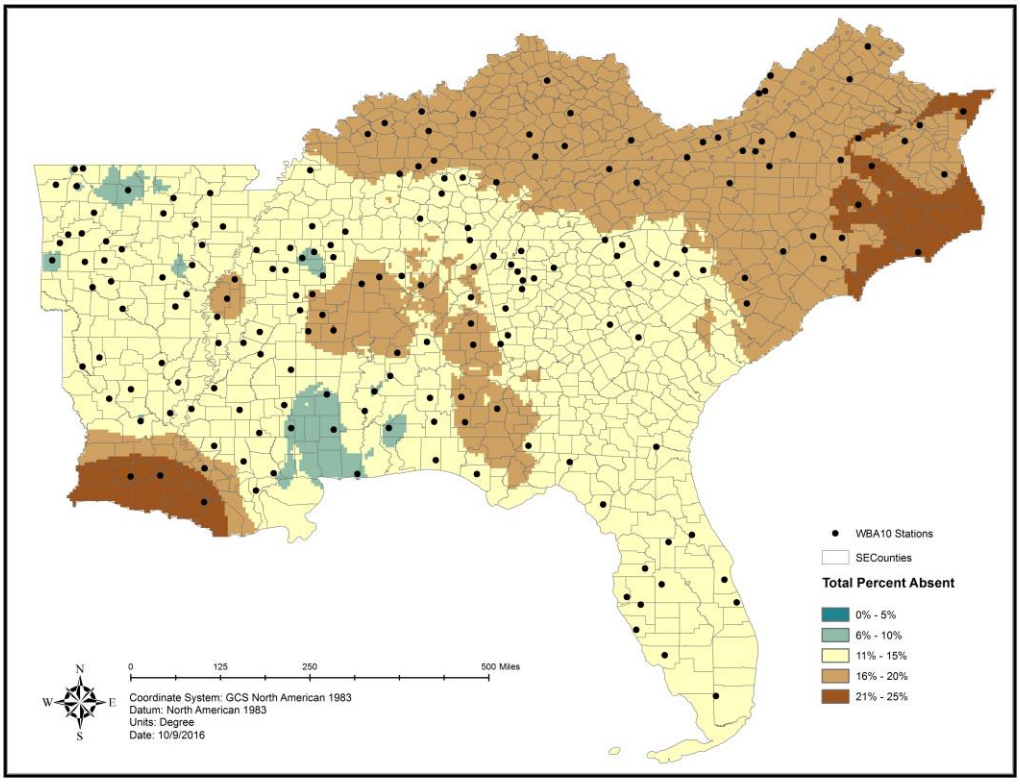

Figure 7 Total Missing and Deleted Percentage for the 20.10 Screening Method

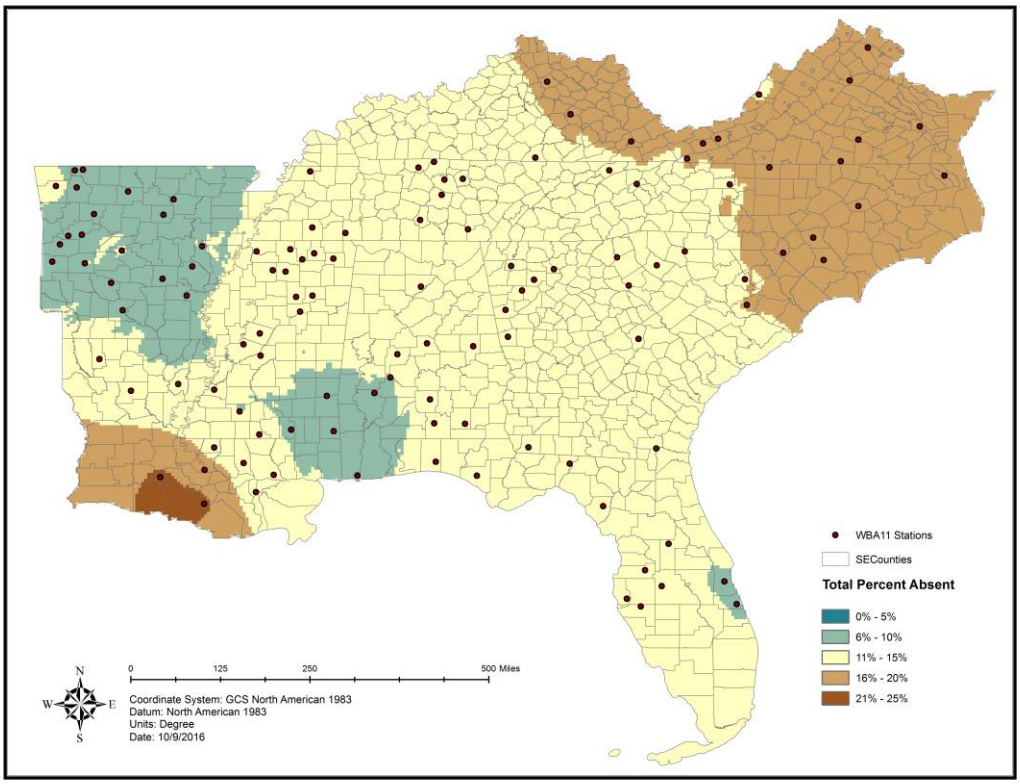

Figure 8 Total Missing and Deleted Percentage for the 20.11 Screening Method

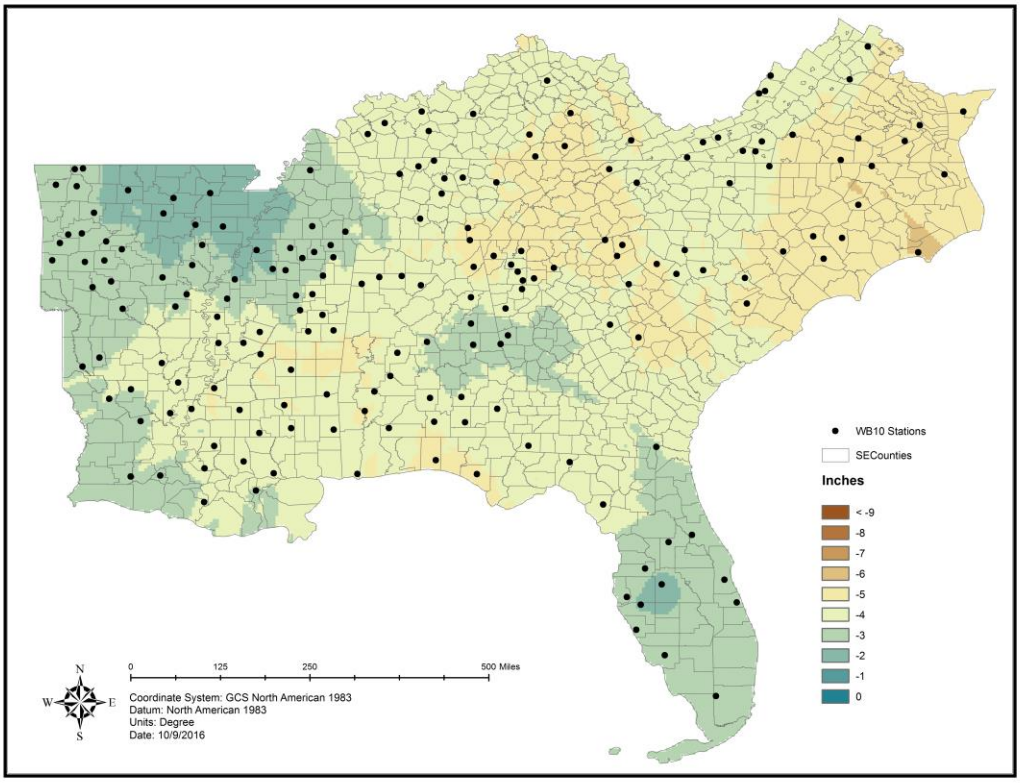

Figure 9 Absolute Difference from Normal Precip. for the 20.10 Screening Method

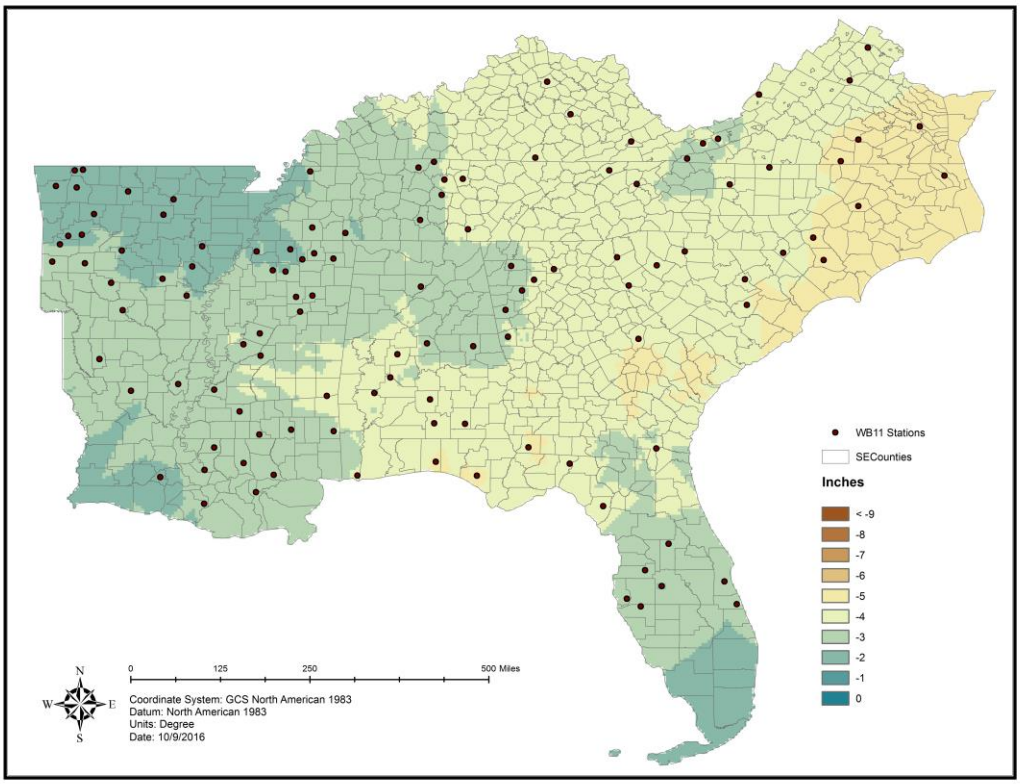

Figure 10 Absolute Difference from Normal Precip. for the 20.11 Screening Method

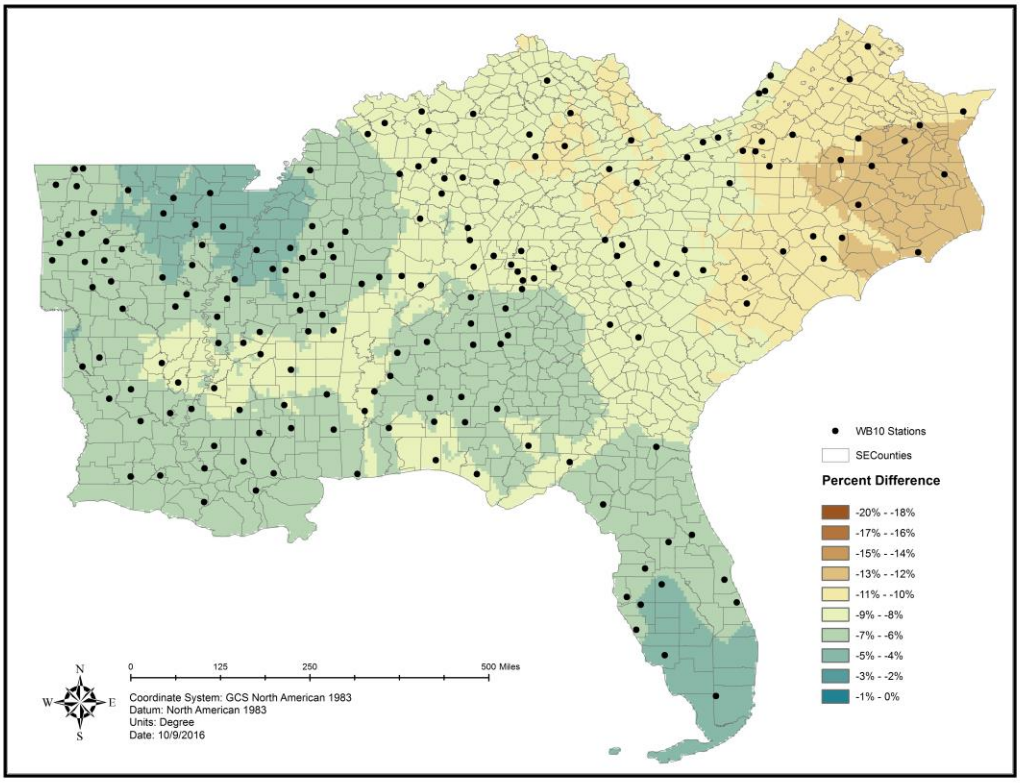

Figure 11 Relative Difference from Normal Precip. for the 20.10 Screening Method

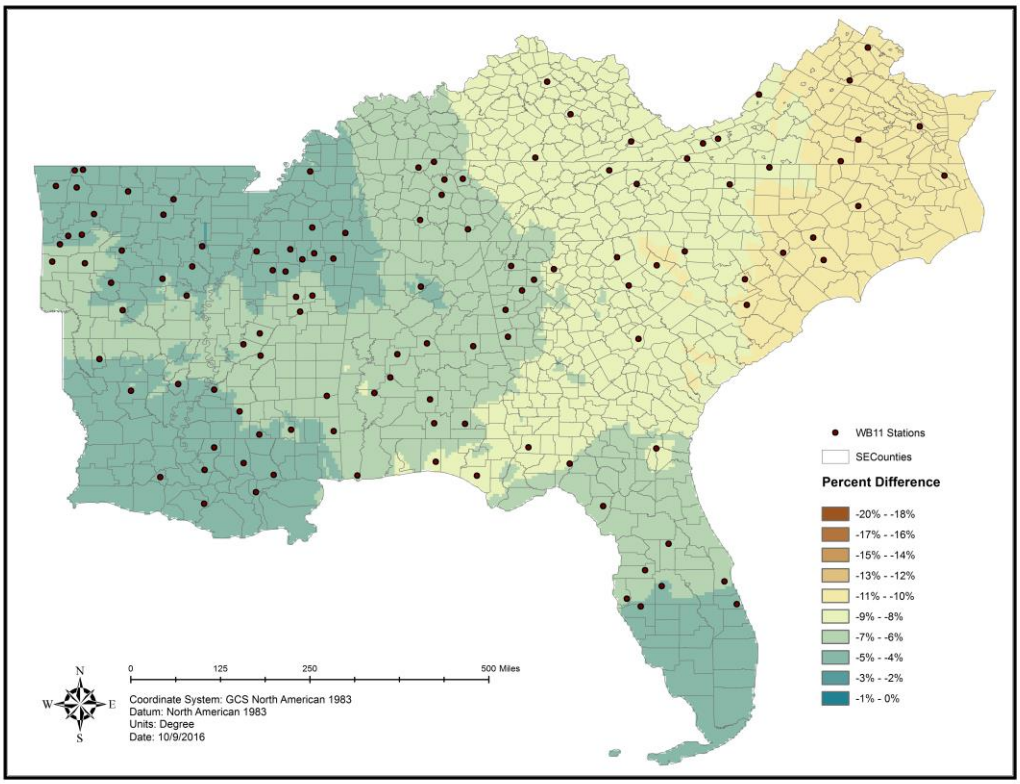

Figure 12 Relative Difference from Normal Precip. for the 20.11 Screening Method

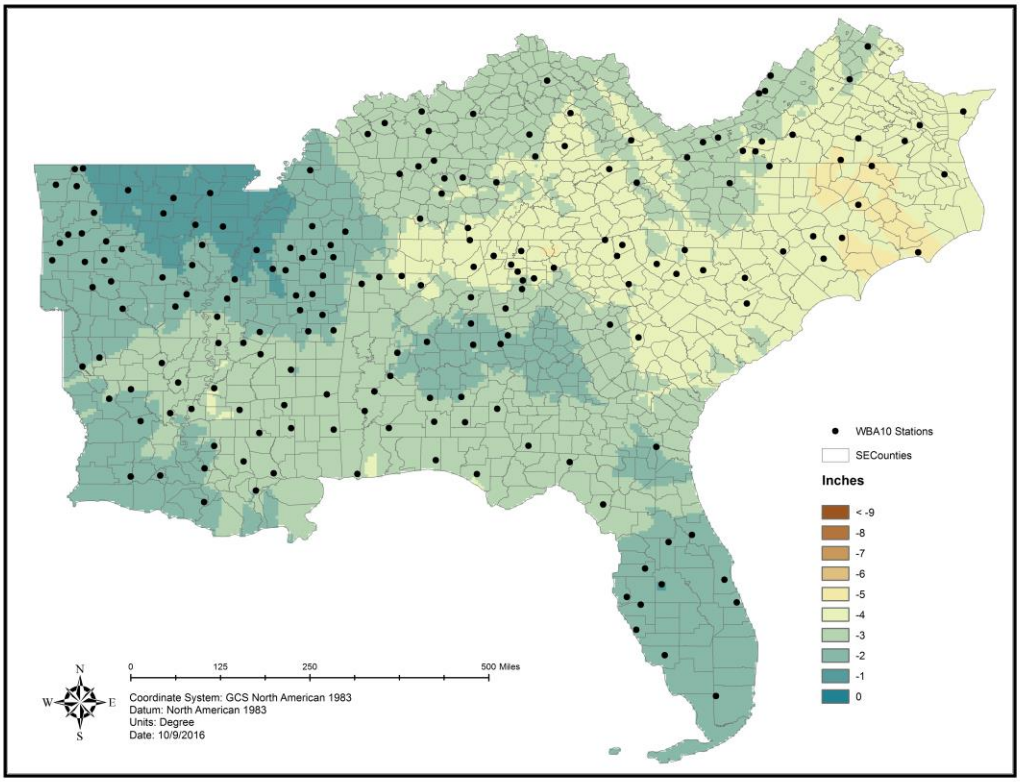

Figure 13 Absolute Difference for the 20.10 Screening Method with Accumulations

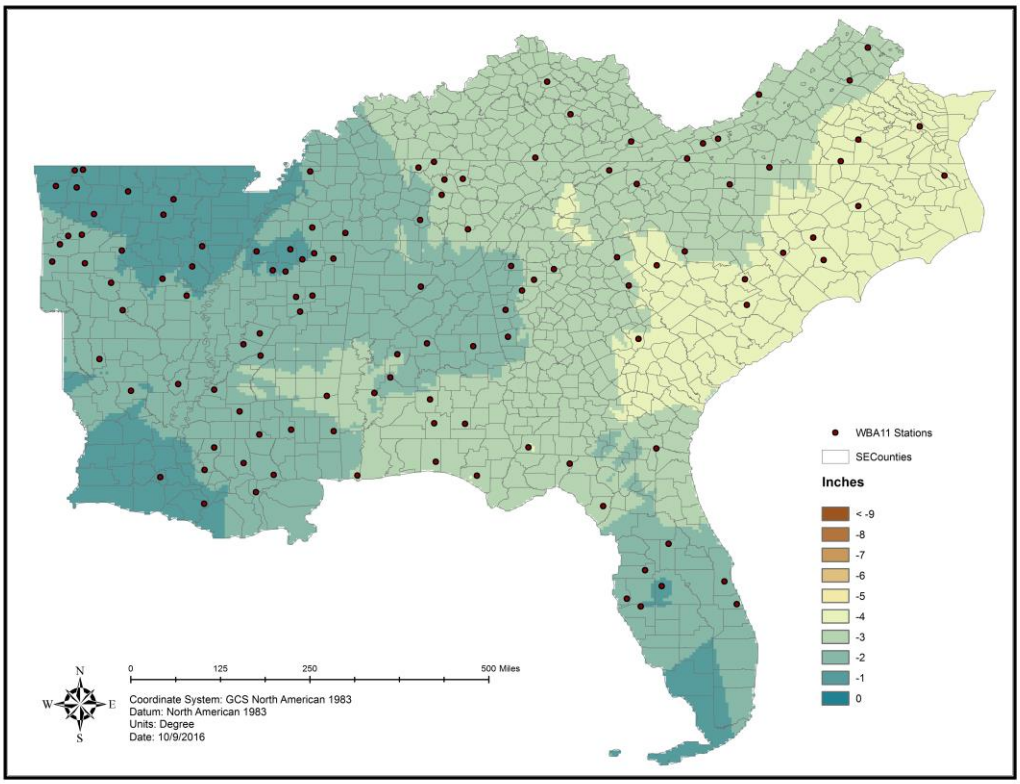

Figure 14 Absolute Difference for the 20.11 Screening Method with Accumulations

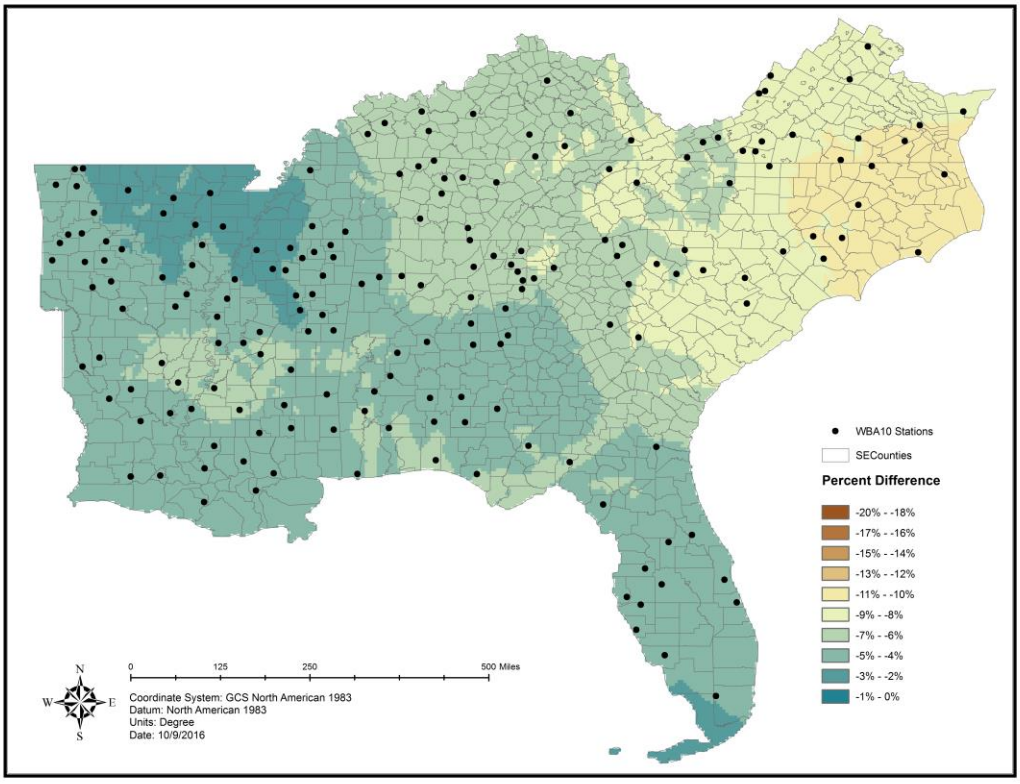

Figure 15 Relative Difference for the 20.10 Screening Method with Accumulations

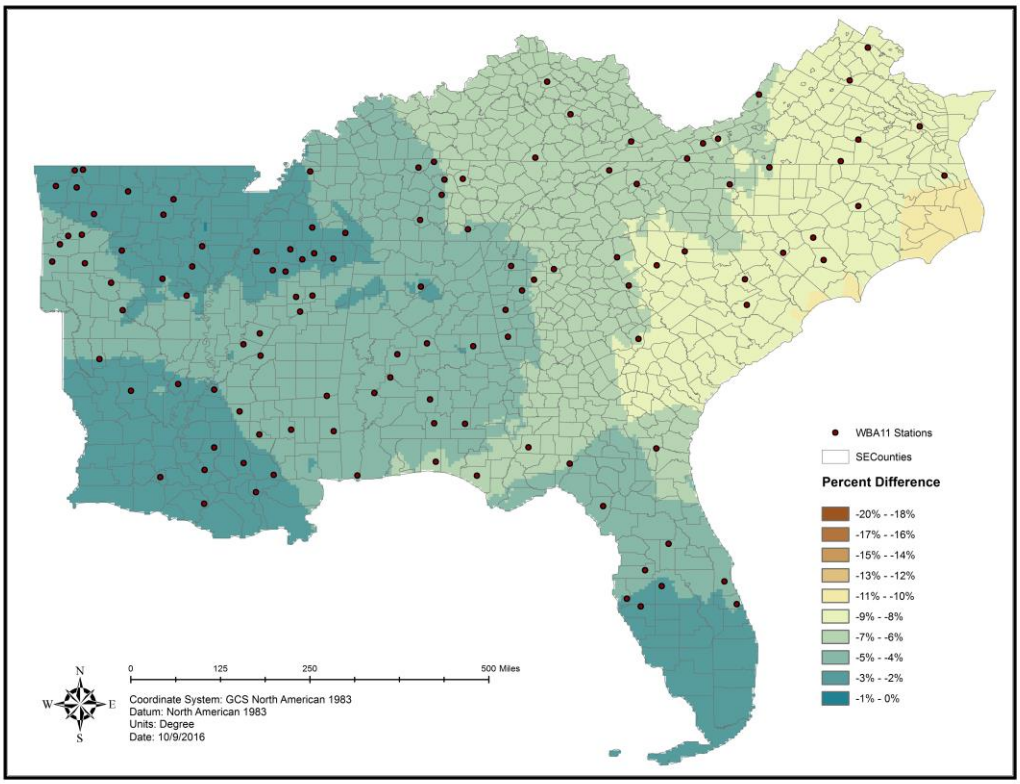

Figure 16 Relative Difference for the 20.11 Screening Method with Accumulations

Table 1 Generalized Water Balance Statistics for All Station Screening Methods

Relative Difference in Avg. Annual Precip. and Normal Annual Precip.							
SCREENING METHOD ID	MEAN %		MEDIAN %		STANDARD DEV. %		NUMBER OF STATIONS
	-	+	-	+	-	+	
20.10	-8.03	-6.15	-8.19	-6.09	3.96	4.15	280
20.11	-7.21	-5.43	-7.59	-5.86	4.11	4.15	172
25.10	-7.55	-5.56	-7.96	-5.44	3.46	3.54	167
25.11	-6.78	-5.11	-6.25	-4.84	3.48	3.49	78
30.10	-6.62	-4.81	-6.57	-4.67	3.06	3.07	68
20.12	-5.64	-4.60	-5.63	-3.81	3.65	3.80	31
30.11	-6.50	-4.93	-6.74	-4.70	2.91	3.00	22

Notes: (+/-) Headers Denote with and without Accumulations. Statistics are Calculated for All Stations in the Water Balance (Screened Stations that have Matching Climate Data for the Same Period). Negative Results Indicate a Deficit for the Period, and Positive Results Indicate a Surplus.

Table 2 Comparison of Deficits to Station Metadata for All Screening Methods

Comparison of Water Deficits to Missing, Deleted, and Total Absent Data							
SCREENING METHOD ID	MEAN MISSING		MEAN DELETED		MEAN TOTAL		NUMBER OF STATIONS
	-	+	-	+	-	+	
20.10	-1.76	0.12	-0.02	1.86	6.25	8.13	280
20.11	-1.85	-0.07	-0.28	1.50	5.08	6.86	172
25.10	-2.15	-0.16	-0.74	1.26	4.66	6.66	167
25.11	-2.80	-1.13	-1.77	-0.10	2.21	3.88	78
30.10	-2.69	-0.87	-1.66	0.16	2.27	4.09	68
20.12	-2.60	-1.57	-1.50	-0.47	1.53	2.57	31
30.11	-3.51	-1.93	-2.24	-0.67	0.75	2.33	22

Notes: (+/-) Headers Denote with and without Accumulations. Statistics are Calculated for All Stations in the Water Balance (Screened Stations that have Matching Climate Data for the Same Period). Negative Results Indicate a Deficit for the Period, and Positive Results Indicate a Surplus.

Appendix C

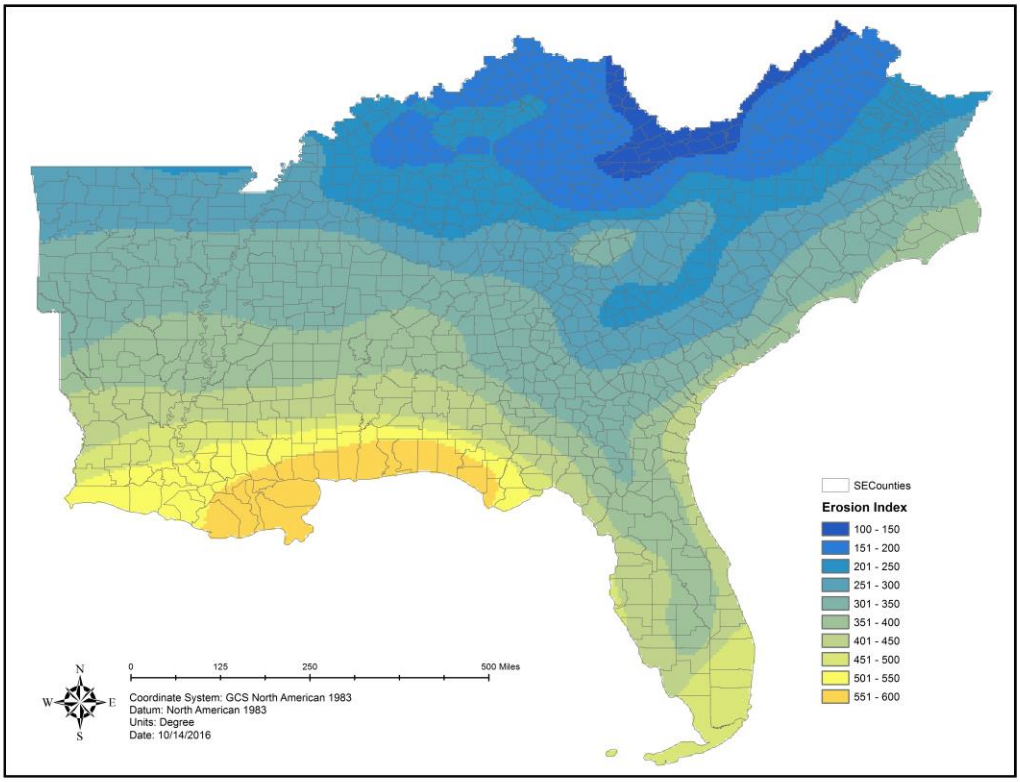

Figure 1 Digitized Isoerodent Map (R-Factor) Published in AH537 (Published 1978)

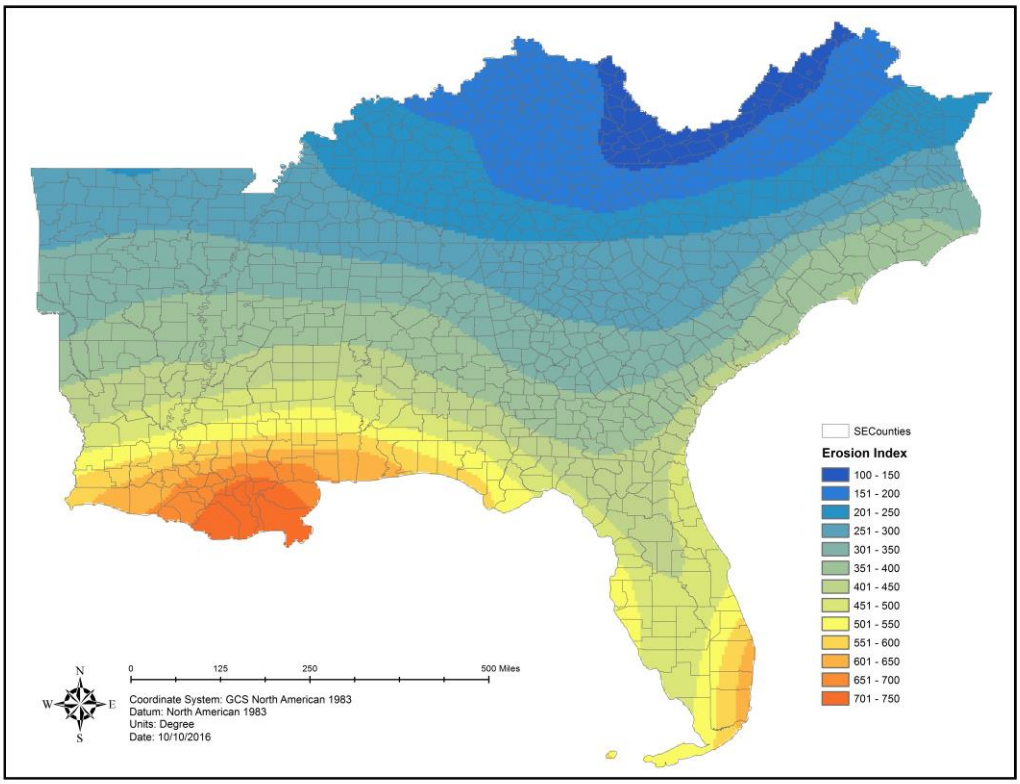

Figure 2 Digitized Isoerodent Map (R-Factor) Published in AH703 (Published 1997)

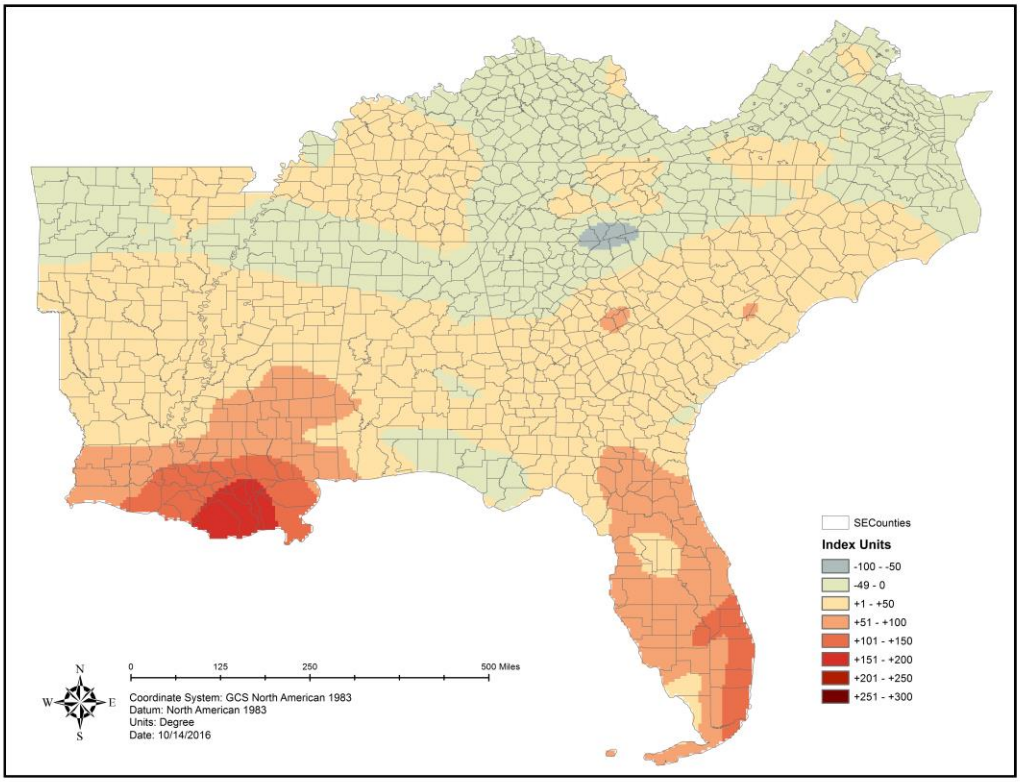

Figure 3 Absolute Difference of AH537 (Baseline) and AH703

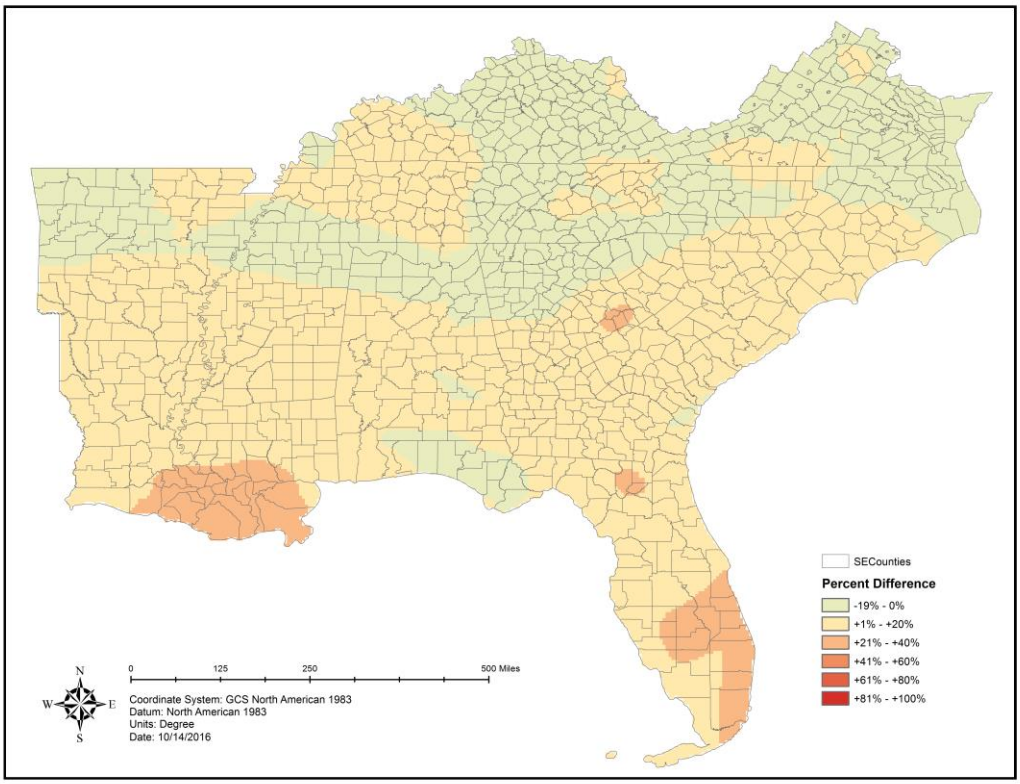

Figure 4 Relative Difference of AH537 (Baseline) and AH703

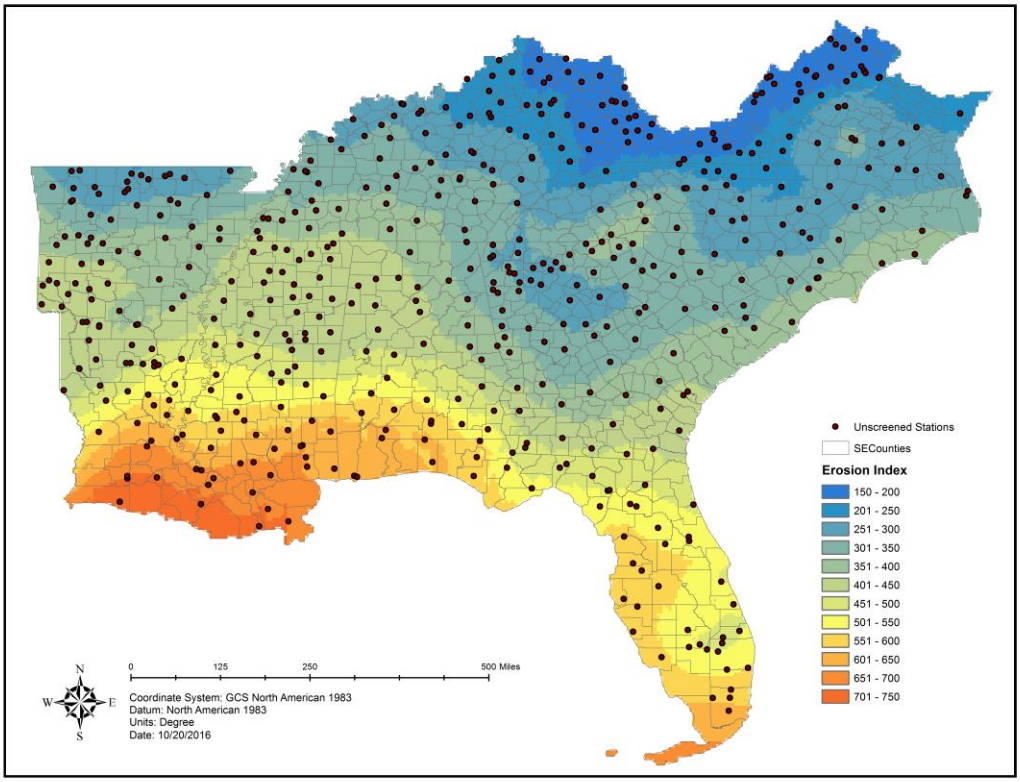

Figure 5 R-Factor Calculated from Unscreened Stations (I_{30} Not Limited)

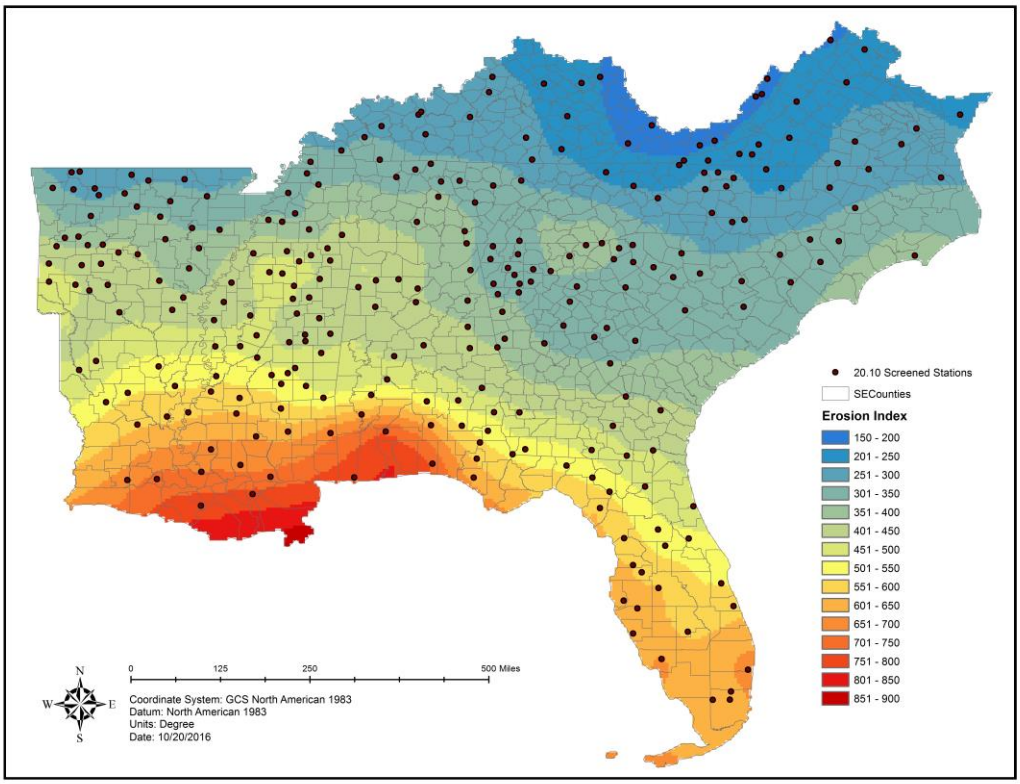

Figure 6 R-Factor Calculated from 20.10 Screened Stations (I_{30} Not Limited)

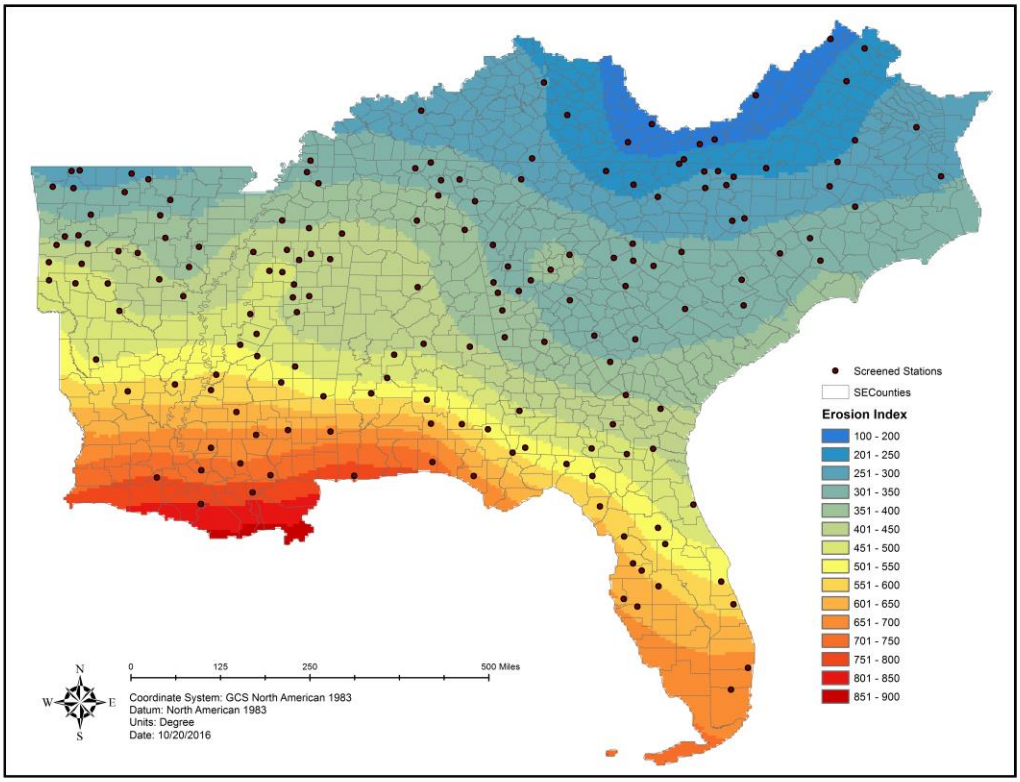

Figure 7 R-Factor Calculated from 20.11 Screened Stations (I_{30} Not Limited)

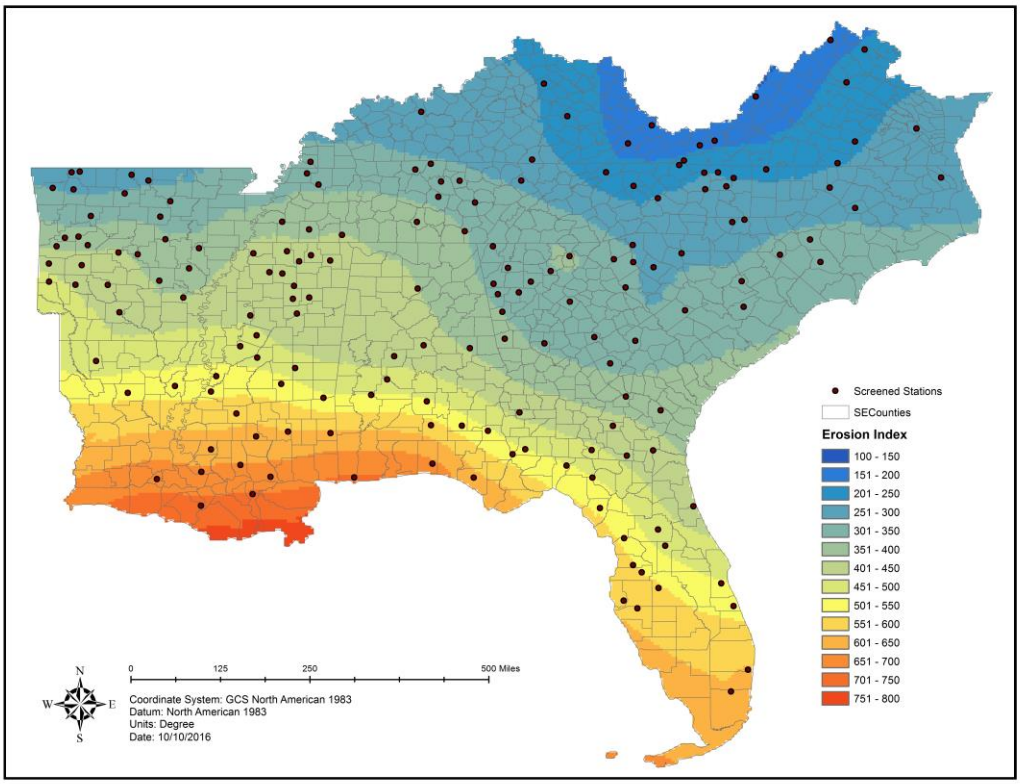

Figure 8 R-Factor Calculated from Screened Stations (I_{30} Limited—Prefered Method)

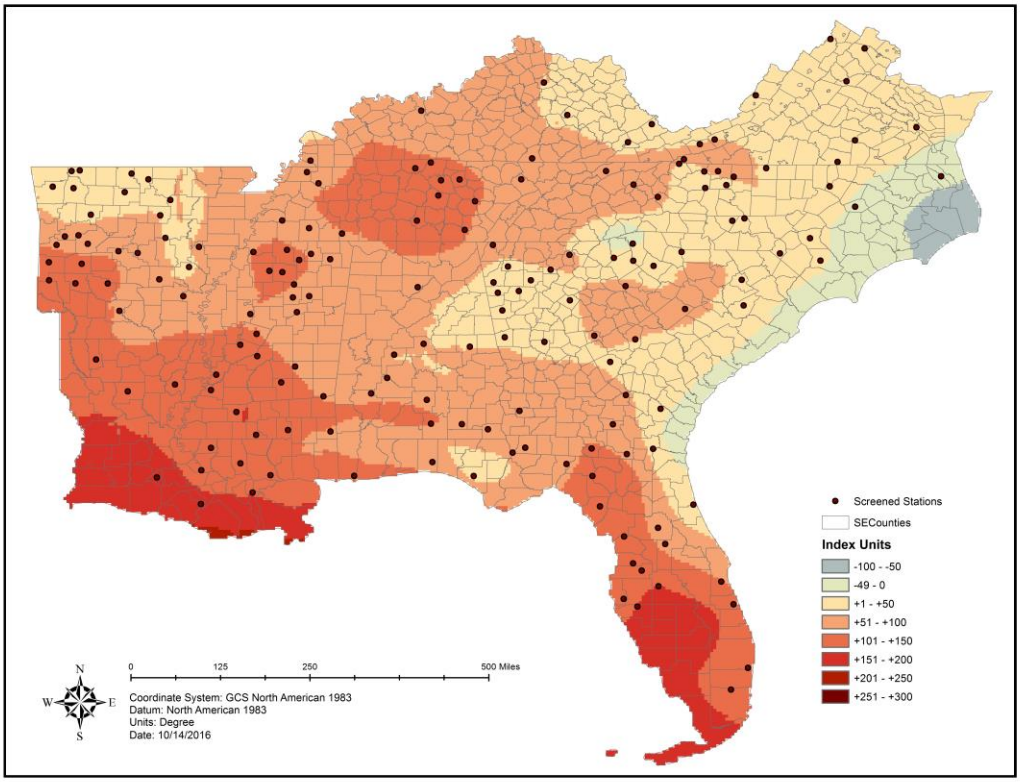

Figure 9 Absolute Difference from AH537 Using Prefered Method

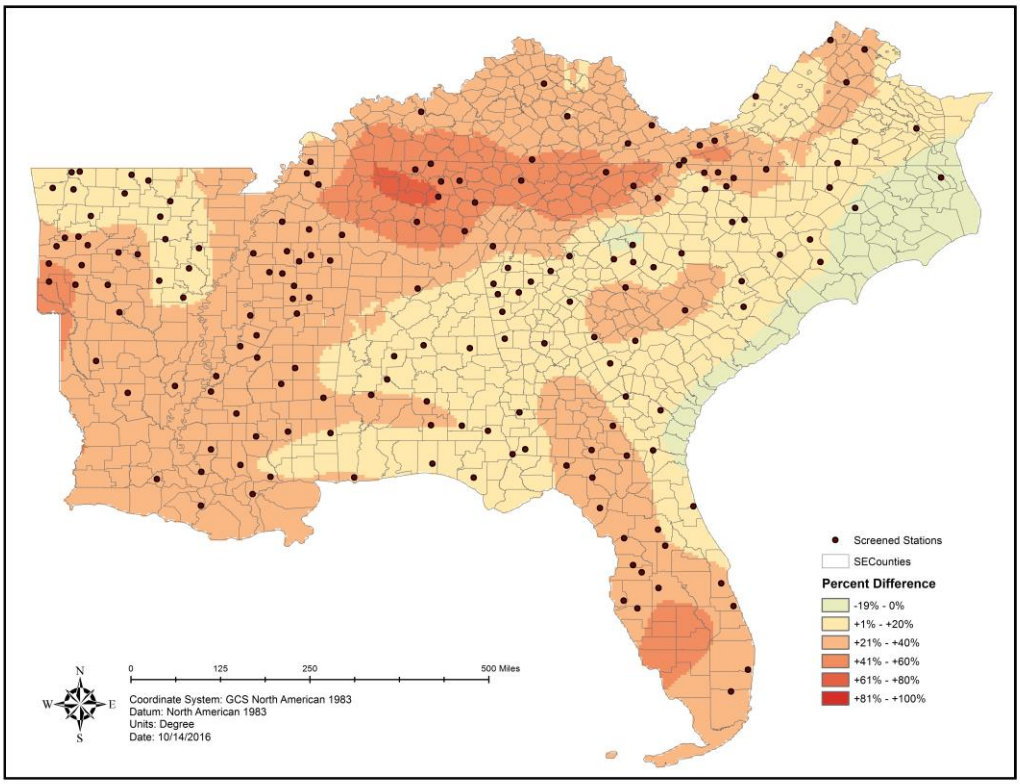

Figure 10 Relative Difference from AH537 Using Prefered Method

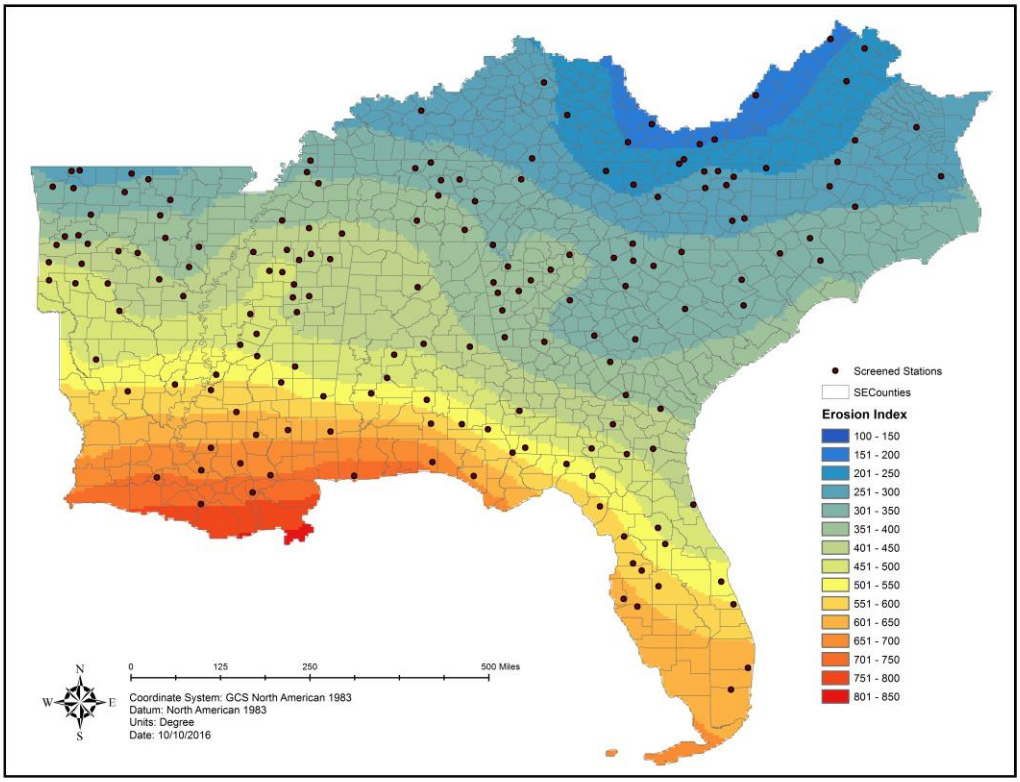

Figure 11 R-Factor Calculated with I_{30} Adjusted +4% to Mimic Breakpoint Data

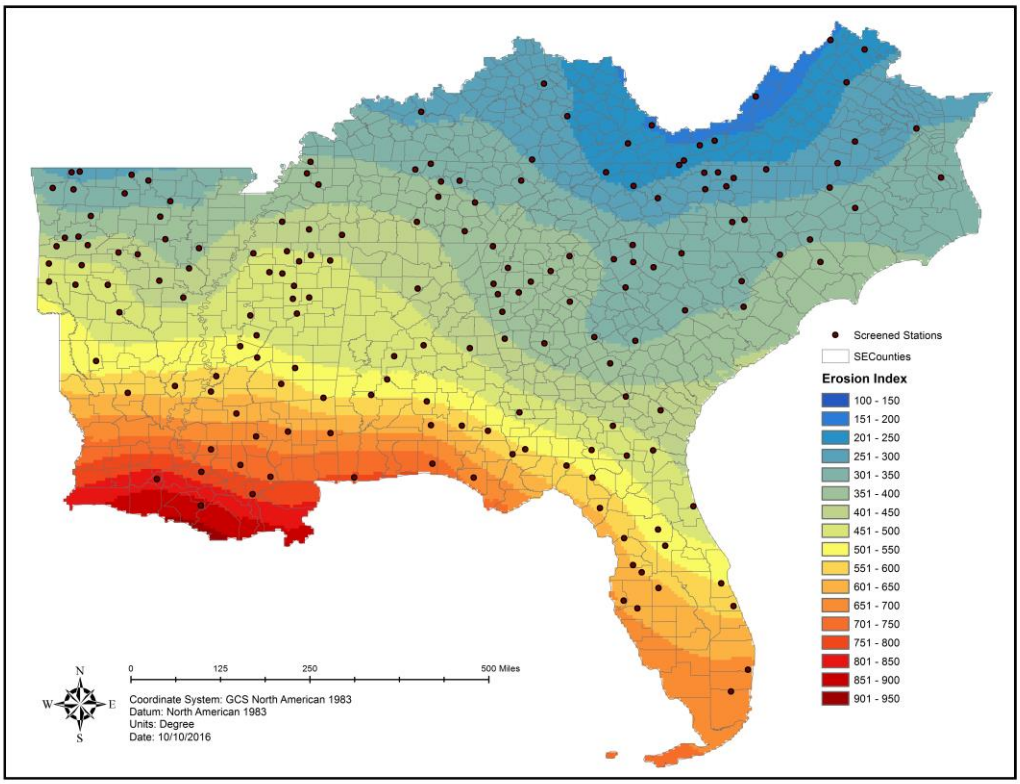

Figure 12 R-Factor Calculated with I_{30} and Missing Percentage Adjustment

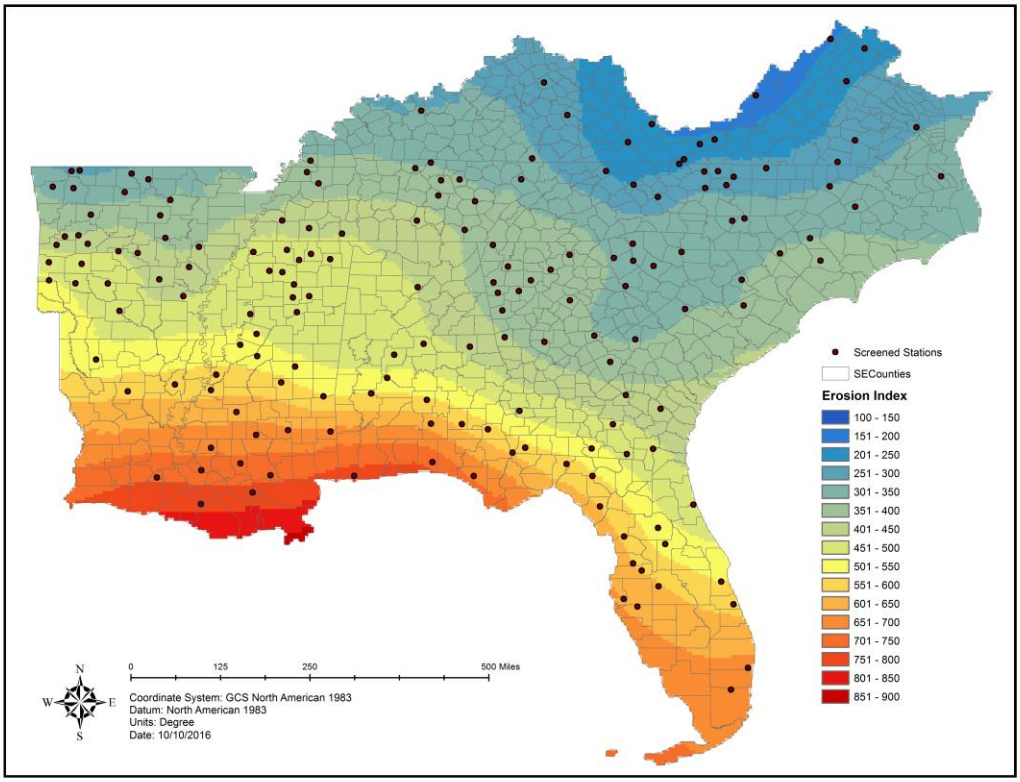

Figure 13 R-Factor Calculated with I_{30} and Deleted Percentage Adjustment

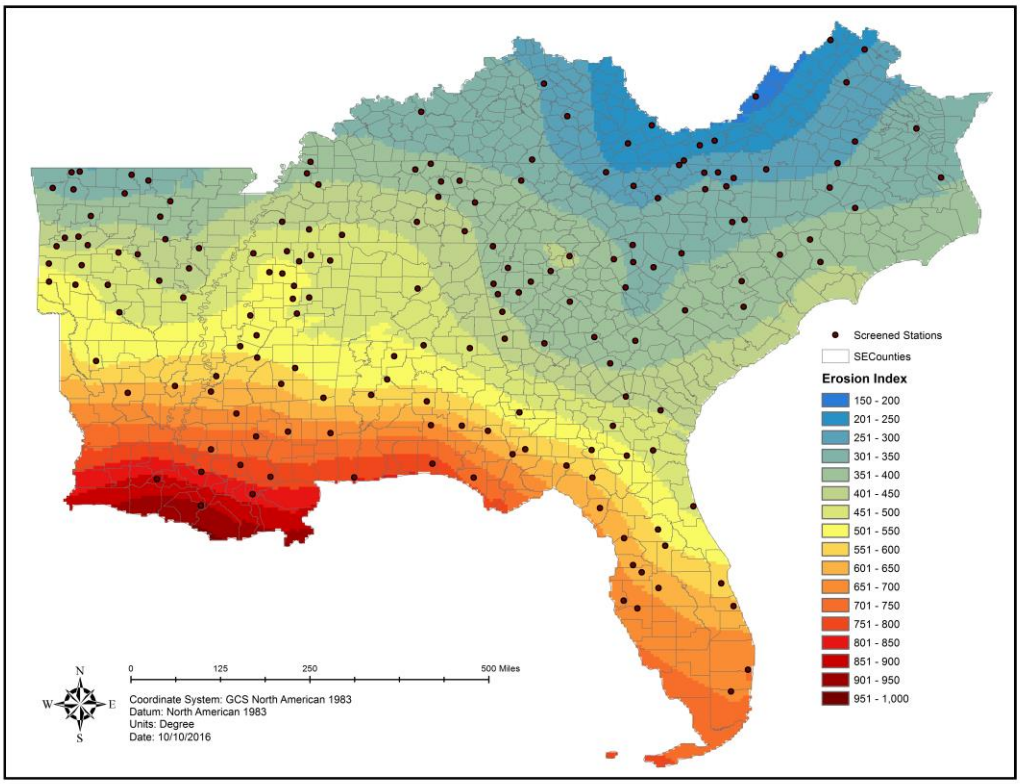

Figure 14 R-Factor Calculated with I_{30}, Missing, and Deleted Percentages Adjustment

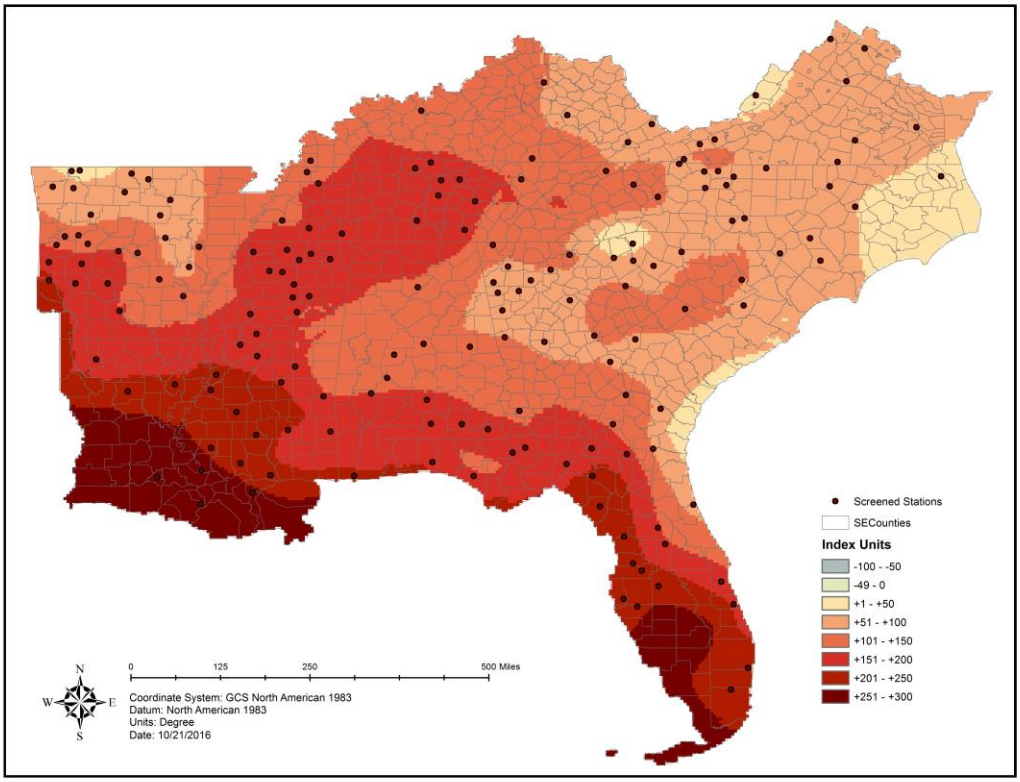

Figure 15 Absolute Difference from AH537 Using Adjusted Data (All)

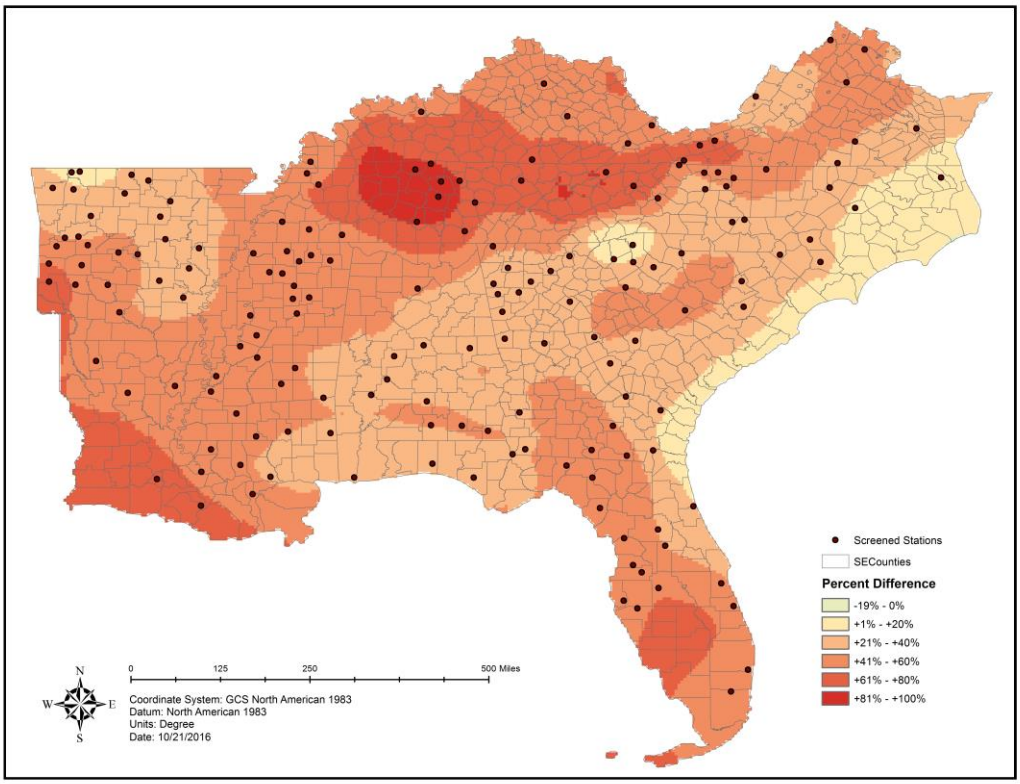

Figure 16 Absolute Difference from AH537 Using Adjusted Data (All)

Appendix D

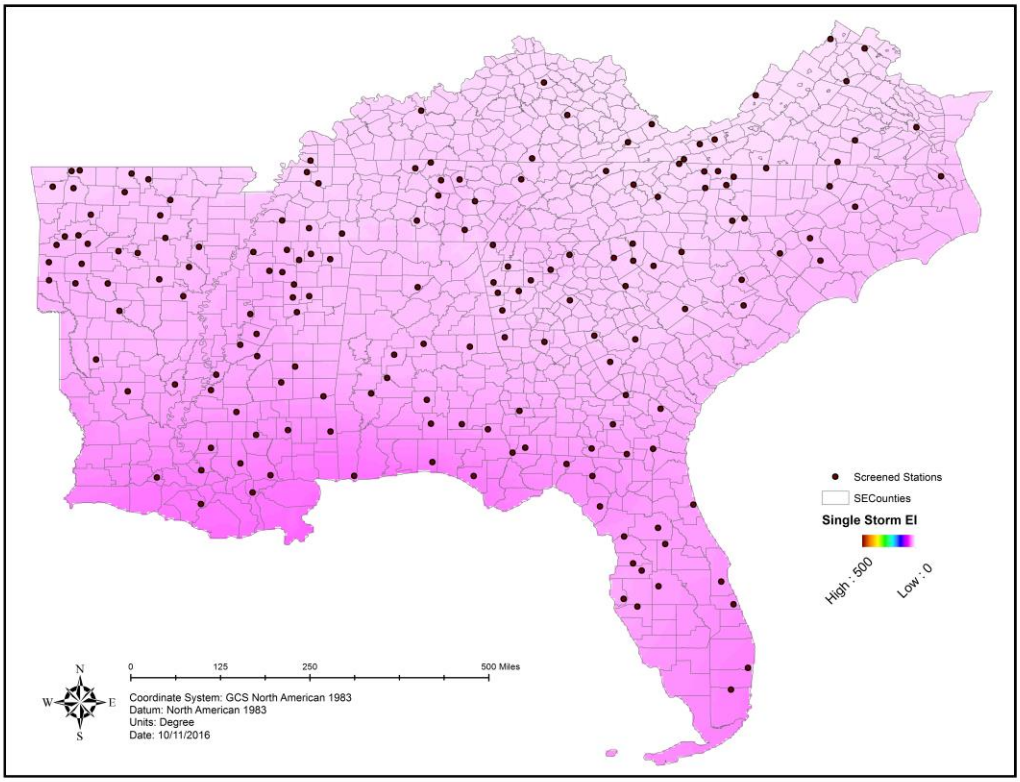

Figure 1 Single Storm EI (1YR RP) Calculated from Screened Stations (I_{30} Unlimited)

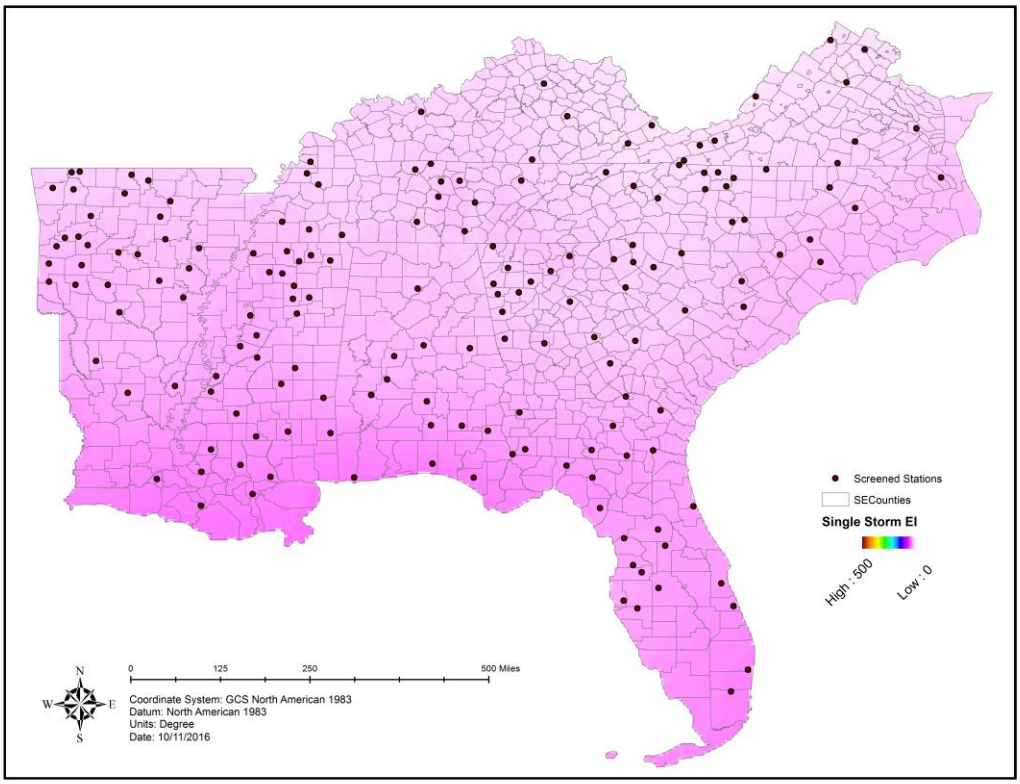

Figure 2 Single Storm EI (1YR RP) Calculated from Screened Stations (I_{30} Limited)

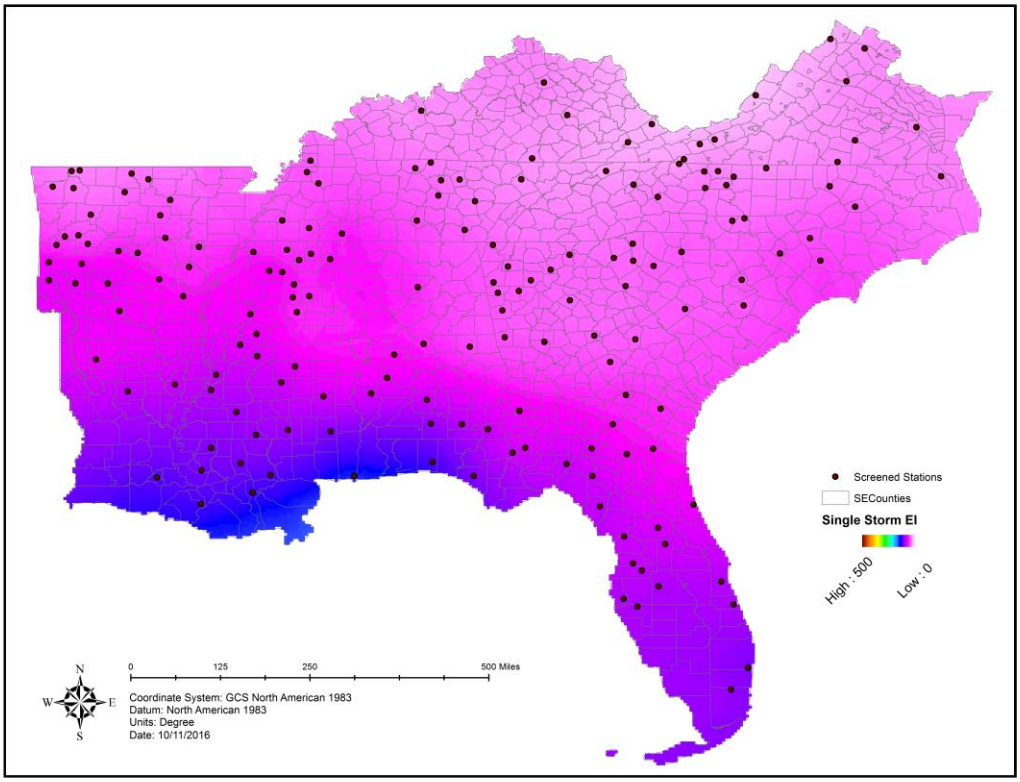

Figure 3 Single Storm EI (2YR RP) Calculated from Screened Stations (I_{30} Unlimited)

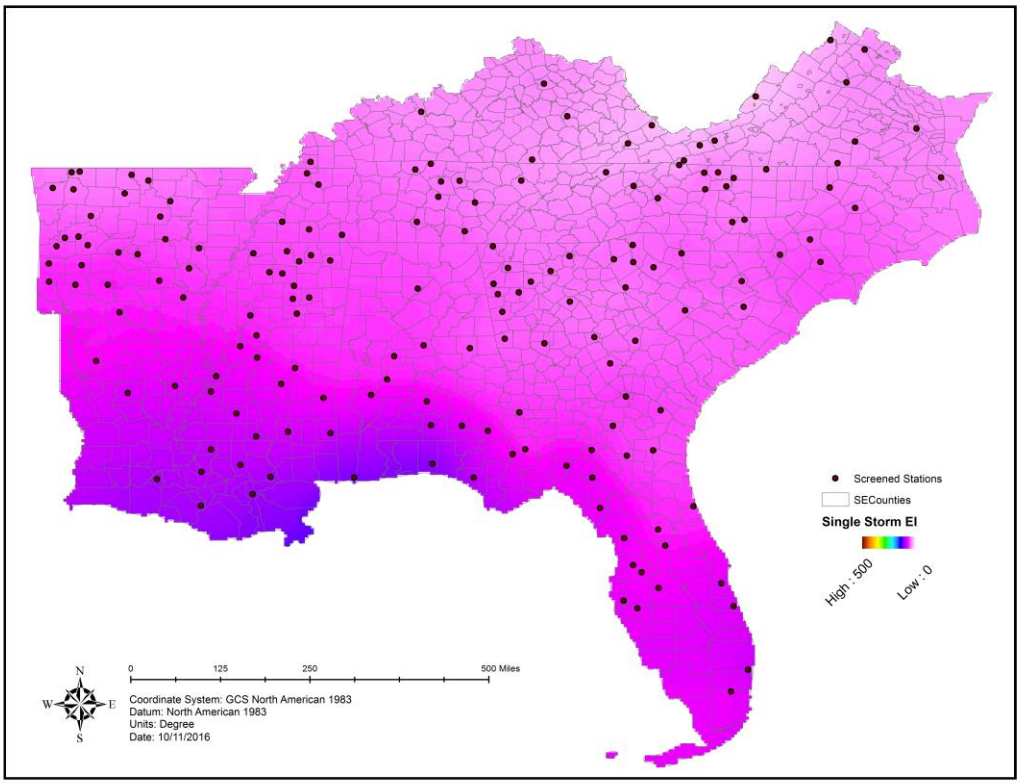

Figure 4 Single Storm EI (2YR RP) Calculated from Screened Stations (I_{30} Limited)

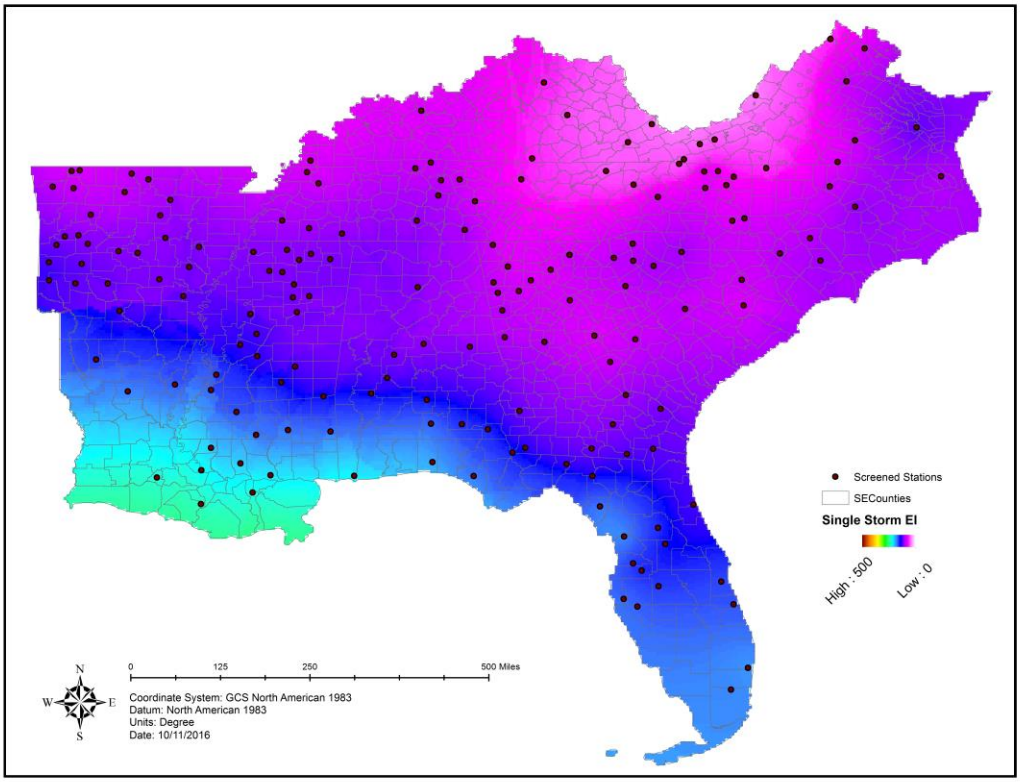

Figure 5 Single Storm EI (5YR RP) Calculated from Screened Stations (I_{30} Unlimited)

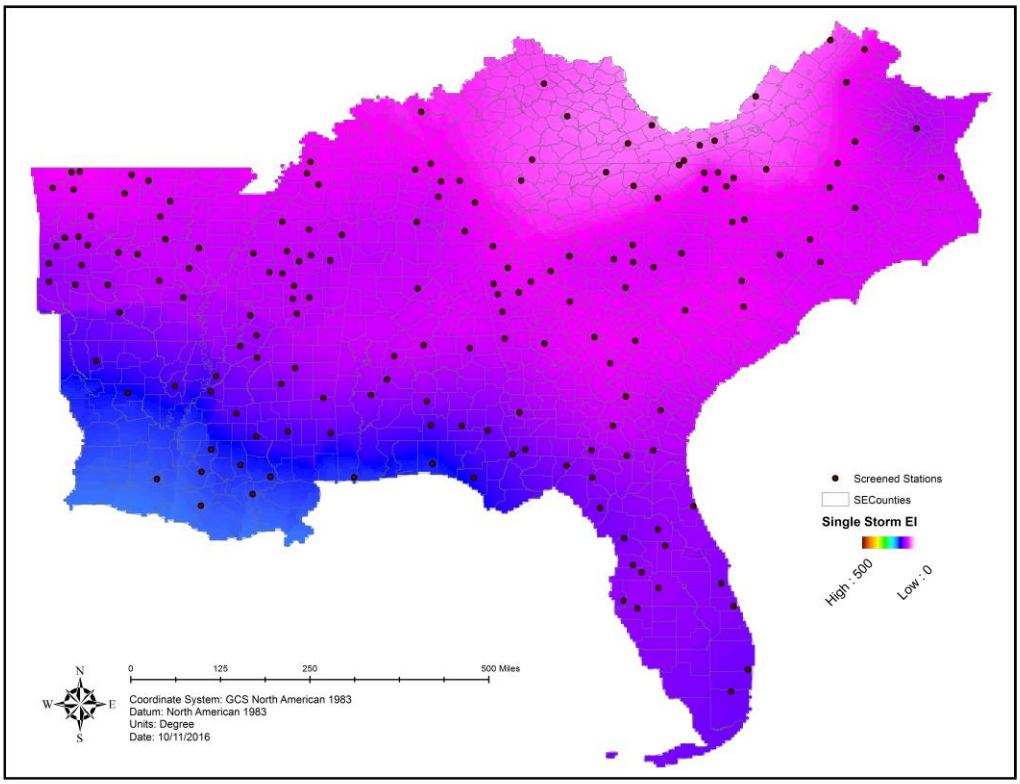

Figure 6 Single Storm EI (5YR RP) Calculated from Screened Stations (I_{30} Limited)

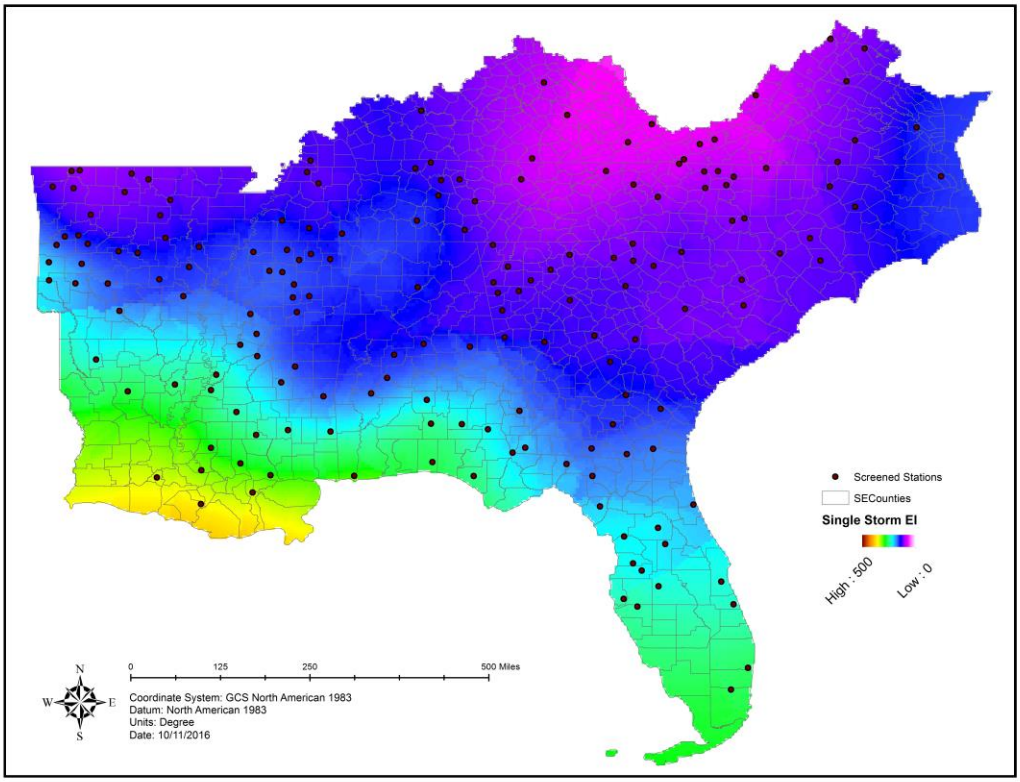

Figure 7 Single Storm EI (10YR RP) Calculated from Screened Stations (I_{30} Unlimited)

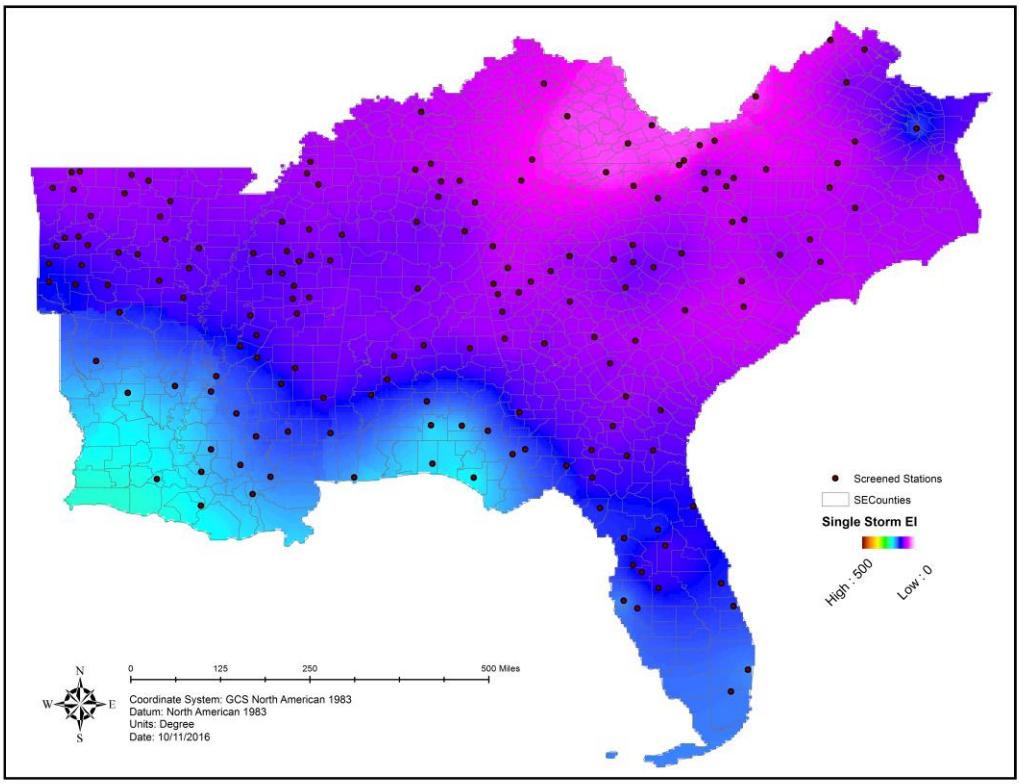

Figure 8 Single Storm EI (10YR RP) Calculated from Screened Stations (I_{30} Limited)

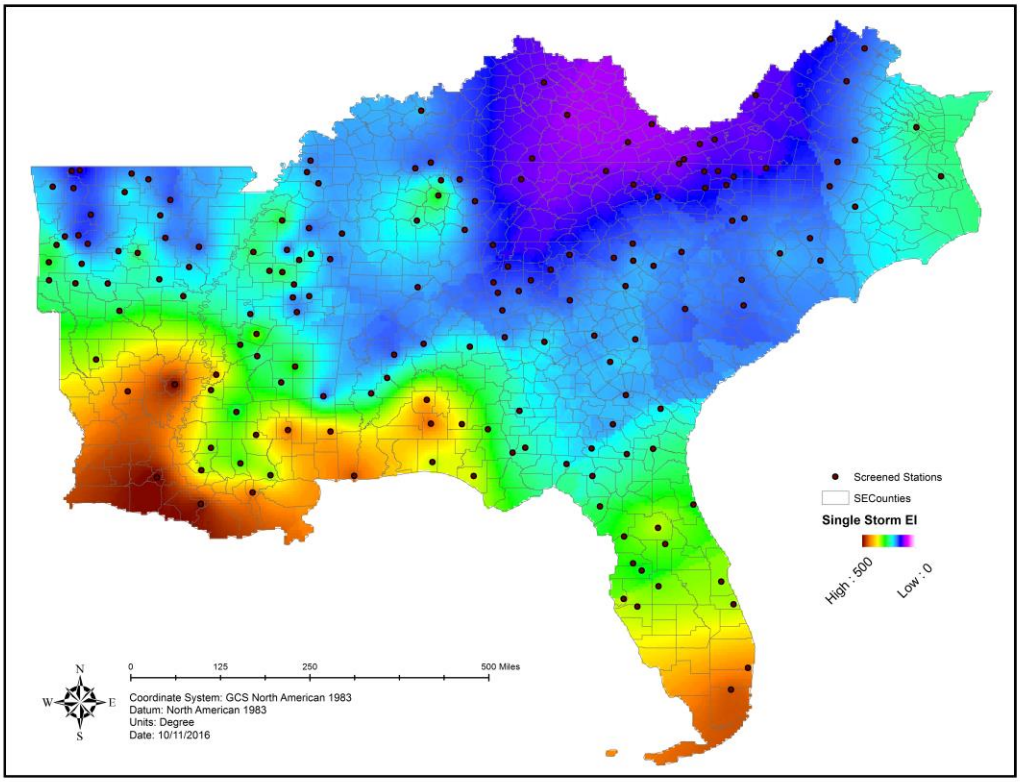

Figure 9 Single Storm EI (20YR RP) Calculated from Screened Stations (I_{30} Unlimited)

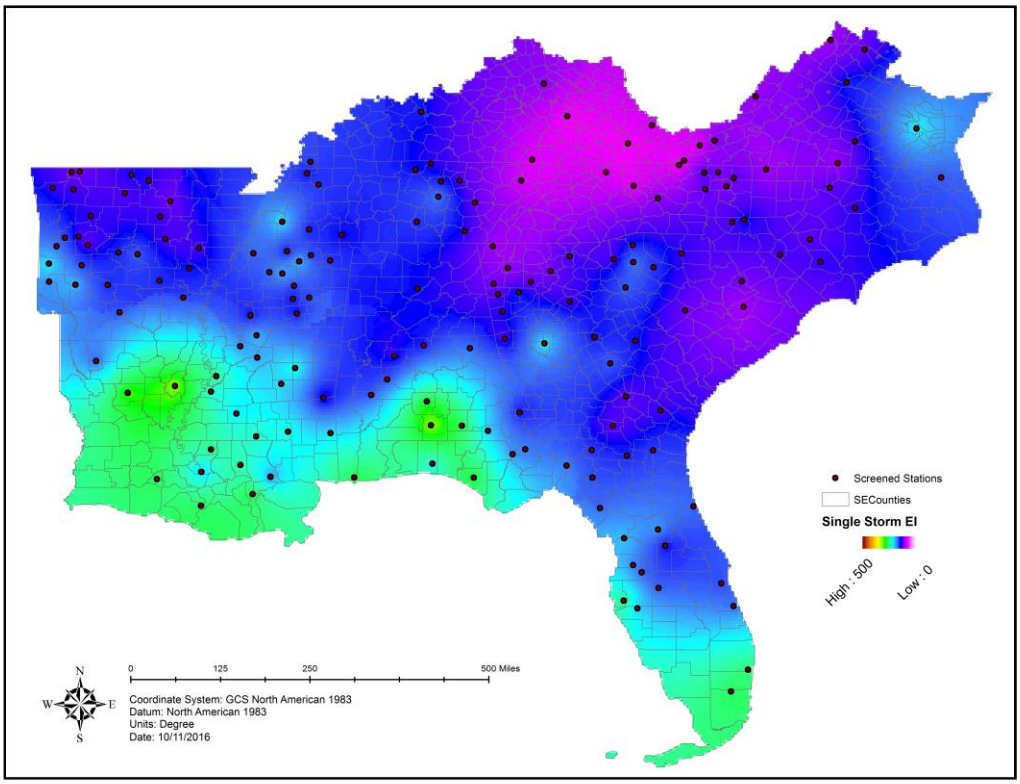

Figure 10 Single Storm EI (20YR RP) Calculated from Screened Stations (I_{30} Limited)

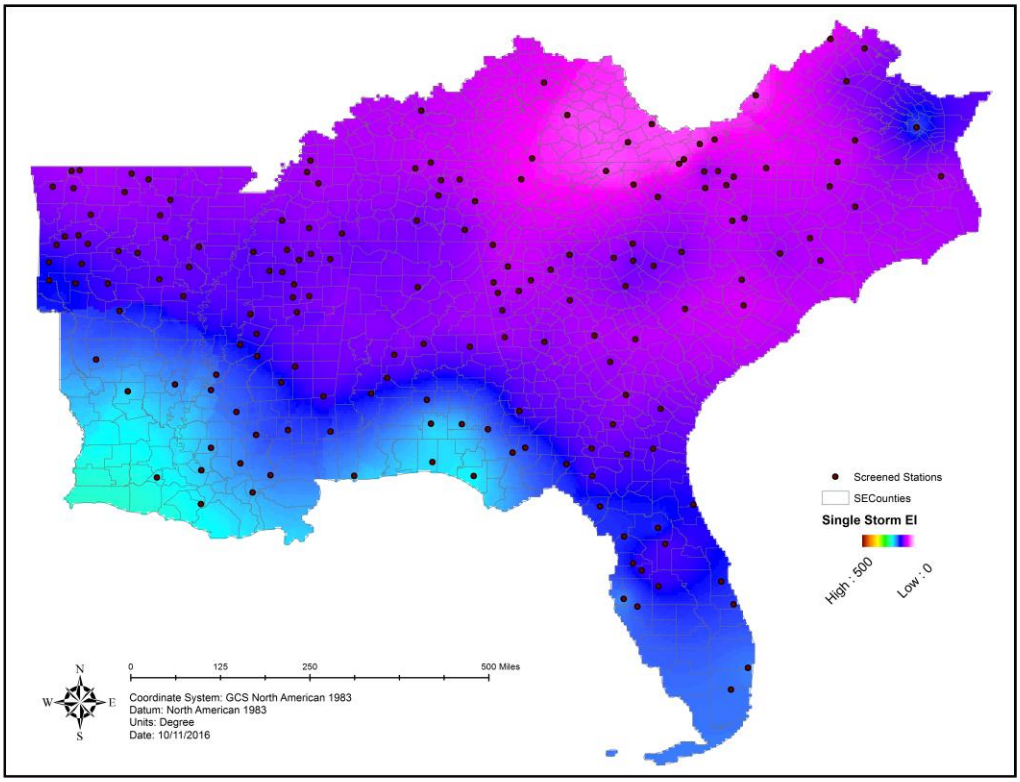

Figure 11 Single Storm EI (10YR RP) without Log-Transformation

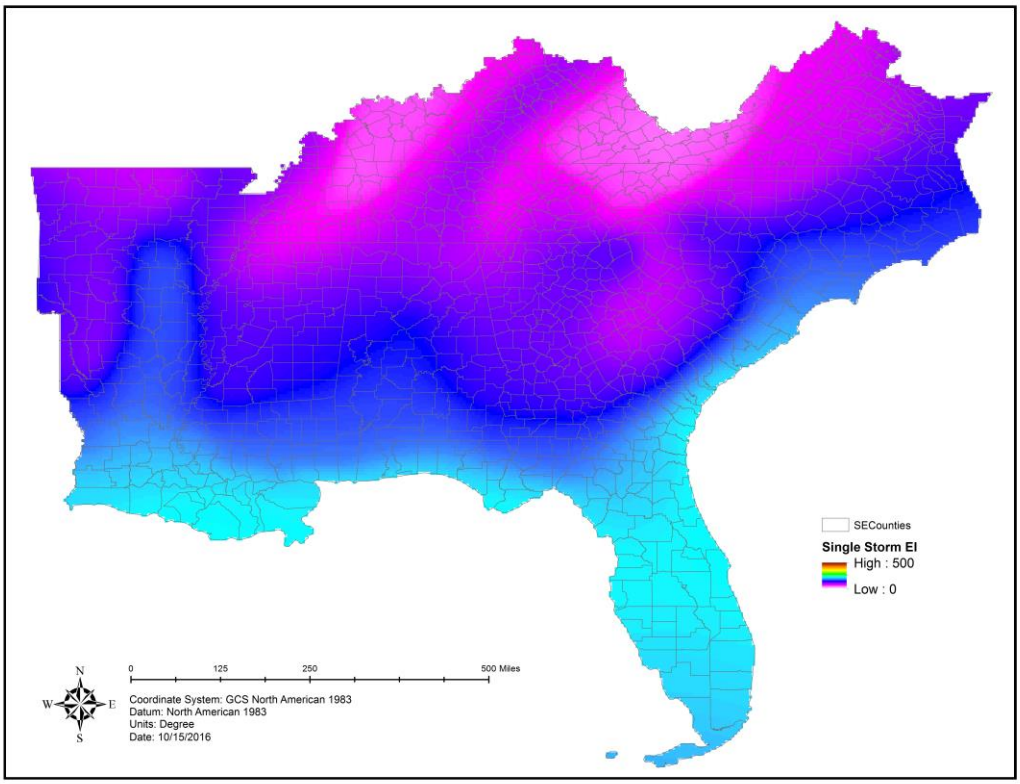

Figure 12 Single Storm EI (10YR RP) from AH537 and AH703

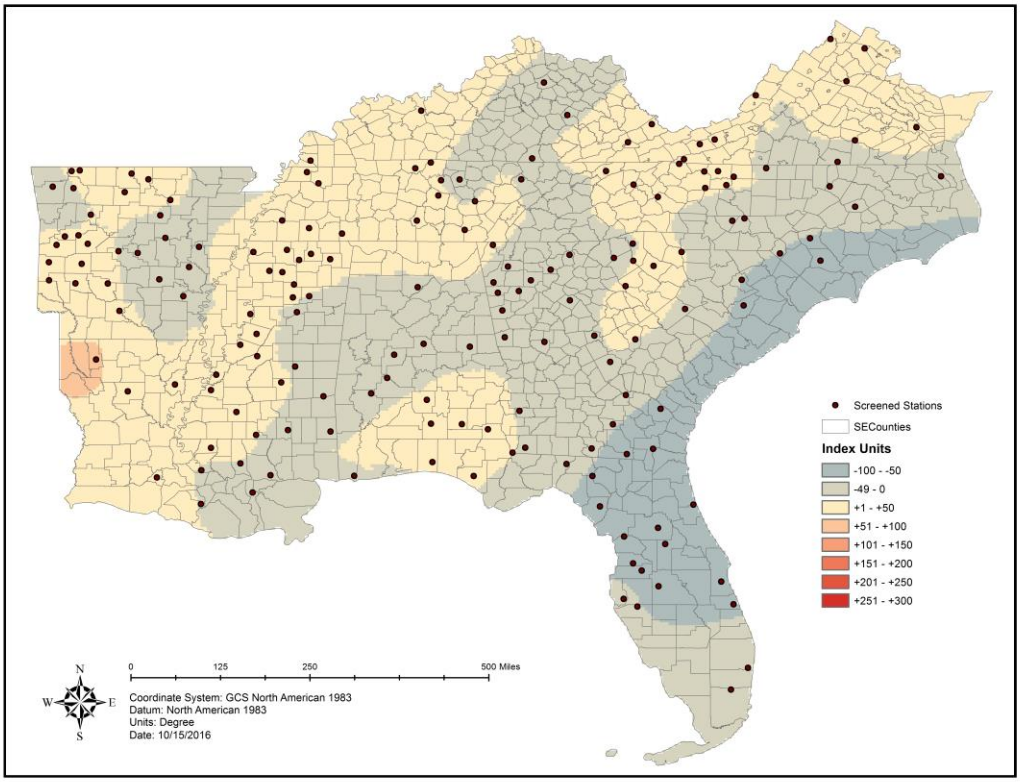

Figure 13 Absolute Difference from AH703 (10YR RP) for I_{30} Limited Data

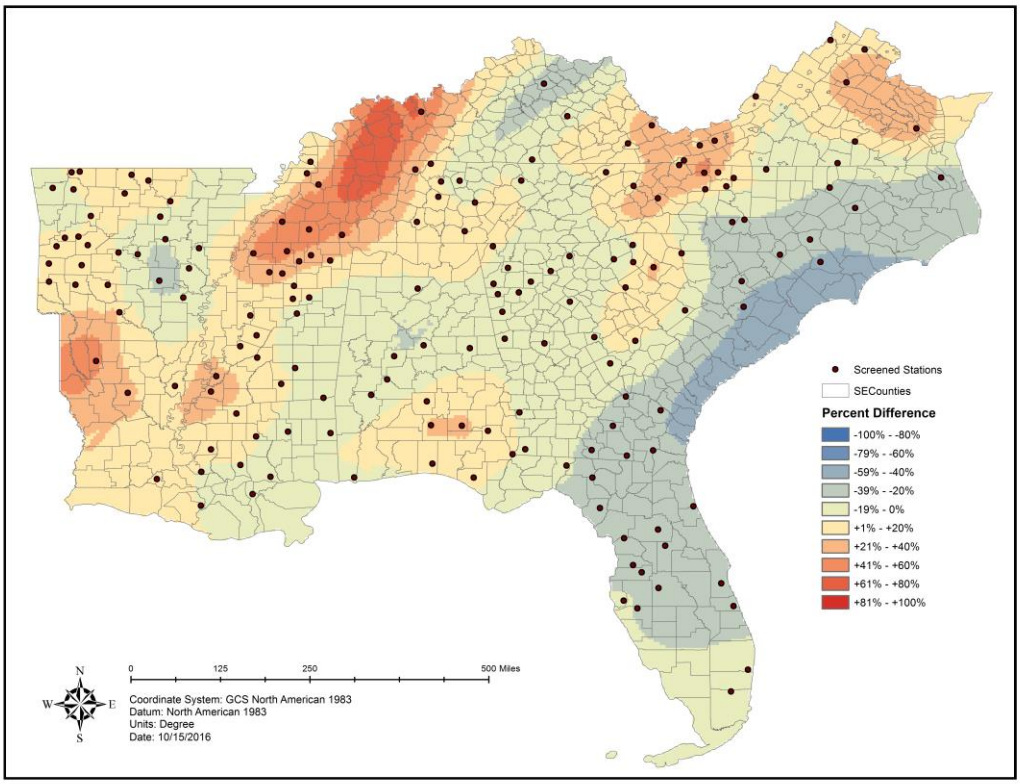

Figure 14 Relative Difference from AH703 (10YR RP) for I_{30} Limited Data

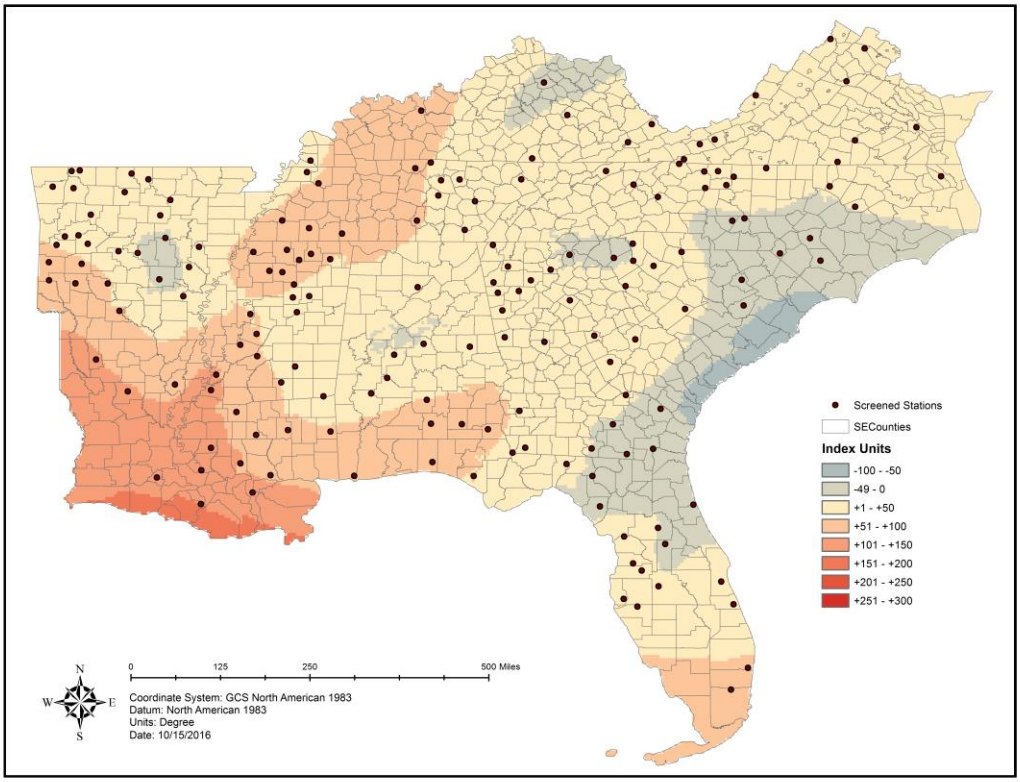

Figure 15 Absolute Difference from AH703 (10YR RP) for I_{30} Unlimited Data

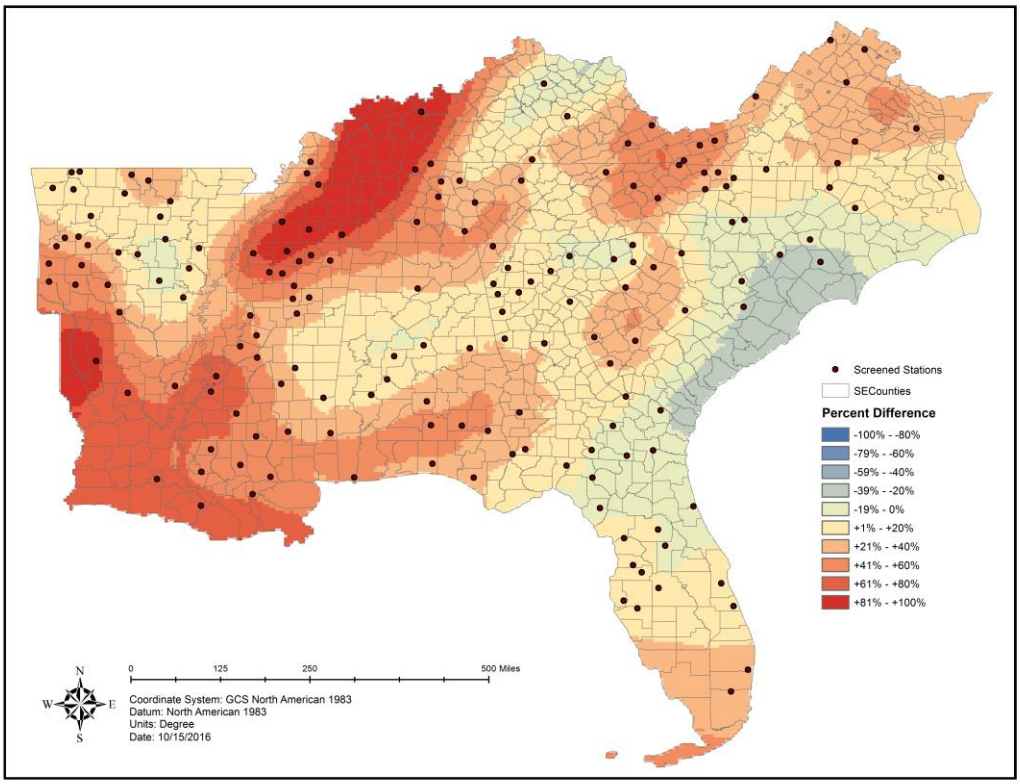

Figure 16 Relative Difference from AH703 (10YR RP) for I_{30} Unlimited Data

Appendix E

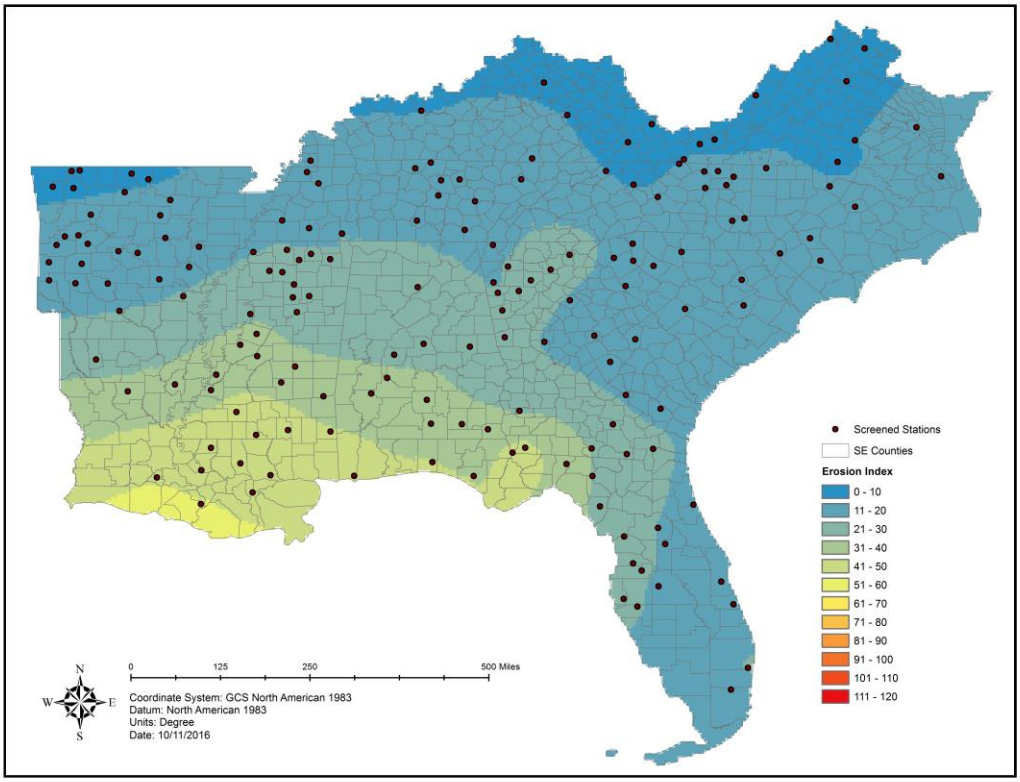

Figure 1 Mean EI for January

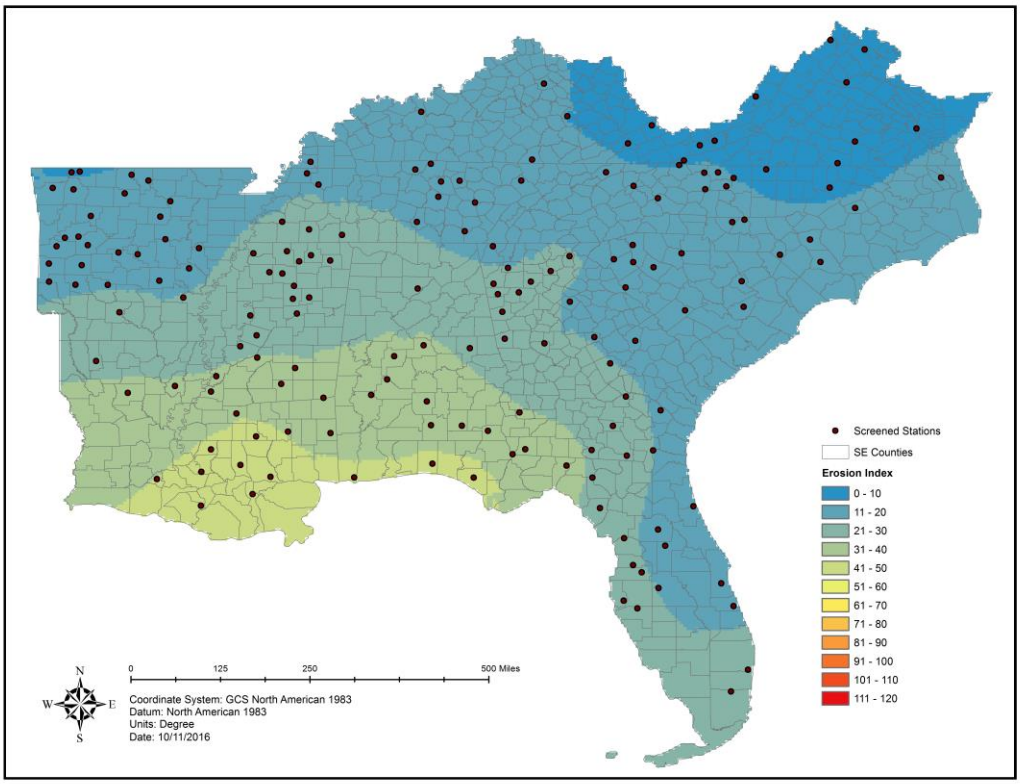

Figure 2 Mean EI for February

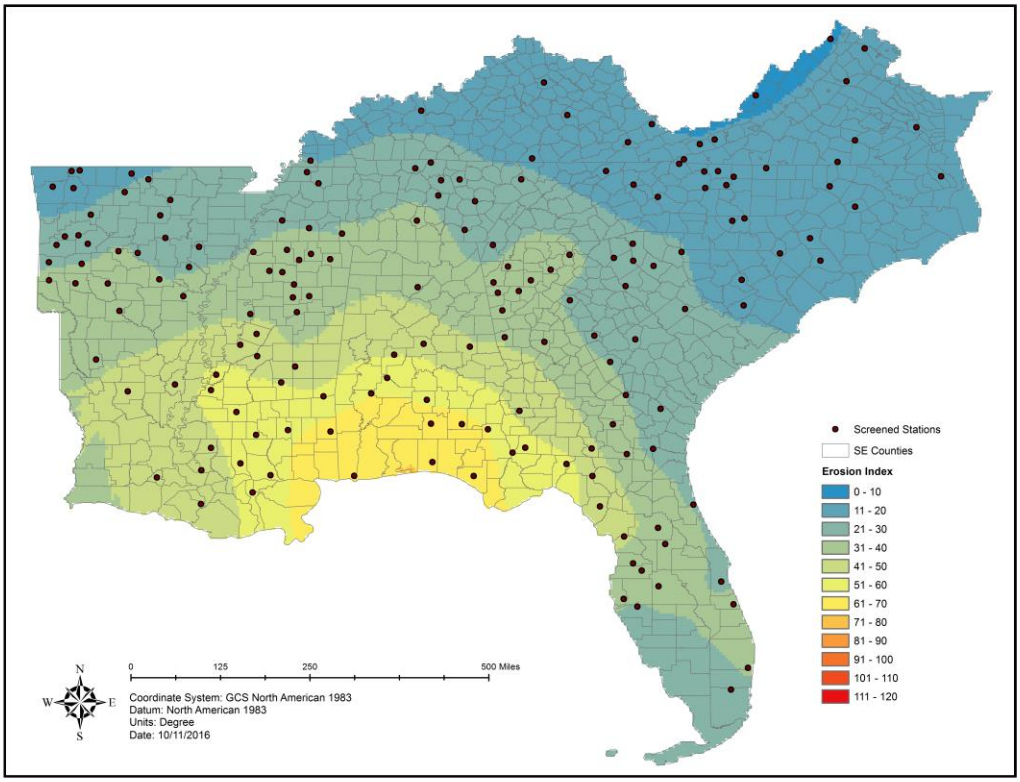

Figure 3 Mean EI for March

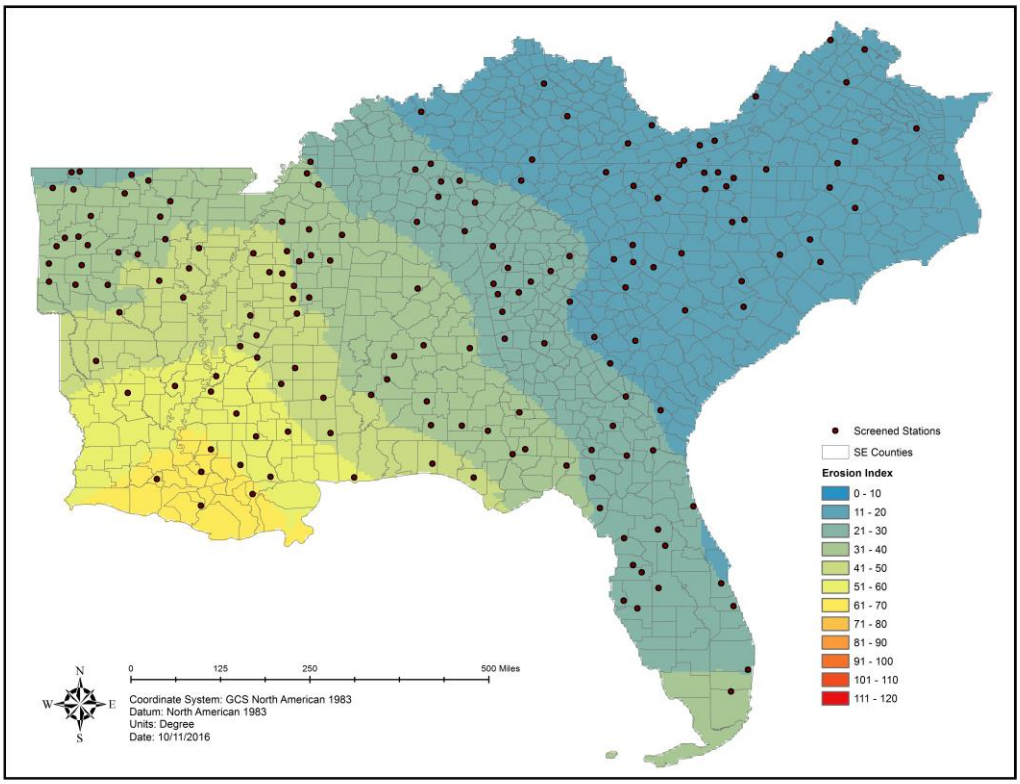

Figure 4 Mean EI for April

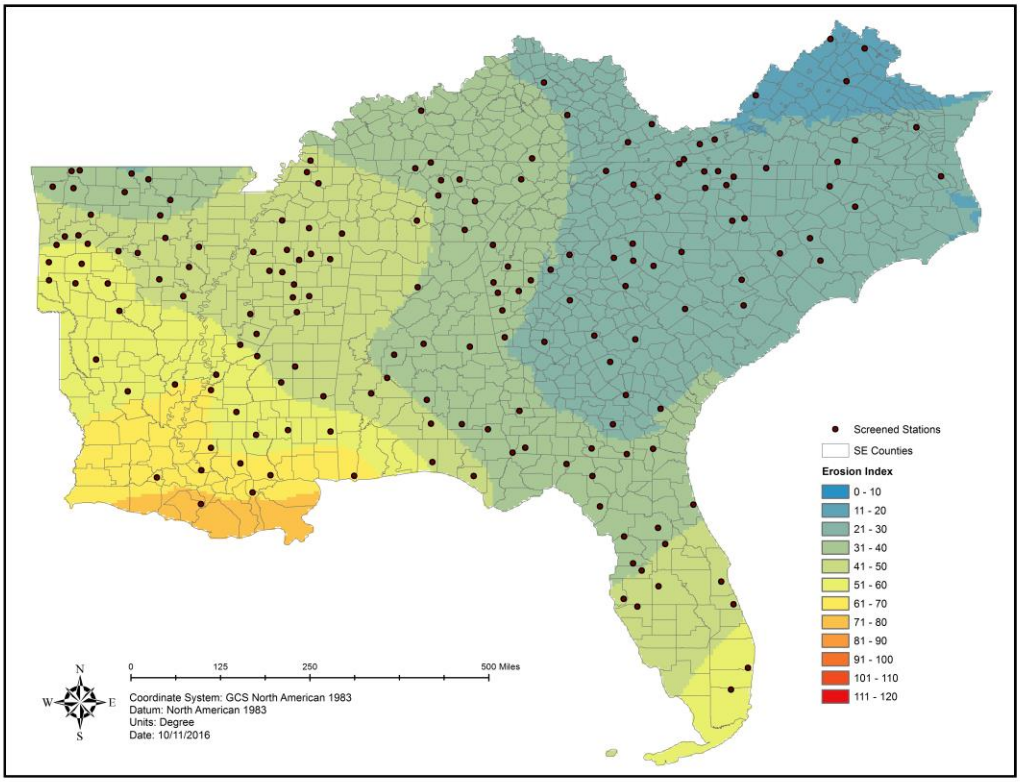

Figure 5 Mean EI for May

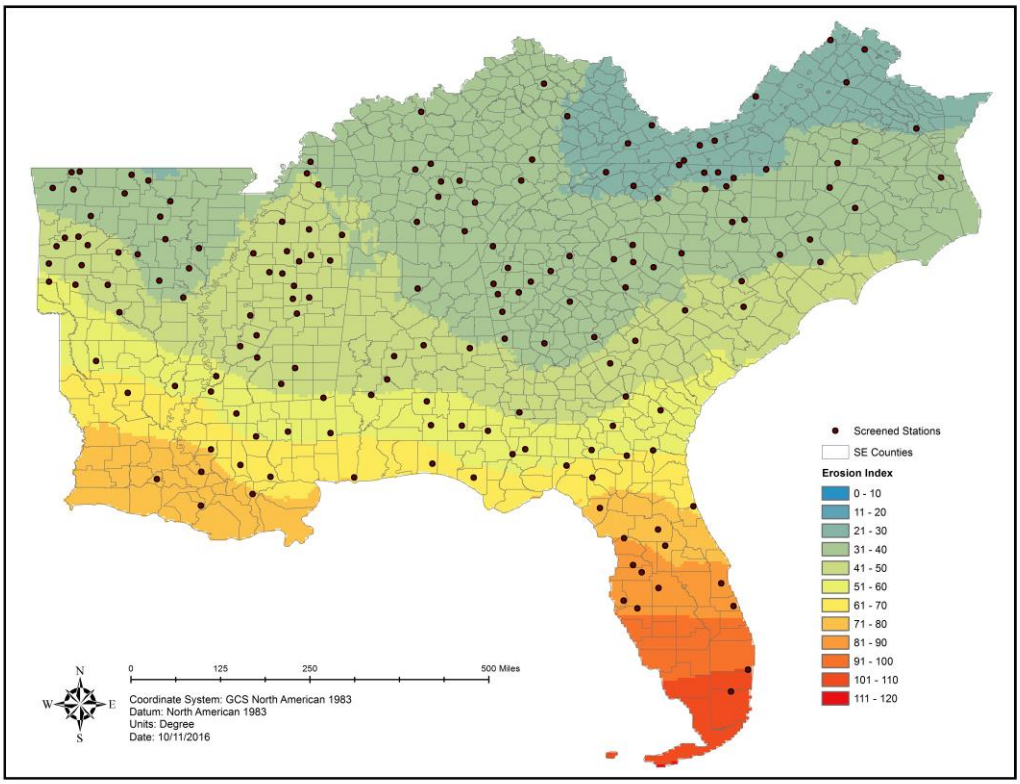

Figure 6 Mean EI for June

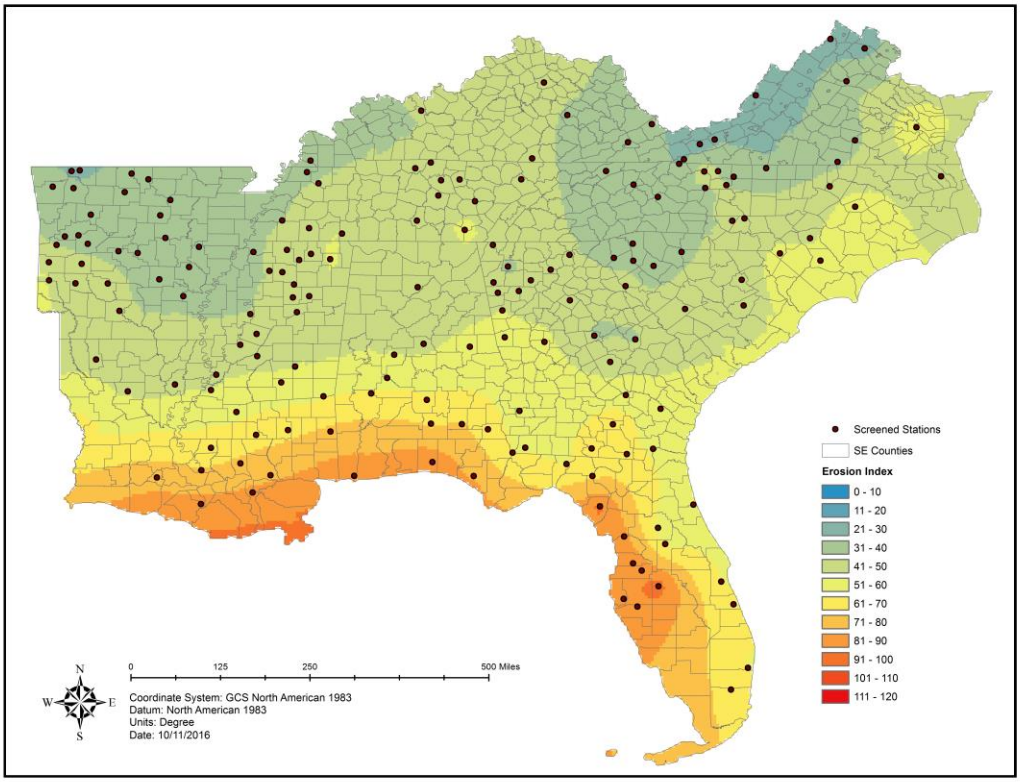

Figure 7 Mean EI for July

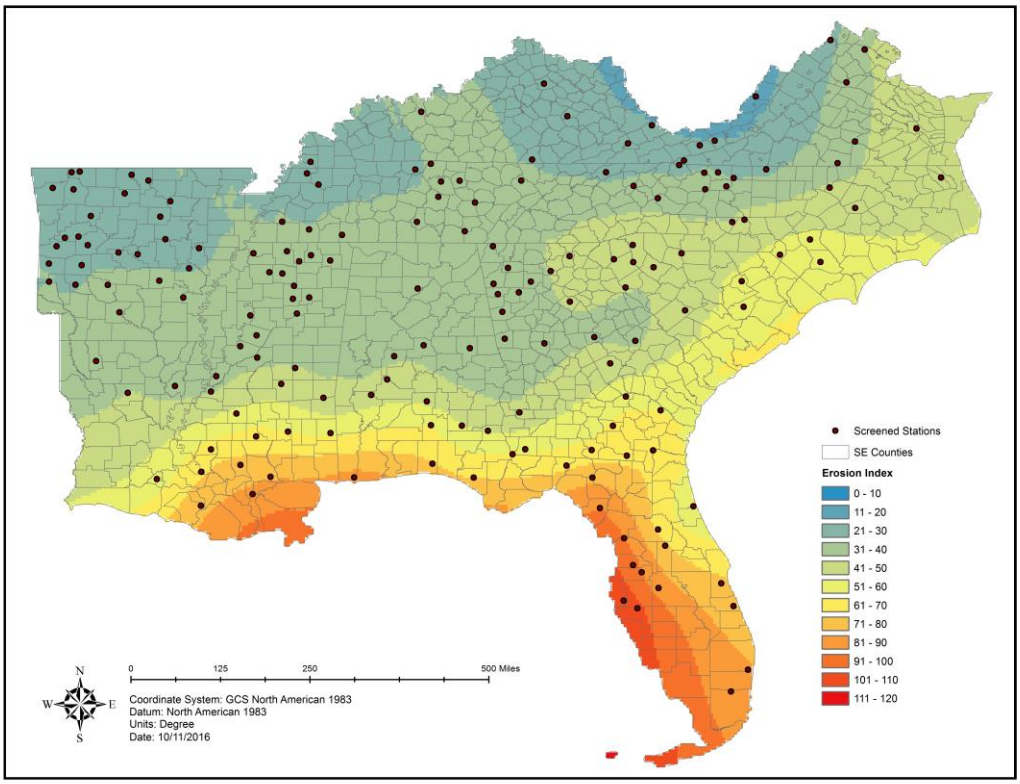

Figure 8 Mean EI for August

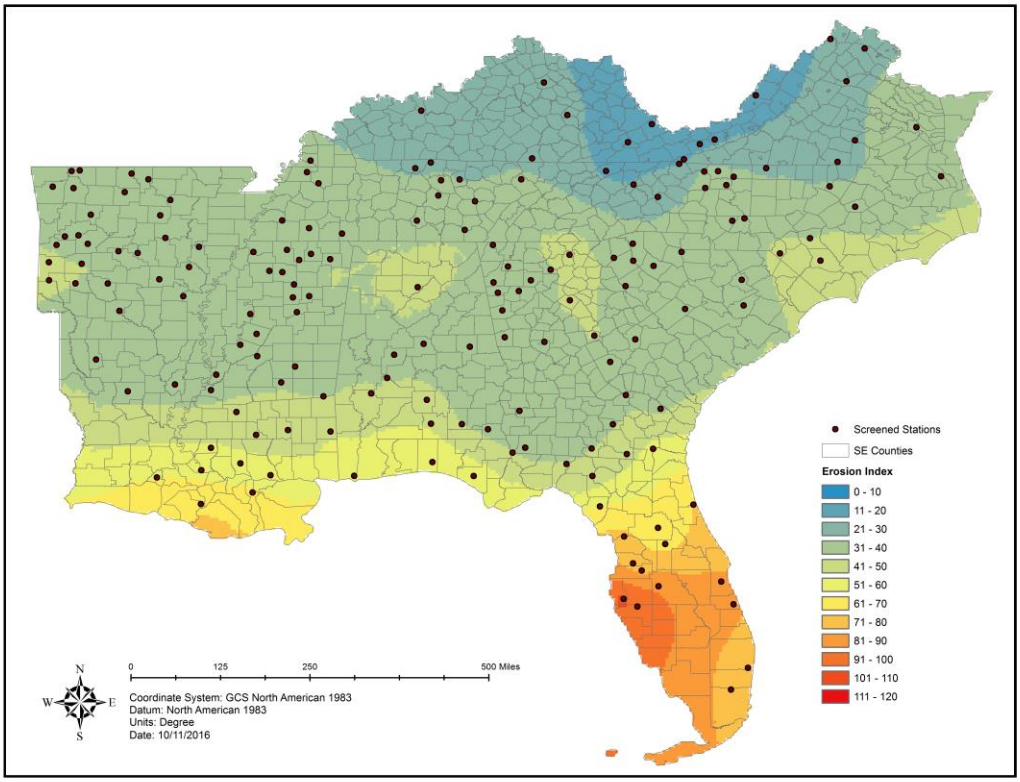

Figure 9 Mean EI for September

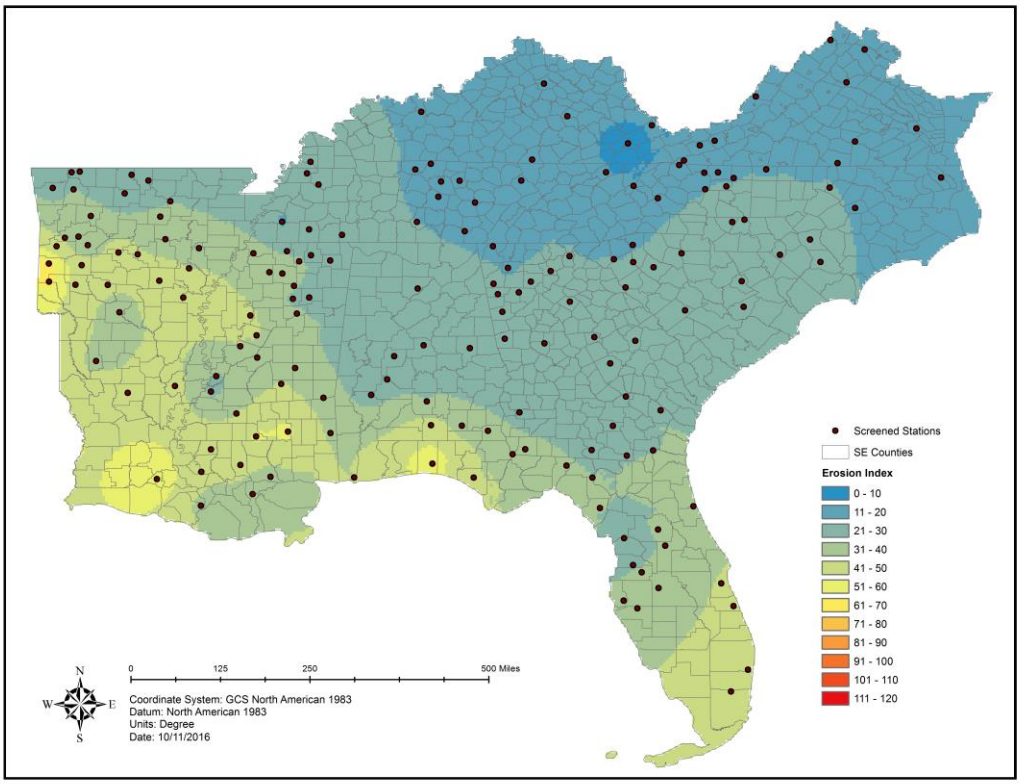

Figure 10 Mean EI for October

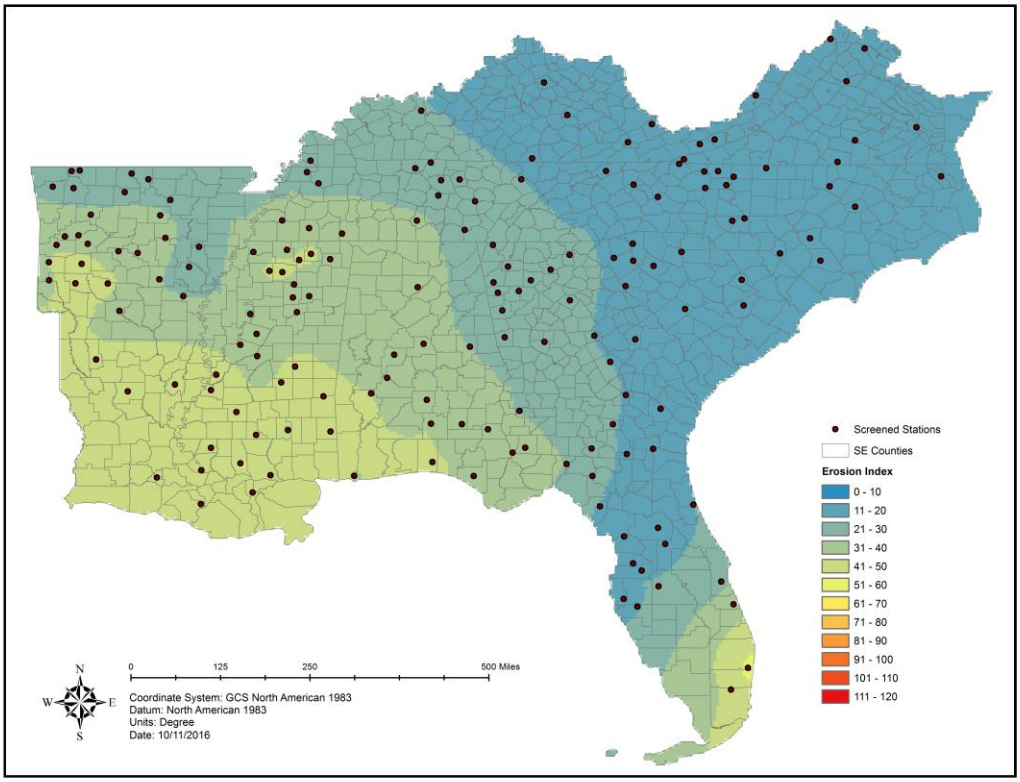

Figure 11 Mean EI for November

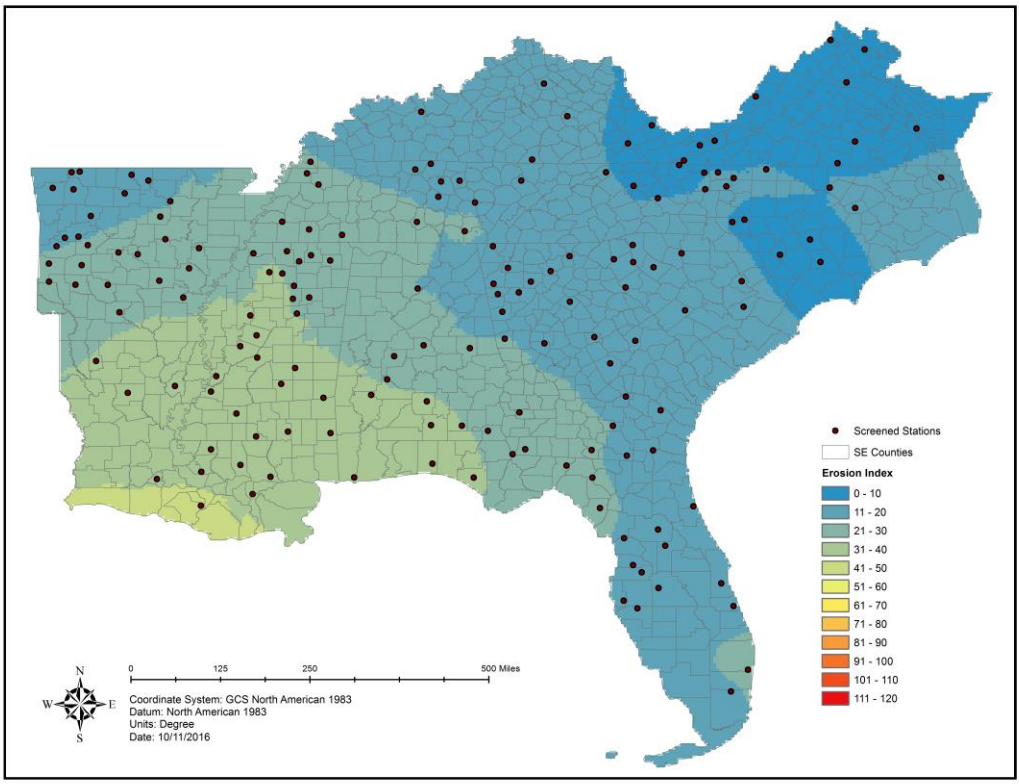

Figure 12 Mean EI for December

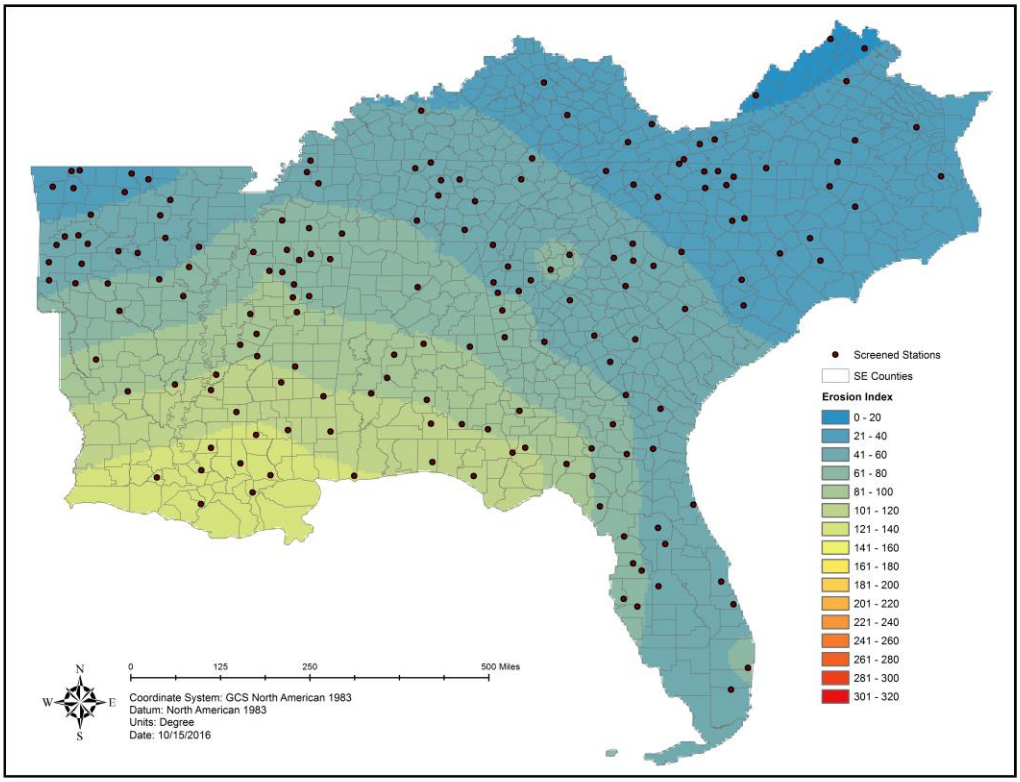

Figure 13 Mean EI for Winter

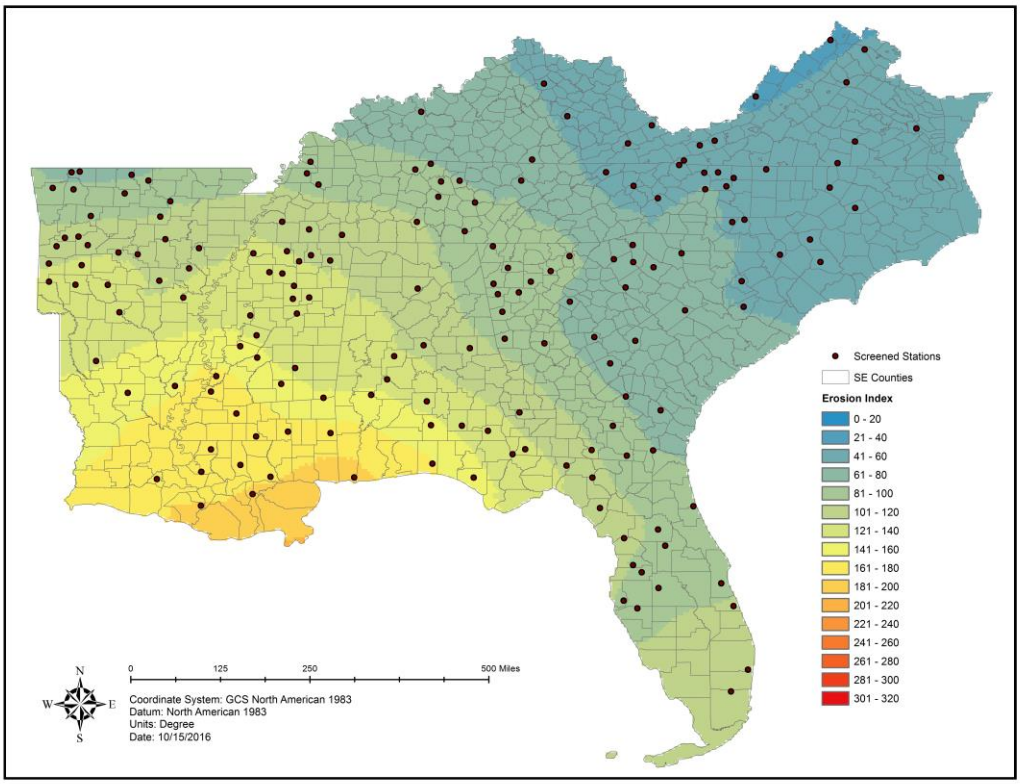

Figure 14 Mean EI for Spring

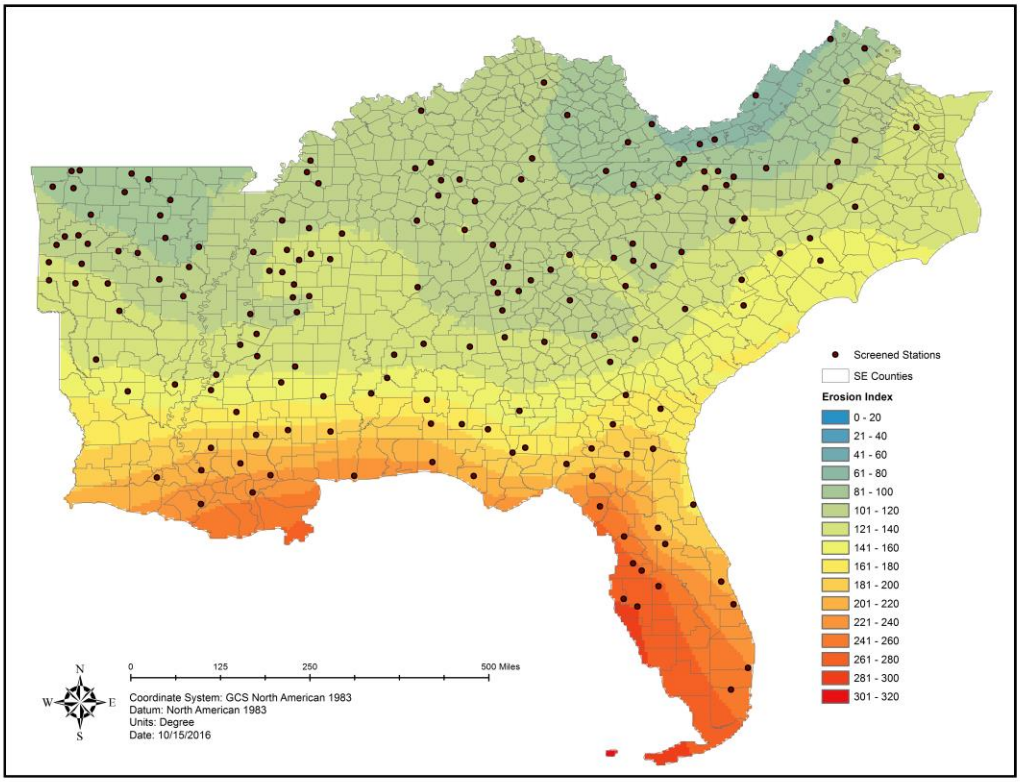

Figure 15 Mean EI for Summer

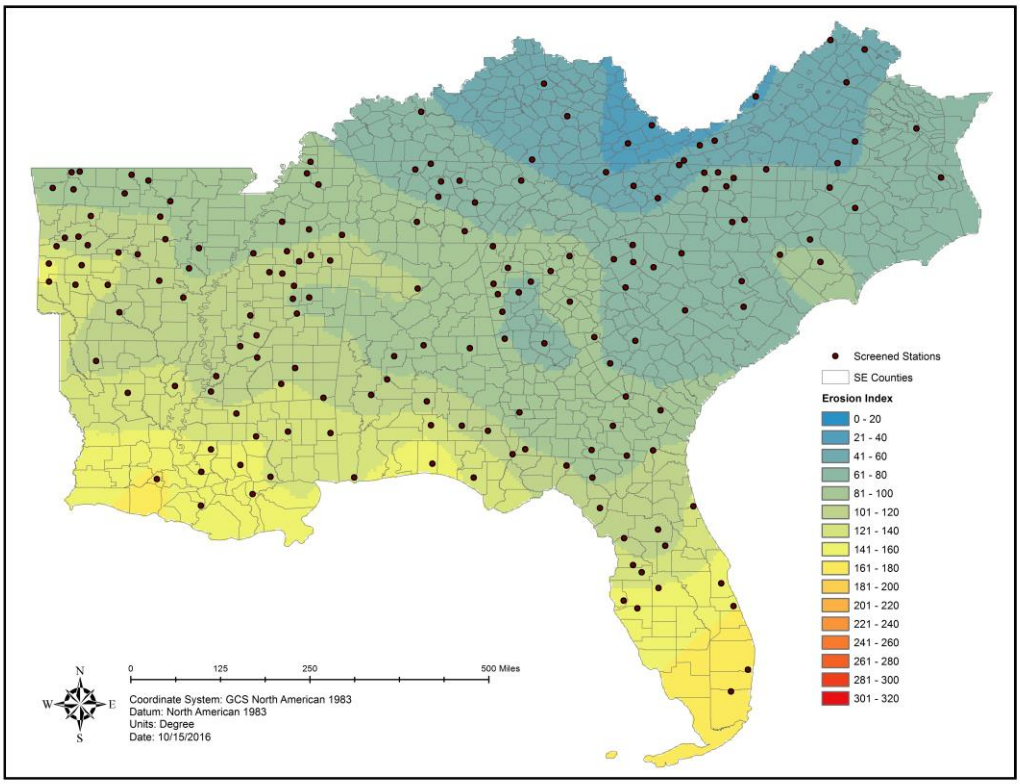

Figure 16 Mean EI for Fall

Appendix F

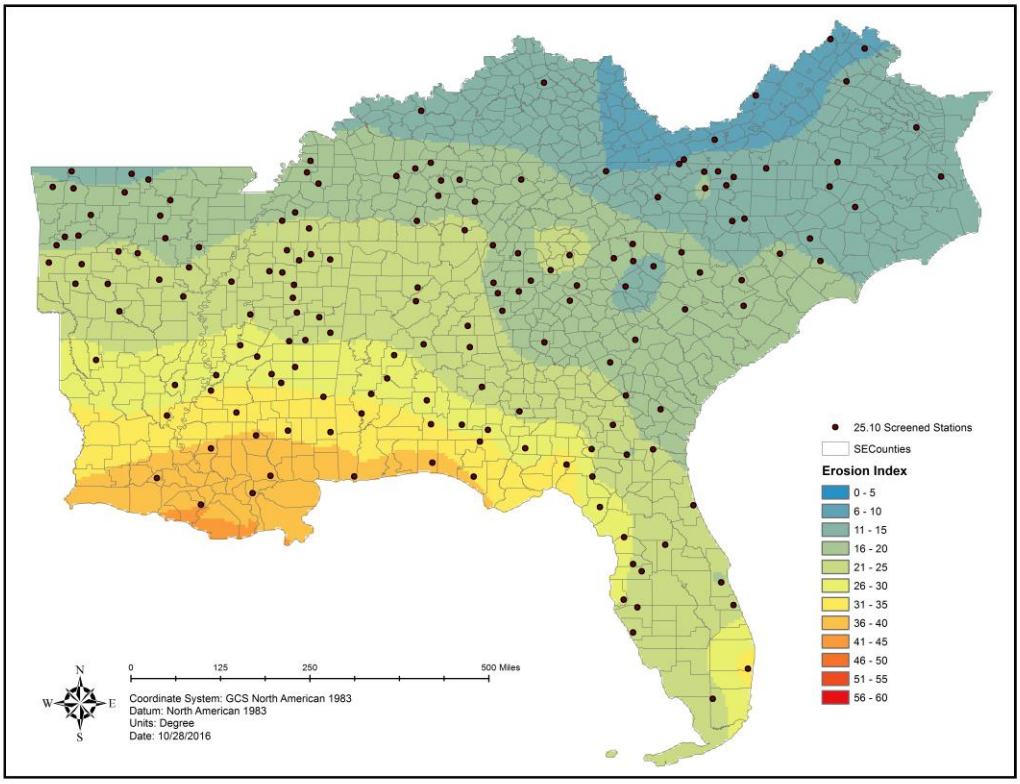

Figure 1 Median Monthly EI

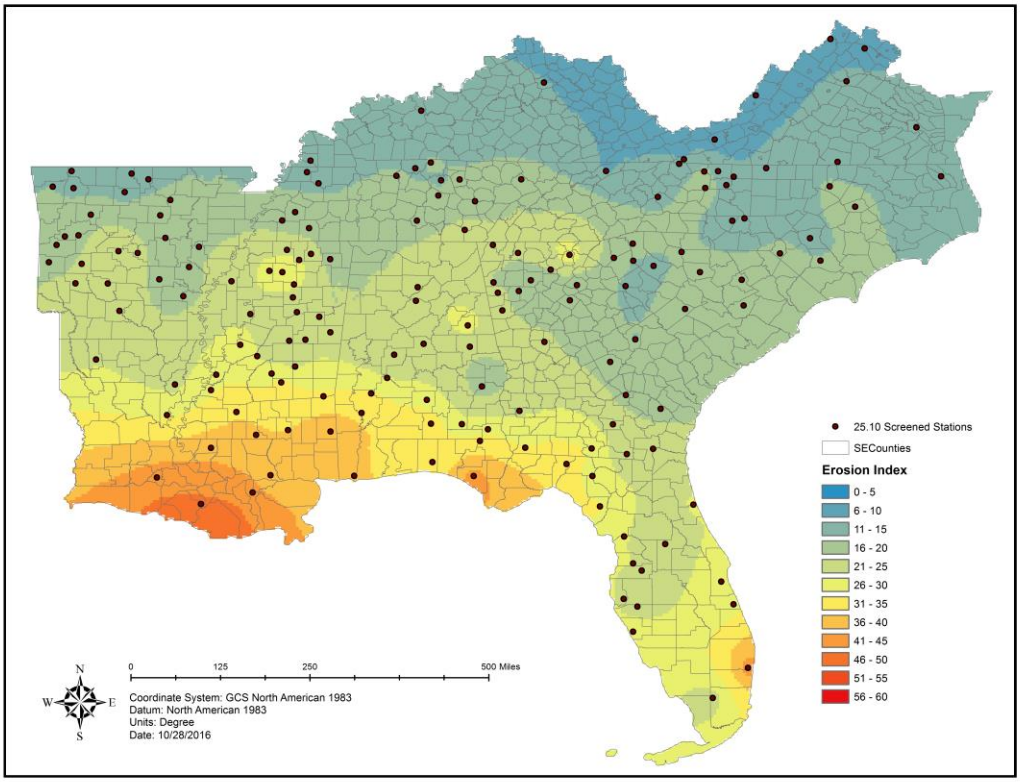

Figure 2 El Nino Median Monthly EI

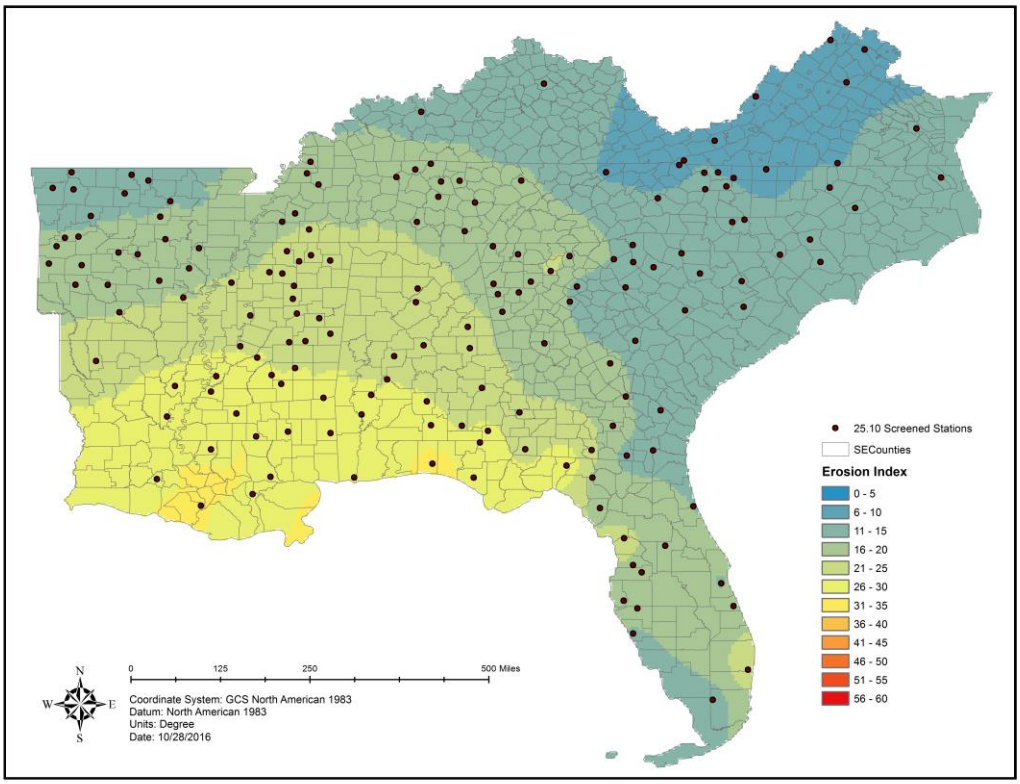

Figure 3 La Nina Median Monthly EI

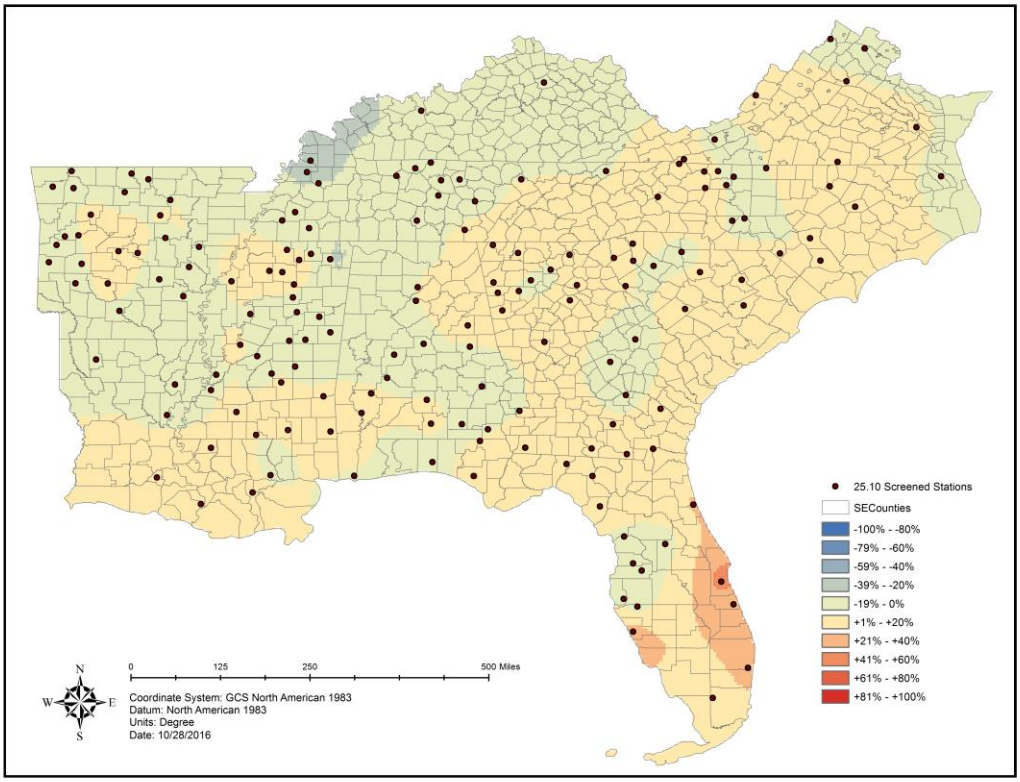

Figure 4 Relative Difference of Normal and El Nino

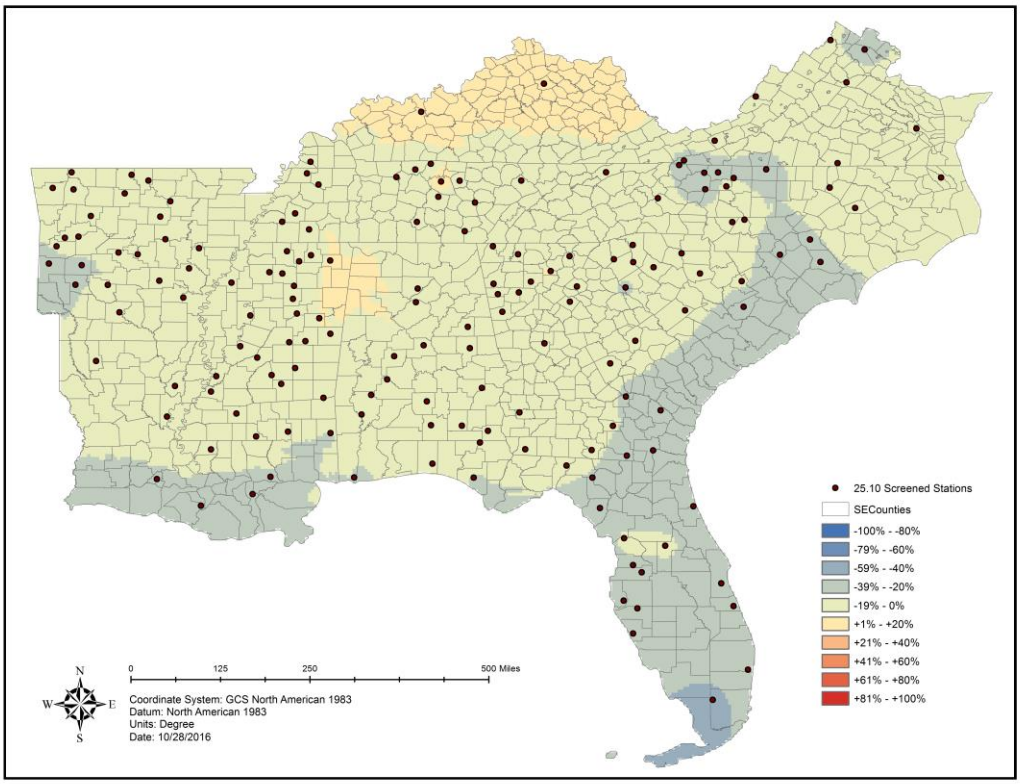

Figure 5 Relative Difference of Normal and La Nina

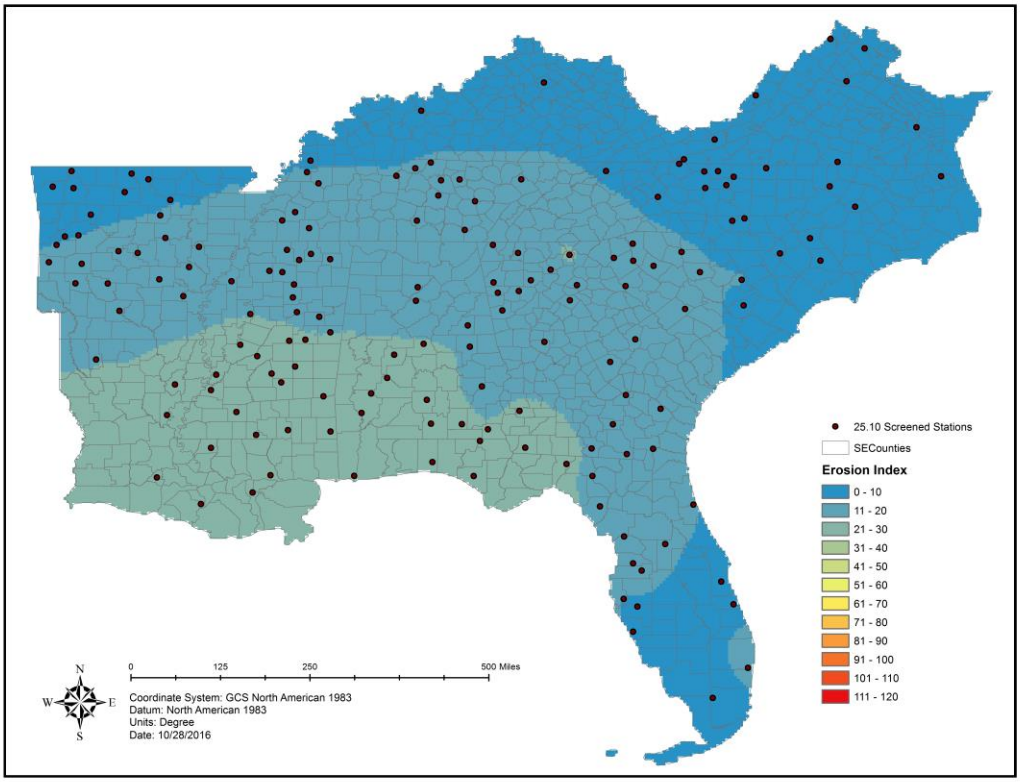

Figure 6 Winter Median Monthly EI

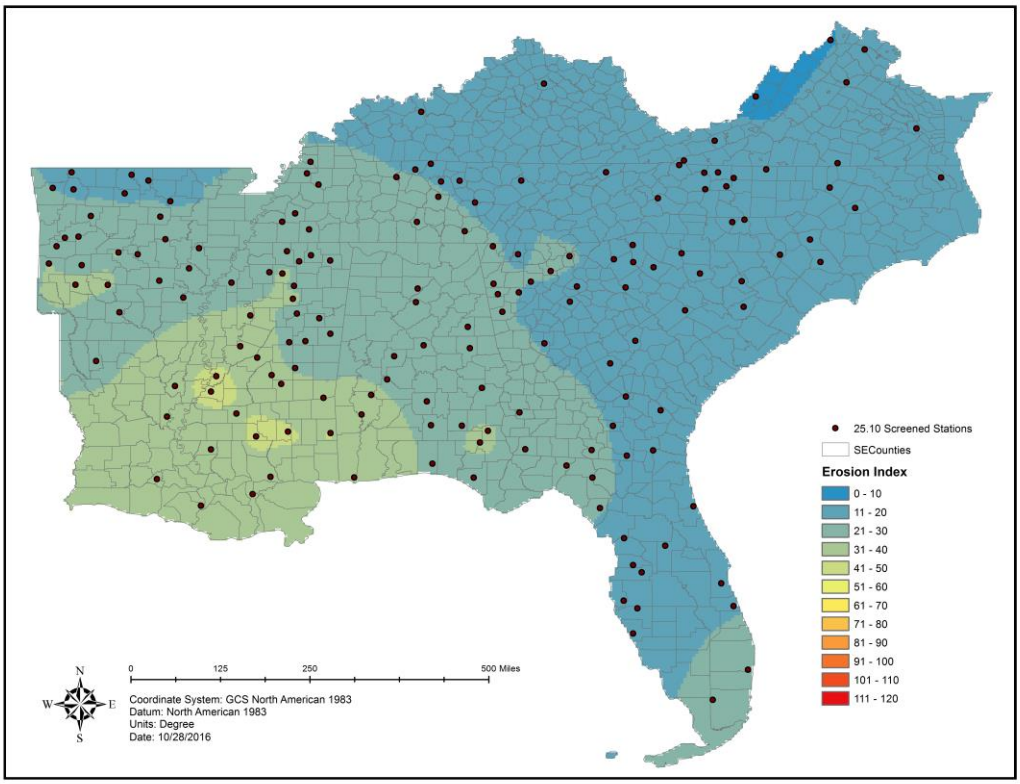

Figure 7 Spring Median Monthly EI

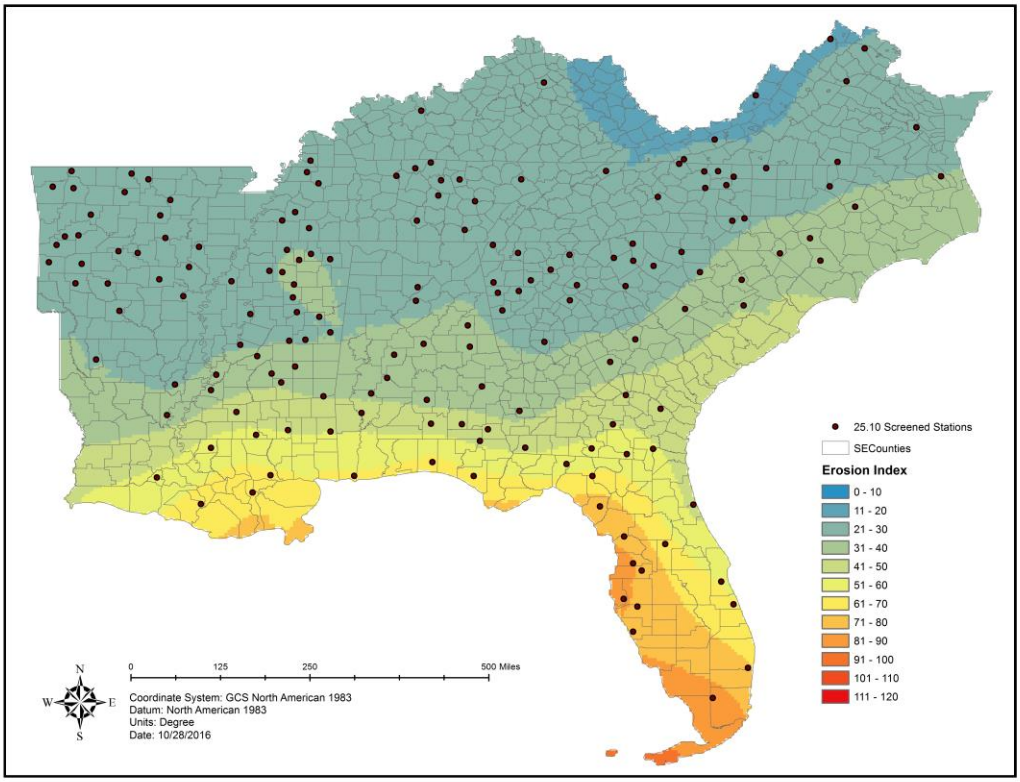

Figure 8 Summer Median Monthly EI

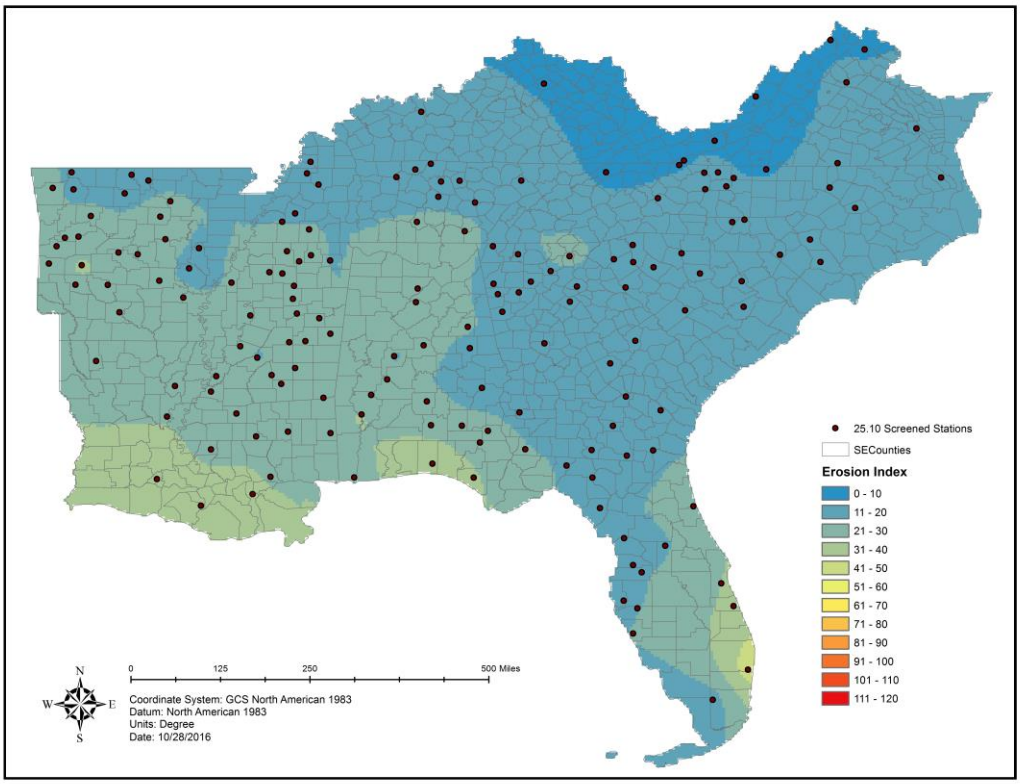

Figure 9 Fall Median Monthly EI

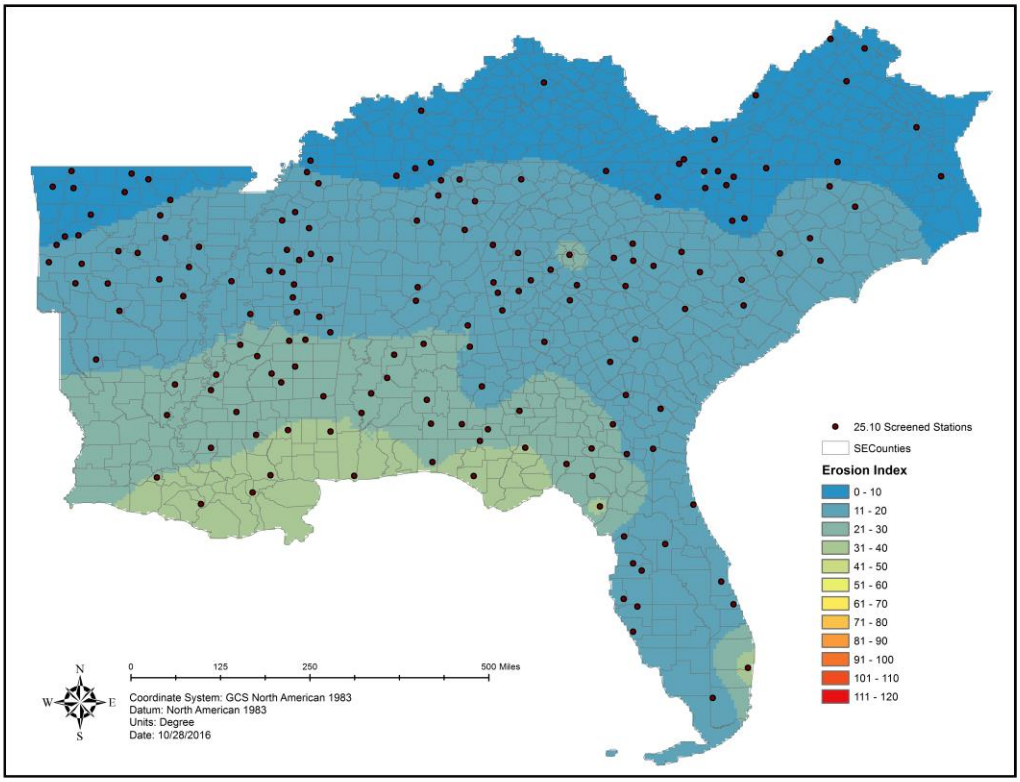

Figure 10 El Nino Winter Median Monthly EI

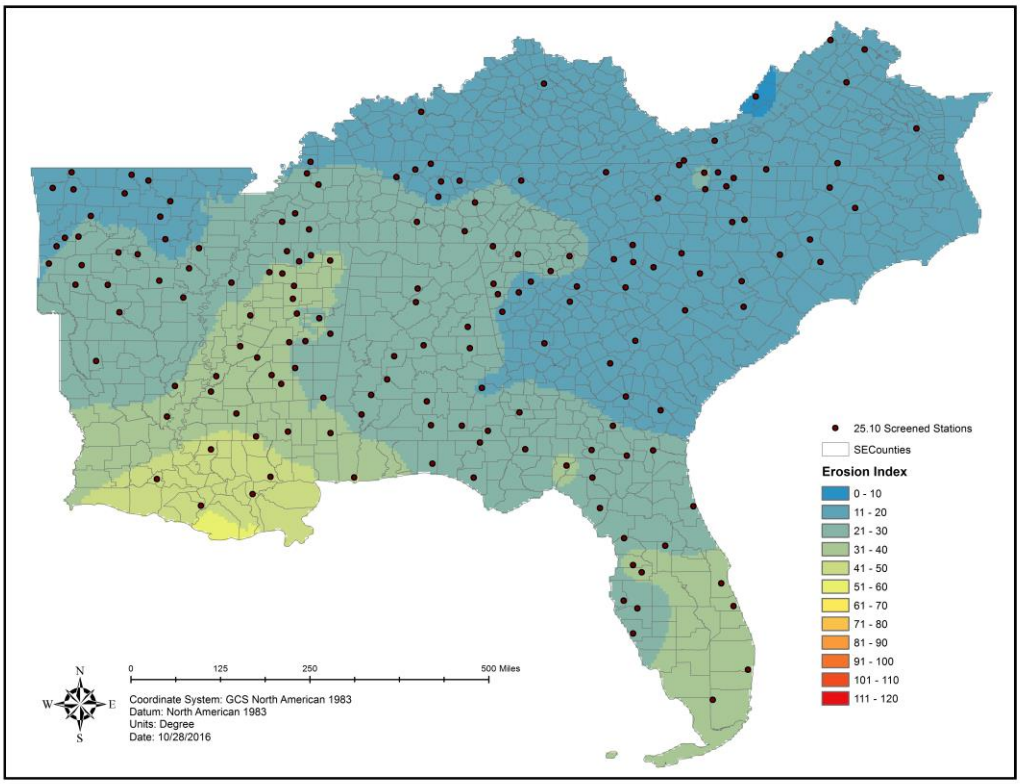

Figure 11 El Nino Spring Median Monthly EI

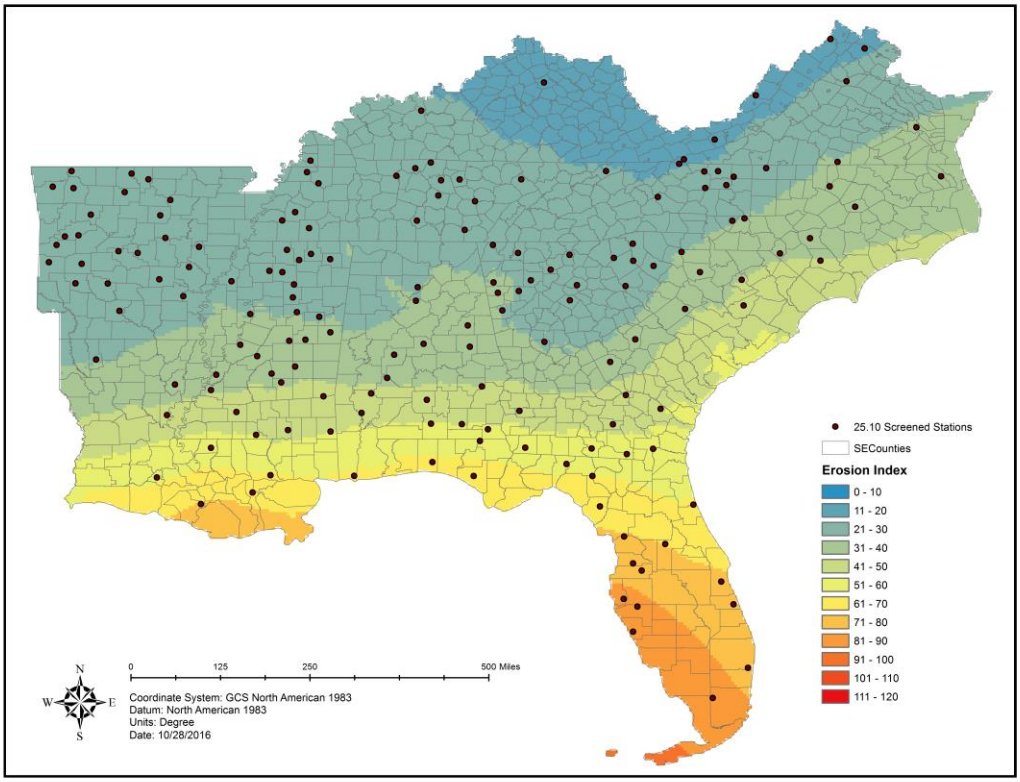

Figure 12 El Nino Summer Median Monthly EI

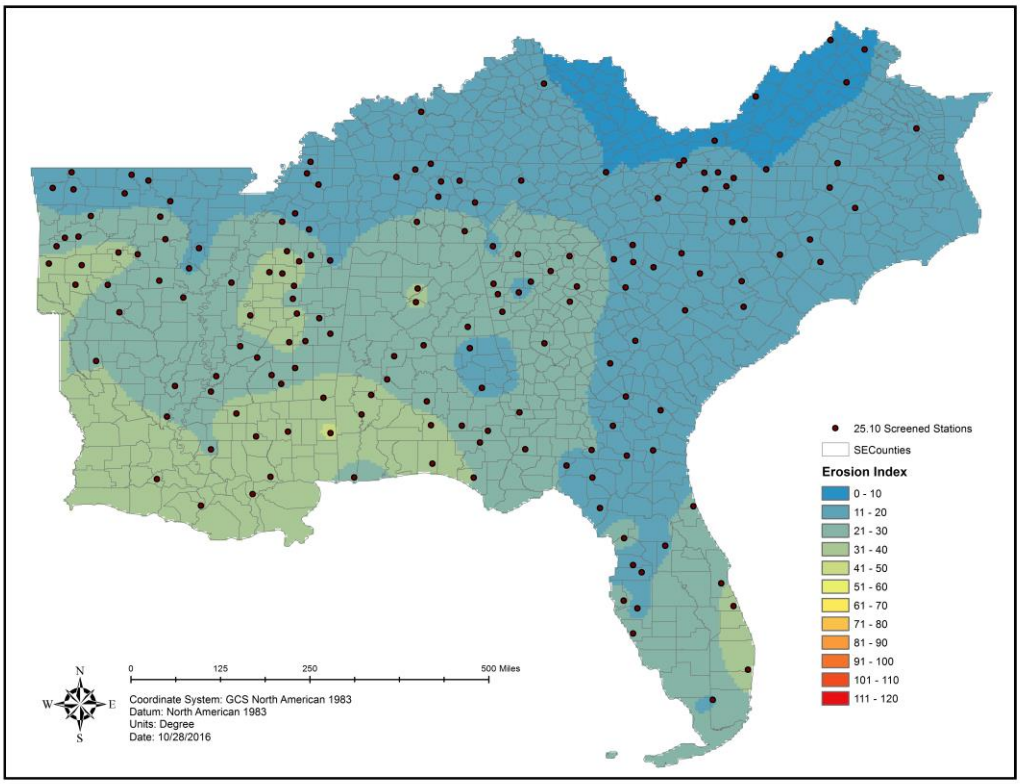

Figure 13 El Nino Fall Median Monthly EI

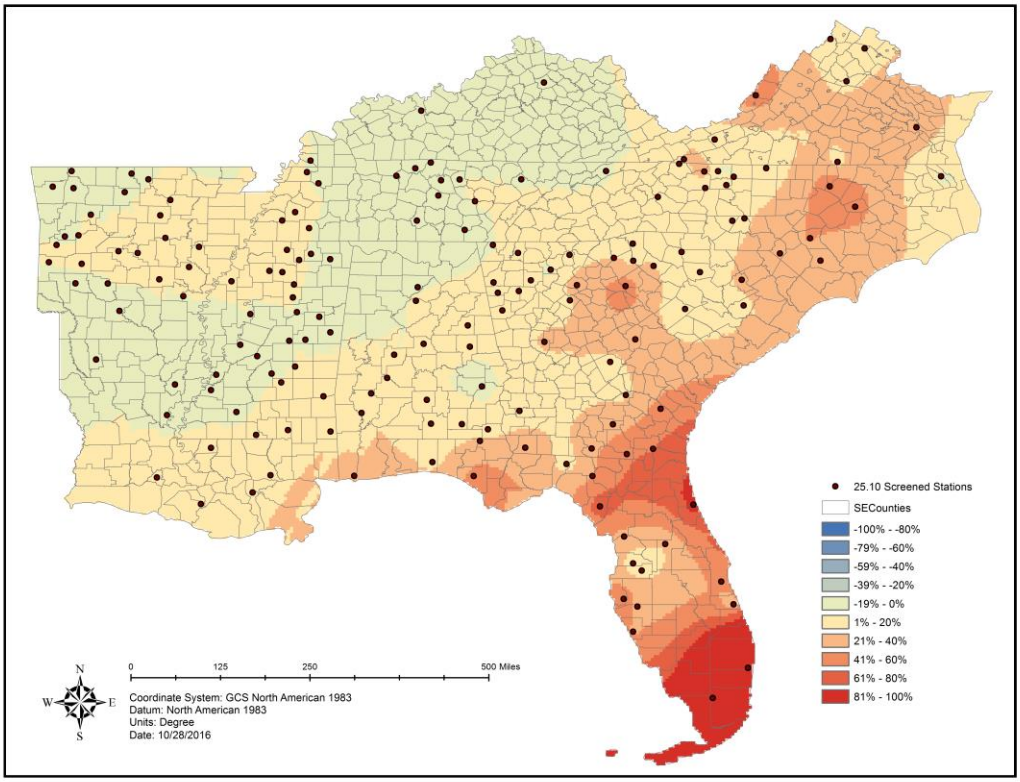

Figure 14 Relative Difference in Normal and El Nino Winter Median Monthly EI

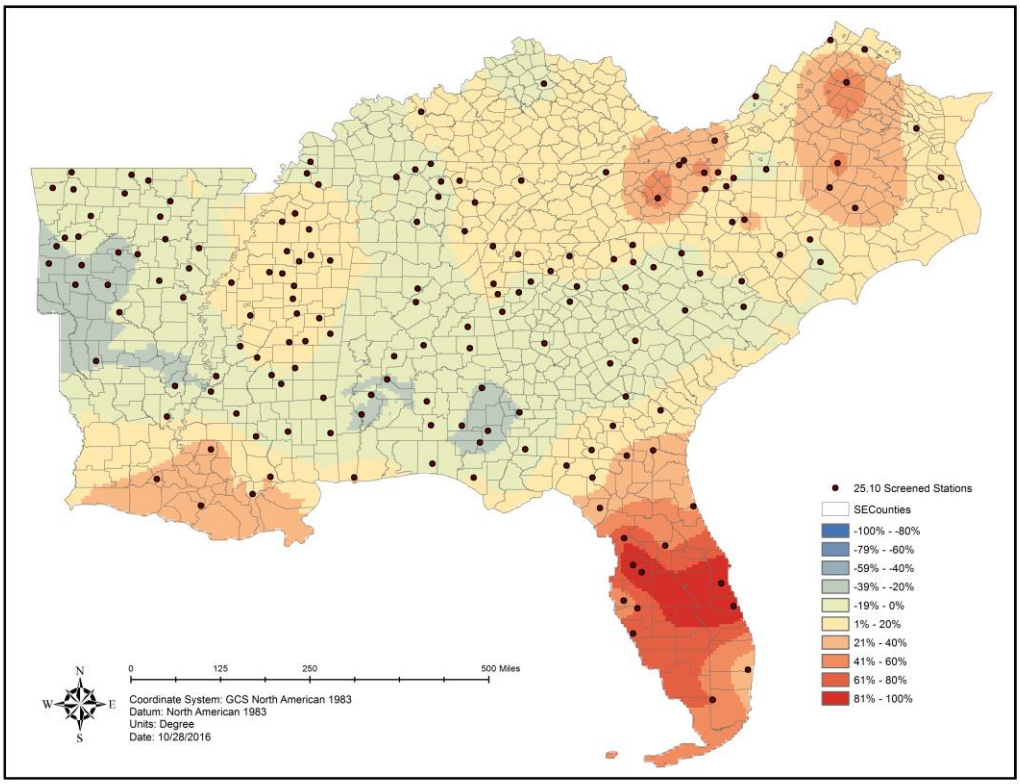

Figure 15 Relative Difference in Normal and El Nino Spring Median Monthly EI

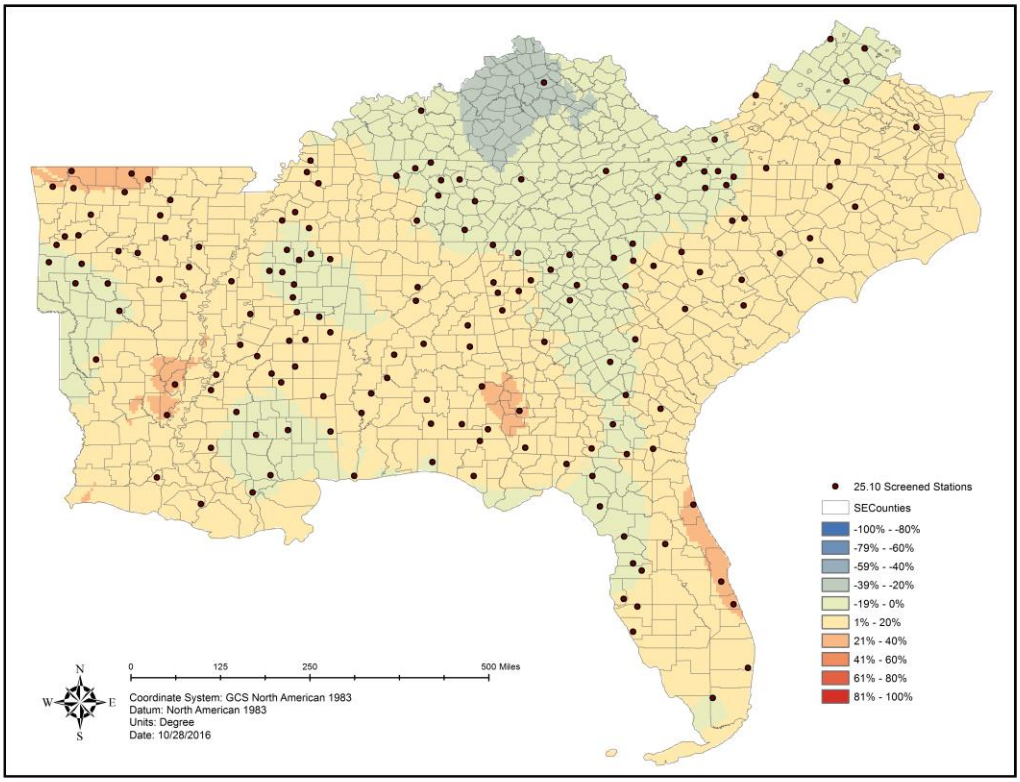

Figure 16 Relative Difference in Normal and El Nino Summer Median Monthly EI

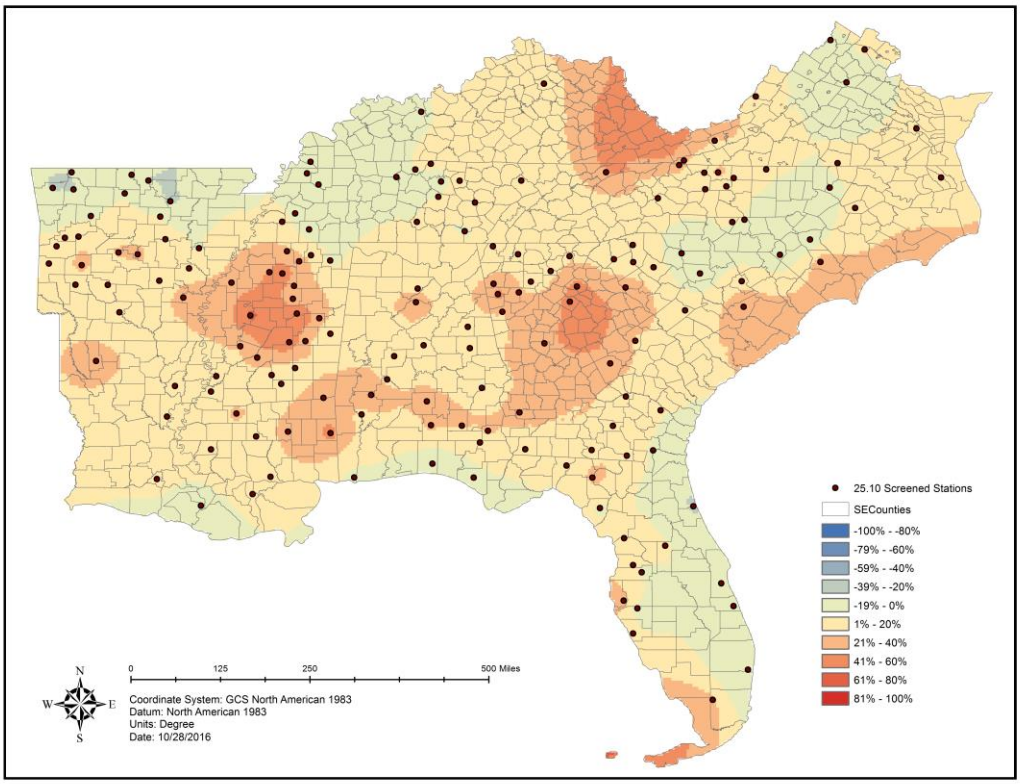

Figure 17 Relative Difference in Normal and El Nino Fall Median Monthly EI

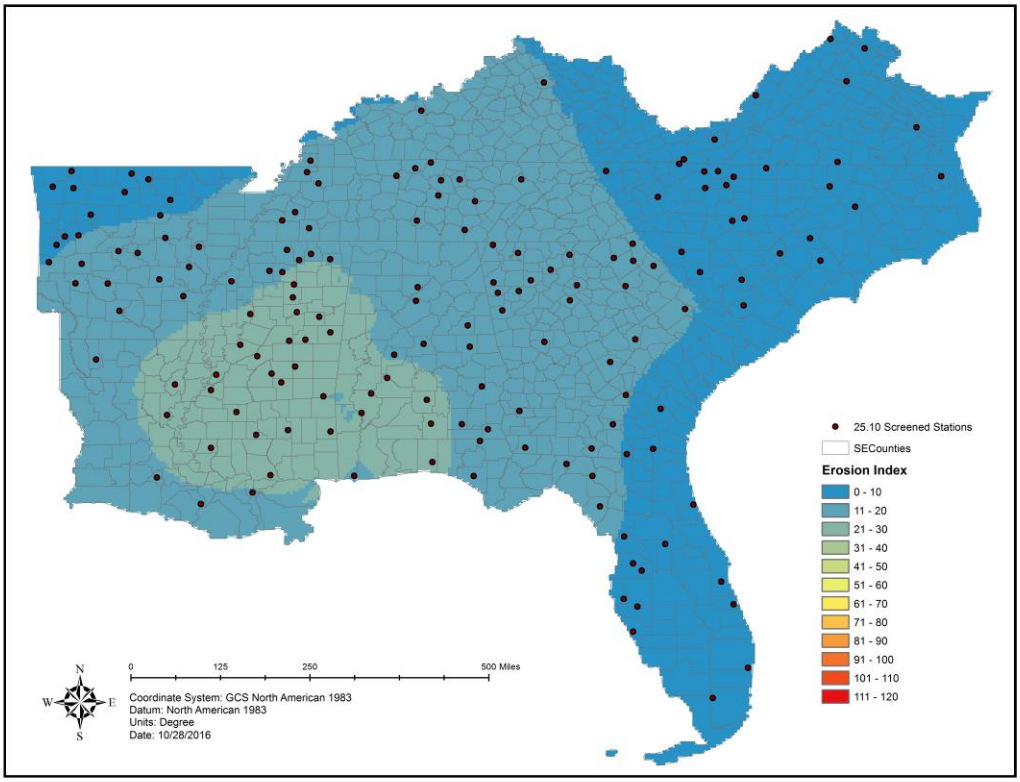

Figure 18 La Nina Winter Median Monthly EI

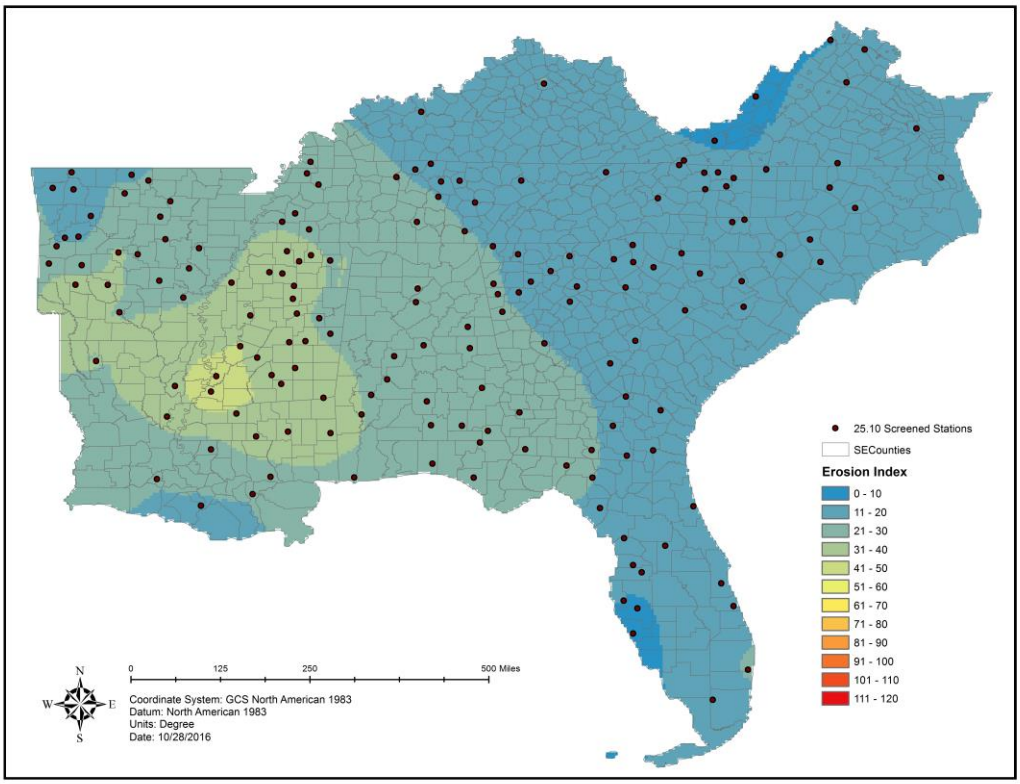

Figure 19 La Nina Spring Median Monthly EI

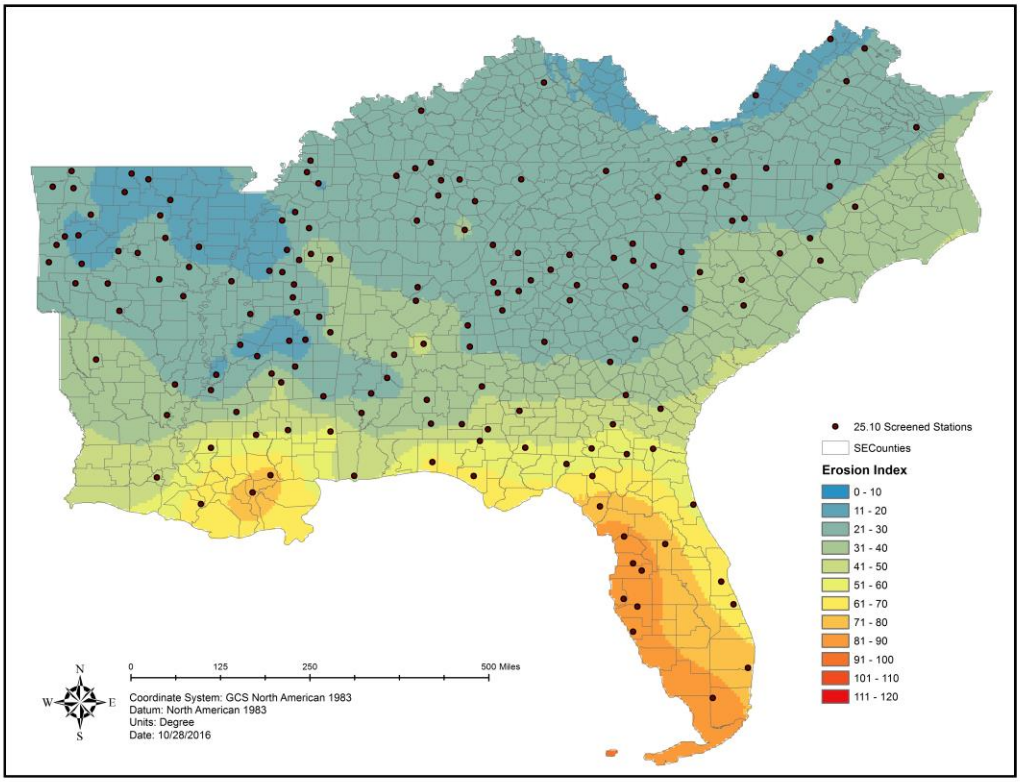

Figure 20 La Nina Summer Median Monthly EI

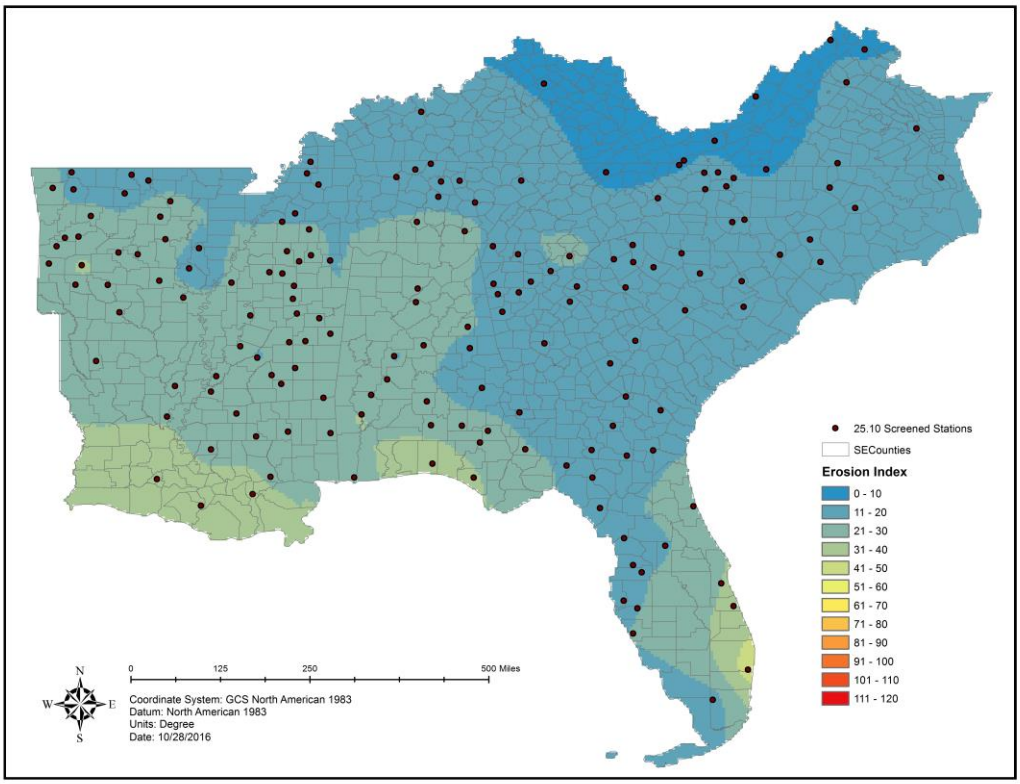

Figure 21 La Nina Fall Median Monthly EI

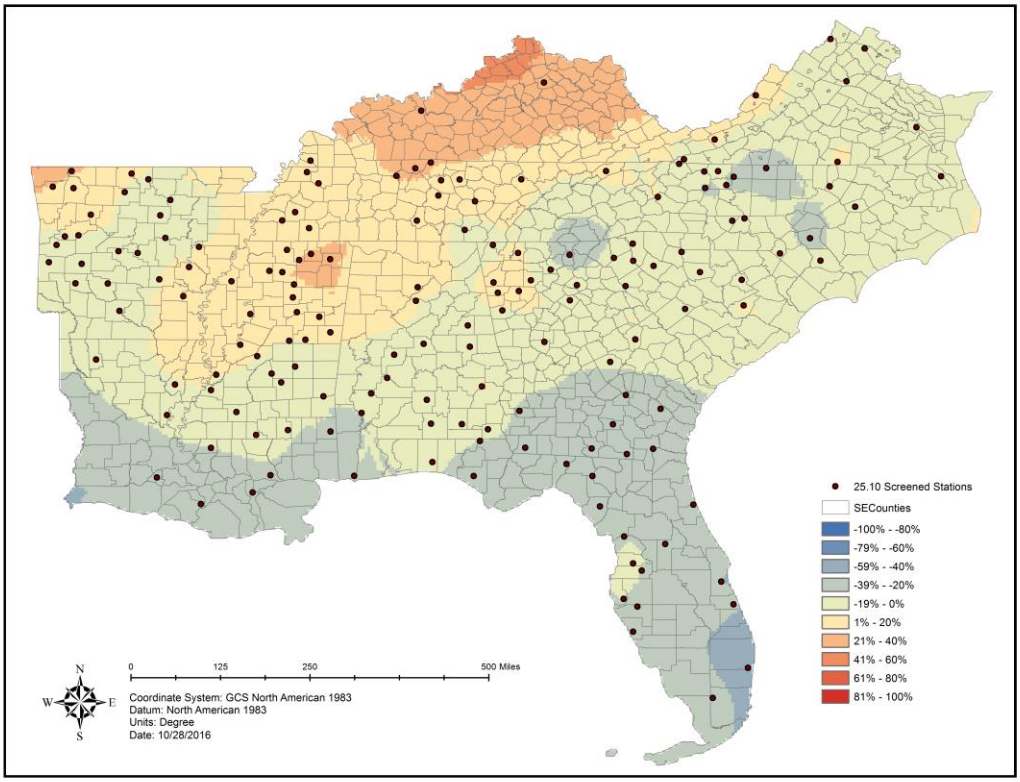

Figure 22 Relative Difference in Normal and La Nina Winter Median Monthly EI

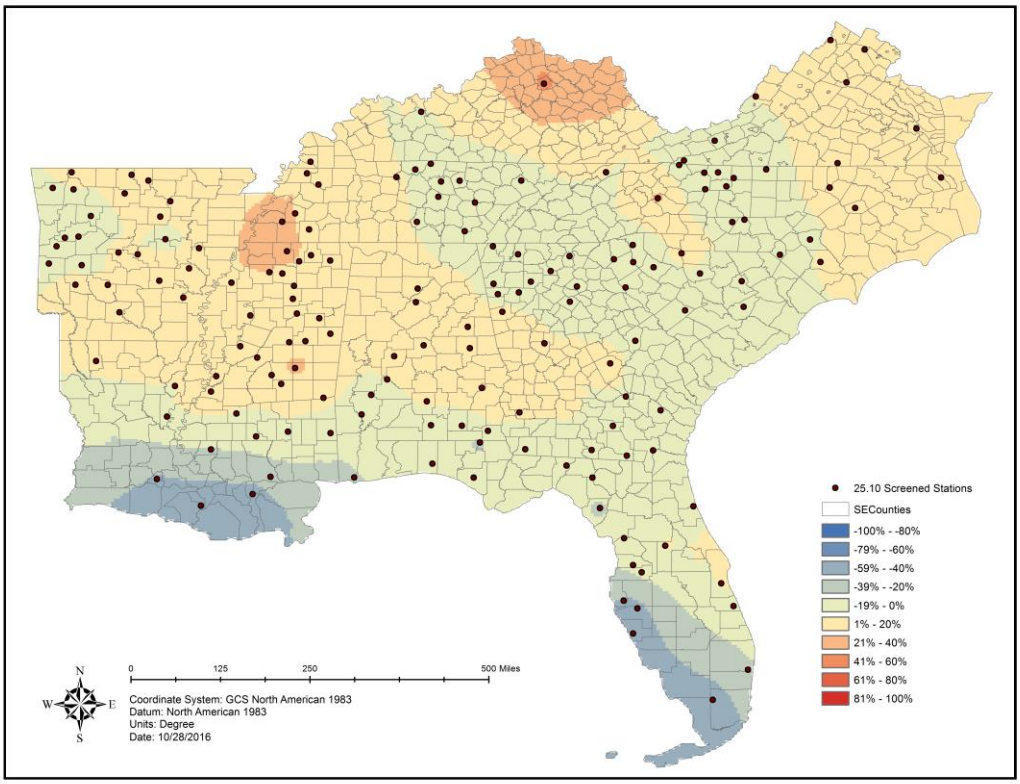

Figure 23 Relative Difference in Normal and La Nina Spring Median Monthly EI

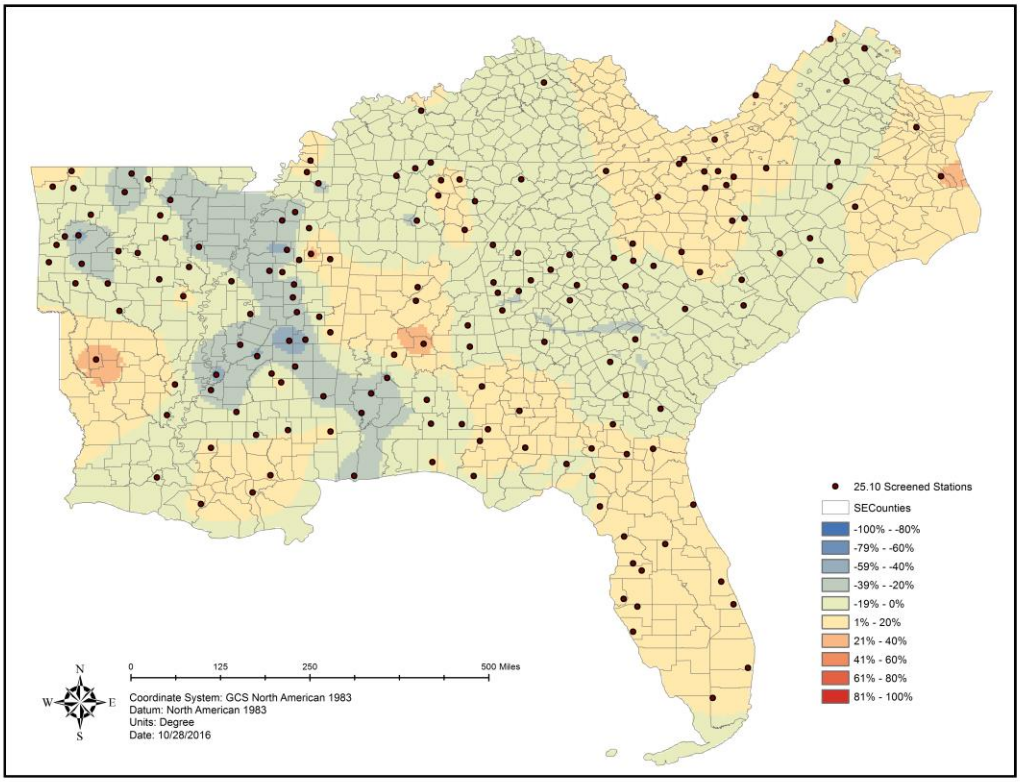

Figure 24 Relative Difference in Normal and La Nina Summer Median Monthly EI

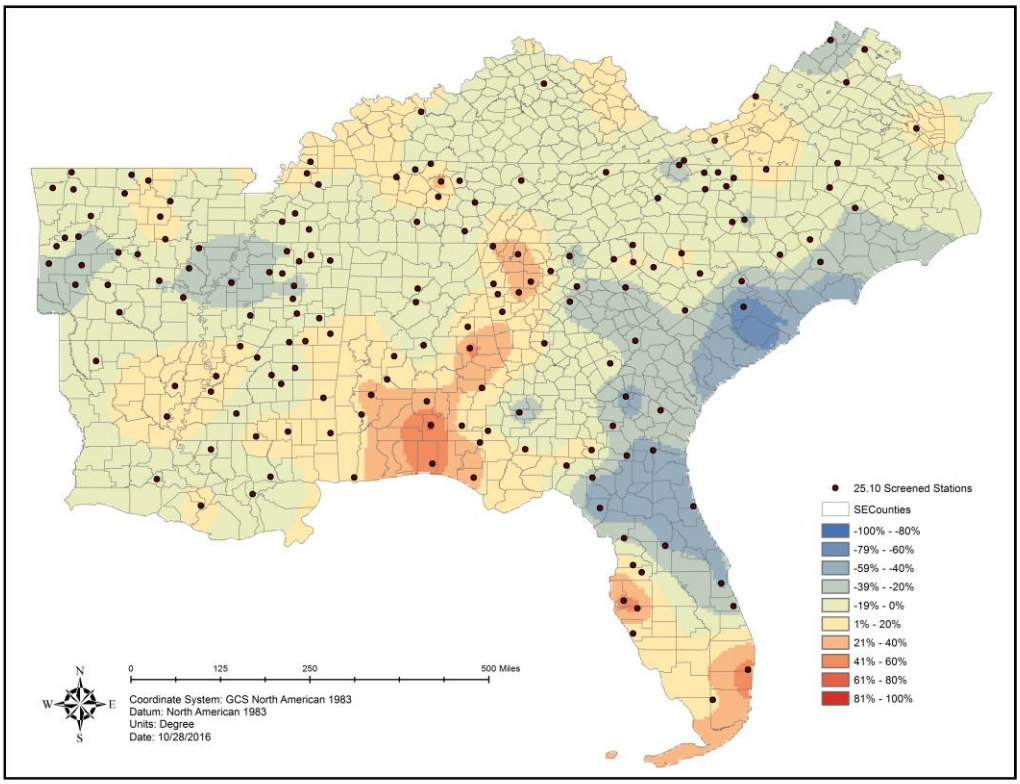

Figure 25 Relative Difference in Normal and La Nina Fall Median Monthly EI

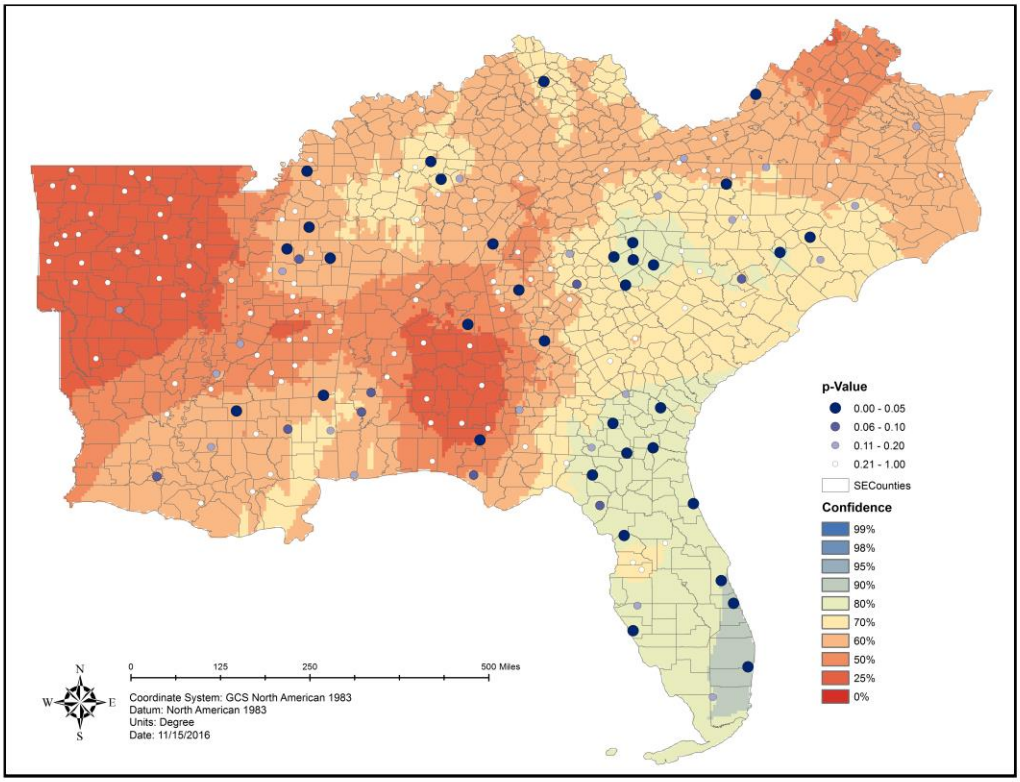

Figure 26 JRFit Test for Significance of ENSO in Winter (Clustered Months)

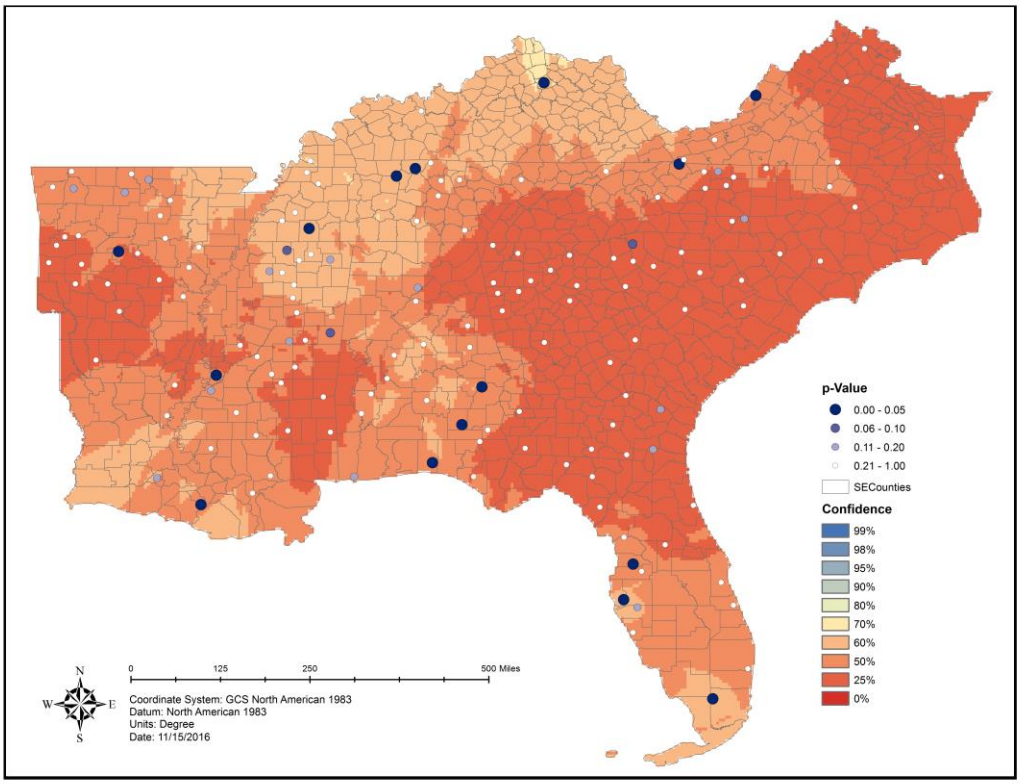

Figure 27 JRFit Test for Significance of ENSO in Spring (Clustered Months)

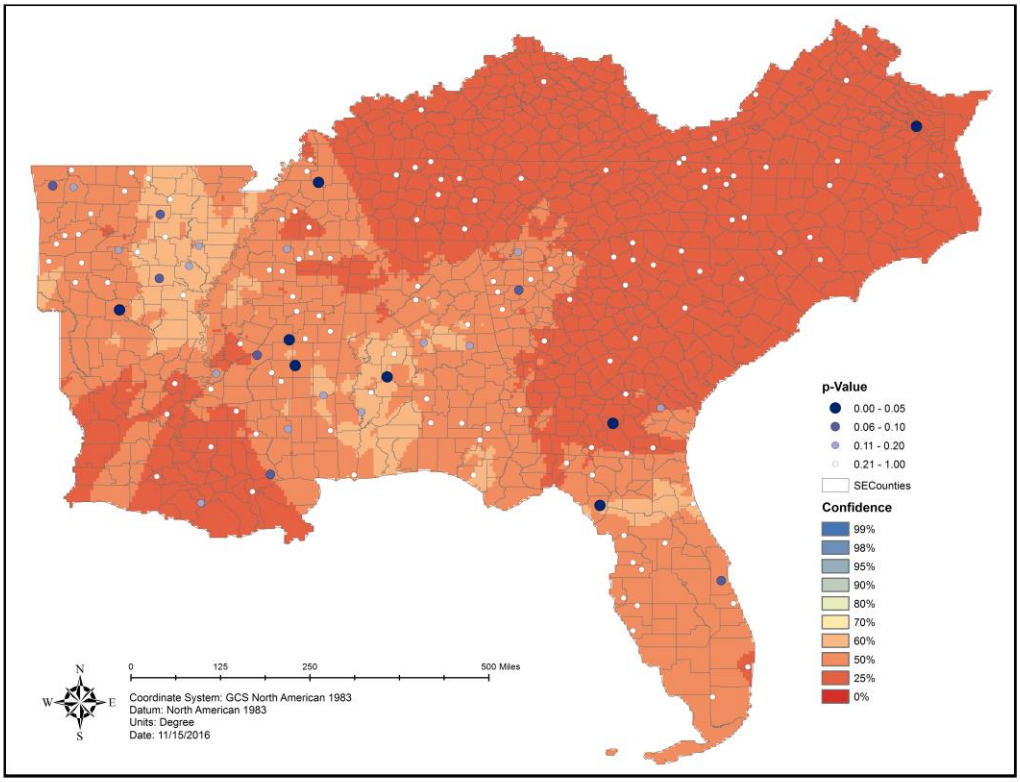

Figure 28 JRFit Test for Significance of ENSO in Summer (Clustered Months)

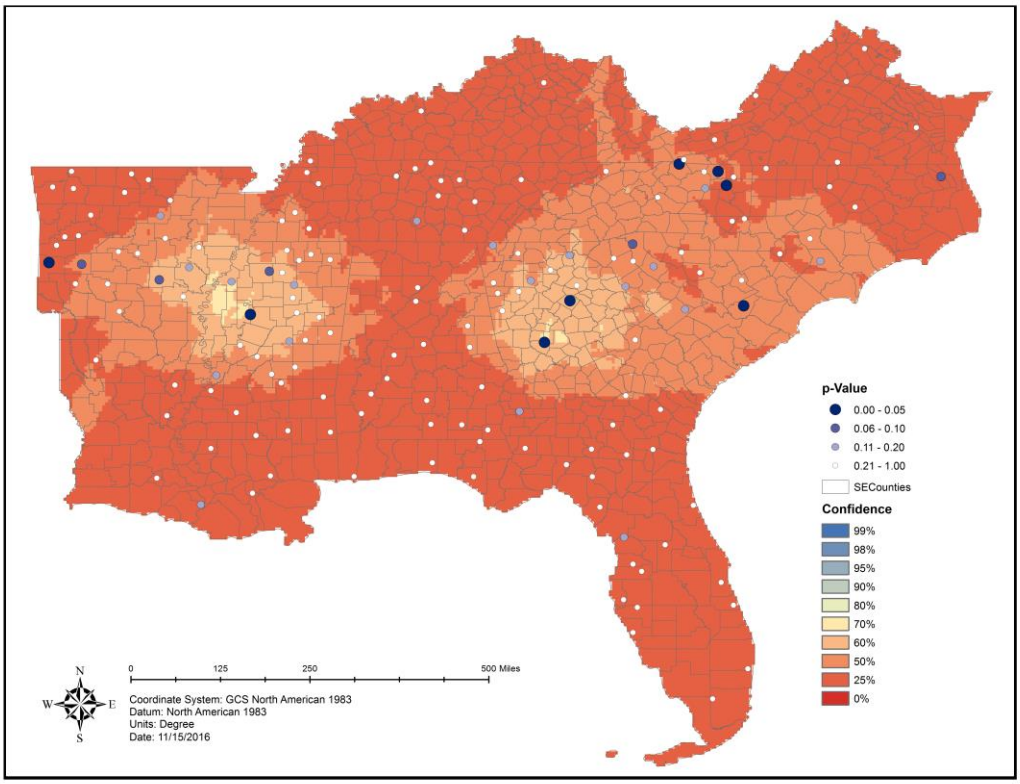

Figure 29 JRFit Test for Significance of ENSO in Fall (Clustered Months)

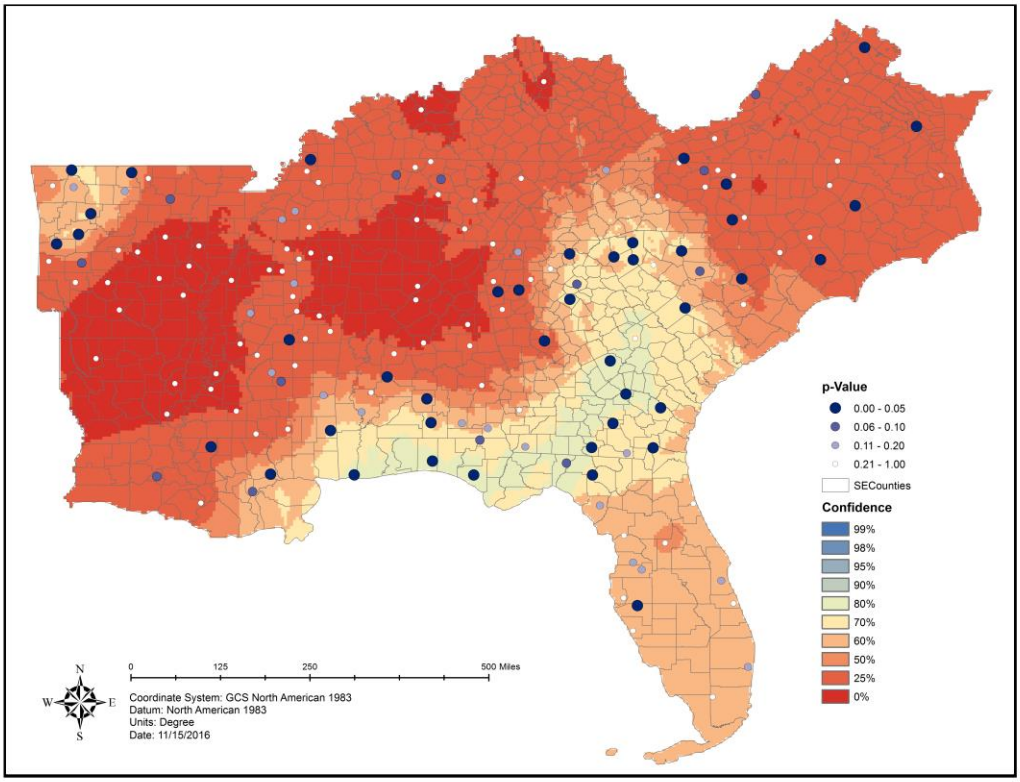

Figure 30 JRFit Test for Significance of ENSO on Number of Events

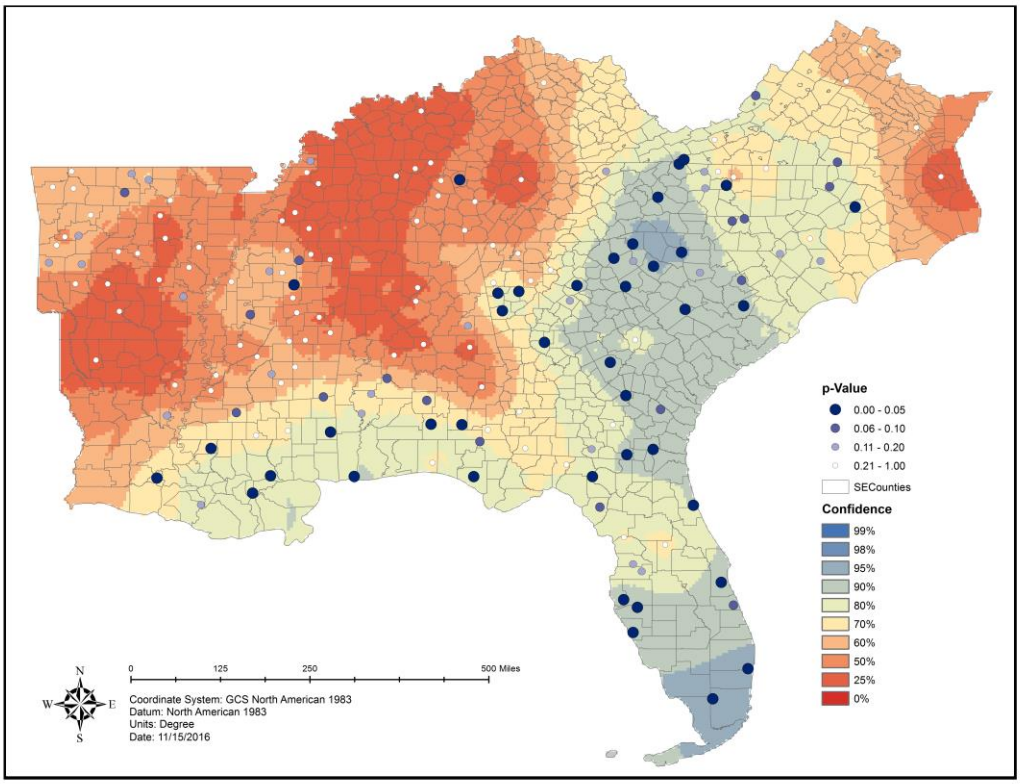

Figure 31 JRFit Test for Significance of ENSO on Depth

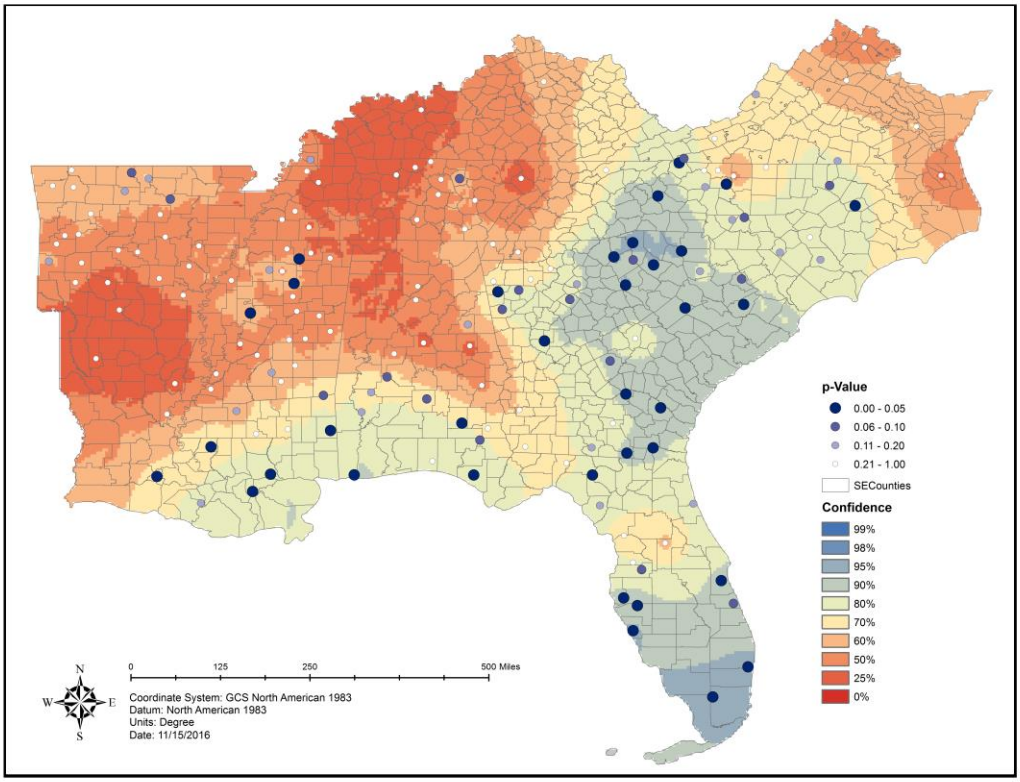

Figure 32 JRFit Test for Significance of ENSO on Kinetic Energy

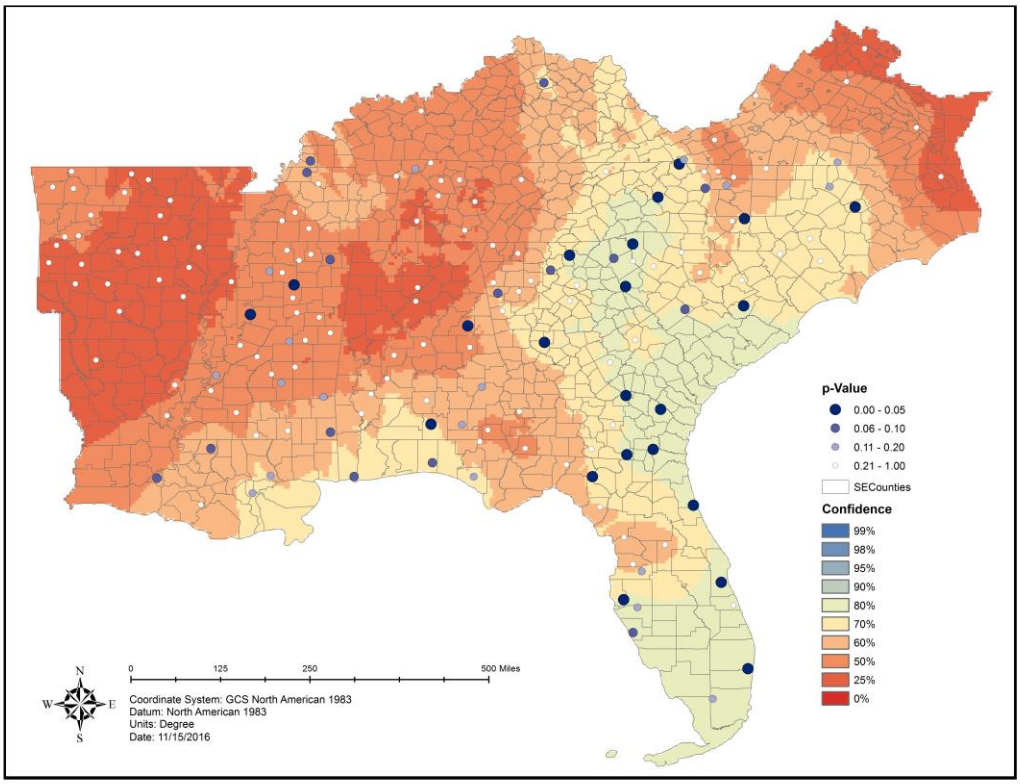

Figure 33 JRFit Test for Significance of ENSO on Erosion Index

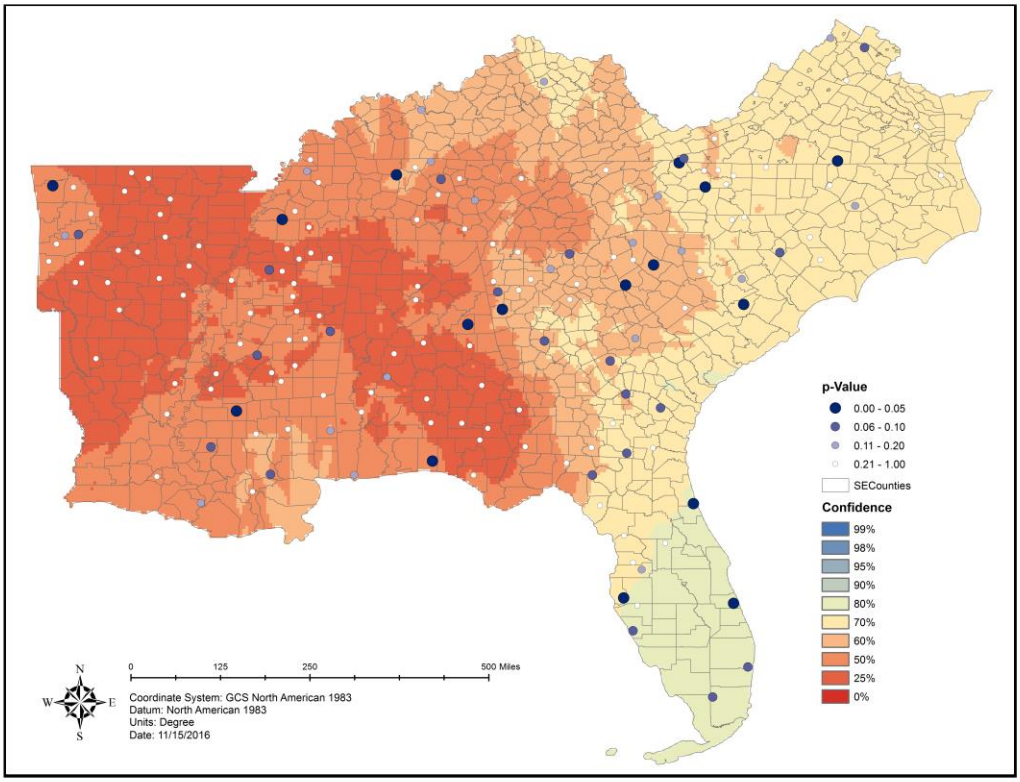

Figure 34 JRFit Test for Significance of ENSO on Mean Depth

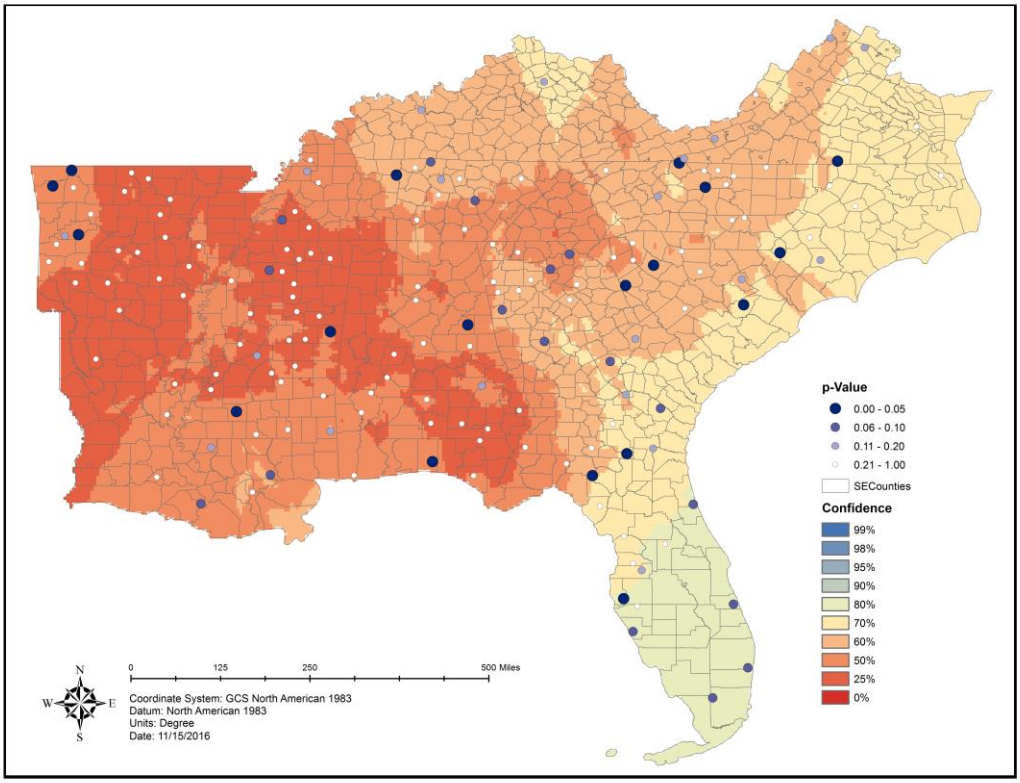

Figure 35 JRFit Test for Significance of ENSO on Mean Kinetic Energy

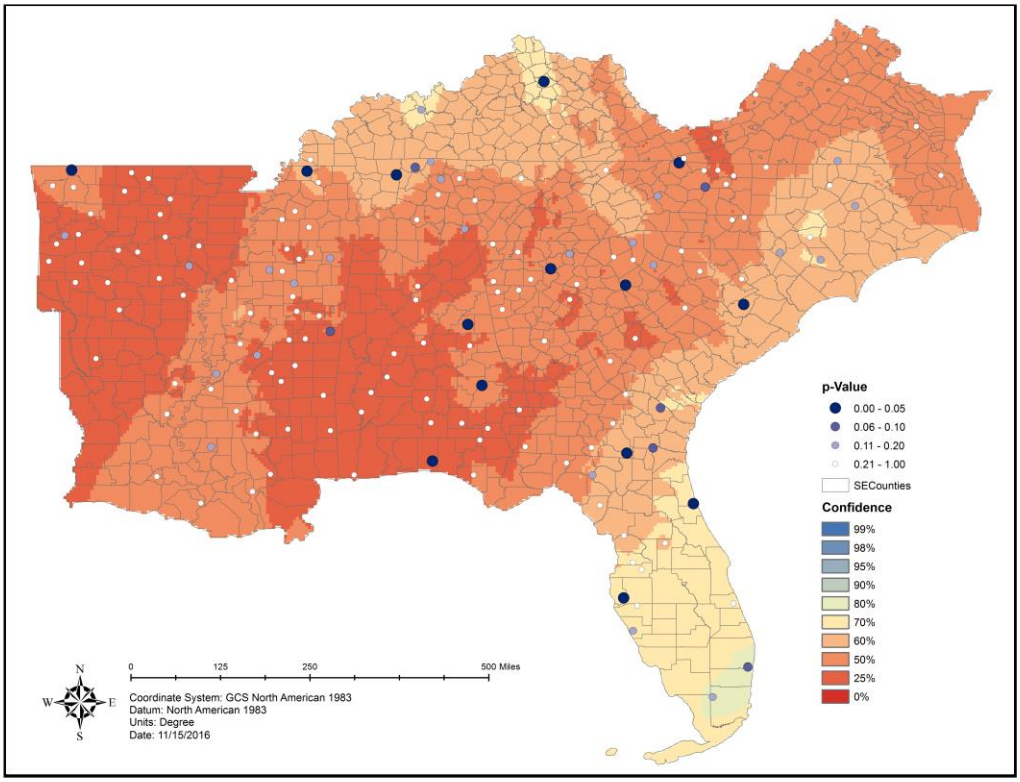

Figure 36 JRFit Test for Significance of ENSO on Mean Erosion Index

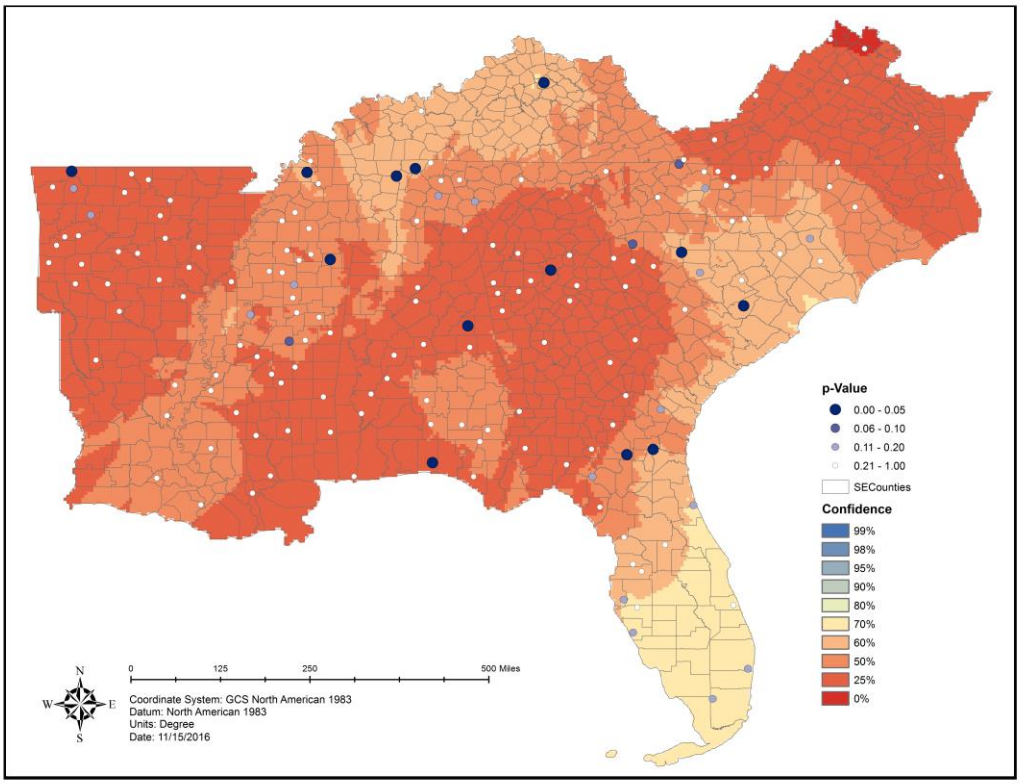

Figure 37 JRFit Test for Significance of ENSO on EI Rate

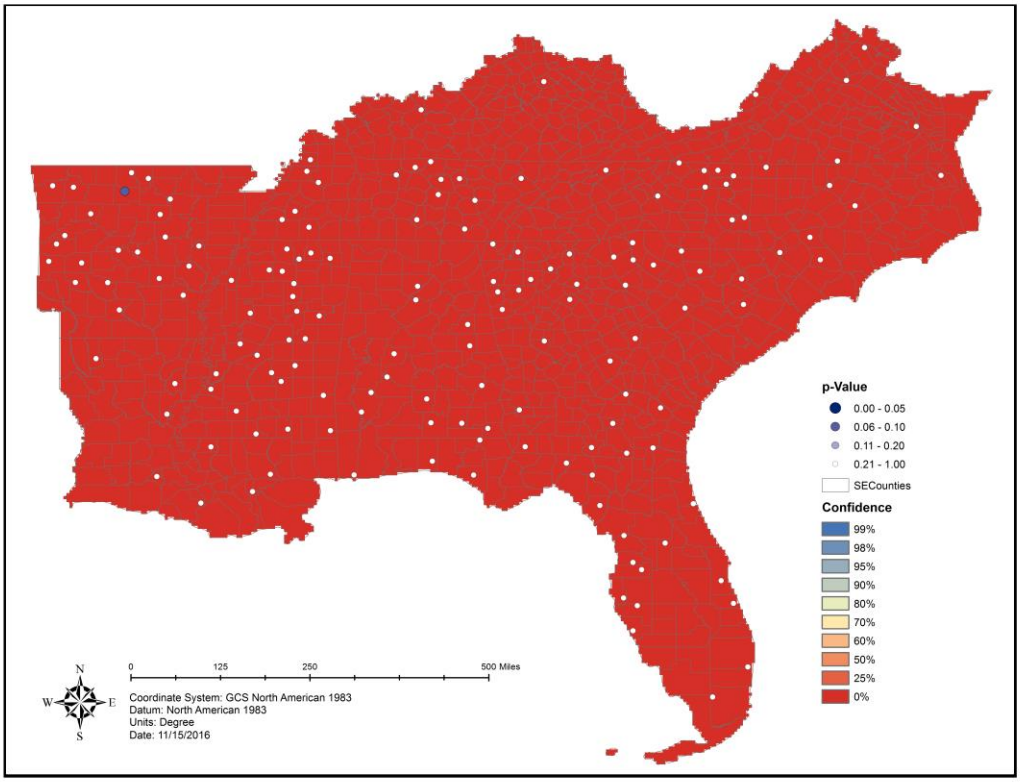

Figure 38 JRFit Test for Significance of ENSO on Median I_{30} (All Storms)

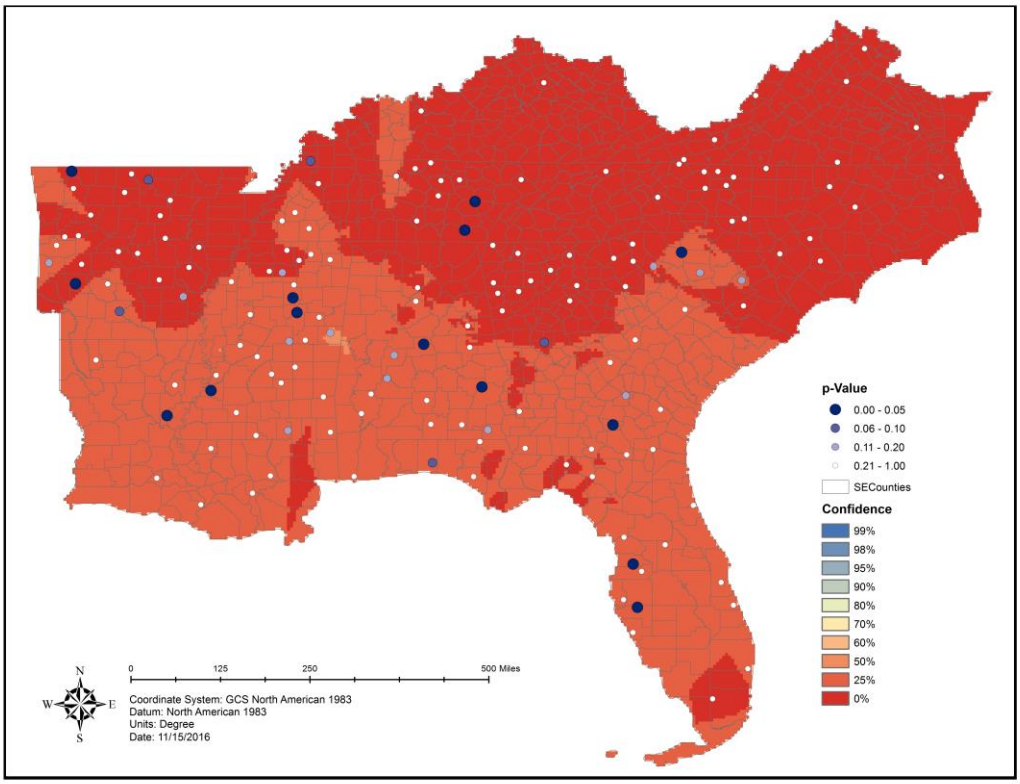

Figure 39 JRFit Test for Significance of ENSO on Median I_{30} (Greater than 0.5 Inches)

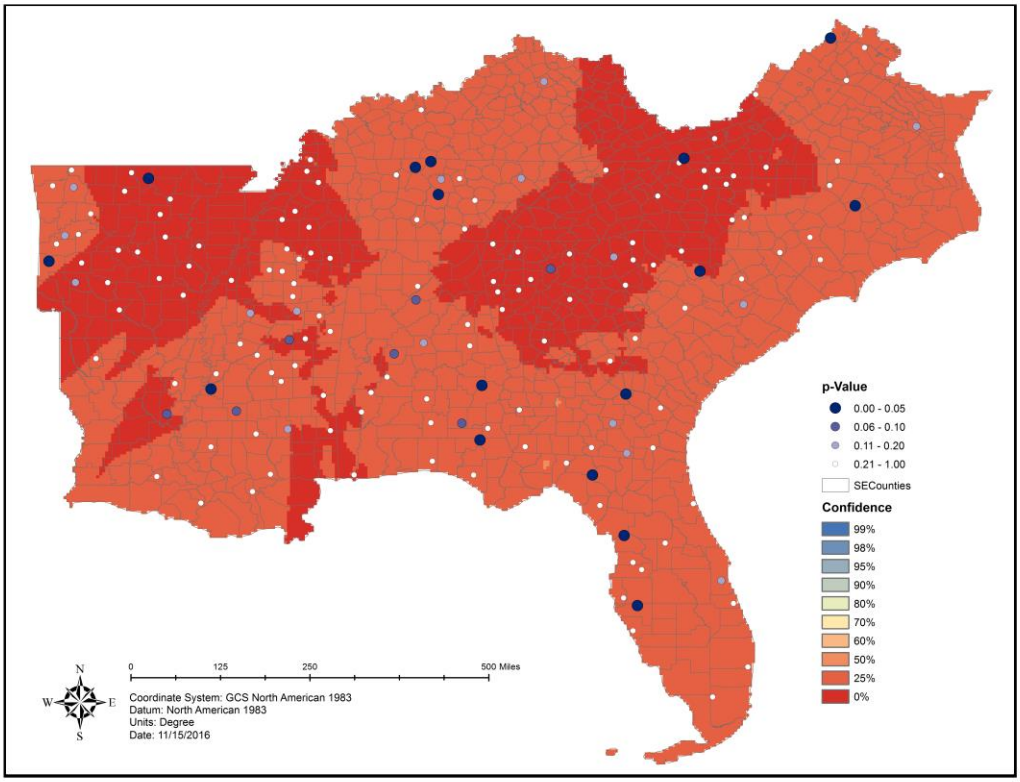

Figure 40 JRFit Test for Significance of ENSO on Median I_{30} (Greater than 1.0 Inch)